AVAILABLE METHODS FOR FUNCTIONAL MONITORING OF DRY CASK STORAGE SYSTEMS

Prepared for

U.S. Nuclear Regulatory Commission
Contract NRC–HQ–12–C–02–0089

Prepared by

Xihua He[1]
Roland Benke[1]
Yi-Ming Pan[1]
Leonard Caseres[2]
Pavan Shukla[1]
Ken Chiang*
Roberto Pabalan[3]
Greg Willden[2]
David Vickers[2]

[1]Center for Nuclear Waste Regulatory Analyses
San Antonio, Texas

[2]Southwest Research Institute®
San Antonio, Texas

[3]U.S. Nuclear Waste Technical Review Board
Arlington, Virginia

November 2014

*Former employee at Southwest Research Institute

CONTENTS

CONTENTS (continued)

CONTENTS (continued)

FIGURES

FIGURES (continued)

TABLES

ACKNOWLEDGMENTS

This report was prepared to document work performed by the Center for Nuclear Waste Regulatory Analyses (CNWRA®) for the U.S. Nuclear Regulatory Commission (NRC) under Contract No. NRC–HQ–12–C–02–0089. The studies and analyses reported here were performed on behalf of the NRC Office of Nuclear Regulatory Research. The report is an independent product of CNWRA and does not necessarily reflect the view or regulatory position of NRC.

The authors acknowledge the valuable contributions of the NRC project managers D. Dunn and M. Hiser and NRC staff members G. Oberson, O. Torres, B. Jagannath, and R. Einziger for their guidance, input, and information provided over the duration of this project.

The authors thank J. McMurry and O. Pensado for technical review and G. Wittmeyer for programmatic review. The authors also thank A. Ramos for support in report preparation and L. Mulverhill for editorial review.

QUALITY OF DATA, ANALYSES, AND CODE DEVELOPMENT

DATA: All CNWRA-generated original data contained in this report meet the quality assurance requirements described in the Geosciences and Engineering Division Quality Assurance Manual. Sources for other data should be consulted for determining the level of quality for those data. Scientific Notebook 1165E was used (Benke, 2013).

ANALYSES AND CODES: Scientific software MCNPX Version 2.6.0 was used in the analyses contained in this report.

REFERENCE

Benke, R. "Radiation Shielding Calculations for Dry Cask Monitoring." Scientific Notebook 1165E. San Antonio, Texas: Center for Nuclear Waste Regulatory Analyses. pp. 1–6. 2013.

EXECUTIVE SUMMARY

Spent nuclear fuel at a number of U.S. locations is maintained at independent spent fuel storage installations (ISFSIs) in dry cask storage systems (DCSSs). These systems commonly consist of a bolted cask or a welded austenitic stainless steel canister containing spent nuclear fuel. The welded canister is put in a larger concrete overpack or horizontal storage module that is vented to the external atmosphere to allow airflow cooling. A number of technical issues and data needs associated with extended storage of SNF have been identified in the U.S. Nuclear Regulatory Commission (NRC) gap assessment. Following direction from the Commission in SRM–COMSECY–10–0007, NRC staff identified and prioritized the technical information needs (NRC, 2014). Functional monitoring of environmental conditions to assess the condition of safety-significant structures, systems, and components (SSCs) was identified as one of the top priority, crosscutting issues. The purpose of this report is to evaluate the current state of technology for monitoring environmental conditions and the degradation of dry cask components to ensure the safe operation of DCSSs.

A broad literature review of monitoring techniques was conducted for important internal and external environmental conditions (temperature, humidity, chloride concentration, and microbes) affecting materials degradation process, as well as degradation features of welded canister materials, concrete overpacks, cask bolts, and cask internals. Overall, because of geometry, space limitations, and the high ionizing radiation of DCSSs, many of the monitoring methods must either be modified for this application, and all proposed monitoring methods would require testing and validating to assure that the sensors would not affect the performance of DCSS SSCs.

Technologies reviewed to monitor parameters of interest for DCSSs are summarized in Table ES–1 (external and internal environmental conditions, including temperature and relative humidity); Table ES–2 (chloride concentration and microbial activity for the external environment); Table ES–3 (internal pressure); and Table ES–4 (materials degradation inside and outside the system, including canister stress corrosion cracking and potential degradation of the concrete overpack, cask bolts, cladding, and other internal components). Although further assessment is necessary, a variety of techniques are potentially suitable for monitoring component degradation. They include sensors and monitoring methods that have been effectively deployed in nuclear applications as well as in non-nuclear applications, such as chemical process industries, manufacturing, or oil and gas production and refining. Substantial advancement in technology may be necessary for methods that are not presently designed or packaged for field use.

Temperature measurements are routinely performed in nuclear applications using nuclear qualified thermocouples and resistance temperature detectors (RTDs). Other methods for measuring temperature are available but would require significant advancement or development to overcome operational limitations such as (i) having a limited temperature tolerance or unknown radiation tolerance or (ii) requiring complex instrumentation and data analyses.

Table ES–1. Potential Monitoring Techniques for Temperature and Relative Humidity					
Parameter	**Monitoring Method**	**Level of Development**	**Strengths**	**Weaknesses**	**Report Section**
Temperature	Thermocouples	Field deployed for nuclear applications	High T and radiation tolerance	Calibration and drift, physical contact for surface temperature	2.1.1
				Penetration needed for internal use	3.2.1
	Resistance Temperature Detectors	Field deployed for nuclear applications	High T and radiation tolerance	Physical contact for surface temperature	2.1.2
				Penetration needed for internal use	3.2.1
	Radiation Thermometers	Field deployed for non-nuclear applications	Noncontact	Low temperature and radiation tolerance	2.1.3
				Window needed for internal use	3.2.1
	Ultrasonic Measurement	Field deployed for nuclear applications	Mature, high T tolerance	Low radiation tolerance	2.1.4
				Penetration or wireless transmission needed for internal use	3.2.1
	Fiber Optic Sensors	Field deployed for non-nuclear applications	Mature, high T tolerance	Radiation-induced darkening	2.1.5
				Penetration needed for internal use	3.2.1
	Semiconductor	Field deployed for non-nuclear applications	High sensitivity	Low T and radiation tolerance	2.1.6
				Not applicable for internal use	3.2.1
	Thermistors	Field deployed for non-nuclear applications	Small size, high radiation tolerance	Temperature tolerance	2.1.7
				Penetration needed for internal use	3.2.1
	Johnson Noise	Not commercially available	High T and radiation tolerance	Complex with advanced instrumentation necessary	2.1.8
				Penetration needed for internal use	3.2.1
	Bimetallic Sensor	Field deployed for non-nuclear applications	No penetration needed for internal use	Imaging system uncertain	3.2.2
	Pyrometric Cones, Thermoscope Bars	Field deployed for non-nuclear applications	No penetration needed for internal use	Imaging system uncertain	3.2.3

Table ES–1. Potential Monitoring Techniques for Temperature and Relative Humidity					
Parameter	**Monitoring Method**	**Level of Development**	**Strengths**	**Weaknesses**	**Report Section**
Relative Humidity	Ceramic-Capacitance-Based	Field deployed for non-nuclear applications	Small size	Frequent calibration	2.2.1.1
				Penetration needed for internal use	3.3
	Polymer-Capacitance-Based	Field deployed for non-nuclear applications	High precision, no hysteresis	Radiation-induced damage	2.2.1.2
				Radiation hardening and penetration needed for internal use	3.3
	Chilled-Mirror-Based	Field deployed for non-nuclear applications	High accuracy	Size modification	2.2.2
				Radiation hardening, wireless transmission needed for internal use	3.3
	Electrical Resistance-Based	Field deployed for non-nuclear applications	Small size, broad T range	Low precision	2.2.3
				Wireless transmission and internal power supply needed for internal use	3.3
	Fiber Optic Sensor	Limited commercial availability	Size, resistant to electromagnetic interference	Limited availability, unknown temperature and radiation tolerance	2.2.4
				Radiation hardening needed for internal use	3.3
	Leakage Monitoring Air Sampling	Field deployed in nuclear applications	Spatial humidity measurement	System sophistication, size and operational requirements	2.2.5
				Significant size reduction needed for internal use	3.3
	Psychrometer	Field deployed for nuclear applications	High accuracy and small size	Unknown temperature and radiation tolerance, requires water source	2.2.6
				Not applicable for internal use	3.3

Table ES–2. Potential Monitoring Techniques for Chloride and Microbial Activity					
Parameter	**Monitoring Method**	**Level of Development**	**Strengths**	**Weaknesses**	**Report Section**
Chloride	Conductivity-based	Field deployed for nuclear applications	Automated, no sealing needed	Limited to T<100 °C [212 °F], one-time use	2.3.1
	Long-period grating-based	Laboratory instrument	Potential real-time monitoring	Response sensitive to temperature changes	2.3.2
	Fluorescence-based optic	Laboratory instrument	Potential real-time monitoring	Other halide ions and oxygen may interfere	2.3.3
	High-electron mobility transistor-based	Laboratory instrument	Small size and sample volume	Temperature change interference	2.3.4
	Absorption spectroscopy	Trial field testing	Designed for field use, automated data acquisition	Limited information available	2.3.5
	Quantum dots	Under development	Can measure chloride concentration in small volumes of liquid	Limited information available	2.3.6
	Electrochemical sensors	Commercially available	Designed for field use, automated data acquisition	Limited information available	2.3.7
	Electromechanical sensors	Under development	Designed for field use	Limited information available	2.3.8
Microbial Activity	Electrochemical sensor	Field deployed for non-nuclear applications and limited use in nuclear applications	Field deployed, simple, rugged, automated, and provides real-time data	Unknown temperature and radiation tolerance	2.4.1
	Hydrogenase-based bioanalyzer	Field deployed for non-nuclear applications	Designed for field monitoring of microbes associated with microbially influenced corrosion	Limited to T<40 °C [104 °F]	2.4.2
	Sulfide oxidase-based biosensor	Concept	Real-time monitoring, provides assessment of corrosion and microbial activity	Unknown temperature and radiation tolerance, limited short-term laboratory testing	2.4.3
	Culturing methods	Field deployed for non-nuclear applications	Routinely used, formulations for specific microbes associated with microbially influenced corrosion	Requires sampling and long incubation periods	2.4.4

Table ES–3. Potential Monitoring Techniques for Internal Pressure					
Parameter	**Monitoring Method**	**Level of Development**	**Strengths**	**Weaknesses**	**Report Section**
Pressure	Bourdon tube pressure gauges	Field deployed for non-nuclear applications	Internal monitoring of components without penetration	Retrofit required	3.4.1
	Ball bearing strikes generated sound resonance spectra	Laboratory testing	Internal monitoring of components without penetration	Mechanical impact on canister	3.4.2
	Remote sensing of pressure transducer inside system	Laboratory testing	Internal monitoring of components without penetration	Retrofit required	3.4.3
	Booth-Cromer type, null balance pressure transducer	Old technology, laboratory testing	Continuous monitoring	Need electrical wires and cables	3.4.4
	Container material hoop strain-based embedded sensor	Field deployed for non-nuclear applications	In-service, nondestructive monitoring	Radiation interference	3.4.5
	Container material deflection-based measurement	Laboratory testing	Internal monitoring of components without penetration	Possible low sensitivity	3.4.6

Table ES–4. Potential Monitoring Techniques for Component Degradation Processes					
Component/Degradation	**Monitoring Method**	**Level of Development**	**Strengths**	**Weaknesses**	**Report Section**
Welded Canister Stress Corrosion Cracking	Fiber optic sensors	Field deployed for non-nuclear applications	High temperature tolerance, small size, corrosion resistant	Unknown radiation tolerance, may be difficult to install	2.5.1
	Luna crack growth sensor	Field deployed for non-nuclear applications	Sensitive to crack formation, can vary applied stress	Surrogate sensor, temperature sensitive, limited field use	2.5.2
	Crack propagation sensor	Not field deployed	Wide operational temperature range, small size	Modest resolution, little or no field testing, highly localized area monitored	2.5.3
Concrete Overpack/ Horizontal Storage Module Mechanical and Environmental Degradation	Embeddable corrosion sensors	Field deployed for non-nuclear applications	Real time, highly sensitive, wide temperature operation range	Concrete coring required, surrogate sensor for rebar corrosion	2.6.1
	External corrosion sensors	Field deployed for non-nuclear applications	Easy to operate, high sensitivity to rebar corrosion	Manual operation limited to outer surface layer assessment	2.6.2
	Ultrasonic pulse velocity	Field deployed for non-nuclear applications	No modification to structure required	Limited to outer surface layer assessment	2.6.3
	Acoustic emission	Field deployed for non-nuclear applications	Real time, no modification to system	Qualitative analysis, complex data, better for physical degradation processes	2.6.4
Bolts of Direct-Load Bolted Cask Corrosion, Stress Corrosion Cracking, and Mechanical Degradation	Ultrasonic testing	Field deployed for nuclear applications	Compatible in high radiation	Hardware not portable	2.7.1
	Multielectrode array sensor	Field deployed for non-nuclear applications	Small size, can be customized	Unknown temperature and radiation tolerance	2.7.2
	Electrochemical noise	Field deployed for non-nuclear applications	Small size, can be customized	Unknown temperature and radiation tolerance	2.7.3
	Electrical resistance probe	Field deployed for non-nuclear applications	Aqueous and nonaqueous environments	Sensitive to temperature, unknown longevity and radiation tolerance	2.7.4
	Acoustic emission	Field deployed for non-nuclear applications	Real-time monitoring	Only identifies active cracking	2.7.5
	Impedance-based *in situ*	Experimental	Real-time monitoring	Limited information available	2.7.6

Table ES–4. Potential Monitoring Techniques for Component Degradation Processes					
Component/Degradation	**Monitoring Method**	**Level of Development**	**Strengths**	**Weaknesses**	**Report Section**
Cladding and other internal components	Gamma-ray spectrometry for Kr-85	Feasibility assessed	Internal monitoring of components without penetration	Retrofit required	3.5.1
	Piezoelectric probes for speed of sound measurement	Proposed idea only	Small size and nondestructive examination of internal components	Require internal free space and significant release of the total noble gas inventory	3.5.2
	Gamma-ray radiography and computed tomographic imaging	Field deployed for non-nuclear applications	Nondestructive examination of internal components	Require significant modification to gamma-ray energies and emission intensities	3.5.3

Relative humidity measurements are used in leak detection systems in operating nuclear power plants. These systems have been developed with automated air sampling and analysis for the early identification of pressure boundary leaks. Although the instrumentation and methods have been demonstrated in operating nuclear power plants, the instrumentation is complex and not presently designed for portable field use. Relative humidity measurement using a psychrometer has been reported in nuclear applications. One potential drawback to use a psychrometer is the need to have water present in the environment where the measurement is conducted. Other methods to measure relative humidity are available but would require significant advancement or development to overcome operational limitations, such as low temperature tolerance and/or low or unknown radiation tolerance.

No suitable method was identified for detecting and monitoring of atmospheric deposition of solid chloride-containing salts that may lead to degradation of safety significant SSCs, such as welded stainless steel canisters used in the majority of DCSSs. Sample collection methods exist and have been previously attempted at an operating ISFSI, but these methods rely on manual collection of a sample and were not designed to be used in harsh environments with high temperatures and ionizing radiation. Sample analysis, accomplished by measuring the conductivity of the collected sample dissolved in water, can be subject to significant error, depending on the composition of the deposit. Other methods to measure chloride have significant limitations, such as low temperature and/or radiation tolerance or unknown radiation tolerance, or they are laboratory analytical methods designed for the analysis of solutions rather than solid salts.

Sensors to detect the onset of microbially-influenced corrosion have been developed and deployed in industrial service environments such as oil and gas, but these sensors are designed to be used in bulk liquid environments. Some sensors are temperature and/or radiation tolerance limited, under development, or designed for non-nuclear applications and rely on manual sample collection and culturing techniques.

Stress corrosion cracking sensors are limited. Surrogate sensors, which are an instrumented SCC coupon, have been developed for condition monitoring in field applications. Significant advancement and qualification testing would likely be necessary to use the sensor for DCSS monitoring. Other methods, such as fiber optic sensors or crack propagation sensors, have significant limitations (e.g., unknown temperature and radiation tolerances). Fiber optic sensors appear to be the only direct method of monitoring the actual component of interest. Implementation of this type of system would be challenging, given the temperatures and radiation near the canister surface. Such an application also would need to consider the possible detrimental effects of attaching a sensor to the canister surface.

Concrete degradation monitoring methods are well developed and have sufficient sensitivity to detect degradation before physical deterioration begins. However, these methods also have limitations, such as being labor intensive and limited to interrogation depths of 10 cm [4 in] or requiring access to the interior surfaces. Embeddable sensors have been developed and are commercially available; however, significant effort would be required to install these sensors in existing DCSSs. In addition, determining an optimized location for sensor placement may require analysis or knowledge of susceptible areas for degradation.

Methods are available to monitor cask bolts degradation including general and localized corrosion, stress corrosion cracking, and mechanical degradation. Ultrasonic testing has been field deployed for nuclear applications. Most other sensors have been deployed for non-nuclear

applications. The main limitation for some methods is the deployment difficulty. Modification of DCSS is needed and its effect on the system will require evaluation.

Monitoring the canister internal environment poses several challenges because of high temperatures, radiation, and accessibility difficulty. The sensors can be brought in contact with the internal environment by penetrating the confinement boundaries. Some methods require imaging or reading from outside using a “sight glass” or by using sensing techniques in which the cask is transparent. Current designs of storage canisters used in DCSSs do not include instrument penetrations or a sight glass. Any penetrations or instrumentation features would have to be designed and evaluated for confinement and leakage under normal, off-normal, and accident conditions. Methods to conduct internal monitoring also are limited. External gamma-ray spectrometry for Kr-85 monitoring in canister voids for cladding confinement integrity monitoring does not require physical penetration of sealed canisters and provides good sensitivity for detecting the loss of cladding confinement. A Bourdon tube pressure gauge for monitoring internal pressure through an external shield plug port could provide a direct measure of internal cask pressure without the need for a pressure boundary penetration. Significant analyses and tests would be necessary to qualify these methods. In addition, adverse effects, such as material incompatibility, would need to be rigorously evaluated.

1 INTRODUCTION

1.1 Background

The U.S. Department of Energy (DOE) ended development of a proposed geologic repository at Yucca Mountain, Nevada, for the disposal of spent nuclear fuel (SNF). The termination of the repository program and limited at-reactor pool capacity to store SNF necessitate continued use of dry storage of SNF until a permanent waste management solution is available. A number of technical issues and research and data needs associated with extended SNF storage, focusing on long-term aging issues important to the performance of the structures, systems, and components (SSCs) of the dry cask storage systems (DCSSs), have been identified in recent gap assessments by Savannah River National Laboratory (SRNL) (Sindelar, et al., 2011), DOE (Hanson, et al., 2012), the U.S. Nuclear Waste Technical Review Board (NWTRB) (NWTRB, 2010), and the Electric Power Research Institute's Extended Storage Collaboration Program (EPRI-ESCP) (EPRI, 2011).

The U.S. Nuclear Regulatory Commission (NRC) staff has developed a project plan for the Extended Storage and Transportation Regulatory Program Review (COMSECY–10–0007) to evaluate the adequacy of the existing regulatory framework for ensuring the safety and security of extended storage and transportation of SNF beyond 120 years. Following direction from the Commission in SRM–COMSECY–10–0007 (NRC, 2010a), NRC staff reconciled the technical information needs in recent gap assessments by SRNL, DOE, NWTRB, and EPRI-ESCP and prioritized them in NRC (2014), where functional monitoring was identified as one of the top priority, crosscutting areas that are significant in identifying potential degradation mechanisms of various dry cask components.

Because monitoring dry cask components to identify the onset of conditions conducive to component degradation could be essential in establishing inspection programs and maintenance schedules to assure safe storage of SNF over extended periods, evaluation of the present state of monitoring technology has been the subject of several NRC-sponsored projects. An NRC-sponsored survey of potential methods to monitor the long-term performance of DCSSs was reported by Argonne National Laboratory (ANL) (ANL, 2012). The methods evaluated include temperature measurements, surface inspection of components, monitoring cask/canister leak tightness, canister internal conditions, gamma-ray scanning, and inspection methods for concrete. Recently, NRC sponsored another project at Pacific Northwest National Laboratory (PNNL) to evaluate nondestructive examination methods for detecting stress corrosion cracking (SCC) of welded stainless steel canisters (Meyer, et al., 2013). The NRC-sponsored project presented in this report focuses on measurement methods that have not been used for DCSSs but appear to have the potential to be used. This project is intended to complement the evaluations conducted by ANL (2012) and PNNL (Meyer, et al., 2013).

Because the monitoring methods described in this report are not routinely used in DCSSs, the information and assessments presented must be viewed as preliminary. A number of technical issues must be evaluated prior to considering any sensor or monitoring system for DCSS application. At a minimum, the application of any type of sensor, detector, or monitoring system in a DCSS would require (i) consideration of calibration and established recalibration intervals based on the requirements or measurement accuracy and precision; (ii) sensor size and the dimensions of the DCSS; (iii) the effects of sensor placement on the required functions of the DCSS SSCs; (iv) the operating environment, which includes significant gamma and neutron radiation and elevated temperatures; (v) material compatibility; and (vi) the potential negative effects of sensor placement on the DCSS SSCs. These considerations should be addressed in

qualification tests and analyses performed under an acceptable quality assurance (QA) and maintenance plan and are outside the scope of this report.

The currently applicable regulatory requirements for DCSSs also are significant for sensor placement and monitoring systems. Most sensors for material or atmospheric condition monitoring require either electrical power and/or signal transmission; this is commonly achieved through electrical transmission via signal wires or transmission through optical fiber cables. Because sensor power and/or output transmission through electrical or optical fiber cables would require a connection to the sensor element, the routing of power and data transmission lines must be considered. For monitoring of environmental conditions and degradation to components inside DCSSs, current designs of storage canisters used in DCSSs do not include instrument penetrations, which would have to be designed and evaluated for confinement and leakage under normal, off-normal, and accident conditions. In the course of this literature review, several sensors were identified that do not require electrical or optical hardwired cables. Although no qualification and testing of the sensors has been performed for this application and a demonstrated means to obtain the data from such sensors has not been established, the possible use of these sensors for monitoring internal conditions is addressed.

1.2 Technical Information Needs of Dry Cask Storage System Structures, Systems, and Components

There are several DCSS designs; most can be grouped loosely into two main types based on how they are loaded: (i) direct-load bolted cask systems where SNF assemblies are loaded directly into a cask and (ii) canister-based systems where assemblies are loaded into a relatively thin-walled canister that is placed in a storage overpack or module (Hanson, et al., 2012). The overpack or module typically consists of a steel-lined and reinforced concrete cylinder that provides neutron and gamma shielding. The concrete thickness can be >59 cm [2 ft] (Hanson, et al., 2012). Some examples of direct-load bolted cask system designs include the General Nuclear Systems, Inc. CASTOR V/21, X/32, and X/33; the Transnuclear, Inc. (TN), series of casks (TN–24, 32, 32, 40, and 68); and the Westinghouse MC–10. Examples of canister-based systems include the Holtec International HI–STAR 100 and HI–STORM 100, the NAC International, Inc., NAC–MPC, NAC-UMS, and MAGNASTOR systems, and the TN NUHOMS System®.

Most DCSSs use canister-based systems (ANL, 2012), for which there are several design variations that merit discussion. The majority of canister-based designs emplace the canister vertically within the overpack structure, as shown in Figure 1-1 (NRC, 2012a). The welded stainless steel canister functions as the confinement boundary to retain the radioactive material under normal and accident conditions. Generally the gap between the canister and overpack of vertical systems is small. For the HI-STAR 100 system, the gap between the welded stainless steel canister and overpack is 1.59 cm [0.625 in] at the top and 0.476 cm [0.188 in] at the sides and there is no available space at the bottom based on the dimensions of the canister and overpack (Holtec International, 2009). The space above the canister lid for the HI-STORM 100 series storage modules ranges from 1.3 to 46 cm [0.5 to 18 in] depending on the variations of the overpack design (Meyer, et al., 2013). In addition, the gap between the canister and overpack at the sides is approximately 6.4 cm [2.5 in].

Some canister-based designs load and store the canister in a horizontal storage module (HSM), similar to that depicted in the generic schematic in Figure 1-2 (NRC, 2012a) for the TN NUHOMS System®. The gap between the canister and storage module for the

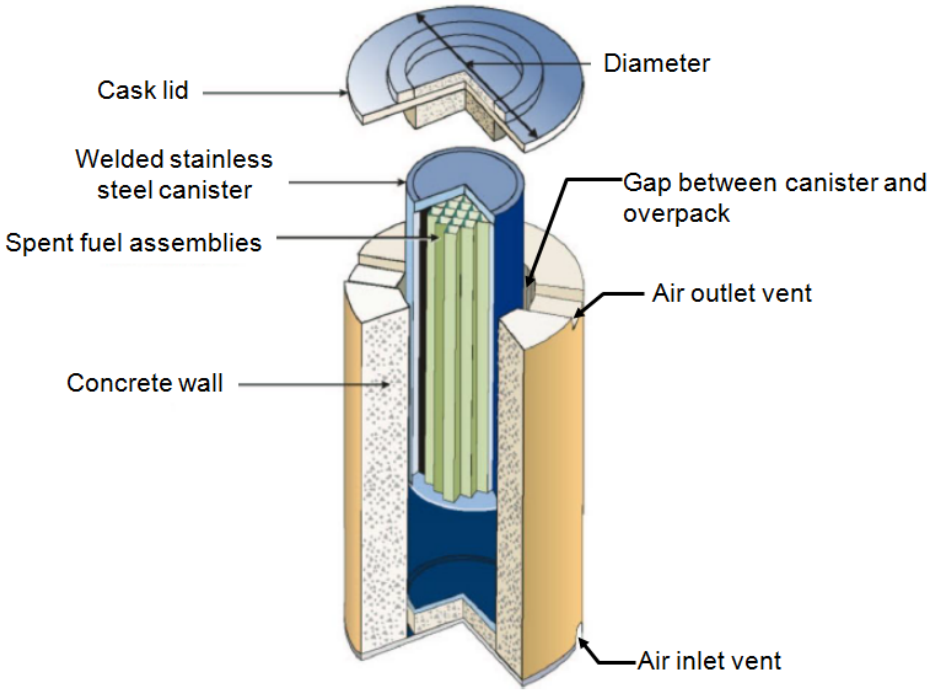

Figure 1-1. Schematics of Vertical Canister-Based System (NRC, 2012a)

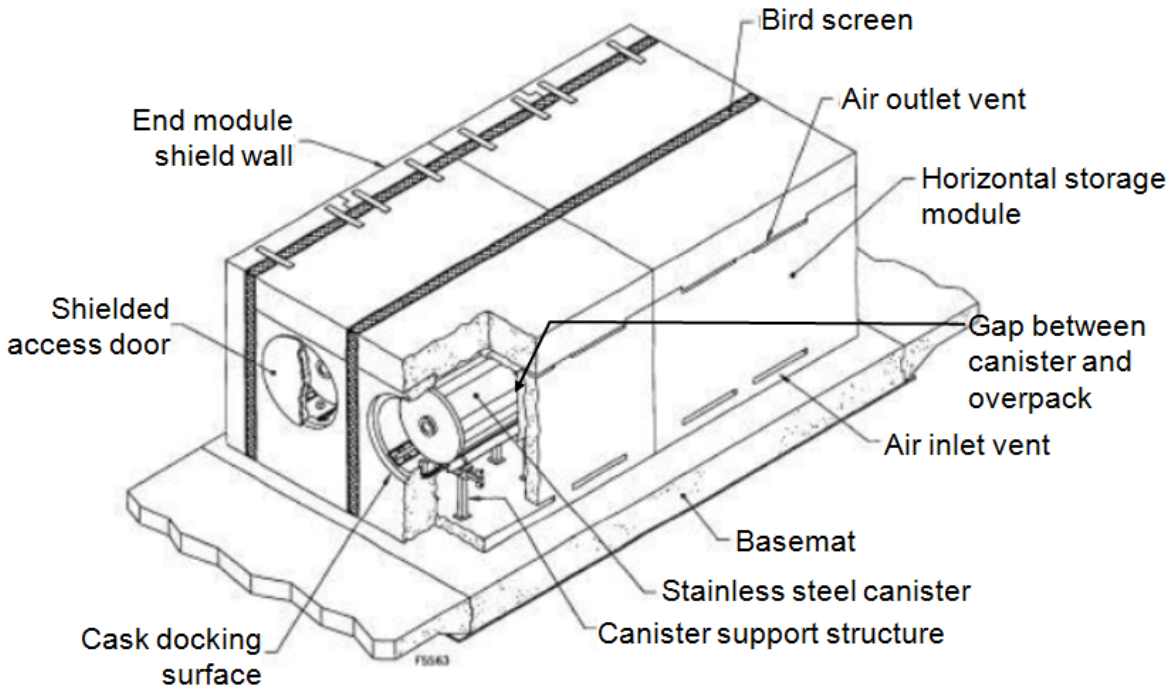

Figure 1-2. Schematics of Horizontal Canister-Based System (NRC, 2012a)

TN NUHOMS System® at the entrance is less than 2.54 cm [1 in], although an additional 10.16─101.6 cm [4─40 in] may be available inside the cross section of the storage module. Figure 1-2 also shows air inlet and outlet vents near the bottom and roof of the storage module that allow convective cooling by natural circulation. The vent opening is on the order of 15 cm [5.9 in] wide, which allows direct access to the external surface of the canister. Another design variation that has been introduced to reduce cask tip over during seismic events is the loading of canisters into below-grade vaults or modules.

Although the proportion of the direct-load bolted cask systems in the total population of DCSSs is dwindling, Chopra, et al. (2012) discuss several design variations with more detailed information than are noted here. Figure 1-3 shows a generic schematic of the TN-68 direct-load bolted cask system as one example. This cask system consists of the following components: (i) confinement vessel with bolted lid closure; (ii) basket for fuel assemblies, gamma and neutron shield; (iii) pressure/leak tightness monitoring system; (iv) weather cover; and (v) trunnions. In contrast to the canister-based designs, there is no concrete overpack or module around the circular cylinder cask body. The confinement boundary to retain the radioactive material under normal and accident conditions is commonly sealed via vessel closure from primary (inner) and secondary (outer) lids, which are fastened to the metal cask vessel using bolts and gaskets made from metallic or elastomeric materials. The entire closure system, including the seals and bolts, is important to confinement. The free space between the primary and secondary lids is evacuated and backfilled with helium and the helium pressure is monitored with instrumentation placed between the lid and the protective cover. The materials used for metallic cask vessels are typically nodular cast iron, carbon steel, low-alloy steel, and forged steel (NWTRB, 2010). Materials used for confinement lids include 304/304L SS, 193 Gr B7, 230 Gr L43, SB637 Gr N07718, SA 564, and Type 630 H1150 (NWTRB, 2010). Commonly used metallic gaskets are Inconel X730 spring, aluminum jacket, Nimonic 90 spring, Inconel X750, aluminum, and 304L SS. Commonly used elastomer gaskets are ethylene propylene copolymer, silicone rubber, propylene, Viton, and polytetrafluoroethylene (NWTRB, 2010). Cask closure lid bolt materials include stainless steels, low alloy steels, and nickel alloys.

Table 1-1 lists the technical information needs for NRC-identified Priorities 1 and 2 for the degradation of specific dry cask components covering both types of systems (NRC, 2014) and the parameters to be monitored. Some parameters are directly related to the degradation processes of the cask components of interest, and some parameters are related to the environmental conditions that may affect the extent of degradation (i.e., temperature, humidity, chloride ion, microbes). A broad literature review of monitoring techniques was conducted to address technical information needs with NRC-identified Priorities 1 and 2 (NRC, 2014) covering (i) internal and external environmental conditions (temperature, humidity, chloride concentration, microbes, and pressure) and (ii) degradation mechanisms affecting welded canister materials, the concrete overpack, cask bolts, SNF cladding, and other cask internal components. For cask internal environment and component degradation monitoring, priority for the investigation was given to monitoring techniques based on external measurements taken without cask or inner canister penetration and without the sensor installed inside the primary confinement boundary. This report covers most of the parameters presented in Table 1-1 in grey boxes. The parameters not covered in this report are noted in Table 1-1. The covered parameters will be specified in the following sections.

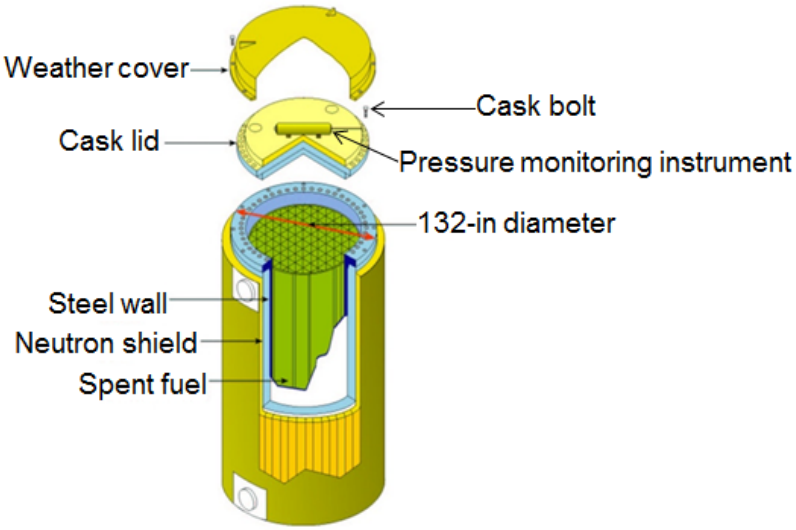

Figure 1-3. Schematics of Direct Load Bolted Cask System (NRC, 2012c)

Table 1-1. Technical Information Needs* and Monitoring Parameters

Components	Degradation Phenomena	Parameters That May Be Monitored
Fuel-Cladding Interactions	Fission gas release during accident	Fission gasses
	Helium release	Helium pressure†
	Pellet swelling	Cladding stress and geometry†
	Additional fuel fragmentation	Cladding stress, oxygen, and fission gasses†
Cladding	Galvanic corrosion	Humidity, water, oxygen
		Corrosion rate†
	Stress corrosion cracking	Humidity
		Cladding stress, oxygen, and crack growth rate, Xe, I, Cs, Kr†
	Delayed hydride cracking	Hydrogen, oxygen
		Cladding stress and crack growth rate†, Xe, I, Cs, Kr
	Low temperature creep	Cladding stress†
	Propagation of existing flaws	Cladding stress and crack growth rate†
Fuel Assembly Hardware and Damaged Fuel Cans	Metal fatigue caused by temperature fluctuations	Temperature variations
	Wet corrosion and stress corrosion cracking	Water, humidity
		Oxygen and crack growth rate†
Fuel Baskets	Weld embrittlement	Temperature, humidity, hydrogen
	Metal fatigue due to temperature fluctuations	Temperature variations
Neutron Absorber	Thermal aging effects	Temperature and humidity

Table 1-1. Technical Information Needs* and Monitoring Parameters		
Components	**Degradation Phenomena**	**Parameters That May Be Monitored**
Stainless Steel Canister Body and Weld	Atmospheric stress corrosion cracking	Temperature, humidity, chloride, crack growth rate
		Stress †
	Pitting	Temperature, humidity, chloride
		Deposited salts other than chloride and corrosion rate†
	Crevice corrosion	Temperature, humidity, chloride
		Deposited salts other than chloride and corrosion rate†
	Microbially influenced corrosion	Temperature, humidity, microbial activity, and corrosion rate
Concrete Overpack	Freeze-thaw, chemical attack (Cl^- or SO_4^{2-} induced), aggregate reactions/expansion, corrosion of embedded steel, leaching of $Ca(OH)_2$, settlement, creep, gamma/neutron irradiation, high temperature steel rebar corrosion, carbonation	Cracking, spalling, scaling, crazing, delaminations, popouts, voids, honeycombing, bug holes, staining, dusting, efflorescence, radiation fluence/dose, temperature, corrosion potential, surface potential/resistivity
Cask Bolts	Stress corrosion cracking, general corrosion, localized corrosion	Temperature, humidity, chloride, and crack growth rate
		Deposited salts other than chloride†
	Embrittlement	Temperature and humidity
	Thermal mechanical degradation	Temperature, temperature variations
		Dimensional change and crack initiation†
Steel, Cast Iron Body, Welds, Lids, and Seals	Microbially influenced corrosion	Temperature, humidity, microbial activity, and corrosion rate

*NRC. "Identification and Prioritization of the Technical Information Needs Affecting Potential Regulation of Extended Storage and Transportation of Spent Nuclear Fuel." ML14043A423. Washington, DC: U.S. Nuclear Regulatory Commission. 2012.
†Not reviewed

1.3 Objectives and Organization of the Report

The objective of this NRC-sponsored project is to provide NRC reviewers with a tool to evaluate the potential success of a monitoring technique suggested by an applicant in an aging management program by (i) reviewing and assessing existing monitoring technologies that have not yet been used for DCSSs, but are applicable to monitoring degradation of dry cask components; and (ii) identifying possible advances for future monitoring technology development and deployment. The results of this project may be used to support the development of regulatory guidance, including the technical basis for monitoring requirements and evaluation of proposed industry actions. The monitoring techniques included in this review and assessment were prioritized to address these technical information needs for both existing and new DCSSs.

This report is organized into four chapters, including an introduction and the technical information needs that are presented in Chapter 1. The reviewed and assessed monitoring

techniques potentially applicable for existing or new DCSSs are categorized by the parameters being monitored and are organized into two chapters: Chapter 2 describes monitoring of the external environment and degradation of external components, and Chapter 3 details monitoring of the internal environment and degradation of internal components. Chapter 2 has seven sections: (i) temperature, (ii) humidity, (iii) chloride ion, (iv) microbially influenced corrosion, (v) SCC of the welded stainless steel canister, (vi) concrete overpack degradation, and (vii) cask bolt degradation. Chapter 3 has five sections: (i) internal monitoring challenges, (ii) temperature, (iii) humidity, (iv) pressure, and (v) cladding confinement and other internal components. A table summarizing the key features of the applicable techniques is provided in each section in Chapters 2 and 3. A summary of potentially applicable techniques is included in Chapter 4. The radiation levels inside and outside casks and the materials radiation tolerance are used as supporting information to determine the radiation tolerance of monitoring techniques, these are documented in Appendix A.

2 TECHNIQUES FOR FUNCTIONAL MONITORING OF EXTERNAL ENVIRONMENTS AND DEGRADATION OF COMPONENTS OUTSIDE THE CONFINEMENT BOUNDARY

Dry cask storage systems (DCSSs) have vents in the shielding structure to allow airflow around the canister for convective cooling. Thus, the canister may, to a certain extent, be exposed to the ambient environmental conditions of the site where the independent spent fuel storage installation (ISFSI) is located, including temperature, humidity variations, and airborne particulates that vary in composition depending on their source and origin. In evaluating the DCSS designs, a scenario has been identified whereby airborne salts could enter through the vents and deposit on the canister surface. A brine could then form by the process of deliquescence, in which salt absorbs water vapor from air to form a saturated aqueous solution. Deliquescence takes place when the ambient relative humidity (RH) is greater than the thermodynamic equilibrium RH for the saturated salt solution, referred to as the deliquescence relative humidity (DRH). The reverse process is called efflorescence and involves the loss of water from the aqueous solution and resulting in salt precipitation when the ambient RH is below the thermodynamic equilibrium RH for the saturated salt solution. Deliquescence of chloride salts on the canister surface could lead to a condition of susceptibility known as stress corrosion cracking (SCC), particularly for austenitic stainless steel exposed to chloride-rich salts. Steel, the cast iron body, and the welds and seals of the DCSS may be susceptible to microbially-influenced corrosion (MIC) at RH values above the DRH of deposited salts.

This chapter summarizes the reviewed and assessed techniques for monitoring the most significant external environmental conditions (temperature, humidity, chloride concentration, and microbes) and degradation of components outside the confinement boundary. The potentially applicable techniques for existing or new DCSSs are categorized by the parameters being monitored and are organized into the following seven sections: (i) temperature, (ii) humidity, (iii) chloride ion, (iv) MIC, (v) SCC of the welded stainless steel canister, (vi) concrete overpack degradation, and (vii) cask bolt degradation. A table summarizing the key features of the applicable techniques is provided in each section. Details of the sensor capabilities, operational requirements, advantages, and limitations are provided for each sensor or indicator. Based on an assessment of the information available for each sensor or monitoring method, potential applications for DCSSs are described along with a listing of the unknowns for each application.

To backfit existing DCSSs that were not originally designed to have sensors or condition monitors would require extensive analyses, testing, and planning to assure that the sensors or monitors are functional while not degrading or interfering with the function of the DCSS SSCs. In addition, the radiation exposure of personnel needs to be considered when obtaining data and during the initial placement, maintenance, repair, and replacement of the sensors and monitors. Although it is understood that these are significant issues that require additional study, the challenges and complexities of backfitting the identified sensors and monitoring methods to DCSSs are not addressed in this report.

2.1 Temperature Monitoring

As indicated in Table 1-1, temperature is one parameter that may be monitored to assess degradation of welded canisters and bolted casks. Temperatures of the canisters, overpacks, and concrete horizontal storage modules (HSMs) are expected to decrease from 200 °C [392 °F] to ambient and will vary, depending on the location of the ISFSI facility, loading age, DCSS design, and spatial position within the DCSS. Numerous methods have been developed

to measure temperature because it is an important parameter for many industrial and manufacturing operations. Several methods for measuring temperature have been utilized in nuclear applications. The U.S. Nuclear Regulatory Commission (NRC)-sponsored study mentioned in Section 1.1 (ANL, 2012) assessed type N thermocouples, Johnson noise thermometers, ultrasonic temperature sensors, Fabry-Perot fiber optic temperatures sensors, and thermal imaging. The present work reviews temperature measurement methods that may be of interest for monitoring a DCSS, including sensors that may be considered for measuring the temperatures both at the canister surface and inside the cask. This section focuses on the external temperature monitoring techniques, including (i) thermocouples, (ii) resistance temperature detectors, (iii) radiation thermometers, (iv) ultrasonic measurement, (v) fiber optic sensors, (vi) semiconductor temperature sensors, (vii) thermistors, and (viii) Johnson noise thermometers. Bimetallic sensors, pyrometric cones, and thermoscope bars are considered for internal temperature monitoring in Section 3.1, and although these types of sensors also could be considered for external temperature monitoring, given the many other options available for external temperature measurement, it is unlikely that these more specialized sensors would be a preferred choice for external temperature monitoring.

The main features of these techniques are summarized in Table 2-1 and are described in more detail in the subsequent sections. Note that Table 2-1 is a compilation of general information for each type of sensor. Actual specifications that the manufacturer determines and reports may differ somewhat from the typical values shown in Table 2-1. Also, note that measuring air temperature of an ISFSI site is not addressed in this report because the air temperature can be readily and reliably measured by using many commercially available sensors.

2.1.1 Thermocouples

Measurement Principle

A thermocouple consists of a junction of two wires of dissimilar materials, usually metal alloys, that produces a voltage at its terminals proportional to the temperature of the junction (e.g., Figure 2-1) (Watlow, 2013; Texas Instruments Incorporated, 2013; Michalski, et al., 2001). The thermocouple is placed in physical contact with the component or structure whose temperature is to be measured. External data acquisition equipment or devices are required to measure the voltage present at the terminals of a thermocouple.

Maturity

Thermocouples are rugged sensors that have been used for many years in industrial applications and in a wide range of nuclear applications where tolerance to high radiation is required. ASTM International Specification E235 describes the requirements for Type K and Type N thermocouples for nuclear or other high reliability applications (ASTM International, 2012a). Thermocouples are commercially available that meet the requirements (IEEE, 2003, IEEE 323) for safety-related electric equipment located in harsh environments and for certain post-accident monitoring equipment.

Measurement Range, Sensitivity, and Longevity

Thermocouple type, identified by a letter designation, indicates the type of materials that compose the junction and also dictates the measurement range. The temperature ranges and

Table 2-1. Temperature Monitoring Sensors				
Features	**Thermocouples (Section 2.1.1)**	**Resistance Temperature Detectors (Section 2.1.2)**	**Radiation Thermometers (Section 2.1.3)**	**Ultrasonic Measurement (Section 2.1.4)**
Maturity	Field deployed in nuclear applications	Field deployed in nuclear applications	Field deployed in non-nuclear applications	Field deployed in nuclear applications
Measurement Ranges	−270 to 1,480 °C [−454 to 2,700 °F]	−200 to 650 °C [−328 to 1,202 °F]	Typically −50 to 825 °C [−58 to 1,517 °F], device tolerance: 40–70 °C [104–158 °F]	20 to 2,500 °C [68 to 4,532 °F]
Sensitivity	Temperature and thermocouple type dependent, ~3 °C [5 °F] for Type K or N at 400 °C [752 °F]	Temperature and device dependent, ~1.9 °C [3.5 °F] at 400 °C [752 °F]	~ 0.1 °C [0.2 °F]	Temperature and system dependent, can be ~0.001 °C [0.002 °F]
Longevity	Decades	Decades	Years	Unknown
Space Requirements	Typically 3–6 mm [0.125–.250 in] diameter × 10 mm [3.9 in] length, various sizes available	Typically 3–6 mm [0.125–0.250 in] diameter × 10 mm [3.9 in] length, various sizes available	1,000 cm^3 [61 in^3]; 10 cm [3.9 in] L × 10 cm [3.9 in] W × 10 cm [3.9 in] H	200–2,000 cm^3 [12.2–122 in^3]; diameter of measuring wire <1 mm [39 mils]
Power Requirements	On the order of 10–20 watts	On the order of 10–20 watts	On the order of 20–100 watts	On the order of 20–100 watts
Monitoring Area	Point at surface contact or immediate surrounding when immersed	Point at surface contact or immediate surrounding when immersed	Surface area in direct field of view	Integral portion of the measuring medium
Data Acquisition Mode	Continuous or intermittent	Continuous or intermittent	Continuous or intermittent	Continuous or intermittent
Radiation Tolerance	Commercially available sensors with reported tolerance of 300 Mrads TID	Commercially available sensors with reported tolerance of 300 Mrads TID	Unknown	Not specified, but likely high
Strengths	Mature, small size, high-temperature and radiation tolerance, long lifetime	Mature, small size, high-temperature and radiation tolerance, long lifetime	Mature technique, noncontact method, wireless	High temperature tolerance
Weaknesses	Requires signal cable, good thermal bonds are essential for surface temperature measurements	Requires signal cable, good thermal bonds are essential for surface temperature measurements	Low temperature range, likely low radiation tolerance of instrumentation, emissivity of surface must be known	Systems with high radiation tolerance still under development, complex compared to other sensors

Table 2-1. Temperature Monitoring Sensors				
Features	**Fiber Optic Temperature Sensors (Section 2.1.5)**	**Semiconductor Temperature Sensors (Section 2.1.6)**	**Thermistors (Section 2.1.7)**	**Johnson Noise Thermometers (Section 2.1.8)**
Maturity	Field deployed in non-nuclear applications	Field deployed in non-nuclear applications	Field deployed in non-nuclear applications	Not commercially available but has been used in nuclear applications
Temperature Measurement Ranges	−50 to 2,000 °C [−58 to 3,632 °F]	−55 to 150 °C [−58 to 302 °F]	−196 to 300 °C [−320 to 572 °F]. Some can be up to 600 °C [11,112 °F].	Not available but has been used up to 1,500 °C [2,732 °F]
Sensitivity	Temperature and system dependent, can be ~0.1 °C [0.2 °F]	0.5 °C [1.0 °F]	0.5 °C [1.0 °F]	Not available
Longevity	Years—Decades	Years	Years	Not available
Space Requirements	2,000 cm^3 [122 in^3]; diameter of optical fibers <5 mm [197 mils]	3 × 3 × 2 mm [0.25 × 0.25 × 0.2 in]	0.8 mm diameter × 1.6 mm length [0.032 in diameter × 0.064 in length]	Not available
Power Requirements	On the order of 20–100 watts	~2 watts	0.1 watts	Not available
Monitoring Area	Direct thermal contact with the optical fiber	Immediate surroundings	Immediate surroundings or surface contact	Not available
Data Acquisition Mode	Continuous or intermittent	Continuous or intermittent	Continuous or intermittent	Not available
Radiation Tolerance	Commercial systems up to 98 Mrads and 2.4 × 10^{16} n/cm^2	Unknown, no radiation-hardened devices located	Not available, but devices are marketed for harsh environments including nuclear radiation	Not available, used for in-pile measurements with high neutron and gamma radiation
Strengths	High-temperature and moderate radiation tolerance, less susceptible to electromagnetic interference	Small sensor, low power requirements, easily integrated into circuits	Small sensor, low power requirements, designed for harsh environments	Fundamental measurement of temperature, low drift
Weaknesses	Potential fiber darkening and embrittlement, complex compared to other sensors	Limited temperature range and easily damaged at elevated temperatures, likely low radiation tolerance	Low temperature tolerance, radiation tolerance not defined	Not commercially available, complex instrumentation necessary

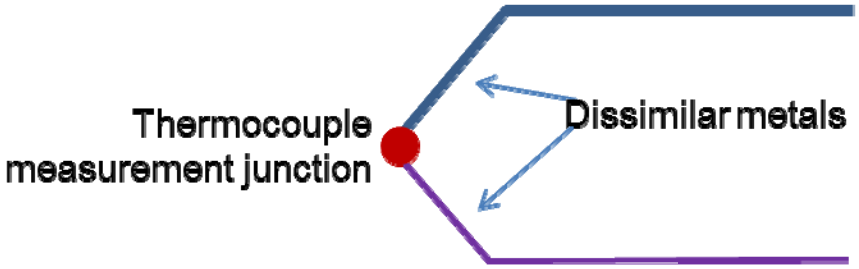

Figure 2-1. Schematics of Thermocouple Measurement Junction

sensitivities of thermocouple types also are well characterized (Table 2-2). Note the upper temperature limit for thermocouples depends on both the type of thermocouple and the thermocouple wire diameter. However, the diameter of the thermocouple is variable and involves a tradeoff between sensitivity, longevity, and response time (Burns and Scroger, 1989).

In general, larger diameter thermocouples have greater longevity but longer response times. Thermocouple sensitivity is based on the Seebeck coefficient of the materials used to make the thermocouple junction. The electromotive force (EMF)–temperature relationship is a nonlinear function of temperature that is unique for each thermocouple junction (Burns and Scroger, 1989). The measurement sensitivity is dependent on the thermocouple junction, instrumentation sensitivity, and temperature. For commonly used Type K and Type N thermocouples, the measurement tolerance is the greater of 2.2 °C [4.0 °F] or 0.75 percent over the temperature range from 0 to 1,260 °C [32 to 2,300 °F] (ASTM International, 2012b). Thermocouples can have lifetimes for years to decades but are subject to long-term drift, which requires recalibration, and a nonlinear response of many degrees over an operating temperature range requires compensation to be applied in the measurement circuitry.

Space and Power Requirements

Diameters of standard thermocouples range from 0.1 to 6.5 mm [3.9 to 256 mils]. The sensing element of the thermocouple is approximately 10 mm [394 mils] long, although the cable extending from it can be much longer. The space requirement of thermocouples is less than 5 cm^3 [0.3 in^3]. Specialized thermocouples are available that are designed to be attached to components for surface temperature measurements. Attachment to surfaces has been accomplished by several means including adhesives, spring-loaded fixtures, and mechanical clamps. The use of attached thermocouples to measure surface temperatures where a significant temperature gradient exists (e.g., a heat transfer surface) may require qualification to assure that the measured temperatures accurately reflect the measurement of interest.

The thermocouple cable is connected to external data acquisition equipment or devices mostly powered by battery. The power required to measure temperatures using thermocouples depends on the power requirements of the measurement circuitry and any compensation circuitry, if present. The interval between measurements affects the power requirements, in that the more frequent the sampling, the greater the power requirements.

Monitoring Area and Data Acquisition

A thermocouple may be used to measure the temperature of the air surrounding the junction, or it may be configured to measure the temperature of an object or structure. To accurately measure the temperature of an object or structure, the thermocouple must have a strong

Table 2-2. Temperature Range of Various Types of Thermocouples*		
Junction Type	**Temperature Range (°C) [°F]**	**Suggested Maximum Temperature (°C) [°F]**
E	−270 to 1,000 [−454 to 1,832]	870 [1,600]
J	0 to 760 [32 to 1,400]	750 [1,382]
K	−270 to 1,372 [−454 to 2,500]	1,260 [2,300]
R	−50 to 1,768 [−58 to 3,214]	1,480 [2,700]
N	−270 and 1,300 [−454 to 2,372]	1,260 [2,300]
*ASTM. "Standard Specification and Temperature-Electromotive Force (emf) Tables for Standardized Thermocouples." Designation E230. West Conshohocken, Pennsylvania: ASTM International. 2012.		

thermal bond at the point of measurement. If a thermal bond is not established or is broken after being made, the temperature measured will represent the air temperature immediately surrounding the junction. Data from thermocouple measurements are typically stored in an electronic data acquisition file that records temperature at specified time intervals. Both continuous and intermittent data acquisitions are possible using thermocouples. Numerous data acquisition systems are commercially available, ranging from systems that have multiple thermocouple inputs to portable, battery operated data acquisition systems, allowing data acquisition to be performed over a period of time and at multiple locations as a function of time and position.

Temperature and Radiation Tolerance

Thermocouples are available for a wide range of operating temperatures. Table 2-2 provides an overview of various thermocouple types and their associated temperature ranges and sensitivities. Most commonly used thermocouple types have temperature tolerance that exceeds the range of expected temperature ranges for DCSSs. Thermocouples qualified to the requirements of IEEE (2003, IEEE-323) have been reported to have a radiation tolerance of 300 Mrads (Weed Instrument Company, 1999). The data acquisition equipment would generally have far higher radiation susceptibility than the thermocouple itself and would need to be sufficiently shielded or placed at a safe distance from the high-radiation environment. Thermocouple lead cables could be made to allow the more radiation sensitive instrumentation and data acquisition system to be placed in a less aggressive environment than the thermocouple itself.

Strengths and Weaknesses

Strengths of thermocouples are their small size, high-temperature and radiation tolerance, and long lifetimes. Thermocouples are robust and have been used in a variety of aggressive environments, and thermocouples meeting the requirements of IEEE (2003, IEEE-323) are readily available in a variety of configurations.

Weaknesses of thermocouples include that they are subject to drift and periodic recalibration, which is usually required to ensure measurement accuracy. Also, high quality thermal bonds are essential to minimize measurement error for surface temperature measurements.

Potential DCSS Use

Thermocouples are capable of measuring temperatures in the ranges expected for DCSSs. Their small size, relative ease of deployment, and high radiation tolerance may be

advantageous for the measurement of air temperatures of new or existing DCSSs. Commercially available thermocouples are available that are physically small enough to fit in the gap between the canister and overpack for the measurement of the air temperature in close proximity to the canister.

External surface temperature monitoring would require a reliable thermal contact between the thermocouple and the canister surface. There are numerous commercially available thermocouples designed for surface temperature measurement, including spring-mounted contacts, adhesive mounts, and clamping systems. While such systems exist and have been routinely utilized in commercial applications, deployment in either existing or new DCSSs would require considerable effort to verify reliable operation. Thermocouples require a cable connection to a thermocouple instrument to calculate temperature from the measured potential of the thermocouple junction. Typical thermocouple instrumentation and the associated data acquisition systems usually are not radiation tolerant and would need to be shielded to avoid damage.

Unknowns

- The extent of DCSS modification and preparation required to obtain accurate surface temperature measurements on existing systems that were not designed to have temperature monitoring.
- Effects of oxides and accumulated atmospheric deposits on surface temperature measurements.
- Reliability and replacement difficulty of thermocouples for DCSS surface temperature measurements.
- Effects of neutron and gamma radiation on drift.

2.1.2 Resistance Temperature Detectors

Measurement Principle

A resistance temperature detector (RTD) contains a wire of a single metallic material whose resistance varies in a predictable way with its temperature, as shown in Figure 2-2. A data acquisition device can apply a known voltage (V), measure the resulting current (I), and then calculate the equivalent resistance (R) using Ohm's Law (V = I*R). The conversion of measured resistance to temperature is straightforward because the resistance-temperature curve for an RTD is nearly linear and any nonlinearity is highly predictable and repeatable. RTDs can be used across a wide operating range. Higher currents through the device can lead to significant self-heating and can result in erroneous temperature measurements. In general, it is best to minimize power usage and self-heating effects by only energizing the device while taking a measurement. As in the case for thermocouples, RTDs require external data acquisition devices, with their accompanying radiation susceptibilities, to measure the resistance of the sensor (Texas Instruments Incorporated, 2013).

The sensitive portion of an RTD, called an element, is usually a coil of small-diameter, high-purity wire such as platinum, copper, or nickel. Thin-film elements also are used, where a thin film of platinum is deposited onto a ceramic substrate. Platinum is a common choice for RTD sensors because it is known for its long-term stability at high temperatures.

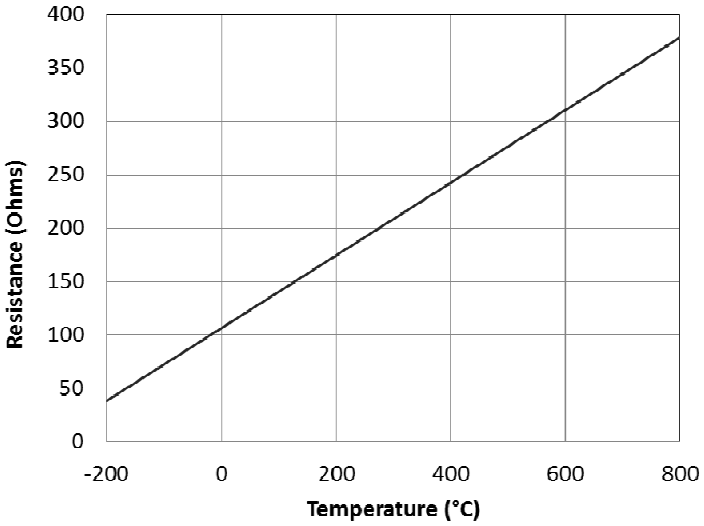

Figure 2-2. Resistance Temperature Detector Resistance Versus Temperature (Texas Instruments Incorporated, 2013)

Maturity

RTDs are rugged sensors that have been used for many years in industrial applications and in a wide range of nuclear applications where tolerance to high radiation is required. RTD applications are commercially available that meet the requirements of IEEE (2003, IEEE 323) for safety-related electric equipment located in harsh environments and for certain post-accident monitoring equipment (Weed Instrument Company, 1997).

Measurement Range, Sensitivity, and Longevity

RTDs can be used across a wide operating range from approximately −200 to +650 °C [−392 to 1,202 °F] (ASTM, 2012c). The sensitivity of platinum RTD is 0.385 Ω/Ω/°C. Nickel and copper RTDs have higher sensitivities but are limited to lower temperatures. Platinum RTDs have a stated accuracy of 0.1 °C [0.2 °F] or better (Stephenson, et al., 1999). Longevity is a function of temperature, especially at elevated temperatures. At temperatures below 400 °C [752 °F], contamination and drift of platinum RTDs are not significant concerns. Industrial RTDs rated to 480 °C [896 °F] have advertised drifts of 0.56 °C [1 °F] over 40 years. At temperatures above 500 °C [932 °F], drift can be as large as several degrees per year.

Space and Power Requirements

Space and power requirements for RTDs are generally similar to thermocouples. RTD elements are available in a variety of sizes and have been tailored to specialized measurements, such as air temperature, immersions in liquids such as oil, and surface temperature measurements. General purpose RTDs are available in diameters ranging from 3 to 6 mm [0.125 to 0.250 in], with various lengths available. Surface mount systems are available in a variety of sizes, but surface mount probes for industrial applications are typically larger than general surface probes. Mounting options include spring, adhesive threaded, and bolt on systems.

Power requirements for RTDs are low and are dominated by the data acquisition systems. The power requirements depend on the number of sensor inputs and the frequency of measurements. Data acquisition systems are available that operate on AC or DC power.

Monitoring Area and Data Acquisition

The monitoring area and data acquisition for RTDs are similar to those of thermocouples and have the same requirements for thermal bonding in order to be used to measure surface temperature. Data from RTD measurements are typically stored in an electronic data acquisition file that records temperature at specified time intervals. The amount of data accumulated during monitoring is dependent on the measurement frequency. Small, rugged, submersible, self-contained, and battery operated data acquisition loggers that are designed to be used in harsh environments are commercially available. These systems can log data for a period of up to a year at a rate of one point per hour.

Typically, data acquisition is performed over a period of time and at multiple locations. Data acquisition systems for RTDs are similar to those used for thermocouples. Systems are commercially available that can take both RTD and thermocouple inputs. Both continuous and intermittent data acquisitions are possible. Numerous data acquisition systems are commercially available, ranging from systems that have multiple inputs to portable, battery operated data acquisition systems. Small, rugged, submersible, self-contained data acquisition loggers are available that are designed to be used in harsh environments. These systems are typically battery operated but can record data for up to a year at the rate of one point per hour.

Temperature and Radiation Tolerance

Nickel RTDs are limited to temperatures below 300 °C [572 °F], as a result of nonlinear behavior at elevated temperatures. Copper has slightly greater sensitivity but also is limited to temperatures below 150 °C [302 °F]. At higher temperatures, copper RTDs have significant oxidation that degrades performance (Stephenson, et al., 1999). Platinum RTDs can operate at temperatures up to 660 °C [1,220 °F] (Wilkins and Evans, 2005), but the stability and accuracy at temperatures above 500 °C [932 °F] are significantly diminished. Commercially available RTDs for nuclear applications are available that can operate at temperatures up to 482 °C [900 °F] and 300 Mrads total integrated dose.

Strengths and Weaknesses

Strengths of RTDs are similar to thermocouples. They are small in size, have high-temperature and radiation tolerance, and have long lifetimes. RTDs are robust and have been used in a variety of aggressive environments, and RTDs meeting the requirements of IEEE (2003, IEEE-323) are readily available in a variety of configurations.

Weaknesses also are similar to those noted for thermocouples. RTDs are subject to drift, and periodic recalibration is usually required to ensure measurement accuracy. For surface temperature measurements, high quality thermal bonds are essential to minimize measurement error. Compared to thermocouples, RTDs have a more limited measurement range but greater accuracy.

Potential DCSS Use

RTDs are capable of measuring temperatures in the ranges expected for DCSSs. Their small size, relative ease of deployment, and high radiation tolerance may be advantageous for the measurement of air temperatures of new or existing DCSSs. Commercially available RTDs are available that are physically small enough to fit in the gap between the canister and overpack for the measurement of the air temperature in close proximity to the canister.

External surface temperature monitoring would require a reliable thermal contact between the RTD and the canister surface. Commercially available RTDs for surface temperature measurement are available. Although such systems exist and have been routinely utilized in commercial applications, deployment in either existing or new DCSSs would require considerable effort to verify reliable operation. Replacement difficulty is similar to thermocouples and is dependent on the intended application. Replacement of an RTD measuring the temperature of the air space between the canister and an overpack would not be easy, but depending on the probe location and DCSS design, it may be possible to replace a probe remotely and thereby significantly reduce worker dose. Replacement of a surface-mounted probe would prove to be more difficult because of the challenges associated with securing the probe and making an adequate thermal contact of the probe to the surface.

RTDs require a cable connection to an instrument to calculate temperature from the measured resistance. Typical RTD instrumentation, which is similar to that used for thermocouples, and the associated data acquisition systems are usually not radiation tolerant and would need to be shielded to avoid damage.

Unknowns

- Dry cask system modification and preparation required to obtain accurate surface temperature measurements on existing systems that were not designed to have temperature monitoring.
- Effects of oxides and accumulated atmospheric deposits on surface temperature measurements.
- Reliability and replacement difficulty of RTDs for DCSS surface temperature measurements.
- Effects of neutron and gamma radiation on drift.

2.1.3 Radiation Thermometers

Measurement Principle

Radiation thermometers measure a portion of the thermal radiation emitted by the object being measured (Ng and Fralick, 2001; Olinger, et al., 2007; Michalski, et al., 2001). Optical pyrometers, infrared thermometers, and radio-frequency-based thermal radiation measurements are examples of this class of instruments. Although they may differ in the specific frequency bands of thermal radiation that the device uses to measure temperature, the techniques can be considered as a group for the purposes of this evaluation. Computing the temperature of a device under test conditions requires a line-of-sight measurement of the emitted thermal radiation and an estimated or known value of the object's emissivity. For some radiation

thermometers, the emissivity of the object under examination is configured via keypad or user display. In these cases, the device internally calculates the conversion and provides a temperature readout of the object.

Maturity

Radiation thermometers of all types are mature instruments that have been widely deployed in non-nuclear industrial environments. Commercially available radiation thermometers are available that span various temperature ranges. At present, there are no known uses of radiation thermometers as temperature sensors in gamma and neutron radiation environments similar to those expected in DCSSs.

Measurement Range, Sensitivity, and Longevity

Radiation thermometers are available that cover a variety of temperature ranges. A number of manufacturers produce commercially available infrared thermometer systems that can measure temperatures between −50 and 825 °C [−58 and 1,517 °F], but higher temperature models are available that can measure temperatures up to 1,800 °C [3,252 °F]. The sensitivity of radiation thermometers can be on the order of 0.1 °C [0.2 °F]. In industrial environments, radiation thermometers can reliably operate for years.

Space and Power Requirements

The size of these devices varies, and technological advances continue to reduce the size, weight, and power requirements. In general, the size and battery life of the device is similar to that of a mid-range video camera (about 2–6 hours for portable systems). The space requirement of radiation thermometers is on the order of 1,000 cm^3 [61 in^3] or 10 cm × 10 cm × 10 cm [3.9 in × 3.9 in × 3.9 in]. Systems also are available that operate exclusively from 110 V AC power.

Monitoring Area and Data Acquisition

The monitoring area of a radiation thermometer is dependent on the field of view of the sensor. For many sensors, the field of view is similar to that of a camera, while others obtain data from a small area identified by a laser sight or pointer. The temperature at any given point can be reduced to a single number. The data acquisition mode of some devices in this class of instruments is similar to a video camera. However, whereas a video camera collects radiation in the visible spectrum, these devices are sensitive to other frequency bands and, like a camera, provide temperature measurements at many points within the field of view. Other devices of this class measure the thermal radiation at only a very small point. Both continuous and intermittent data acquisitions are possible.

Temperature and Radiation Tolerance

Although radiation thermometers are available to measure very high temperatures {greater than 1,000 °C [1,832 °F]}, the devices themselves contain semiconductor components that are generally limited to temperatures less than 40–70 °C [104–158 °F]. Similarly, although the exact maximum total integrated permissible dose for these classes of devices is unknown, commercial off–the–shelf radiation thermometers are likely to exhibit high-radiation sensitivity due to extensive use of semiconductors and electronics that are not radiation hardened.

Strengths and Weaknesses

The strengths of radiation thermometry include its being a mature technique that has been widely deployed in many industrial environments. The noncontact nature of the approach, coupled with the standoff distances possible with some devices, can, at least partially, mitigate some of the drawbacks of the devices, such as low temperature tolerances of the instrumentation.

Weaknesses include the accuracy of emissivity values, which has a large effect on the accuracy of infrared thermometers. For example, accurate measurement of the surface temperatures of metals and alloys is a known issue with infrared thermometers. For clean or unoxidized metals, emissivity is strongly dependent on the angle of incidence, and clean metal surfaces are poor emitters (Stephenson, et al., 1999). The emissivity of oxidized metals and alloys is generally higher than polished or unoxidized metals but also is variable and influenced by surface finish. Emissivity values for most alloys, including stainless steel, depend on surface finish and oxidation (Stephenson, et al., 1999; Scigiene Corporation, 2013). In the polished condition, emissivity can be 0.35 or less, while emissivity values for oxidized alloys are typically 0.85 to 0.95. Changes in emissivity associated with deposits on metal surfaces also could be significant. For example, concrete and soil typically have emissivity values of 0.9 to 0.95. For long-term remote deployment, the effect of deposits on the collection optics, changes in the surface emissivity as a result of oxidation or atmospheric deposits, and radiation-induced degradation of the collection optics also would need to be evaluated prior to remote deployment for extended periods.

Potential DCSS Use

Radiation thermometers are capable of measuring temperatures in the ranges expected for DCSS canister and cask temperatures. The line-of-sight measurement capability, combined with large standoff distances and the availability of portable systems, may be advantageous for temperature monitoring of new or existing DCSSs.

Shielding the measurement electronics from damaging radiation would likely be necessary. Also, the error associated with the difficulty of determining a correct emissivity value would need to be considered for stainless steel canisters. Given the emissivity issue, it appears that infrared thermometers are better suited for measuring or monitoring the temperatures of painted surfaces or nonmetallic structures, systems, and components (SSC).

Unknowns

- Expected change in emissivity of canister and cask surfaces with time as a result of oxidation and accumulation of atmospheric deposits on the canister or cask surface.
- Error in temperature measurement as a result of atmospheric deposition on the sensor optics.
- Neutron and gamma radiation tolerance of radiation thermometer optics and electronics.

2.1.4 Ultrasonic Temperature Measurement

Measurement Principle

Two methods for ultrasonic temperature measurement have been explored: (i) pulse-echo and (ii) acoustic-resonance. Both methods can be used to measure temperatures up to at least 2,000 °C [3,632 °F]. The pulse-echo method has been used to measure temperatures of in-pile tests (Wilkins and Evans, 2005) and is based on the thermal dependence of the speed of sound in materials (Tasman, et al., 1982; Lynnworth, 1989). The time difference between the transmission of an ultrasonic pulse and the signal reflected from a calibrated location allows for calculation of the temperature of the material through which the pulse travels. In contrast with other devices that measure temperature at a single point, ultrasound measures the bulk mean temperature throughout the measuring medium. For in-pile measurements, the ultrasonic transducer is connected to a specific measurement medium, the most common of which have been thoriated tungsten and tungsten ruthenium alloys (Daw, et al., 2010).

Maturity

Thin wire sensors have been used in nuclear and industrial applications where conditions preclude the use of thermocouples, resistance devices, or optical pyrometers (Wilkins and Evans, 2005). Development of ultrasonic transducer materials for improved temperature measurements is continuing (Daw, et al., 2012), and development of ultrasonic temperature probes for monitoring DCSSs is ongoing at Argonne National Laboratory (Bakhtiari, et al., 2013). While the technique has been used for many years, ultrasonic thermography is not widely used, owing to the cost and specialized nature of the measurement system. The most common use has been for in-pile measurements characterized by high thermal neutron fluence and temperatures that typically exceed the operational limits of other measurement methods, such as thermocouples.

Measurement Range, Sensitivity, and Longevity

Measurement range of ultrasonic thermometers is dependent on both the properties of the material for the ultrasonic measurement and the temperature tolerance of the transducer. Daw, et al. (2010) have shown that 2 percent thoriated tungsten materials could be used at temperatures up to 2,500 °C [4,532 °F]. Bakhtiari, et al. (2013) demonstrated temperature measurements from 20 to 400 °C [68 to 752 °F] using a cobalt/iron alloy and a magnetostrictive transducer. Measurement sensitivities using this technique can be as small as 0.001 °C [0.002 °F]. Bakhtiari, et al. (2013) reported a measurement resolution of 0.79 °C [1.4 °F] with a system under development for the specific purpose of DCSS temperature monitoring. For those applications where the measuring medium is a solid (thin wire and calibrated rod), the accuracy of the measurement may be affected by corrosion, ablation, or erosion of the material. However, the longevity of the measuring medium is likely to far exceed that of the ultrasonic equipment, which is designed for years of service in industrial settings.

Space and Power Requirements

The length of the measuring medium also is calibrated for the specific application. The diameter of the measuring medium can be similar to that of a thin rod or a wire less than <1 cm [0.4 in]. The length of the wire or rod is determined by the physical separation of the sites that require monitoring. There is no specific information on the minimum length of the probe: it depends on the frequency of the waveform of the input ultrasonic signal and the speed of sound of the

material of which the probe is made. In Bakhtiari, et al. (2013), 15 cm [5.9 in] corresponded to about 250 μsec and was detectable using a 200 kHz pulse. The space requirement of the ultrasonic equipment is on the order of 200–2,000 cm^3 [12.2–122 in^3]. Continuous access to power is likely required for the measurement equipment, although portable equipment is available for conducting manual measurements.

Monitoring Area and Data Acquisition

This approach measures the average temperature between known locations along the wire or rod medium. The system collects a large amount of intermediate data and then calculates temperature readings for each segment of the medium based on the known dependence of acoustic velocity or resonance frequency, as a function of temperature. The data acquisition mode can be continuous or intermittent. The measurement system captures a large amount of intermediate data from the ultrasonic sensor that are used to measure the time difference between the arrivals of reflections from known locations along the medium. A temperature for each section of the medium is calculated based on the offset from the expected arrival time. The offset is due to the temperature-dependent effect on the speed of sound through the medium and measures the temperature at various points along the medium.

Temperature and Radiation Tolerance

The technique has been demonstrated at temperatures greater than 2,000 °C [3,632 °F] in plasmas (Carnevale, et al., 1967). Tasman, et al. (1982) reported on the capability for continuous measurement of temperatures greater than 2,000 °C [3,632 °F] in nuclear reactors using thin wire sensors. It is unknown whether the main features of this technique (i.e., calibration, longevity, and sensitivity) will be affected for this temperature range.

In previous testing of ultrasonic temperature measurements, neither tungsten nor rhenium were attractive choices for reactor use because decalibration from transmutation arises, similar to that experienced by tungsten−rhenium alloy thermocouples under irradiation. Rhenium sensors decalibrated by as much as −50 percent for a thermal neutron fluence of 1.2 E+22 n/cm^2 during in-pile tests (Wilkins and Evans, 2005). Although ultrasonic temperature sensors have been used for in-pile measurements, specific gamma and neutron radiation tolerance information is not available. However, development of ultrasonic transducer materials for in-pile temperature measurements in high gamma and neutron radiation environments is continuing (Daw, et al., 2012).

Strengths and Weaknesses

A strength of ultrasonic temperature measurement is that it is a mature technique that has been demonstrated in extremely harsh environments, including those with high-radiation fields.

Weaknesses include the care that must be taken to shield the measurement electronics from high radiation. Alloys used for ultrasonic measurements are affected by high neutron damage. Because calibrated sensor materials are required to conduct ultrasonic temperature measurements, the measurement material must be immersed in the environment of interest. This requirement limits the applicability of ultrasonic temperature measurements, and it is unclear whether this method could be used for surface temperature measurements. Degradation of the measurement materials in humid environments has not been thoroughly investigated. The data acquisition and data processing are complex and expensive.

Potential DCSS Use

Ultrasonic temperature measurement can be used at temperatures much greater than operational temperatures for DCSSs. In addition, ultrasonic temperature measurements have been conducted in high radiation environments.

The size and operation of the systems may be better suited to providing air temperature measurements, but it is unclear whether these systems could be placed in the gap between the canister and overpack for external temperature monitoring. Use of ultrasonic temperature measurements to monitor surface temperatures is uncertain. In addition, it would be necessary to shield the sensitive measurement electronics from damaging radiation. The entire system, with the measurement medium, transducer, and data acquisition system, appears to be more complex than typical thermocouple or RTD temperature systems that are widely used in other industrial and nuclear applications. Consequently, replacement of the wire or rod measurement medium of a transducer could pose challenges that require significant planning, cost, and efforts to minimize worker dose.

Unknowns

- Neutron and gamma radiation tolerance of sensor materials and transducers.
- Degradation of measurement materials and transducers in humid air environments.
- Applicability for surface temperature measurements.
- Size of the systems.

2.1.5 Fiber Optic Temperature Sensors

Measurement Principle

Optical fibers can be used as sensors to measure strain, temperature, pressure, and other quantities by modifying a fiber so the quantity to be measured modulates the intensity, phase, polarization, wavelength, or transit time of light in the fiber (Tasman, et al., 1982; Engineers Handbook.com, 2013). Sensors that vary the intensity of light are the simplest, because only a simple source and detector are required.

Maturity

Fiber optic sensors are a mature technology for industrial and medical applications. Fiber optic temperature sensors have been evaluated for possible nuclear applications (Cheymol, et al., 2008; Korsah, et al., 2006; Liu, et al., 2003; Miller, et al., 1999).

Space and Power Requirements

The size of the sensor is approximately the diameter of a fiber optic cable: less than 5 mm [197 mils]. The length of the sensors is dependent on the physical location of the sites that require monitoring. The size of accompanying electronics is on the order of 20 cm × 10 cm × 10 cm [7.9 in × 3.9 in × 3.9 in], so the space requirement of the measurement system is on the order of 2,000 cm^3 [122 in^3]. The system would require continuous access to 110 V AC power.

Measurement Range, Sensitivity, and Longevity

The measurement range of fiber optic temperature sensors is dependent on the measurement principle. Fiber optic sensors have been employed to measure temperatures in excess of 2,000 °C [3,632 °F] in industrial applications. Commercially available fiber optic temperature sensors based on an interferometric sensing mechanism are readily available, with measurement ranges from −50 to 300 °C [−58 to 572 °F] and a measurement accuracy of ±0.15 °C [0.3 °F]. Specialty fibers are available that can operate at temperatures up to 800 °C [1,472 °F]. A highly sensitive fiber Bragg grating (FBG) temperature sensor using a temperature-sensitive Pb/Ge-codoped fiber has been demonstrated experimentally with the average temperature sensitivity of the resonance wavelength shift about 0.0176 nm/ °C [2.2×10^{-5} mils/ °F] (Ju, et al., 2009). Advertised minimum measurement sensitivity for industrial systems can be as low as 0.1 °C [0.2 °F]. The sensor lifetime is between 7–10 years for industrial applications.

Monitoring Area and Data Acquisition

Optical fiber, when used as a temperature sensor, provides real-time measurement of the longitudinal temperature profile along the fiber. The amount of data depends on the length of the fiber, with one temperature value for every 0.5 to 2 m [1.6 to 6.6 ft]. Data processing and acquisition are dependent on the phenomena exploited in the optical techniques for temperature measurement, including (i) collection and detection of blackbody radiation; (ii) changes in refractive index of external media with temperature; (iii) changes in fluorescence spectra and/or fluorescence rise times with temperature; (iv) changes in Raman or Brillouin scatter with temperature; (v) phase transitions in carefully selected materials imposing mechanical modulation on optical fiber transmission properties; and (vi) temperature changes within an optical path length, either within the fiber or an external interferometer element (Stephenson, et al., 1999). Both continuous and intermittent data acquisitions are possible.

Temperature and Radiation Tolerance

Fiber optic sensors have been employed to measure temperatures in excess of 2,000 °C [3,632 °F] in industrial applications. Although they are subject to gamma-induced fiber darkening that introduces temperature offsets, it may be possible to mitigate or compensate for these effects through calibration. Fox, et al. (2007) investigated gamma-induced darkening for space-based applications. Results indicated that the specific fibers studied exhibited "reasonable radiation resistance to gamma exposures typical of a 5-year, low-Earth-orbit environment. Maximum transmittance losses of less than 10 percent were observed for total gamma exposures of 20–50 Gy [2,000–5,000 rad]" (Fox, et al., 2007). Different kinds of fiber have varying sensitivities to gamma-induced effects. In EPRI-sponsored testing of commercial off–the–shelf sensors under conditions corresponding to a gamma dose of 98.5 megarads and a total neutron fluence of 2.4×10^{16} n/cm^2, the sensor element experienced a degradation that affected either its calibration, signal amplitude or both (Miller, et al., 1999). Subsequent development of hollow core photonic bandgap (PBG) fibers has yielded significant improvement in terms of radiation resistance over conventional fibers. The PBG fibers showed radiation resistance up to 10^{20} n/cm^2 and gamma dose of 10GGy (10^6 Mrads) (Cheymol, et al., 2008).

Strengths and Weaknesses

Strengths of fiber optic temperature sensors include corrosion resistance (due to their glass-based construction) and the ability to operate at temperatures that are too high for

semiconductor sensors. Fiber optic sensors can provide accurate and stable measurement in hazardous environments, including environments with high ambient electromagnetic fields. Specialized fibers have been developed with improved gamma and neutron radiation resistance.

Weaknesses include the fact that few fiber optic temperature sensors satisfy the criteria outlined in IEEE (2003, IEEE-323).

Potential DCSS Use

Fiber optic temperature measurement can be used at temperatures that are within the operational temperature ranges expected for DCSSs. The fibers are small, which may allow them to be applied on DCSS SSC surfaces where space and clearance tolerances are limited.

The measurement electronics for the fiber optic temperature sensors would need to be shielded from damaging radiation. This could potentially be accomplished by routing the optical fiber from the high-radiation environment to a location outside of the high-radiation environment.

Unknown

- Temperature and radiation stability of hollow core PBG fibers.

2.1.6 Semiconductor Temperature Sensors

Measurement Principle

Most semiconductor junction temperature sensors use a diode-connected bipolar transistor operating with a constant current passed through the base-emitter junction that produces a junction voltage between the base and emitter. The junction voltage is a function of temperature (approximately 2 mV/°C).

Maturity

Semiconductor temperature sensors are commercially available, and the technology is mature. These sensors are typically configured to allow incorporation onto electronic circuit boards and are not usually packaged as standalone temperature sensors.

Space and Power Requirements

Semiconductor temperature sensors are available in a range of sizes but are usually small to allow incorporation onto circuit boards. A typical component is 3 mm × 3 mm × 2 mm [0.12 in × 0.12 in × 0.08 in] in size and requires up to 2 milliwatts of power.

Measurement Range, Sensitivity, and Longevity

Measurement range is generally limited to the nominal integrated circuit (IC) operating range of −55 to +150 °C [−67 to 302 °F]. Typically a semiconductor temperature sensor has a temperature coefficient of approximately 2 mV/°C. This is small but similar to a thermocouple. The temperature sensitivity is usually 0.5 °C [1.0 °F] or better. Explicit information on the longevity of semiconductor temperature sensors was not identified in this study; however, it is

well known that the lifetimes of the sensors are considerably reduced at elevated temperatures (Stephenson, et al., 1999).

Monitoring Area and Data Acquisition

The monitoring area is the immediate vicinity of the sensor. The output of semiconductor temperature sensors is a voltage that is proportional to temperature. Packaged solid state components include compensation and linearization circuitry. The output is generally a digital value of the measured temperature. Data acquisition systems and data file format are similar to those of a thermocouple or an RTD. Both continuous and intermittent data acquisitions are possible.

Temperature and Radiation Tolerance

Like other integrated circuits, the operating range is generally limited to the nominal IC operating range of −55 to +150 °C [−67 to 302 °F]. Radiation tolerance information for semiconductor temperature sensors is not known, but many semiconductors are highly susceptible to radiation effects.

Strengths and Weaknesses

Strengths include sensitivity, small size, and low power requirements for semiconductor temperature sensors. These attributes facilitate their use on electronic devices where temperature measurement is necessary.

Weaknesses include limited operational range. Most semiconductor temperature sensors are limited to temperatures less than 150 °C [302 °F]. Radiation tolerance of semiconductor temperature sensors was not available. In general, semiconductor devices are known to be susceptible to radiation damage.

Potential DCSS Use

Semiconductor temperature sensors are low-cost ICs for temperature measurement. The devices are small, allowing their incorporation into circuit boards. They have a limited temperature range and are easily damaged at elevated temperatures. Given this drawback, semiconductor temperature sensors are not likely to be suitable for temperature monitoring in close proximity to DCSSs.

Unknowns

- Radiation tolerance of semiconductor temperature sensors.
- Combined effects of elevated temperature, humidity, and radiation on accuracy and drift.

2.1.7 Thermistors

Measurement Principle

Thermistors are another type of device whose resistance varies with temperature. Unlike a wire wound or metal film RTD, a thermistor is a ceramic semiconductor. Depending on the type of material system used, a thermistor can have either a large positive temperature coefficient of resistance (PTC device) or a large negative temperature coefficient of resistance (NTC device).

PTC thermistors are silicon semiconductor devices and have a temperature coefficient of resistance of 0.7 to 0.8 percent $°C^{-1}$, whereas NTC thermistors are typically metal oxides, such as the oxides of chromium, cobalt, copper, iron, manganese, nickel, and titanium, and have nonlinear resistance–temperature characteristics. Although the resistance–temperature characteristic of an NTC thermistor is nonlinear, it is possible to achieve good linearity of the conductance–temperature and resistance–temperature characteristics using thermistor-resistor networks.

Maturity

Thermistors are a mature technology used in many commercial applications. No reported literature on thermistors meeting the requirements of IEEE (2003, IEEE-323) was identified in this review, but thermistors that have significant radiation tolerances are commercially available.

Measurement Range, Sensitivity, and Longevity

Commercial versions of thermistor devices typically have a range of –80 to 300 °C [−112 to 572 °F]. However, some units are rated for intermittent operation at 600 °C [1,112 °F], and special cryogenic devices are rated for operation as low as −196 °C [−320 °F] (Stephenson, et al., 1999). Thermistors have excellent sensitivity over a small temperature range because of orders of magnitude changes in resistivity as a function of temperature. Longevity can be on the order of years at moderate temperatures. At elevated temperatures the lifetime of thermistors can be significantly shortened.

Space and Power Requirements

Thermistors are one of the smallest commercially available temperature sensors. Commercial thermistors are available with diameters of 0.8 mm [0.032 in] and lengths of 1.6 mm [0.064 in], excluding the lead wires. Power requirements for thermistor sensors are very low, on the order of 0.04 watts. Sensor power requirements are similar to thermocouples and RTDs. Instrumentation and data acquisition power requirements are greater than the sensor power requirements.

Monitoring Area and Data Acquisition

Thermistors are used for a point measurement of temperature. In contrast to the highly linear operation of RTDs, the resistance–temperature curve for the more commonly used NTC type thermistors is very nonlinear, which requires the application of substantial linearization when attempting measurement across large temperature ranges. Data acquisition systems and data file formats are comparable to those for thermocouples and RTDs. Both continuous and intermittent data acquisitions are possible.

Temperature and Radiation Tolerance

Most thermistors are rated for use up to +150 °C [302 °F], but devices are available within the range from −196 to +600 °C [−302 to 1,112 °F]. There are commercially marketed thermistors that are advertised to be unaffected by radiation (General Electric, 2006), but specific information on neutron and gamma radiation tolerance was not located in this review.

Strengths and Weaknesses

Strengths of thermistors are their small size and low power requirements. Compared to RTDs, thermistors have a large temperature coefficient, which improves sensitivity to small temperature changes.

Weaknesses are that most thermistors have upper temperature limits that are either close to or below the maximum temperatures expected for DCSSs. Self-heating due to current flow at elevated temperatures must also be considered, because this can lead to measurement errors. Radiation tolerance of some devices is high (General Electric, 2006), but comparisons to thermocouples and RTDs were not found. In addition, thermistors meeting the qualifications of IEEE (2003, IEEE 323) were not located.

Potential DCSS Use

Thermistors can be used at temperatures that are within the operational temperature ranges expected for DCSSs. Their small size may allow application on DCSS SSC surfaces or locations where space and clearance tolerances are limited. They have a low power requirement, which is attractive for remote applications.

The long-term stability of these devices in high radiation environments at elevated temperatures has not been determined. Surface mountable thermistors are available, but given the temperature limitations, it is not clear whether these devices would be suitable to measure surface temperatures of canisters or casks. Similarly to thermocouples and RTDs, the measurement electronics would need to be shielded from damaging radiation.

Unknowns

- Gamma and neutron radiation tolerance.
- Long-term stability in elevated temperature environments.

2.1.8 Johnson Noise Thermometers

Measurement Principle

Johnson noise thermography is a fundamental first principle measurement of temperature using the Nyquist equation, as in Eq. (2-1), which gives the relationship between temperature, resistance, and voltage generated as follows:

$$V^2=4k_BTR\Delta f \qquad (2\text{-}1)$$

where V^2 is the mean squared value of the voltage—also called power spectral density—across a resistor of resistance R, k_B is Boltzmann's constant, T is the absolute temperature of the resistor, and Δf is the measurement bandwidth. To measure temperature using Johnson noise, the frequency response of the total system must be known, as well as the resistance. Temperature is then computed by dividing the power spectral density of the noise voltage by $4k_BR$ (Lambert, et al., 2012).

Maturity

Johnson noise has been utilized to measure temperatures in very aggressive environments and has been evaluated for Earth orbit and space exploration applications (Kisner, et al., 2004). This method also has been used in high temperature reactors, and recent work has been conducted to develop Johnson noise thermometers for small modular reactors where temperature measurements are necessary with minimal drift between recalibration intervals (Britton, et al., 2012). Although used in highly demanding applications, Johnson noise thermometers are not commercially available. This is largely attributed to several difficulties that make this technique either technically or economically unattractive. The sophisticated electronic signal processing for very low-level current and voltage measurements has been shown to be at least as costly as that required for ultrasonic thermometers. Also, Johnson noise thermometers are susceptible to the same electrical shunting limitations in lead cabling as those that limit the temperature range of refractory-metal thermocouples. Finally, Johnson noise generated in the instrument lead cable is an error source that requires special compensation, which increases instrument complexity and cost (Wilkins and Evans, 2005).

Space and Power Requirements

Not available.

Measurement Range, Sensitivity and Longevity

Johnson noise thermometers have been used at temperatures up to 1,500 °C [2,732 °F], but specific information on measurement range, sensitivity, and longevity is not available.

Monitoring Area and Data Acquisition

Not available.

Temperature and Radiation Tolerance

Although Johnson noise thermometers have been constructed and used in past decades, these devices are not commercially produced and details of temperature and radiation tolerance are not available. However, Johnson noise thermometers have been reportedly used successfully for temperatures up to 1,500 °C [2,732 °F] and for in-core measurements where high levels of neutron and gamma radiation are expected.

Strengths and Weaknesses

The strength of a Johnson noise thermometer is its capability to provide reliable temperature measurements in high temperature and high radiation environments.

Weaknesses are the lack of commercial systems and standard specifications.

Potential DCSS Use

In principle, Johnson noise thermometers could be used in severe environments where traditional instruments have limited operability. Johnson noise thermometers are not commercially available, and detailed information on data acquisition and instrumentation has not been reported.

Unknowns

There are many unknowns for Johnson noise thermometers because these systems are not commercially available. Some of the key unknowns include

- Sensor and system size, complexity, and overall system requirements.
- Range of measurement, especially low temperatures.
- Radiation and temperature tolerance.
- Ability to provide surface temperature measurements.
- Environmental compatibility.

2.2 Humidity Monitoring

The humidity at the outside surface and inside an SNF canister could be an indicator for the initiation of various degradation phenomena. On the exterior of the canister, dust, salts, or other airborne species that deposit on the surface could deliquesce at high relative humidity. NRC and the industry have recognized the potential for chloride-rich brines to form in this manner, raising concerns for the occurrence of corrosion and SCC. Likewise, a warm and moist environment could be favorable for MIC of the canister and other metal structures inside the overpack. In principle, humidity at the canister external surface could be measured by placing a sensor directly on the canister surface or estimated by measuring absolute humidity of the nearby ambient air and calculating the RH at the canister surface, provided the canister surface temperature is known.

Humidity measurement techniques are well established for industrial applications, and many types of sensors are commercially available (Rittersma, 2002; Chen and Lu, 2005; Pieter, 1997). Compared to temperature sensors, however, there appears to be only limited use of humidity sensors for nuclear applications in which the sensors could be exposed to elevated temperatures and radiation fields. This section reviews the most common commercially available sensors, as well as novel techniques that have been proposed for nuclear applications. The main features of these techniques are summarized in Table 2-3, with additional details described in subsequent sections.

The reviewed and assessed humidity sensors are (i) capacitance-based humidity sensors, (ii) chilled-mirror-based humidity sensors, (iii) electrical-resistance-based humidity sensors, (iv) fiber optic sensors, (v) leakage monitoring systems, and (vi) psychrometers.

2.2.1 Capacitance-Based Humidity Sensors

Measurement Principle

For capacitance-based humidity sensors, a ceramic or polymer is deposited as a thin film between two conductive electrodes. The dielectric constant of the material varies in a known manner as a function of humidity, thereby allowing the determination of humidity by measuring the capacitance of the sensor. Ceramic and polymer humidity sensors are described as follows.

Table 2-3. Humidity Monitoring Sensors				
Features	**Ceramic-Capacitance-Based (Section 2.2.1.1)**	**Polymer-Capacitance-Based (Section 2.2.1.2)**	**Chilled Mirror (Section 2.2.2)**	**Resistance-Based (Section 2.2.3)**
Maturity	Field deployed in non-nuclear applications	Field deployed in non-nuclear applications	Field deployed in non-nuclear applications	Field deployed in non-nuclear applications
Measurement Ranges	Up to 80 °C [176 °F]	Up to 100 °C [212 °F]	Up to 115 °C [239 °F]	Up to 200 °C [392 °C] for certain designs
Sensitivity	± 2 to 3 °C [3.6 to 5.4 °F] dew point	±1 to 4 percent RH	±0.1 percent RH	±1 to 5 percent RH
Longevity	Years	Years	Years	Years
Space Requirements	Probe: 5–10 cm [2–4 in] long and 2–4 cm [0.8–1.6 in] in diameter; larger analyzer unit	Probes: 10–15 cm [4–6 in] long and 1–3 cm [0.4–1.2 in] in diameter; chips: 1.0 cm × 0.5 cm × 0.5 cm [0.4 in × 0.2 in × 0.2 in]; larger analyzer unit	Probes: 13 cm long [5 in] and 5 cm [2 in] diameter; larger analyzer unit	Depends on design, but typically few cm^2; larger analyzer unit
Power Requirements	Continual by batteries or AC source	Continual by batteries or AC source	Continual by batteries or AC source	Continual by batteries or AC source
Monitoring Area	Immediate area	Immediate area	Immediate area	Immediate area
Data Acquisition Mode	Continuous or intermittent	Continuous or intermittent	Continuous or intermittent	Continuous or intermittent
Temperature Tolerance	Aluminum oxide sensors: 80 °C [176 °F], $MgCr_2O_4$–TiO_2 sensors: 300 °C [572 °F]	100 °C [212 °F]	115 °C [239 °F]	Up to 200 °C [392 °C] but varies significantly from one manufacturer to another
Radiation Tolerance	Largely unknown, limited testing on $MgCr_2O_4$–TiO_2	Unknown, but polymers typically low	Unknown	Some designs tested up to 100 Mrad
Strengths	Temperature tolerance, small size	High accuracy, lack of hysteresis, small size	High accuracy, less calibration needed	High temperature tolerance, small size
Weaknesses	Hysteresis effects, no radiation tolerance data	No radiation tolerance data	No radiation tolerance data, potentially degraded by dust or particulates on mirror	Limited radiation tolerance data for certain designs

Table 2-3. Humidity Monitoring Sensors			
Features	**Fiber Optic Sensors (Section 2.2.4)**	**Leakage Monitoring Systems (Section 2.2.5)**	**Psychrometer (Section 2.2.6)**
Maturity	Limited commercial availability	Commercially available and used for nuclear applications	Field deployed in non-nuclear applications
Measurement Ranges	Up to 100 °C [212 °F] for some designs]	Temperature tolerant for RPV head and primary piping	Up to 50 °C [122 °F]
Sensitivity	Few percent RH	±1.5 percent RH	± 3 percent relative humidity
Longevity	Unknown	Years	Intermittent use expected
Space Requirements	Micros to few mm optical fibers; larger analyzer unit	Narrow sensing lines up to several hundred meters long; analyzer unit larger than 1 m [3.28 ft] in height, width, and depth	Few 10s of millimeters in height, width, and depth
Power Requirements	Continual by batteries or AC source	Continual by batteries or AC source	Battery expected for intermittent use
Monitoring Area	Immediate area	Many locations along sensing line	Immediate area
Data Acquisition Mode	Continuous or intermittent	Continuous or intermittent	Intermittent
Temperature Tolerance	100 °C [212 °F]	85 °C [185 °F] for analyses, maximum temperature for air sampling not specified but expected to be >200 °C [392 °F] based on reactor applications	100 °C [212 °F] for commercially available systems
Radiation Tolerance	Limited testing up to 10 kGY	Radiation tolerant for RPV head and primary piping	Unknown
Strengths	Small size, resistant to electromagnetic interference	Lack of electronics on sensing line; demonstrated for nuclear applications; spatial RH data	High accuracy, small size
Weaknesses	Not commonly commercially available, unknown effects of dust or particulates, no radiation tolerance data	Large analyzer unit, complex installation	No radiation tolerance data

2.2.1.1 Ceramic-Capacitance-Based Humidity Sensors

Measurement Principle

The ceramic-capacitance-based capacitive humidity sensors are typically fabricated from porous ceramics, which have high surface area for adsorption of water (Dickey, et al., 2002; Chen and Lu, 2005). These humidity sensors operate on the principle of proton conduction through the hydrogen bond network of water molecules, referred to as the Grotthuss or proton-hopping mechanism. When a first layer of molecules is adsorbed onto the ceramic surface, a dissociative mechanism leads to the formation of a hydroxyl ion and a proton. The hydroxyl ion is chemisorbed onto a surface-activated site, and the proton associates with a surface oxygen atom to form a second hydroxyl ion. Then, another water molecule is physisorbed by hydrogen bonding to the two hydroxyl ions. This layer is not conductive because there are no hydrogen bonds formed between the water molecules. As humidity increases, however, additional layers are formed, creating a liquid-like network in which hydrogen bonding between water molecules becomes predominant, increasing proton conductivity by the Grotthus method. The water-like network of single bonded water molecules has a high dielectric constant as the molecules form dipoles and reorient freely under an externally applied electric field. Chen and Lu (2005) reviewed ceramic humidity sensors made from materials including aluminum oxide (Al_2O_3), titanium dioxide (TiO_2), silica (SiO_2), and spinel compounds.

Maturity

Aluminum oxide humidity sensors are the most common type of ceramic-capacitance-based humidity sensors available on the commercial market. An internet search indicated that these sensors are available from General Electric Measurement & Control Solutions (GE, 2005) and Teledyne Analytical Instruments (Teledyne Cormon, 2013), among others. There is no known use of a ceramic-capacitance-based humidity sensor for a nuclear application where it would be exposed to the temperature and radiation fields analogous to a DCSS.

Measurement Range, Sensitivity, and Longevity

The product literature from the vendors indicates that these sensors have a dew point accuracy of ± 2 to 3 °C [± 3.6 to 5.5 °F], with response time from a few seconds to a minute or more. Vendors indicate that in nonradiation environments, these sensors could last 5 to10 years in operation. Aluminum oxide, as a sensing material, also may be compromised by hysteresis effects (Hasegawa, 1980).

Space and Power Requirements

A typical aluminum oxide probe is in the range of 5–10 cm [2–4 in] long and 2–4 cm [0.8–1.6 in] in diameter. A length of cable is used to connect the probe to a signal analyzer. The size of the analyzer is not specified. A constant power supply from electrical connection or batteries is required.

Monitoring Area and Data Acquisition

The monitoring area is in the immediate vicinity of the sensor. For applications where there is a spatial gradient in temperature, multiple sensors would be needed to monitor the spatial humidity variations. The data acquisition mode for the commercially available aluminum

oxide-based humidity sensors is digital and can be either continuous or intermittent. The data size per measurement is expected to be small.

Temperature and Radiation Tolerance

Chen and Lu (2005) indicate maximum operating temperatures for aluminum oxide sensors in the range of 70 to 80 °C [158 to 176 °F]. There is little information about the radiation tolerance of aluminum oxide sensors. However, aluminum oxide has been used as a radiation hardening material in the semiconductor industry (Sickafus, et al., 2000; Zaininger, 1969). For example, Solanki, et al. (1983) proposed aluminum oxide as a substitute for silicon oxide in ionizing radiation environments.

The only known study of ceramic humidity sensors for a nuclear application involved the use of $MgCr_2O_4$–TiO_2 sensors for leakage detection in piping systems, such as the main steam line (Lee, et al., 2001). Tests were conducted to demonstrate resilience up to 300 °C [572 °F]. Tests also were performed where the sensors were exposed to mild gamma radiation {1 cm [0.4 in] from a 1 μCi Co-60 source at room temperature} with no reported loss of performance.

Strengths and Weaknesses

Strengths of these sensors include commercial availability, temperature tolerance, and small sensor size.

Weaknesses include the lack of demonstrated radiation resistance for extended periods of time, and hysteresis effects.

Potential DCSS Use

Ceramic-capacitance-based humidity sensors are capable of measuring humidity over a wide range of conditions, but limited information exists on the temperature and radiation tolerance of these sensors. The size of the sensors also may limit their placement locations in possible DCSS applications. The associated measurement electronics also would require shielding from damaging radiation. Given these limitations, it does not appear that ceramic-capacitance-based humidity sensors are suitable for DCSS applications.

Unknowns

- Radiation tolerance.
- Effects of hysteresis on long-term accuracy.
- System modifications and preparation required for deployment on a DCSS that was not designed for monitoring.
- Effects of dust and particulates on sensor longevity.

2.2.1.2 Polymer-Capacitance-Based Humidity Sensors

Measurement Principle

Certain insulating polymers absorb or release water from the free space between molecules based on the relative humidity, thereby changing the dielectric properties of the material and, in turn, the capacitance of the polymer material. Polymers used include poly (methyl methacrylate) and cellulose acetate butyrate (Chen and Lu, 2005).

Maturity

Polymer-capacitance-based humidity sensors are readily available on the commercial market and are commonly used for non-nuclear applications. For example, an internet search indicated that Honeywell International (2011), Vaisala (2013, 2012), and Sensirion (2011) provide a variety of humidity sensors, including cylindrical probes and hand-held analyzers. However, there is no known use of a polymer-capacitance-based humidity sensor for a nuclear application where it would be exposed to the temperature and radiation fields analogous to a DCSS.

Measurement Range, Sensitivity, and Longevity

The product literature for the polymer-based capacitive humidity sensors describes accuracy in the range of 1 to 4 percent RH with response time of 10 seconds or more. Vendors indicate longevity of 5 to 10 years in nonradiation environments.

Space and Power Requirements

Polymer-capacitance-based humidity sensors are available from different vendors as cylindrical probes and printed rectangular chips. For example, cylindrical probes are in the range of 10–15 cm [4–6 in] long and 1–3 cm [0.4–1.2 in] in diameter, whereas chips are approximately 1.0 cm × 0.5 cm × 0.5 cm [0.4 in × 0.2 in × 0.2 in]. A length of cable is used to connect the probe to a signal analyzer. The size of the analyzer is not specified in the product literature, but is likely to be larger than the probe itself. If the analyzer cannot be placed inside the overpack to wirelessly transmit data to a receiver outside, a cable would need to pass through the vents or other opening to connect the probe to the analyzer. A continuous power supply is needed. Sensors may operate for up to 2 years on batteries or be connected to an AC source.

Monitoring Area and Data Acquisition

For applications where there is a spatial gradient in temperature, multiple sensors would be needed to assess spatial humidity variations. The data acquisition mode for the commercially available polymer-based capacitive humidity sensors is digital and can be either continuous or intermittent. The data size per measurement is expected to be small.

Temperature and Radiation Tolerance

The product literature for the polymer-based capacitive humidity sensors indicates that they can operate effectively up to temperatures of at least 100 °C [212 °F]. There is little information available on the radiation tolerance of the sensors, but it is known that polymeric materials undergo extensive chemical changes in a high-radiation environment (Schweitzer, 2007).

Strengths and Weaknesses

Strengths of polymer-based capacitive humidity sensors include high accuracy, lack of hysteresis, and small probe size. Vendors also indicated that these sensors are relatively insensitive to dust or other airborne contaminants.

Weaknesses include the lack of radiation tolerance data and low temperature tolerances.

Potential DCSS Use

Limited information exists on the temperature and radiation tolerance of polymer-based capacitance humidity sensors. The size of the sensors also may limit their placement locations in possible DCSS applications. The associated measurement electronics also would require shielding from damaging radiation. Given these limitations, it appears that polymer-capacitance-based humidity sensors are not suitable for DCSS applications.

Unknowns

- Radiation tolerance.
- System modifications and preparation required for deployment on a DCSS that was not designed for monitoring.

2.2.2 Chilled-Mirror-Based Humidity Sensors

Measurement Principle

Chilled-mirror-based sensors operate by measuring the dew point or frost point temperature: the temperature at which a sample of air at constant pressure becomes saturated with water vapor. At this saturation temperature, further cooling of air results in condensation of water either in a liquid or solid phase. The condensation is allowed to occur on a chilled-mirror surface. A light from a lamp is projected onto the chilled mirror, and the reflection is received by a photo resistor, as schematically shown in Figure 2-3. If water condenses on the mirror, the photo resistor picks up the optical signal and records the change in intensity of the reflected light from the mirror. The mirror temperature is recorded when the change in the intensity of the light occurs. The temperature of the mirror is controlled by electronic feedback to maintain a dynamic equilibrium between evaporation and condensation on the mirror, thus closely measuring the dew point temperature. The measured dew or frost point temperature values are used to estimate saturation vapor pressure and, in turn, to estimate water concentration in air. Chen and Lu (2005) reported that recent improvements have increased precision of the sensors. These recent improvements include use of fiber optics for projecting and receiving the light on the mirror surface and a laser source as the light.

Maturity

Chilled-mirror humidity sensors are readily available on the commercial market and are commonly used for non-nuclear applications. An internet search indicated that they are available from various vendors, including Omega Engineering (2013), GE (2007; 2011), Michell Instruments (2012), and Kahn Instruments, Inc. (2012), among others.

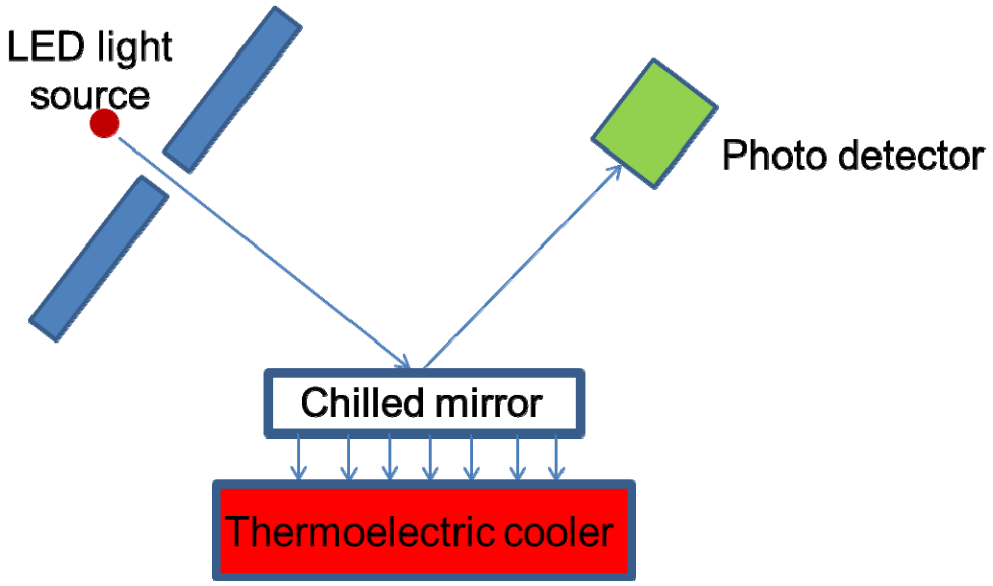

Figure 2-3. Schematics Showing the Measurement Principle of a Chilled-Mirror-Based Sensor

Measurement Range, Sensitivity, and Longevity

Product literature indicates that a dew point measurement precision of ±0.2 °C [0.4 °F] is attainable with the sensors, which correlates to the measurement precision of ±0.1 percent RH at high temperatures {e.g., 85 °C [185 °F]}. Response time of the commercially available chilled-mirror-based sensors is typically in the range of a minute to a few minutes. Vendors stated that the service life may be in the range of 5 to 15 years in nonradiation environments.

Space and Power Requirements

Configurations are available in which a sensor and data analyzer are integrated into a single unit or in which a probe is connected to the data analyzer by a length of cable. The integrated units and analyzer piece of the separate unit have size of 25 cm × 20 cm × 12 cm [10 in × 8 in × 5 in], equivalent to approximately 0.006 m^3 [0.2 ft^3]. A probe is 13 cm long [5 in] and 5 cm [2 in] diameter, with cable length up to several meters. A continuous power supply of batteries or an AC source is needed for the units.

Monitoring Area and Data Acquisition

The monitoring area of the chilled-mirror-based sensors is expected to be larger compared to the capacitance-based sensors because these sensors measure absolute rather than relative humidity. Nevertheless, multiple sensors would be needed to assess spatial humidity variations, particularly if airflow or temperature gradients cause local differences. The data acquisition mode for the commercially available chilled-mirror-based sensors is digital and can be either continuous or intermittent. The data size per measurement is expected to be small.

Temperature and Radiation Tolerance

Chilled-mirror humidity sensors can operate up to 115 °C [239 °F]. If the cooling mechanism of the mirror of the sensor were modified, it is possible that the sensors could operate at higher temperatures. There are no known studies on the radiation tolerance of these sensors. The measurement principle of the sensor is not expected to be affected by gamma radiation because the wavelength of the gamma rays is several orders of magnitude smaller than the visible light. This suggests that the chilled-mirror-based sensors could operate without interference from radiation. However, radiation could affect the semiconductor-based device that reads the temperature of the mirror when condensation is detected, the light source emitter, photo detectors that detect reflected light from the mirror, and other instruments inside the analyzer.

Strengths and Weaknesses

Strengths of chilled-mirror sensors include high reliability because of their optic-based operating principle. They have an additional advantage in that there is no need to convert parameters, such as capacitance, resistance, and voltage to humidity through a calibration chart. This eliminates the need for frequent calibration of the sensors.

Weaknesses include the lack of radiation tolerance data. These sensors also may be affected by dust or other particulates in the DCSS that would contaminate the mirror. Filters or compensation algorithms may alleviate this issue, but the effectiveness in the DCSS environment is not certain. There is no known use of a chilled-mirror humidity sensor for a nuclear application where it would be exposed to the temperature and radiation fields analogous to a DCSS.

Potential DCSS Use

The large size of integrated sensor/analyzer units along with uncertain temperature and radiation tolerance makes them an unlikely choice for humidity monitoring in a DCSS without specific modifications to the overpack or canister. For the separate probe/analyzer units, the size of the sensor may limit DCSS applications. It is unknown whether the sensors could be made to tolerate the temperatures and radiation expected in the narrow space between the canister and overpack. The sensor system electronics would need to be shielded and protected from damaging radiation. Replacement of the sensors would require remote access to the proximity of the canister surface with tools that allow for the insertion and attachment of the probes in desired locations. Cables also may need periodic replacement. The difficulty of replacement will depend on the configuration of the DCSS. Given these limitations, it appears that the chilled-mirror humidity measurement sensors are not suitable for DCSS applications.

Unknowns

- Radiation tolerance.
- Long-term effects of dust and particulates.
- System modifications and preparation required for deployment on a DCSS that was not designed for monitoring.

2.2.3 Resistance-Based Humidity Sensors

Measurement Principle

Electrical resistance-based humidity sensors operate on different measurement principles, depending on the system design. Some examples follow:

- Ohmic Instruments Company (2013) has a unit with a sensor of two matched resistors. One resistor is glass encapsulated in an inert gas (i.e., nitrogen or helium), and the second resistor is exposed to the environment. As the resistors are energized, the heat dissipated from the sealed resistor is different from the exposed resistor due to the difference in thermal conductivity of nitrogen or helium with respect to air containing moisture. As a result, the two resistors are at different temperatures. The difference in the resistors' temperatures is directly proportional to the absolute humidity of the environment.

- Hygrometrix, Inc. (2005) has developed a sensor in which a thin cellulosic material is deposited on the top surface of cantilever beams machined from the substrate of a silicon chip. Each beam has a strain gauge that operates by piezoresistance. Adsorption and desorption of water causes the cellulosic material to expand or contract, inducing a measurable deflection in the beams that is correlated to the humidity.

- TDK Co. (2011, 2010) has a sensor with a film of a conductive material, like gold printed onto a substrate, then deposited with a hygroscopic polymer. As the polymeric material adsorbs moisture, functional ionic groups dissociate and increase conductivity, which is correlated to the humidity.

Maturity

Resistance-based humidity sensors are available on the commercial market and used for non-nuclear applications. As indicated previously, they are available from a number of vendors.

Measurement Range, Sensitivity, and Longevity

Based on information in the product literature, the respective units have accuracy in the range of 1 to 5 percent RH, with response time from less than a minute to a few minutes, depending on the system design. Sensors are reported to operate for 10 years or longer in nonradiation environments.

Space and Power Requirements

Resistance-based humidity sensors involve a probe connected to a signal analyzer via cable. Probes are relatively small—a few centimeters in length and diameter. The size of the analyzer unit is not described in the literature but is likely to be somewhat larger than the probe. A continuous power supply by batteries or an AC source is needed for the units.

Monitoring Area and Data Acquisition

The monitoring area is in the immediate vicinity of the sensors, and multiple sensors would be needed to assess spatial humidity variations, particularly if airflow or temperature gradients

cause local differences in humidity. The data acquisition mode for the sensors is digital and can be either continuous or intermittent. The data size per measurement is expected to be small.

Temperature and Radiation Tolerance

The operating temperature range for the resistance-based humidity sensors varies depending on the design. The TDK sensor is recommended only for use up to 35 °C [95 °F], whereas the Hygrometrix sensor can be used up to 125 °C [257 °F] and the Ohmic Instruments sensors can be used up to 200 °C [392 °F]. The only sensor of this type known to have been radiation tested is the Hygrometrix unit. Studies for the Large Hadron Collider at the European Organization for Nuclear Research (CERN) reported that the sensor was qualified for exposure to 100 Mrad over a 10-year period (Brenner, et al., 2007). There was no notable loss in performance tests with an equivalent cumulative neutron fluence of 10^{14} n/cm^2.

Strengths and Weaknesses

Strengths of resistance-based humidity sensors are their small sensor size and long operational life.

Weaknesses include less precision than capacitance-based or chilled-mirror sensors, low temperature tolerance, and the limited radiation tolerance data for an environment similar to the DCSS.

Potential DCSS Use

Resistance-based humidity probes may be small enough to be positioned in various locations within an overpack (Figure 1-1) or an HSM (Figure 1-2) in order to obtain relative humidity information in the environment adjacent to canister surfaces. Long-term use as a humidity monitor for DCSS applications may be limited by the temperature and radiation tolerance. Sensor electronics would need to be shielded or kept out of the high radiation areas.

Unknowns

- Long-term radiation tolerance.
- Effects of dust and particulates.
- System modifications and preparation required for deployment on a DCSS that was not designed for monitoring.

2.2.4 Fiber Optic Sensors

Measurement Principle

A number of humidity monitoring techniques have been proposed that take advantage of the attributes of fiber optics, which include small size, remote measurement capability, and resistance to electromagnetic interference. Yeo, et al. (2008) described four general measurement techniques.

- Direct spectroscopic

For this method, moisture-sensitive chemical species are attached to the tip of a fiber and the optical signal analyzed for changes in absorption or fluorescence that relate to changes in humidity. For instance, cobalt chloride ($CoCl_2$) changes in color and absorption wavelength as it hydrates, whereas Rodamine 6G ($C_{28}H_{31}N_2O_3Cl$) fluoresces at different wavelengths depending on relative humidity.

- Evanescent wave

When light traveling through an optical fiber reflects at the fiber core and fiber cladding interface, interference of the incident light and reflected light generates an evanescent wave that penetrates the fiber cladding. The amplitude of the wave decays with increasing distance from the interface. For an evanescent wave humidity sensor, a portion of the normal fiber cladding material is replaced by a moisture-sensitive chemical species, such as $CoCl_2$ or polyvinyl alcohol, which then affects transmission along the fiber (e.g., by changing the optical absorption or refractive index as a function of humidity).

- Fiber Bragg grating sensors

For a grating sensor, a periodic variation is induced in the refractive index of the fiber core such that only certain wavelengths are reflected, whereas others are transmitted. The wavelength at which light is reflected is referred to as the Bragg wavelength. The fiber optic-based humidity sensor is coated with a moisture-sensitive chemical species, such as polyimide, which is hygroscopic and has a relatively linear volume expansion with increasing humidity. Thus, the period of the grating increases as the polyimide swells, thereby shifting the Bragg wavelength to longer values.

- Interferometric sensors

For this method, a species whose refractive index depends on moisture absorption, such as TiO_2 and SnO_2, is deposited on the end of an optical fiber. Interference between a source wave traveling along the fiber and the wave reflecting from the species gives a spectral response with maximum intensity at specific wavelengths. The wavelengths will shift in a known manner as a function of humidity.

Maturity

Fiber optic humidity sensors have been the subject of laboratory studies at least since the 1980s, but do not yet appear to be commonly available on the commercial market. There is no known use of a fiber optic humidity sensor for a nuclear application where it would be exposed to the temperature and radiation fields analogous to a DCSS.

Measurement Range, Sensitivity, and Longevity

Laboratory studies indicate that fiber optic humidity sensors have sensitivity on par with those of common commercial sensors and are able to detect changes of at least a few percent RH (Yeo, et al., 2005; Mathew, et al., 2010; Gaston, et al., 2003; Consales, et al., 2011). Because they are not yet in common use, the longevity of fiber optic humidity sensors is uncertain, but fiber optic temperature sensors are described as lasting up to 10 years in service.

Space and Power Requirements

The optical fiber itself is very small, on the order of microns to a few millimeters. The analyzer unit, however, may be 10 cm [3.9 in] or more in height, width, and depth, with the need for a continual power supply. If the analyzer cannot be placed inside the overpack to wirelessly transmit data to a receiver outside, a cable would need to pass through the vents or other opening to connect the probe to the analyzer.

Monitoring Area and Data Acquisition

The monitoring area is in the immediate vicinity of the sensors, and multiple sensors would be needed to assess spatial humidity variations, particularly if airflow or temperature gradients cause local differences in humidity. The data acquisition mode for the sensors is digital and can be either continuous or intermittent. The data size per measurement is expected to be small.

Temperature and Radiation Tolerance

The literature describes reliable performance of the fiber optic humidity sensors at temperatures up to 100 °C [212 °F]. An operational temperature limit may be imposed if temperature-sensitive species, such as polymers, are used for moisture absorption. Some work on radiation tolerance of novel fiber optic humidity sensors has been done for the collider at CERN (Berrutti, et al., 2013, 2011). A polyimide in-fiber grating sensor was still functional after exposure to 10 kGy of ionizing radiation, whereas a commercial electric hygrometer was described as being damaged at the same exposure.

Strengths and Weaknesses

Strengths of these systems include the small size of the fibers and resistance to electromagnetic interference.

Weaknesses include lack of commercial availability and lack of demonstrated performance at the temperature and radiation field conditions of the DCSS.

Potential DCSS Use

Fiber optic sensors may be small enough to be positioned in various locations within an HSM or overpack in order to obtain relative humidity information in the environment adjacent to canister surfaces. Long-term use as a humidity monitor for DCSS applications may be limited by the temperature and radiation tolerance. Sensor electronics would need to be shielded or kept out of the high radiation areas.

Unknowns

- Long-term radiation tolerance.
- Effects of dust and particulates.
- System modifications and preparation required for deployment on a DCSS that was not designed for monitoring.

2.2.5 Leakage Monitoring Systems

The leakage monitoring systems described in this section represent a somewhat different approach for humidity measurement. Rather than measuring humidity at the site of the sensor, air is captured with a passive element and transferred to a remote humidity analyzer, thereby eliminating the need for an electronic sensor in a potentially adverse environment. This technology has been developed to detect moist air, which could indicate leakage from nuclear power plant pressure boundary components. Two systems have been identified and seem to operate in a similar manner: the Areva Flüs system (Areva, 2009) and the Westinghouse Leakage Monitoring Systems (Westinghouse Electric Company, 2011).

Measurement Principle

A sensor tube is routed along a piping system or on a component surface, such as the reactor pressure vessel head. Diffusion windows through which moisture can enter the sensing tube are spaced at intervals along the length. Air is circulated through the tube and is passed through a central humidity measurement station. When there is a leak in the pipe or component, the local moisture content in the air increases and then enters the sensor tube through the diffusion windows. Depending on the humidity-time profile calculated at the monitoring station and the known flow velocity in the tube, the location of the leak can be determined. The type of humidity sensor inside the measurement station is not described in the product literature, but is likely to be one of those described in previous sections.

Maturity

These are generally mature technologies that have already been deployed in nuclear plant service. Therefore, they would be accepted into a plant qualification and quality assurance program.

Measurement Range, Sensitivity, and Longevity

Product literature for the Areva Flüs system describes its sensitivity in terms of leakage detection capability. It states that field experience and leak simulations showed a threshold leakage rate of less than 1 kg/hr [2.2 lb/hr], with the ability to identify the leakage location to within 2 m [6.6 ft] along the length of the sensing line. Literature for the Westinghouse Leakage Monitoring System states that it has relative humidity accuracy of ±1.5 percent at 23 °C [73 °F]. An Areva Flüs system has been used on the reactor pressure vessel head at the Davis-Besse plant since 2003 (NRC, 2010b).

Space and Power Requirements

Product literature for the Areva Flüs system states that the sensing line itself can be made of stainless steel or flexible corrugated tubes. The monitoring station through which the sensor lines are circulated appears to be at least 1 m [3.3 ft] in height, width, and depth, with the need for a continual power and water supply. For the nuclear power plant applications, this unit is typically deployed at an accessible area of containment. With a data link, a separate analysis and control unit can be set up outside of containment. If the monitoring station could not fit inside the overpack, the sensor lines would need to pass through the vents or other opening. Product literature for the Westinghouse Leakage Monitoring System indicates that it is similar in size and setup to the Areva Flüs system.

Monitoring Area and Data Acquisition

Product literature for the Areva Flüs system states that a single sensing line may be up to 300 m [984 ft] in length and that a single monitoring station can manage up to eight lines. Typical spacing of diffusion windows is given as 50 cm [20 in]. Data from analyzed samples are stored as an electronic data file. Both continuous and intermittent data acquisitions are possible.

Temperature and Radiation Tolerance

Areva Flüs system sensor lines are made of stainless steel tubing. The product literature states that it is temperature and radiation resistant and would be suitable for deployment in such locations as the reactor pressure vessel head and primary piping systems. The Westinghouse Leakage Monitoring System is described as having a sensor operating temperature from −15 to 85 °C [5 to185 °F] with no sensitivity degradation at a background radiation level of 100 mR/hr.

Strengths and Weaknesses

Strengths of these systems include the small size of the sensing lines, lack of electrical equipment exposed to aggressive environments, and the ability to monitor humidity at many locations along a single line that can provide spatial humidity information. Further, they have already been demonstrated to be suitable for nuclear plant deployment.

Weaknesses include the need for the sizable monitoring station through which the sensing lines are routed. Currently available systems also have significant instrumentation requirements for the data acquisition and require both a source of electrical power and a constant supply of water. The installation of this system also is more complex because it involves positioning of sample collection lines.

Potential DCSS Use

The leakage monitoring systems have been designed to operate in environments that are somewhat similar to those expected for DCSSs. Product literature for the Areva Flüs system specifically states that it is suitable for monitoring the humidity in equipment compartments. These systems could, in principle, be used to supply real-time humidity monitoring capability. Because there are multiple diffusion windows on the sensor line, the units may be useful for determining spatial humidity variations.

Given the unit size and configuration of the sampling lines, it is unlikely that the systems could be utilized in an existing DCSS. Significant planning would be necessary to install or position the sensing line near the canister surface. In addition, the instrumentation required to obtain the samples and conduct the analyses is substantially more complex than the electronics used in other humidity sensor systems. All of the sensing instrumentation would need to be located external to the overpack or HSM and shielded from the elevated temperatures and high radiation environments. It is unclear whether the sampling tube would require periodic maintenance or replacement.

Unknowns

- Type of humidity sensors used in the monitoring station.
- Effects of dust and particulates on system performance.

- Maintenance requirements for DCSS applications.

- System modifications and preparation required for deployment on a DCSS that was not designed for monitoring.

2.2.6 Psychrometers

Measurement Principle

A psychrometer is a device with two temperature measurement sensors, such as thermocouples or RTDs. One of the thermocouples or RTDs is exposed to the environment to be monitored while dry, and the second thermocouple or RTD is exposed to the same environment to be monitored while wet. The former is referred to as the dry bulb and the latter as the wet bulb. A common practice is to have a durable fabric sleeve covering the wet bulb that is kept wet. When exposed to air, the evaporation of water from the wet bulb lowers the temperature relative to the dry bulb. The relative humidity can be calculated by the temperature difference. Lower humidity leads to a greater temperature difference.

Maturity

Handheld psychrometers are readily available on the commercial market and commonly used for nuclear and non-nuclear applications, particularly in the heating, ventilation, and air conditioning sector. Remote or wireless units are more likely to be useful for DCSSs and were the focus of the discussion in this section. An internet search indicated that units with remote probes and wireless transmitters are available from Omega Engineering Inc. (2012) and Fieldpiece Instruments Inc. (2010), among others. Wet and dry bulb temperatures are typically measured by thermocouple. In principle, a psychrometer could be developed using a different temperature measurement technique, such as RTD, but these were not identified on the commercial market.

Measurement Range, Sensitivity, and Longevity

Product literature for commercial psychrometers indicates accuracy within a range of ±3 percent relative humidity. Because of the need to maintain moisture on the wet bulb, these units would be used for intermittent or periodic measurements. Therefore, the longevity is not evaluated as part of this assessment.

Space and Power Requirements

Commercial wireless psychrometers are relatively small, a few 10s of millimeters [hundreds of mils] in height, width, and depth. A probe could wirelessly transmit to a receiver outside the overpack, or cables would need to pass through the vents or other opening to connect the probe to the readout. Because intermittent or periodic use is expected, units may operate on battery power.

Monitoring Area and Data Acquisition

The monitoring area is in the immediate vicinity of the sensors, and multiple sensors would be needed to assess spatial humidity variations, particularly if airflow or temperature gradients cause local differences in humidity. The data acquisition mode for the commercially available

psychrometers is digital and intermittent. The data size per measurement is expected to be small.

Temperature and Radiation Tolerance

Product literature for the commercial psychrometers indicates operable temperature up to 100 °C [212 °F] and is limited to the boiling point of water. There is no known information on the radiation tolerance of psychrometers; however, thermocouples and RTDs can have high radiation tolerance. Measurement instrumentation using standard electronics has low radiation and temperature tolerance. Typically, the instrument is connected to the thermocouples or RTDs via cable, which allows the instrument to be kept in a less aggressive environment.

Strengths and Weaknesses

Strengths of psychrometers include their high accuracy and small probe size. The means by which relative humidity is calculated is straightforward and does not rely on changes to the physical properties, such as capacitance or resistance. The probes can be made using thermocouples or RTDs that have high radiation tolerance.

Weaknesses include the requirement of a water source to obtain a valid wet bulb temperature. There is no known use of a psychrometer for a nuclear application where it would be exposed to the temperature and radiation fields analogous to a DCSS.

Potential DCSS Use

Given the limited temperature range and the need to have one of the temperature measurement sensors continuously wet, it is unlikely that psychrometers would be utilized to monitor humidity in DCSSs.

Unknown

- System modifications and preparation required for deployment on a DCSS that was not designed for monitoring.

2.3 Chloride Ion Monitoring for External Environment

Solutions formed by the dissolution of deposited salts may contain a range of cations and anions. Cations from commonly deposited soluble salts include sodium, calcium, magnesium, and potassium. Commonly deposited anions are numerous and include chloride, nitrate, nitrite, carbonate, bicarbonate, phosphate, and sulfate. The deliquescence of salts that are present in atmospheric particulate matter and deposit on the dry cask storage canister outer surface can result in the formation of a brine solution, as discussed in Section 2.2. If such conditions occur, monitoring the chloride concentration would be relevant because chloride ions can cause corrosion, including SCC of the stainless steel canister, as well as degradation of other materials. There is extensive literature on technologies for specifically detecting and measuring chloride ions using devices and sensors. Some of these devices and sensors can be used to measure the chloride concentration of brines in contact with a DCSS. To be useful for measuring chloride ion concentration, most of the sensors must be immersed in the solution to be analyzed, which means a horizontally positioned sample cell or container is necessary to collect the deposited salts and to contain the deliquescent brine that forms.

The wet candle method specified in ASTM G140 (ASTM International, 2008) uses a wet wick of a known diameter and surface area to measure aerosol deposition. The wick is maintained wet using a reservoir of water or a 40 percent glycol and water solution. Particles of salt or spray are trapped by the wet wick and retained. At intervals, a quantitative determination of the chloride collected by the wick is made and a new wick is exposed. The wet candle method measures the total amount of chloride arriving on a vertical surface, giving an indication of the salinity of the atmosphere rather than the chloride concentration of exposed metal surfaces. There are some commercially available, one-time, conductivity-based devices measuring soluble salt concentration. Note that conductivity is influenced by all soluble species, and the conductivity-based, one-time soluble salt measurement devices measure the total concentration of soluble salts. Features of these systems are described in Section 2.3.1 and summarized in Table 2-4.

Chloride ion-specific sensors can be broadly classified into four types: (i) optical, (ii) electrochemical, (iii) electromechanical, and (iv) electrical. Optical methods can be further subdivided into techniques based on the following technologies: (i) long-period grating, (ii) fluorescence spectroscopy, (iii) absorption spectroscopy, and (iv) quantum dots. Electrochemical methods include technologies that use silver/silver-chloride (Ag/AgCl) electrodes and all-solid-state chloride electrodes. Features of these chloride ion-specific sensors also are summarized in Table 2-4 and are described in more detail in Sections 2.3.2 through 2.3.8.

Of the chloride ion monitoring methods described in this report, none have been qualified or evaluated for service in harsh environments, such as those defined in IEEE-323 (IEEE, 2003). At present, only a conductivity-based method that required manual collection of the deposits has actually been used to evaluate the deposits on a DCSS. While not actually deployed in the field, some of the sensors included here have some notable advantages. For example, the long-period grating optical method offers the advantages of simplicity of fabrication; ease of interrogation; and potential for onsite, real-time, and remote sensing using fiber optic cables. Similarly, the fluorescence optical method has the advantages of ease of interrogation using fiber optics and the potential for onsite, real-time, and remote sensing. The high-electron mobility transistor method has the advantages of a small sample volume requirement and the possibility of onsite, real-time, and remote sensing. Both absorption spectroscopy and electrochemical sensors require a volume of solution to determine chloride ion content and are probably better suited for analyses of bulk solutions rather than the comparatively small volumes that are expected in the formation of deliquescent brines. Quantum dots and electromechanical sensors are not, and additional technology development and testing are necessary to evaluate the applicability of these sensors for DCSS applications.

2.3.1 Conductivity-Based Soluble Salt Measurement Meters

Measurement Principle

Various devices and meters were developed to assess the level of soluble salt ions (i.e., chlorides, sulfates, and nitrates) deposited on substrate and in air in which the conductivity is proportional to the concentration of dissolved salts in the solution. In coastal regions, it is very likely that the soluble salts are from sea salt. Assuming a seawater-derived ion assemblage and using known molar conductivities for the ions, a chloride ion concentration can be inferred from the conductivity measurement results. Although their detailed procedures vary depending on the sampling device, all of them operate in the following basic steps: (i) collect

Table 2-4. Chloride Ion Monitoring Techniques				
Features	**Conductivity-Based Meter* (Section 2.3.1)**	**Long-Period Grating-Based Optical Sensor (Section 2.3.2)**	**Fluorescence-Based Optical Sensor (Section 2.3.3)**	**High-electron Mobility Transistor-Based Sensor (Section 2.3.4)**
Maturity	Field deployed in nuclear applications	Tested in laboratory	Tested in laboratory	Tested in laboratory
Measurement Range	0–0.155 g/m^2 [3.2×10^{-5} lb/in^2]	Not specified	Not specified	Not specified
Sensitivity	0.001 g/m^2 [1.4×10^{-5} lb/in^2]	4 to 320 g/m^2 [5.7×10^{-6} to 4.5×10^{-4} lb/in^2]	4 to 5.8 g/m^2 [5.7×10^{-6} to 8.2×10^{-6} lb/in^2]	4 to 5.8×10^{-6} g/m^2 [5.7×10^{-6} to 8.2×10^{-12} lb/in^2]
Longevity	One-time use device	~1 year†	~1 year†	Less than 1 year
Space Requirements	$10 \times 1.5 \times 1$ cm^3 [$3.9 \times 0.59 \times 0.4$ in^3]	$2.5 \times 2 \times 2$ cm^3 [$0.98 \times 0.79 \times 0.79$ in^3]	$2.5 \times 2 \times 2$ cm^3 [$0.98 \times 0.79 \times 0.79$ in^3]	Less than $1 \times 1 \times 1$ cm^3 [$0.4 \times 0.4 \times 0.4$ in^3]
Power Requirements	Several watts	Tens to hundreds of watts	Tens to hundreds of watts	Tens to hundreds of watts
Monitoring Area	3 cm^2 [0.5 in^2]	Not specified	Not specified	1 cm^2 [0.16 in^2]
Data Acquisition Mode	Intermittent	Continuous or intermittent	Continuous or intermittent	Continuous or intermittent
Temperature Tolerance	Disposable strip: <100 °C [212 °F] Meter: 0–50 °C [32–122 °F]	Maximum is ~100 °C [212 °F] due to solution evaporation	Maximum is ~100 °C [~212 °F] due to solution evaporation	Maximum is ~100 °C [~212 °F] due to solution evaporation
Radiation Tolerance	Up to 10 Mrad	Unknown (estimated to be ~1 Mrad†)	Unknown (estimated to be ~1 Mrad†)	Unknown (estimated to be less than 0.1 Mrad)
Strengths	Fast and automated method, no sealing to the substrate necessary allowing testing of curved or irregular surfaces	Simple fabrication; easy interrogation using fiber optics; potential for onsite, real-time, and remote sensing	Easy interrogation using fiber optics; potential for onsite, real-time, and remote sensing	Small sample volume; potential for onsite, real-time, and remote sensing
Weaknesses	One-time use, the highest working temperature is only 100 °C [212 °F], measure total salt concentration	Response sensitive to temperature changes; unknown thermal and radiation stability; possible interference by other ions and signal attenuation with increased fiber cable length	Other halide ions and oxygen may interfere; thermal and radiation stability is unknown	Temperature could affect measurement; thermal and radiation stability is unknown; possible signal attenuation with increased electrical cable length

*The information is for the SaltSmart™ Meter.
†This is based on the general practice.

Table 2-4. Chloride Ion Monitoring Techniques				
Features	**Absorption Spectroscopy (Section 2.3.5)**	**Quantum Dots (Section 2.3.6)**	**Electrochemical Sensors (Section 2.3.7)**	**Electromechanical (Section 2.3.8)**
Maturity	Trial field testing in bridges	Under development	Commercially available but relatively new	Under development
Measurement Range	Not specified	Not specified	Not specified	Not specified
Sensitivity	Not specified	Not specified	Not specified	Not specified
Longevity	Not specified	Not specified	Not specified	Not specified
Space Requirements	Not specified. Sensor estimated to be 5 cm × 5 cm × 10 cm [2 in × 2 in × 4 in]	Not specified	Not specified	Not specified
Power Requirements	Not specified	Not specified	Not specified	Not specified
Monitoring Area	Not specified	Not specified	Not specified	Not specified
Data Acquisition Mode	Not specified	Not specified	Not specified	Not specified
Amount of Data Per Measurement	Not specified	Not specified	Not specified	Not specified
Temperature Tolerance	Not specified	Not specified	Not specified	Not specified
Radiation Tolerance	Not specified. Target application does not require radiation resistance	Not specified. Target application does not require radiation resistance	Not specified. Target application does not require radiation resistance	Not specified. Target application does not require radiation resistance
Strengths	Designed for field use and automated data collection	Designed for biotechnology applications to measure small solution volumes	Designed for field use and automated data collection	Designed for field use
Weaknesses	Limited information on the sensor or the capabilities of the system.	Little information available on capabilities and limitations.	Little information available on capabilities and limitations.	Little information available on capabilities and limitations.

and dissolve salts, (ii) measure conductivity of soluble salt, and (iii) convert measured conductivity to salt concentration.

Most of the dry methods use mechanical means (i.e., scraping, brushing, and vacuuming) to collect the salts. This section primarily focuses on the wet method to collect the salt. The varieties include, but are not limited to, (i) Bresle standard method, (ii) soluble salt meter, (iii) SaltSmart™ Meter, and (iv) air sampling device from Japan's Central Research Institute for the Electric Power Industry (CRIEPI).

The Bresle standard method complies with the International Organization for Standardization (ISO) (ISO, 2006, ISO 8502-6; 1998, ISO 8502-9) and is operated manually with a chloride test kit as the main component. The kit includes a case, digital conductivity meter, 25 Bresle patches, distilled water, calibration and cleansing solutions, cups and syringes, and an illustrated manual. The test surface can be horizontal, vertical, slanting, or somewhat bulging. There are 16 detailed steps in the measurement; the major steps are shown in Figure 2-4 and include (i) affix patch to substrate with flexible foam seal and press firmly to create a tight seal, (ii) inject water and mix to dissolve the water soluble salts, (iii) extract water into beaker, and (iv) measure conductivity. Because each step is performed manually, the analysis is time consuming and may not be reproducible. In addition, there may be capillary flow under the flexible foam seal and the surface area may vary due to stretching of the patch. Because of these issues, other automated methods have been developed to replace this method.

The soluble salt meter was developed as a direct replacement for the Bresle patch method. It exactly replicates the Bresle method, but the entire process is automated and there are no consumables, sticky residue, and syringe. Each measurement takes only 1 minute, but this meter only works for magnetic material (i.e., carbon steel) because it uses magnets to adhere to the sampling surface.

Another automated method is the commercially available SaltSmart Meter (Louisville Solutions Incorporated, 2013). The salt is extracted from the substrate by a strip, which is a one-time-use disposable device with everything premeasured and in a sealed, contamination-free pouch. The strip uses a patented continuous flow extraction method in a defined area where >99 percent of the salt can be extracted. Figure 2-5 schematically shows the water extraction mechanism. Engineered fiber is used to extract the salt in a defined area and absorb the extract. The meter reads the conductivity. Sealing on the substrate surface is not needed. However, the strip needs to be in direct contact with the measuring surface. The device works on all surface geometries, including vertical, horizontal, curved, overhead, magnetic, and nonmagnetic surfaces. One-time use eliminates cross contamination, syringes, and measurements of liquids in the field.

Japan's CRIEPI developed a salt sampling device in which air is pumped in through an air inlet nozzle. The sea salt in the air is dissolved in the water, and the amount of ions in the sample of this water is measured by conductivity or by ion chromatography, depending on the design (Wataru, et al., 2006). Figure 2-6 shows the view of the air sampling device. Similar to the wet candle method, this CRIEPI device only measures the total chloride concentration in the atmosphere rather than that on the metal surface.

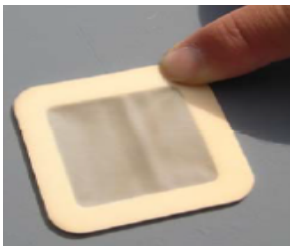

(1) Affix Patch

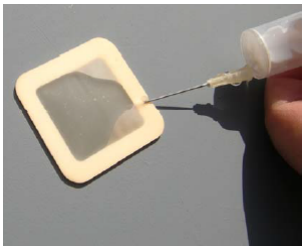

(2) Inject Water

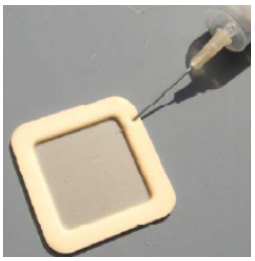

(3) Extract Water

(4) Measure Conductivity

Figure 2-4. Major Steps of the 16 Process Steps for Bresle Method

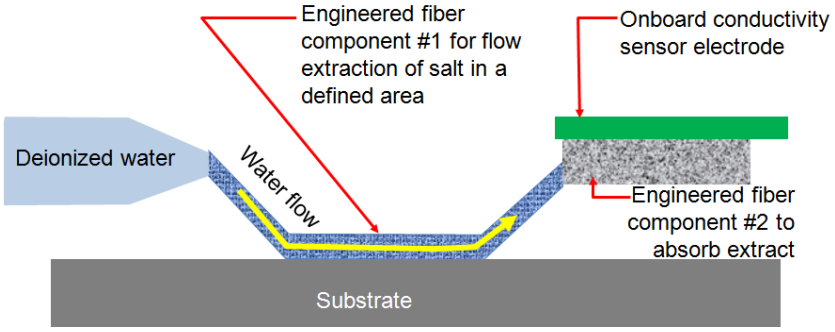

Figure 2-5. Schematics of Disposable Salt Strip

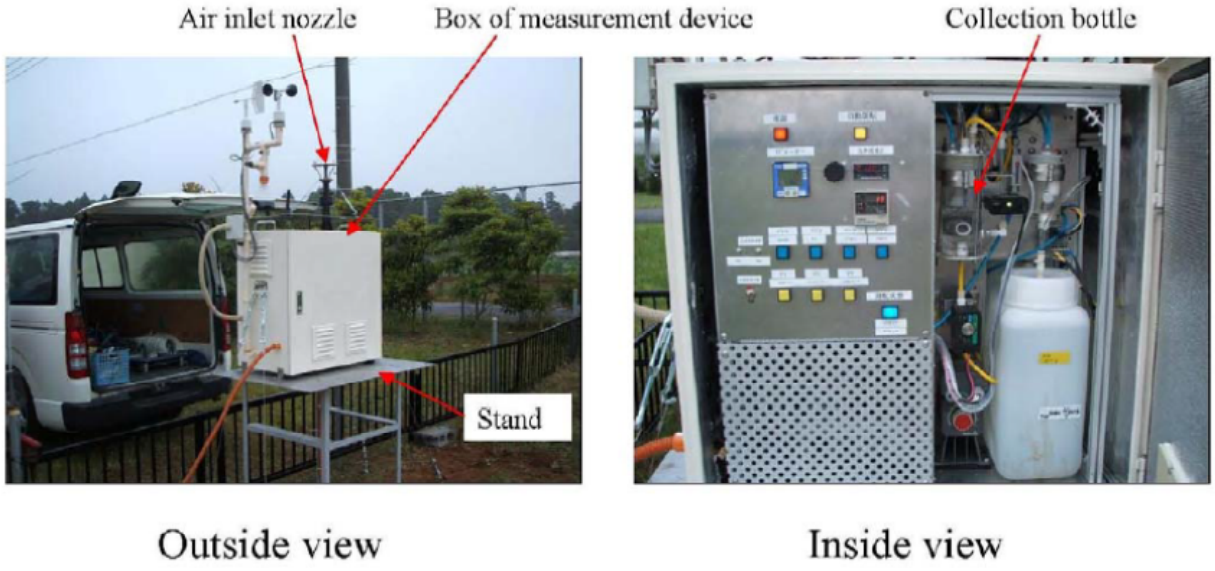

Figure 2-6. Japan's Central Research Institute for the Electric Power Industry Salt Sampling Device (Reproduced With the Permission of Japan's Central Research Institute for the Electric Power Industry)

Maturity

The conductivity-based method was originally developed to assess the level of soluble salt ions (i.e., chlorides, sulfates, and nitrates) on blast-cleaned surfaces prior to coating because these salts may lead to degradation under coating and osmotic blistering.

The Bresle method was first introduced in 1995 and has been widely accepted. Other methods were developed later to replicate the Bresle method with an automated salt sampling device and have been demonstrated to comply with ISO (2006, ISO 8502-6; 1998, ISO 8502-9)standards), as does the manual Bresle method. This type of measurement has been used by the U.S. Navy and the U.S. Department of Transportation on military vehicles, oil rigs, railcars, steel structures, pipelines, bridge repairs, refurbishment pipelines, and water tanks where the coating is used as a protective barrier. The SaltSmart system was developed as a field deployable method for measuring surface salt contamination. It has been utilized by the U.S. Navy for validating adequate cleanliness of surfaces before applying protective coatings. Recently, some mechanical dry salt sampler and the SaltSmart Meter were deployed in the Calvert Cliffs ISFSI inspection to measure the salt concentration for the HSM (NRC, 2012b).

The CRIEPI salt sampling device was used to quantify salt concentration in coastal regions in Japan and has been installed at operating reactor sites where DCSSs for spent nuclear fuel are located (Saegusa, et al., 2010).

Measurement Range, Sensitivity, and Longevity

The Bresle patch method has a reported measurement range of 0 to 0.020 g/m^2 [4 × 10^{-6} lb/ft^2] with a resolution of 0.0001 g/m^2 [2 × 10^{-8} lb/ft^2] (Paul N. Gardner Company, 2013). The Bresle patch method is a one-time use system that requires manual sample collection. The analytical

instrument used to analyze the collected sample can be used repeatedly and would be expected to have longevity of several years.

The SaltSmart system has a reported measurement range of 0 to 0.155 g/m^2 [3.2 × 10^{-5} lb/ft^2] and a sensitivity of 1 × 10^{-3} g/m^2 [2 × 10^{-7} lb/ft^2] (Louisville Solutions Incorporated., 2013). The SaltSmart system is a one-time use collection pad that requires manual sample collection. The analytical instrument used to analyze the collected sample can be used repeatedly and would be expected to have longevity of several years.

No information on the measurement range and resolution of the CRIEPI system is available, but it should be noted that this system collects information on atmospheric salts and is not a direct method for determining the amount of salt deposited on a surface. The correlation between the data obtained and the surface concentration of deposited salts is not available. Longevity of the system is not available.

Space and Power Requirements

The Bresle patch method requires a patch sealed to the sample surface to collect a sample. The patch is approximately 3 cm × 3 cm × 0.3 cm [1.2 in × 1.2 in × 0.12 in]. Note that the space

requirements are larger than the actual area of the collection patch. After applying water to the sampling area defined by the patch, the dissolved salt is collected manually using a syringe. A system to dispense the solution and collect the sample remotely seems possible, but no such system was identified in this review. The hand-held measurement meter uses batteries, and each measurement takes minutes to complete. The power requirement is low—only several watts.

The SaltSmart Meter requires a contact area for the collection strip of approximately 1.5 cm × 2.0 cm [0.59 in × 0.79 in] and does not require sealing to the substrate. The entire strip is 10 cm [3.9 in] long, 1.5 cm [0.59 in] wide, and 1 cm [0.4 in] high, as shown in Figure 2-7. The device uses two AA batteries, and each measurement takes minutes to complete. The power requirement is low—only several watts.

The CRIEPI salt sampling and measurement device shown in Figure 2-6 weighs 60 kg [132 lb], and the size is 70 cm × 70 cm × 40 cm [28 in × 28 in × 16 in]. The dimension of the air inlet nozzle is unknown. By examining the photo in Figure 2-6, the size of the nozzle is 10 times smaller than the box. As such, the size of the nozzle is assumed to be 7 cm × 7 cm × 4 cm [2.8 in × 2.8 in × 1.6 in], which may be able to fit at the air inlet and outlet vents, but the box cannot fit anywhere in the system. The power requirement is 2 kW (20 A at 100 V).

Monitoring Area and Data Acquisition

The sample collection area for the Bresle patch method requires a patch sealed to the sample surface to collect a sample. The patch is approximately 3 cm × 3 cm [1.2 in ×1.2 in]. Each measurement determines the average deposited surface salt concentration defined by the patch area.

The sample collection area of the SaltSmart strip is approximately 3 cm^2 [0.46 in^2] {1.5 cm × 2.0 cm [0.59 in × 0.79 in]}. Measurements can be performed in parallel in different places, covering a larger area. The amount of data per measurement is several bytes.

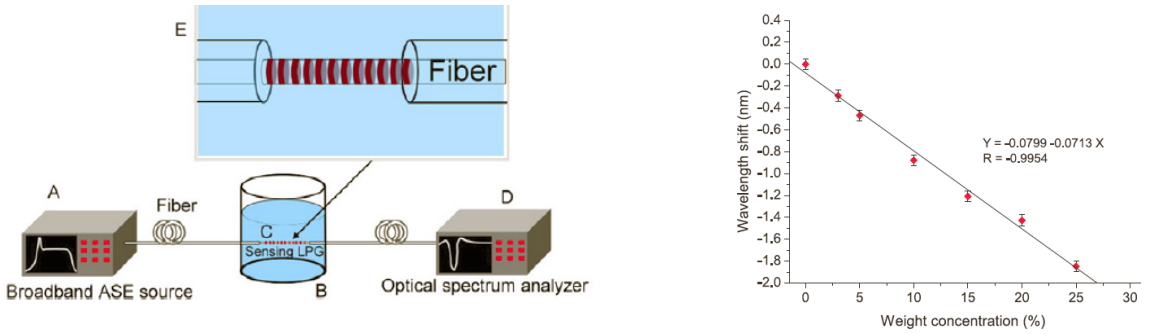

Figure 2-7. (a) Schematic of Experimental Setup Using Long-Period Grating and (b) Data on Wavelength Shift Versus Chloride Ion Concentration (Tang and Wang, 2007) (Reproduced With the Permission of IOP Publishing)

The meter supports electronic capture of 250 measurements for later universal serial bus (USB) download. File formats are compatible with Microsoft® Excel™.

The CRIEPI salt sampling device measures salt concentration in air. Data acquisition details are not reported in literature, but the acquisition mode is intermittent.

Temperature and Radiation Tolerance

Based on the information provided by the manufacturer, the operating temperature range of the Bresle patch system is 0–50 °C [32–122 °F] (Paul N. Gardner Company, 2013).

Based on the information from the manufacturer, the operating temperature range of the SaltSmart Meter also is 0–50 °C [32–122 °F] (Louisville Solutions Incorporated., 2013). The SaltSmart system uses a meter with a liquid crystal display, which may be damaged if heated above 50° C [122 °F]. The manufacturer does not provide the temperature tolerance of the salt strip, but it must be <100 °C [212 °F] because water is used. Because the meter is for external use and each measurement takes only minutes, radiation tolerance of the device is not a main concern. Without additional data to support higher dose levels, the approach for intermittent data collection is expected to be reliable up to 10 Mrad of accumulated dose because detection electronics will not be subjected to the radiation field. Exposure of electronics to high-radiation fields would severely limit the longevity for continuous monitoring.

No specific information on the temperature and radiation tolerance is available for the CRIEPI salt sampling device, but it could be similar to the SaltSmart Meter because the measurement principle is similar.

Strengths and Weaknesses

The Bresle method has a limited range of measurement compared to the SaltSmart system, and its present form requires unrestricted personnel access to the surface of interest and manual testing of the specific area. It also is a single measurement of a collected sample and not a remotely deployable chloride monitoring system. Multiple samples would need to be collected over time to determine the rate of deposition.

Both the Bresle patch method and the SaltSmart system require the use of a hand-held meter to measure conductivity. This allows the meter to be removed from aggressive environments. Both methods also determine salt concentration based on a calculation of the measured conductivity and the surface area sampled. The solution conductivity measured is dependent on the solubility of all the organic and inorganic species sampled. Consequently, chemical analyses are necessary to confirm the calculation of a surface chloride-containing salt concentration from a conductivity measurement is not skewed by non-chloride-containing soluble species.

The SaltSmart Meter does not require sealing to the substrate, which allows for testing of curved or irregular surfaces, including very localized testing of objects. The de-ionized water used as solvent is in premeasured ampoules and requires no measuring or handling. Because a fresh ampoule is used per test, it eliminates chance of cross contamination. There is no residue left on the surface after testing. The sensor requires no manual manipulation while taking the measurement, allowing multiple sensors to be affixed for testing and enabling faster testing of large areas, saving time and labor. The measurements may be stored in the meter for later download, which allows archiving of data. Specialized manipulators have been developed for remotely deploying the disposable salt strip and to collect samples from an actual AREVA/Transnuclear NUHOMS DCSS. The weakness of the SaltSmart Meter is that the strip is a one-time use device. Measurements cannot be performed continuously. The highest working temperature for the strip is 100 °C [212 °F]. The system is based on the deposition of chloride salts, so the deposition of non-chloride-containing soluble salts will result in artificially high chloride concentrations.

The CRIEPI atmospheric monitor is designed for continuous atmospheric monitoring. Additional site-specific surface analysis data would be necessary to correlate the surface salt concentration with a measured atmospheric salt concentration. The system also is quite large and requires periodic access for maintenance. While not specified, the instrumentation and sample collection methods used are likely to have both low temperature and radiation tolerances, making the system unsuitable for remote deployment in aggressive environments.

Potential DCSS Use

The Bresle patch method requires significant manual processing during sample collection. This is a significant limitation that would limit the use of this method to surfaces that are not highly irradiated. The upper temperature limit for sample collection is not stated but would certainly be below boiling, which also limits the use of this method.

The SaltSmart system also used water to dissolve and collect the soluble species on the sample surface and has a temperature limit of 100 °C [212 °F]. This system has been used to collect samples from actual DCSSs, but it must be recognized that the SaltSmart system is not a continuous monitor and is not specific to soluble chloride-containing species. In coastal regions where the atmospheric deposits are likely to have significant chloride-containing salts, the SaltSmart system could potentially be used to periodically determine the amount of salt that is deposited on the DCSS canisters or casks.

The CRIEPI atmospheric monitor is likely to be limited to use in low radiation environments and at near-ambient temperatures. This system could potentially be used to monitor general atmospheric conditions, including the amount of airborne salt that reaches the DCSS air vents shown in Figures 1-1 and 1-2.

Unknowns

- The effect of the range of possible variations in atmospheric conditions on the relationship between conductivity and salt concentration.
- Time- and temperature-dependent decomposition reactions that may result in changes in the chemistry of atmospheric deposits.
- The applicability of atmospheric monitoring to determine surface deposition rates and chemistry.

2.3.2 Long-Period, Grating-Based Optical Sensor

Measurement Principle

This is a fiber optic method. A long-period grating is a periodic perturbation, typically on the order of several hundreds of micrometers [several mils], of the refractive index along the core of a fiber optic cable that is created when the fiber is exposed to ultraviolet light (Lam, et al., 2009). The transmission spectrum of a typical long-period grating comprises a number of attenuation bands in an optical fiber. When there is a concentration change (e.g., in chloride concentration) that causes a refractive index change in the surrounding medium, the center wavelengths of an attenuation band also change. Figure 2-7(a) shows a schematic representation of an experimental setup using a long-period grating sensor. A measuring system that uses a long-period grating sensor requires a broadband amplified spontaneous emission (ASE) fiber source, a sensing long-period grating fiber, a sample cell that contains the solution to be measured, and an optical spectrum analyzer (OSA) (Tang and Wang, 2007).

Maturity

Long-period grating sensors have been tested only in the laboratory.

Measurement Range, Sensitivity, and Longevity

Figure 2-7(b) shows data from Tang and Wang (2007) on the wavelength shift of a bare long-period grating sensor in sodium chloride solution with increasing chloride concentration.

Based on the data, Tang and Wang (2007) estimated a ~0.01 M Cl^- lower detection limit of the long-period grating sensor. The authors stated that a 1 ppm Cl^- detection limit can be achieved using a gold-coated, long-period grating sensor and an OSA with a spectral resolution of 0.1 picometer [4×10^{-8} mils]. Based on a detection limit of 0.01 M Cl^-, the estimated minimum mass of deposited NaCl (e.g., on the canister surface) that can be detected ranges from 4 to 320 g/m^2 [5.7×10^{-6} to 4.5×10^{-4} lb/in^2]. The estimated range will vary with the temperature and RH of the environment. No information was located on the longevity of this analytical method.

Space and Power Requirements

The physical size of a monitoring system (not including the ASE and OSA) would be approximately that of the cell containing the solution to be measured for chloride concentration. The cell must be large enough to immerse the long-period grating sensor in the solution. A typical long-period grating is 20 mm [0.79 in] long and is fabricated using standard

telecommunications (e.g., Corning SMF–28) fibers, which typically have a 0.245-mm [0.01-in] diameter. The dimension of the cell can be less than 2.5 cm^3 × 2 cm^3 × 2 cm^3 [0.98 in × 0.79 in × 0.79 in^3]. As a result, the space required is less than 10 cm^3 [0.61 in^3].

The equipment external to the dry storage system uses 110 V AC. The power requirement is moderate—on the order of tens to hundreds of watts.

Monitoring Area and Data Acquisition

The monitoring area for this method is not established, and it is currently a laboratory method. As a first approximation, the monitoring area can be assumed to be similar to the cross-sectional area of the measurement cell or 2.5 cm^2 × 2 cm^2 [0.98 in^2 × 0.79 in^2]. Data are stored in an electronic data acquisition file, and the amount of data per measurement will be a few kilobytes. Both continuous and intermittent data acquisitions are possible.

Temperature and Radiation Tolerance

Long-period grating can be very sensitive to changes in temperature and to deformations in the fiber. Therefore, changes in temperature and deformations must be compensated or avoided to correctly measure variations in concentrations. Some authors have proposed using two sensors to compensate for temperature effects. For example, Shu, et al. (2001) proposed using an FBG sensor to measure the temperature effect and a long-period grating sensor to measure the change in refractive index in response to a change in chloride concentration. However, further studies are warranted on methods to compensate for temperature effects on long-period grating sensor measurements. In a DCSS, the evaporation of aqueous solutions would limit the application of these sensors to less than ~100 °C [~212 °F].

The thermal and radiation stability of these sensors is unknown and needs to be evaluated. Degradation of optical components due to radiation is known to occur. The effect of the accumulated degradation on the measurement approach is unknown, and there is an absence of radiation tolerance data on this sensor. Given these large uncertainties, the sensor is estimated to function at accumulated doses of 1 Mrad because detection electronics can be located away from the measurement site, so that only optical components would be subjected to the most intense radiation fields (refer to Appendix A for details).

Strengths and Weaknesses

Strengths of long-period grating sensors are their simple fabrication, inexpensive cost, and easy interrogation (Tang, et al., 2006; Tang and Wang, 2007). In combination with fiber optic cables, the sensor has the potential for onsite, real-time, and remote sensing capability and automated measurements.

Weaknesses of this method are its present state of development and limitations of laboratory use. A field-hardened system has yet to be developed. The method is only applicable to the measurement of chloride ions in solution. In addition, the radiation and temperature tolerances are not known. Chloride measurements in the laboratory have used pure sodium chloride solutions, and the possible interference by other species in solution (i.e., sulfate, nitrate, and hydroxide ions) has not been studied. Possible signal attenuation with increased fiber optic cable length also is a concern.

Potential DCSS Use

The long-period, grating-based optical sensor is a laboratory technique that measures chloride ion concentrations in solution. In principle, this type of sensor could potentially be used to monitor chloride concentration and/or deposition rate in remote applications. The ASE and OSA are coupled to the long-period grating sensor through a fiber optic cable. However, given large uncertainties due to a lack of data on the sensitivity of the measurement approach to known radiation-induced degradation effects on fiber optical components, radiation testing would be necessary to provide confidence that reliable data would be obtained. Much more additional information is necessary to evaluate whether this system may be applicable for chloride monitoring in DCSS applications, including specifications and operational limitations.

Unknowns

- Interference by other species in solution (i.e., sulfate, nitrate, and hydroxide ions) has not been studied.
- Possible signal attenuation with increased fiber optic cable length.
- Radiation and temperature tolerance of the system.

2.3.3 Fluorescence-Based Optical Sensor

Measurement Principle

This also is a fiber optic method. Typically, when ultraviolet light illuminates a fluorophore (a chemical compound that can re-emit light upon light excitation), visible fluorescence is produced. Chloride ions can cause collisional quenching in certain fluorophores, which results in a reduced fluorescence intensity that is proportional to the log of chloride ion concentration. The decrease in fluorescence emission intensity can be measured and related directly to the chloride concentration. Several chloride ion-sensitive fluorophores are known, including SPQ (6-methoxy-N-3-sulfoproxyl-quinolinium), SPA (N-sulfopropylacridinium), Lucigenin (N,N'- dimethyl-9-9'-bisacridinium nitrate), MACA (N-methylacridinium-9-carboxamides), and MAMC (N-methylacridinium-9-methylcarboxylate).

Fluorophores are immobilized ("trapped" or covalently linked) either to the surface or within organic or inorganic polymers. The sensor membranes or films that are produced then can be mounted on the tip of optical fibers to produce optrodes (Geddes, 2001). Figure 2-8 is an example of an experimental setup using a fluorescence-based chloride ion sensor. The system includes a light-emitting diode emitting at 365 nm [0.014 mils] that is coupled through a multimode fiber, using collimation and focusing lenses, into a 2 × 1 fiber coupler, with the sensor material located at the distal end of the fiber. The fluorescence from the material is collected by the other end of the fiber coupler, passed to a spectrometer, and then displayed on a computer screen.

Maturity

Fluorescence-based optical sensors have been tested only in the laboratory.

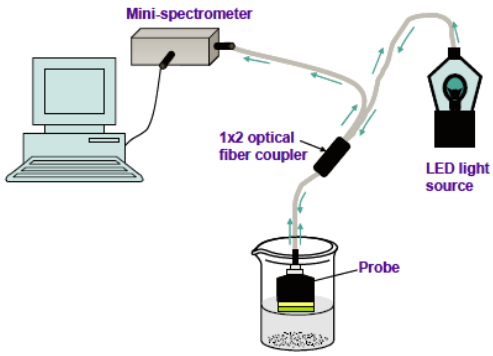

Figure 2-8. Experimental Setup of Fluorescence-Based Chloride Ion Sensors (Nguyen, et al., 2009) (Reproduced With Permission of SPIE)

Measurement Range, Sensitivity, and Longevity

Urbano, et al. (1984) reported a lower detection limit of 0.1 M Cl^- using this type of sensor. Based on a detection limit of 0.1 M Cl^-, the estimated minimum mass of NaCl deposited (e.g., on a surface) that can be detected ranges from 4 to 5.8 g/m^2 [8 × 10^{-4} to 1.2 × 10^{-3} lb/ft^2]. The estimated range is not defined but will vary with the temperature and RH of the environment. The longevity of the sensor is not reported in the literature, and the method is currently limited to laboratory instruments.

Space and Power Requirements

The physical size of the measuring system that uses a fluorescence-based optical sensor (not including the light-emitting diode and spectrometer) would be approximately that of the cell containing the solution to be measured for chloride concentration. The sample cell must be large enough to immerse the fluorescence sensor in the solution. The dimension of the cell can be less than 2.5 cm^3 × 2 cm^3 × 2 cm^3 [0.98 in^3 × 0.79 in^3 × 0.79 in^3], which can fit between the canister and overpack. As a result, the space required is less than 10 cm^3 [0.61 in^3].

The equipment external to the dry storage system uses 110 V AC. The power requirement is moderate—on the order of tens to hundreds of watts.

Monitoring Area and Data Acquisition

The monitoring area of this method is not specified. As a first approximation, the monitoring area may be approximately that of the cell containing the solution to be measured for chloride concentration. The measured decrease in fluorescence emission intensity is used to calculate chloride ion concentration, which is written to a data acquisition file. The estimated file size per measurement is a few kilobytes. Both continuous and intermittent data acquisitions are possible.

Temperature and Radiation Tolerance

The evaporation of aqueous solutions would limit the application of these sensors to less than ~100 °C [~212 °F]. The thermal and radiation stability of these sensors is unknown. Degradation of optical components due to radiation is known to occur. The effect of the accumulated degradation on the measurement approach is unknown, and there is an absence

of radiation tolerance data on this sensor. The detection electronics can be located away from the measurement site, so that only optical components would be subjected to the most intense radiation fields on the canister surface (see Appendix A for details).

Strengths and Weaknesses

Strengths include easy interrogation using fiber optics and their potential for onsite, real-time, and remote sensing capability. The data acquisition mode can be continuous or intermittent, allowing for periodic measurements.

There are several weaknesses of this method. At present, this is a laboratory-based method that has not been packaged for field use. It also is limited to measurement of chloride ions in solution. Fluorescence quenching is not a particularly selective process, and other halide ions (i.e., iodide and bromide), if present, also will be quenched and interfere with the chloride measurement (Geddes, 2001). Dissolved oxygen also could affect the chloride-sensing measurements. However, the effect of interferences can be corrected if the fluorophore response to the interference is known (Geddes, 2001). Leaching of the fluorophore from the sensor (sensor bleeding) also can occur, which usually increases with temperature and is greater in flow cell measurements where fluid is continuously washing over the surface of the sensor (Geddes, 2001). The thermal and radiation stability of these sensors also is unknown and needs to be studied. In addition, signal attenuation with increased fiber optic cable length could occur and needs to be evaluated.

Potential DCSS Use

The fluorescence-based chloride ion optical sensor is a laboratory technique that measures chloride ion concentrations in solution. In principle, this type of sensor potentially could be used to monitor chloride concentration and/or deposition rate in remote applications. However, given large uncertainties due to a lack of data on the sensitivity of the measurement approach to known radiation-induced degradation effects on fiber optic components, radiation testing would be necessary to provide confidence that reliable data could be obtained when subjected to intense radiation fields. Additional information is necessary to evaluate whether this system may be applicable for chloride monitoring in DCSS applications, including specifications and operational limitations.

Unknowns

- Interference by dissolved oxygen and other halide ions in solution.
- Possible signal attenuation with increased fiber optic cable length.
- Radiation and temperature tolerance of the system.

2.3.4 High-Electron Mobility Transistor-Based Sensor

Measurement Principle

This type of sensor uses an aluminum gallium nitride/gallium nitride (AlGaN/GaN) high-electron mobility transistor. Positive countercharges at the high-electron mobility transistor surface layer are induced by the two-dimensional (2-D) electron gas located at the AlGaN/GaN interface. Any slight changes in the atmosphere can affect the surface charge of the high-electron mobility transistor, thus changing the electron concentration in the channel at the AlGaN/GaN interface. The high-electron mobility transistor structure consists of a 1–3 μm [0.04–0.12 mils]-thick

undoped GaN buffer and 250-Å-thick undoped $Al_{0.25}Ga_{0.75}N$ cap layer deposited on 100 mm [3.9 in] (111) silicon substrate. Depending on the gate area modification, AlGaN/GaN high-electron mobility transistor sensors can be used for different applications (i.e., gas sensing) to detect hydrogen, carbon dioxide, and ammonium and liquid sensing to detect protein, deoxyribonuclei acid, lactic acid, solution pH, glucose, chloride ion, and mercury ion (Chu, et al., 2010). For use as a chloride sensor, the gate area of the high-electron mobility transistor structure is deposited with an indium nitride (InN) film (Chu, et al., 2010). The measured drain current of the InN-gated AlGaN/GaN high-electron mobility transistor in chloride-containing solutions is linearly proportional to the logarithm of chloride concentration, consistent with the Nernst equation.

Maturity

This type of sensor has been tested only in the laboratory.

Measurement Range, Sensitivity, and Longevity

The estimated range is not specified but will vary with the temperature and RH of the environment. Figure 2-9 shows a photomicrograph and schematic of a silver/silver chloride (Ag/AgCl) gated high-electron mobility transistor and its signal response to varying chloride ion concentrations. The gate area for sensing typically is 10 × 50 μm^2 [0.016 × 0.8 $mils^2$] and could measure a solution volume of ~3 × 10^{-11} L [8 × 10^{-12} gal] (Chu, et al., 2010). Hung, et al. (2008) reported a detection limit for this device of 1 × 10^{-8} M Cl^-. Based on a detection limit of 1 × 10^{-8} M Cl^-, the estimated minimum mass of NaCl deposited (e.g., on a surface) that can be detected ranges from 4 to 5.8 × 10^{-6} g/m^2 [5.7 × 10^{-6} to 8.2 × 10^{-12} lb/in^2].

The longevity of the sensor is unknown because it is not reported in the literature.

Space and Power Requirements

The dimensions of the sensor are not reported in the literature, but the transistor can be very small because the layers in Figure 2-9(a) are reported to be very thin. The transistor needs to be immersed in solution, and the solution amount can be very small. Considering this, the dimensions of the cell can be made less than 1 cm^3 × 1 cm^3 × 1 cm^3 [0.4 in^3 × 0.4 in^3 × 0.4 in^3]. As such, the space required for the sensor can be less than 1 cm^3 [0.06 in^3].

The equipment external to the dry storage system uses 110 V AC. The power requirement is moderate—on the order of tens to hundreds of watts.

Monitoring Area and Data Acquisition

The monitoring area of this system would be defined by the size of the cell containing the sensing element. The sensing element is typically 10 × 50 μm^2 [0.016 × 0.8 $mils^2$], which would allow a sample cell to be 1 cm^3 × 1 cm^3 × 1 cm^3 [0.4 in^3 × 0.4 in^3 × 0.4 in^3] or smaller. No information is available on the data acquisition system.

Temperature and Radiation Tolerance

The measurement is sensitive to temperature. The temperature tolerance is unknown, but the maximum is ~100 °C [212 °F], due to solution evaporation. The radiation stability of high-electron mobility transistor-based sensors also is unknown.

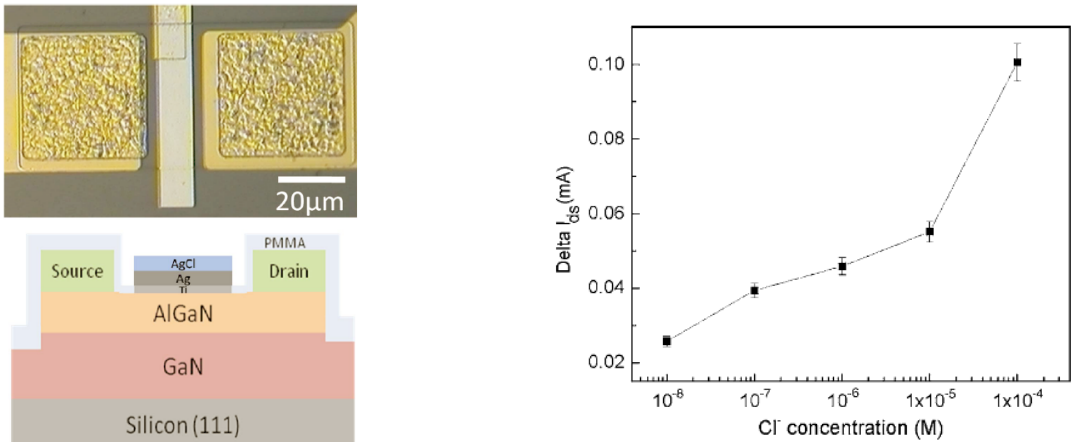

(a) **(b)**

Figure 2-9. (a) Upper Figure Shows a Photomicrograph of an Ag/AgCl Gated AlGaN/GaN High-Electron Mobility Transistor; Lower Figure Shows a Schematic Cross-Sectional View of an Ag/AgCl Gated High-Electron Mobility Transistor and (b) Drain Current Change of an Ag/AgCl Gated High-Electron Mobility Transistor as a Function of Chloride Concentration (Hung, et al., 2008) (Reproduced With the Permission of the American Institute of Physics)

Commercial off-the-shelf microcircuits and analog or digital electronic components typically have total dose tolerance limits that range from a few krad to tens of krad. Individual commercial off-the-shelf components may continue to function at higher accumulated total doses. However, components capable of tolerating a total integrated dose in the range of one hundred krad to a few hundreds of krad (a tenth to a few tenths of Mrad) are commonly referred to as "radiation hardened," after being subjected to standard protocols for irradiation and electronic performance evaluation.

Strengths and Weaknesses

Strengths of the high-electron mobility transistor-based sensors are their very small sample volume requirement and their potential for onsite, real-time, and remote sensing capability.

Weaknesses of this method include limited (laboratory only) use and environmental limitations. The system only measures chloride ions in solution. The method may not be sensitive to the specific anion present in solution, but the possible interference by other anions (i.e., sulfate, nitrate, and hydroxide) has not been studied. Attenuation of the signal as electrical cable length increases also needs to be studied. Radiation tolerance of the transistor is poor.

Potential DCSS Use

The high-electron mobility transistor-based sensor is a laboratory technique that measures chloride ion concentrations in solution. In principle, this type of sensor potentially could be used to monitor chloride concentration and/or deposition rate in remote applications. Without experimental data to support a higher radiation tolerance, the radiation tolerance of this transistor is assumed to be similar to other commercial off-the-shelf electronic components, which raises considerable doubts on operational performance. Additional information is

necessary to evaluate whether this system may be applicable for chloride monitoring in DCSS applications, including specifications and operational limitations.

Unknowns

- Interference by other ions in solution.
- Radiation and temperature tolerance of the system.

2.3.5 Absorption Spectroscopy

Measurement Principle

Fuhr and Huston (2000) tested a chloride ion sensor that uses absorption spectroscopy. Their method relies on spectral changes when AgCl precipitates upon ingress of chloride ions and upon contact with an $AgNO_3$ solution that contains a dichlorofluorescein indicator dye. The anionic dye is attracted to the precipitate, resulting in a pink color. A drawback of this technology is the solution volume required may be too large; therefore, it is not applicable for monitoring dry cask storage systems where the volume of brines that form by salt deliquescence is likely to be small.

Maturity

This sensor has been embedded into three bridges in Vermont for field testing. Fuhr and Huston (2000) (Figure 2-10) indicated that 2 years have passed since installation of the sensors, with no data yet to indicate chloride has penetrated the concrete.

Measurement Range, Sensitivity, and Longevity

Not specified.

Space and Power Requirements

These requirements are not specified, but based on the limited information available, the sensor appears to be approximately 5 cm × 5 cm × 10 cm [2 in × 2 in × 4 in]. Little information is available to estimate the instrumentation and sensor power requirements.

Monitoring Area and Data Acquisition

Not specified.

Temperature and Radiation Tolerance

These tolerances are not specified. Note that the application Fuhr and Huston (2000) reported would not require consideration of gamma or neutron radiation.

Strengths and Weaknesses

One of the strengths of this system is that it is designed for remote deployment in field applications as a chloride-monitoring system.

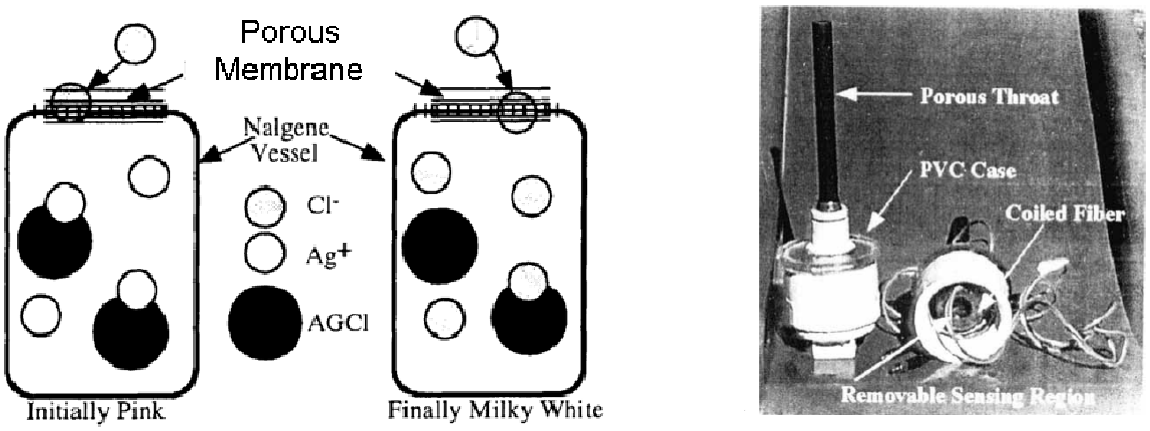

Figure 2-10. Chloride Ion Sensor Based on Detecting Precipitation of AgCl From the Change in Color Due to the Dichlorofluorescein Dye Fuhr and Huston (2000)

Weaknesses include the state of development and the limited availability of information about this sensor. Also, the sensor only measures chloride ions dissolved in solution.

Potential DCSS Use

Additional information is necessary to evaluate whether this system may be applicable for chloride monitoring, including specifications and operational limitations. It is noteworthy, however, that the sensor has been designed for monitoring concrete structures.

Unknowns

- Device specifications including size, power requirements, measurement range monitoring area, and data acquisition requirements.
- Longevity and maintenance requirements.
- Temperature and radiation tolerance.

2.3.6 Quantum Dots

Measurement Principle

Quantum dots are nanometer-sized semiconductor crystals that can be based on a wide range of compound semiconductors (e.g., CdSe, CdTe, ZnS). These materials normally are not fluorescent, but when in quantum dot form, they emit intense, long-lasting colors when excited by ultraviolet or visible light. The uses of quantum dots initially were targeted at biotechnology applications, such as intracellular chloride measurements in epithelial cells (Wang, et al., 2010; Ruedas-Rama, et al., 2012). For example, Figure 2-11 shows the average photoluminescence lifetime, τ_{ave}, of quantum dot-lucigenin conjugates versus chloride concentration in solution determined by Rueda-Ramas, et al. (2012).

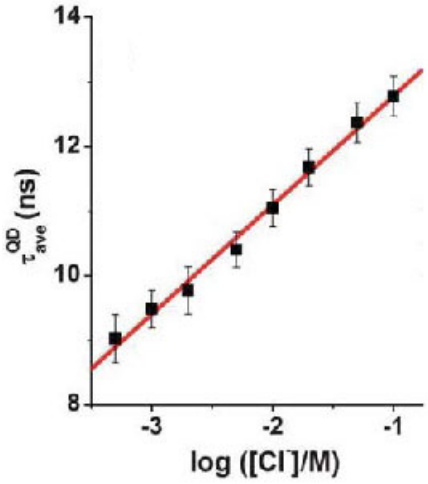

Figure 2-11. Example Data Showing Average Photoluminescence Lifetime, τ_{ave}, of Quantum-Dot-Lucigenin Conjugates Versus Chloride Ion Concentration in Solution (Ruedas-Rama, et al., 2012) (Reproduced With Permission of The Royal Society of Chemistry)

Maturity

This type of sensor technology is still under development. No commercially available systems were identified in this study.

Measurement Range, Sensitivity, and Longevity

Not specified.

Space and Power Requirements

Not specified.

Monitoring Area and Amount of Data per Measurement

Not specified.

Temperature and Radiation Tolerance

Not specified.

Strengths and Weaknesses

Little information is available on this sensor. A potential strength is the fact that this sensor uses nanometer-sized semiconductor crystals that may allow the sensor systems to be very small. Weaknesses include the fact that the system only measures chloride ions in solution.

Potential DCSS Use

Additional information is necessary to evaluate whether this system may be applicable for chloride monitoring, including specifications and operational limitations.

Unknowns

- Device specifications including size, power requirements, measurement range, monitoring area, and data acquisition requirements.
- Longevity and maintenance requirements.
- Temperature and radiation tolerance.

2.3.7 Electrochemical Sensors

Measurement Principle

Electrochemical methods commonly used for measuring chloride ion concentration employ an Ag/AgCl electrode as a working electrode and a reference electrode that has an aqueous reference solution. The use of an aqueous solution is problematic for most field applications. Thus, the literature search on electrochemical sensors focused on technologies that do not use an aqueous reference solution. A chloride ion sensor developed by Gao, et al. (2010) employs an all-solid-state chloride sensor with an Ag/AgCl working electrode and an MnO_2 reference electrode. Other electrochemical-based chloride sensors described in published literature include an all-solid-state chloride electrode based on tin oxide/indium tin oxide (SnO_2/ITO) glass (Cheng, et al., 2011) and ion-selective conducting polymers (e.g., polypyrole) (Zielinska, et al., 2002), which behave as anion exchangers and give potentiometric response to changes in chloride ion concentration.

Maturity

Several systems have been developed and proposed for chloride monitoring in concrete. The Smart Pebble™ wireless sensor developed by SRI International (Watters, et al., 2003) for monitoring chloride ingress into concrete bridge decks does use an aqueous $Cu/CuSO_4$ reference solution, but because it is embedded in concrete, the developers considered the sensor will be protected from freezing ambient conditions that might otherwise damage systems that use a reference solution. Figure 2-12 shows a schematic of the Smart Pebble wireless sensor.

Measurement Range, Sensitivity, and Longevity

Not specified.

Space and Power Requirements

Not specified.

Monitoring Area and Amount of Data per Measurement

Not specified.

Temperature and Radiation Tolerance

Not specified.

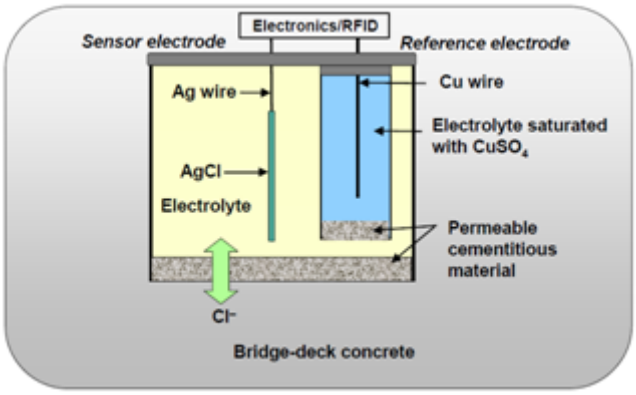

Figure 2-12. SRI International Smart Pebble™ Wireless Sensor (Watters, et al., 2003)

Strengths and Weaknesses

A strength of these systems is the possible large range of chloride concentrations in solutions that could be measured.

Weaknesses include the fact the system only measures chloride ions dissolved in solution and the required volume of solution to conduct a measurement may be significantly larger than for other systems. The limited volume of solution that is expected to form under deliquescence brines from deposited atmospheric deposits may limit the applicability of electrochemical sensors in monitoring systems for surfaces.

Potential DCSS Use

Additional information is necessary to evaluate whether this system may be applicable for chloride monitoring, including specifications and operational limitations.

Unknowns

- Device specifications including size, power requirements, measurement range, monitoring area, and data acquisition requirements.
- Longevity and maintenance requirements.
- Interference by other ions in solution.
- Temperature and radiation tolerance.

2.3.8 Electromechanical Sensors

Measurement Principle

Saafi and Romine (2004) proposed an electromechanical response-based technology for monitoring chloride ion ingress into concrete structures. The sensor is a micro-electromechanical system, which is a collection of microsensors and actuators that can both sense the environment and react to changes in that environment using a microcircuit

control. During sensor operation, chloride ions absorbed into the sensing film surface produce shear stresses at the film/beam interface, which cause a cantilever beam to deflect. The deflection is measured as a resistance change in the embedded strain gauges and is linearly proportional to the shear stress. Thus, the chloride ion concentrations are transduced into a proportional differential voltage change in the bridge circuit.

Maturity

This type of sensor technology is still under development. No commercially available systems were identified in this study.

Measurement Range, Sensitivity, and Longevity

Not specified.

Space and Power Requirements

Not specified.

Monitoring Area and Amount of Data per Measurement

Not specified.

Temperature and Radiation Tolerance

Not specified.

Strengths and Weaknesses

Strengths of this sensor are that it is a solid state system and has been purposely designed for field application for measurements in concrete.

Weaknesses are the early stage of development and lack of specifications, capabilities, and operational limitations. Also, the sensor only measures chloride ions dissolved in solution.

Potential DCSS Use

Additional information is necessary to evaluate whether this system may be applicable for chloride monitoring in a DCSS, including specifications and operational limitations.

Unknowns

- Device specifications including size, power requirements, measurement range, monitoring area, and data acquisition requirements.
- Interference by other species.
- Longevity and maintenance requirements.
- Temperature and radiation tolerance.

2.4 Microbially Influenced Corrosion Monitoring

Stainless steel canisters and their welds, as well as steel and cast iron casks are constructed of materials that have been shown to be susceptible to MIC. Potential microbes include aerobic and anaerobic producers, sulfate-reducing bacteria (SRB), and iron/manganese oxidizing bacteria. The microbes can resist harsh environments, including acidic solutions, high and low temperatures, drying conditions, and radiation environments. The microbes can attach themselves to metal surfaces and develop a protective membrane (biofilm) that changes electrochemistry conditions locally. The biofilm also can cause debonding of coatings from the underlying metal, thereby creating an environment for crevice corrosion. The results of MIC are pitting and crevice corrosion with accelerated corrosion rates of components.

Four potential techniques for detecting and monitoring MIC were identified: (i) electrochemical sensors, (ii) hydrogenase-based bioanalyzer, (iii) sulfide-oxidase-based biosensor, and (iv) culturing methods, including broth bottles and melt agar tubes. The attributes of these techniques are summarized in Table 2-5 and described in detail in the following sections.

2.4.1 Electrochemical Sensor

Measurement Principle

Licina (2001) developed an electrochemical sensor for monitoring biofilms on metal surfaces in real time. The electrochemical sensor system includes a probe, the integrated electronics, interconnecting cable, and display software; data analysis is offline to a personal computer (PC)-based system. The system is designed to be installed inside process water piping or tanks where the sensor is immersed. The electrochemical sensor consists of a stack of identical stainless steel discs configured as a right circular cylinder. The electrodes are electrically isolated from each other with epoxy. One electrode (set of discs) is polarized relative to the other for a short period of time each day. An abrupt increase in current indicates accelerated corrosion that may be related to biofilm formation. A schematic diagram of the device and test results of biofilm activity of the cooling water system of a power plant are shown in Figures 2-13(a) and (b), respectively. Software is included with the system for analyzing test

Space and Power Requirements

The electrochemical biofilm activity monitoring probe is approximately 7.6 cm [3 in] in diameter and 11.4 cm [4.5 in] long. The hardware and software are combined into a small box approximately 12.5 cm × 17.5 cm × 5 cm [5 in × 7 in × 2 in] that contains all of the control and data analysis functions. The entire sensor system requires a space of approximately 1,100 cm^3 [70 in^3], but the installed sensing element is designed to be placed inside components that are difficult to access or inspect (i.e., pipes). The power requirements are 66 or 132 watts and have built-in battery backup.

Monitoring Area and Data Acquisition

The monitoring area is in the immediate vicinity of the sensor. Determinations of the presence and activity of biofilms on the probe electrodes are made from the trend plots, evaluated using logic built into software. The user can adjust the values of the various alarm parameters. An indication light (LED red/green) denotes the probe status. Green indicates no signs of microbial activity, and red indicates microbial activity. The data acquisition mode is continuous and real time.

Table 2-5. Microbially Influenced Corrosion Monitoring Sensors

Features	Electrochemical Sensor (Section 2.4.1)	Hydrogenase-Based Bioanalyzer (Section 2.4.2)	Sulfide Oxidase-Based Biosensor (Section 2.4.3)	Culturing Methods Including Broth Bottle and Melt Agar Tubes (Section 2.4.4)
Maturity	Field deployed in nuclear applications	Field deployed in non-nuclear applications	Concept	Field deployed in non-nuclear applications
Measurement Range	Not specified	Not specified	Not specified	Specific to culture media
Sensitivity	Sensitivity of corrosion rate related to biofilm activity was not reported	As few as 250 bacteria cells can be detected	Responds linearly to abiotic sulfide concentration 0–130 ppm	Dependent on type of microorganisms and culture media
Longevity	Decades	Decades	Unknown	One-time use
Space Requirements, cm^3 [ft^3]	1,100 [0.039], probe is 7.6 cm [3 in] diameter and 11.4 cm [4.5 in] long	Probe is approximately 5 cm [2 in] diameter and 10.7 cm [4.21 in] long	500–2,000 [0.018–0.071]	Not applicable, sample removed and cultured offsite
Power Requirements	66 or 132 watts power and has built-in battery backup	No power needed for probe; 66 watt power, 9 V replaceable battery	66 watts power	Not applicable
Monitoring Area	Immediate vicinity of cask components	Immediate vicinity of cask components	Immediate vicinity of cask components	Point at sampling locations
Data Acquisition Mode	Continuous and real time	Intermittent	Continuous	Single sample
Temperature Tolerance	Unknown	Retrievable probe 260 °C [500 °F]	Unknown	Not applicable
Radiation Tolerance	Unknown	Not specified, but probe could be made radiation-resistant	Unknown for sensor itself	Not applicable
Strengths	Field deployed in nuclear plants in water treatment system; rugged; real-time data	Field deployed in non-nuclear applications	Simultaneous monitoring of corrosion rate and SRB	Custom formulations to detect specific microbes
Weaknesses	The system has mostly been used in a water treatment system with low radiation and has not been operated in a dry system	Unknown radiation tolerance designed for non-nuclear applications; probe may be too large for some sampling sites	Long-term stability of the biosensor is unknown; the sensor has not been field tested	Not real-time monitoring; labor and time intensive; detected microbes may under represent the actual microbes

MIC = microbially influenced corrosion

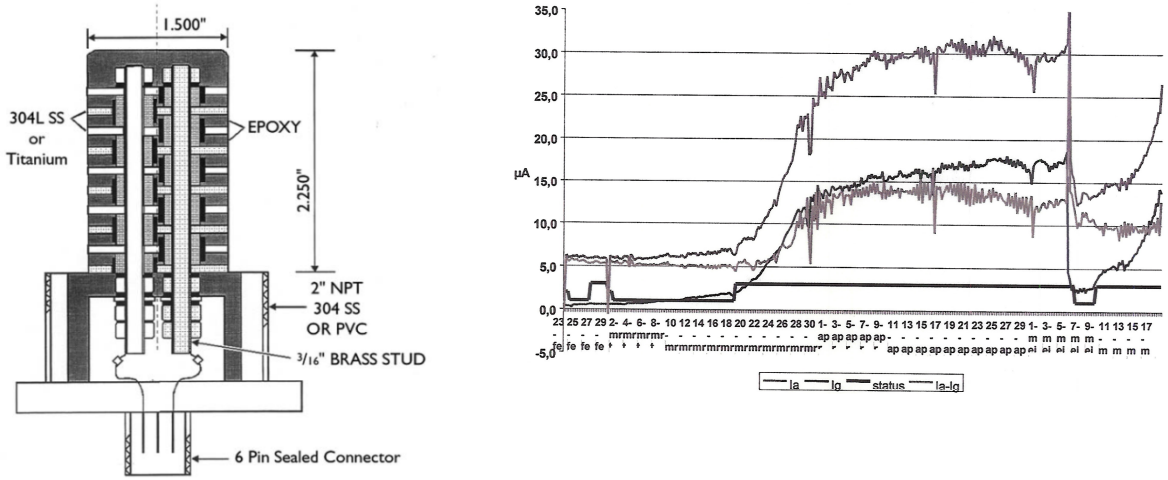

(a) **(b)**

Figure 2-13. Electrochemical Biofilm Activity Monitoring Probe. (a) Schematic Diagram and (b) Biofilm Activity Monitoring Results of Cooling Water System of a Power Plant (Licina, 2001). (Reproduced With the Permission of NACE International)

data and creating detailed trend plots, as shown in Figure 2-13(b). The probe is designed to show a red light signal on an LED display when the applied current exceeds a specified critical value, so that biocide can be added in time to reduce microbial activity.

Marchal, et al. (2005) received a U.S. patent ("Method and Device for Detecting Microbiologically Influenced Corrosion") for inventing a sensor that detects microbiologically influenced corrosion in a metallic structure. The sensor consists of a circular electrode as a cathode and a ring-shaped electrode as an anode and is installed in the vicinity of the metallic structure in contact with a corrosive medium. A conditioning current is applied between the two electrodes to initiate corrosion current. After a specific time, the cathode and anode electrodes are coupled and the corrosion rate calculated from the measured electrical current. The concept of a microbiologically influenced corrosion sensor is similar to that of an electrochemical sensor. It is therefore included here as a variant of the electrochemical sensor. The test data described in the U.S. patent (Marchal, et al., 2005) are limited.

Maturity

The sensor system has been developed primarily for monitoring of industrial liquid handling systems, such as piping systems. It has been field deployed at the Browns Ferry Nuclear Plant in low radiation areas and in other chemical plants to monitor the MIC conditions. In addition to applications in a nuclear power plant, the system has been installed in piping systems, heat exchangers, cooling water towers, and side stream systems.

Measurement Range, Sensitivity, and Longevity

Measurement range and sensitivity of corrosion rate related to biofilm activity were not reported in the referenced literature. System life could be 10 years or longer.

Temperature and Radiation Tolerance

The electrochemical sensor has been used in ambient temperatures and low radiation areas. Temperature and radiation tolerance of the probes are not specified.

Strengths and Weaknesses

A strength of the electrochemical sensor is that it is a simple, rugged, dependable system for MIC monitoring. The technique has been field deployed in the Browns Ferry Nuclear Power Plant, where it was used to monitor microbial activities in the fire protection system and in essential equipment cooling water (Licina and Carney, 1999). It provides continuous, real-time data. The device detects signs of microbial activity to indicate MIC of the canister and cask external materials.

A weakness is the sensor has not been deployed in a dry system. Effects of high-temperature, high-radiation environments on the sensor calibration, and longevity also are unknown.

Potential DCSS Use

The probe is designed and operated so that microorganisms in the environment will settle on the probe surfaces to allow detection. For a DCSS, the current configuration and size of the probe may limit placement location. For example, the probe may not be able to fit in the gap between the canister and overpack, though perhaps it could be placed at the air vents. It might be feasible to place the systems close to or perhaps mounted on the direct-load bolted cask to monitor MIC of steel, cast iron body, welds, lids, and seals, as shown in Table 1-1. Additional information is necessary to evaluate whether this system may be applicable for microbial corrosion monitoring in DCSS applications, including specifications such as operating temperature and radiation tolerance range of the sensor and operational limitations.

Unknowns

- Temperature and radiation tolerance of the sensor.
- Measurement range and sensitivity to the presence of microbial species responsible for MIC.
- Functionality in a “dry” system, where only a thin film of water may be present.

2.4.2 Hydrogenase-Based Bioanalyzer

Measurement Principle

The hydrogenase-based monitoring system (Caproco, 2013) consists of a biofilm probe, a hydrogenase test kit, and a MIC analyzer to detect as well as provide the quantitative indication of bacterial activities in specific environmental conditions. The biofilm probe incorporates a sampling stud design that facilitates accumulation of bacteria. The exposed stud samples are analyzed through a hydrogenase test kit. The biofilm probes are used in testing for anaerobic, SRB and aerobes. The results can be quantified by a MIC analyzer instrument. A schematic diagram and photos of the device are shown in Figures 2-14(a)–(c). As few as 250 bacteria cells can be detected when active hydrogen uptake is occurring. The measurement resolution for H_2S/min is ±0.00001 µmoles, the measurement resolution for H/min is ± 0.0001 µmoles, and

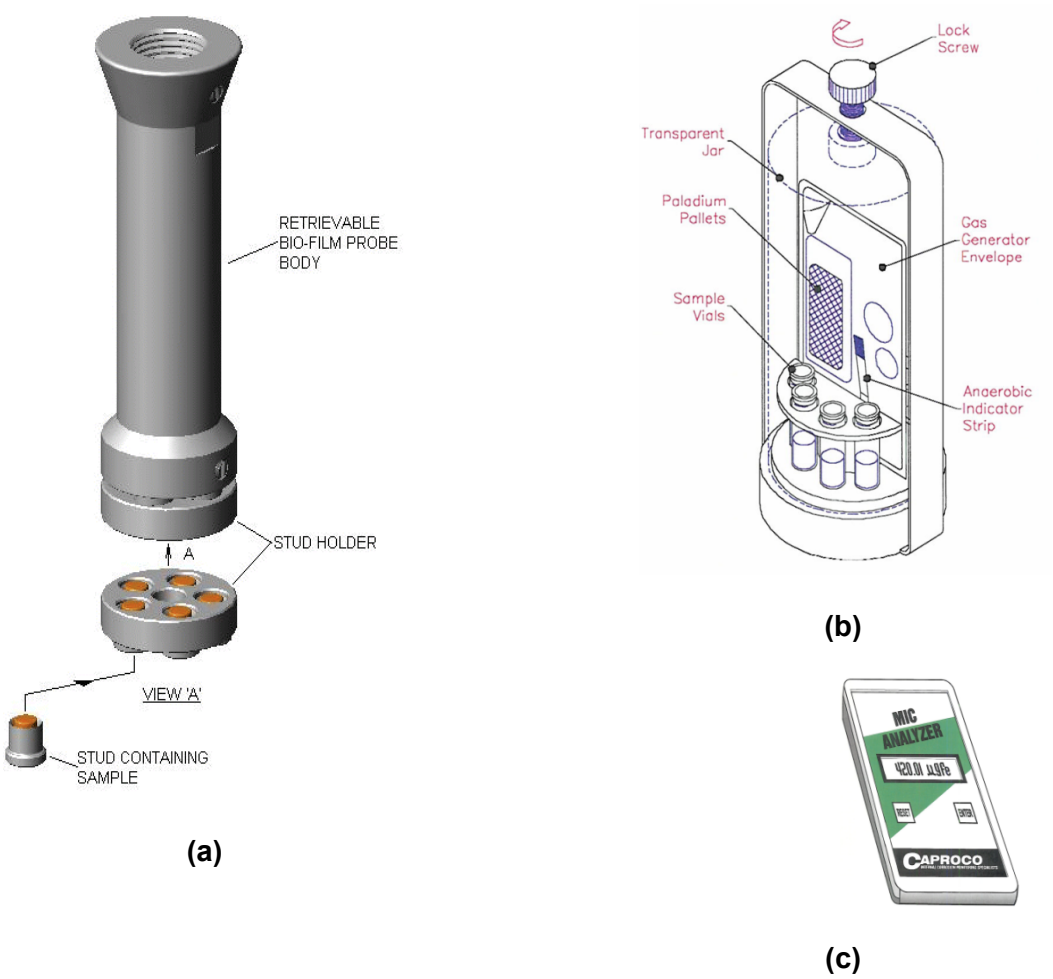

Figure 2-14. Hydrogenase-Based Bioanalyzer. (a) Retrievable Biofilm Probe Body, (b) Schematic Diagram of Anaerobic Test Chamber, and (c) Microbially Influenced Corrosion Analyzer (Caproco, 2013).

the measurement resolution for FeO/min is ± 0.001 µg [4×10^{-11} oz]. A wide range of corrosion-causing anaerobes and aerobes can be detected.

SRB are associated with MIC of iron and steel components. The SRB use an enzyme, hydrogenase, to extract corrosion process energy for their metabolic activities, and the presence of hydrogenase enzyme is therefore considered to be a reliable indicator of MIC. The biofilm probe incorporates a number of sampling studs designed for accumulation of bacteria. The MIC analyzer is connected by cables to the hydrogenase test kit anaerobic chamber. In the test kit, an indicator dye is added to the enzyme extracted from the SRB. If hydrogenase is present, the solution color changes from colorless to blue in several hours.

Maturity

The MIC monitoring system has been field tested in an operating water system and oil and gas pipelines to detect SRB, and it is a proven tool for screening the effectiveness of biocide treatment in industrial settings.

Measurement Range, Sensitivity, and Longevity

The measurement range for this method is not specified, but as few as 250 bacteria cells can be detected where active hydrogen uptake is occurring. The monitoring system life is 10 years or longer.

Space and Power Requirements

The biofilm probe is designed to be mounted flush in the component or pipe wall, with the probe face of five studs exposed to accumulate bacteria. The retractable probe is approximately 5 cm [2 in] in diameter and 10.7 cm [4.21 in] long. The space requirement for the monitoring system is approximately 1,200 cm^3 [73.2 in^3], but only the probe needs to be remotely deployed. The probe does not need power. The power requirement for the analyzer is 66 watts from 110 V AC, with a 9 V replaceable battery.

Monitoring Area and Data Acquisition

The monitoring area is in the immediate vicinity of the sensor. MIC activities are provided in three formats: (i) micromoles of hydrogen uptake per minute, a condition that is directly related to bacterial corrosion activity; (ii) micrograms of iron oxidized per minute, whereby the amount of iron being oxidized by bacteria equals a corrosion rate related to MIC activity; and (iii) micrograms of H_2S per minute, whereby H_2S is a byproduct of the MIC activity. The data acquisition mode is intermittent.

Temperature and Radiation Tolerance

The retrievable probe that needs to be deployed at the site can be used at temperatures up to 260 °C [500 °F]. The upper use temperature of a MIC analyzer is 40 °C [104 °F]. The radiation tolerance of the system is not specified.

Strengths and Weaknesses

Strengths include that the technique has been designed for field monitoring of MIC in industrial applications. The system has been deployed for monitoring microbial activities in non-nuclear applications, such as water treatment plants and pipelines.

Weaknesses of the system include the probe size may need to be modified to fit into the narrow gap between canister and overpack, and radiation tolerance of the system is unknown. The microbes present in a nuclear environment may differ from those the analyzer can detect with certainty. It is unknown whether it can be adapted for nuclear application. Function and sensitivity may be limited in a dry system where only a thin film of water may be present.

Potential DCSS Use

The probe is designed to monitor MIC of external components with intermittent data collection. For DCSS use, the system may be placed in the immediate vicinity of the cask components to continuously accumulate dust, salts, and organic materials in environments similar to dry cask component surfaces. However, additional information on radiation tolerance is necessary to evaluate whether this system may be applicable for microbial corrosion monitoring in DCSS applications.

Unknowns

- Radiation tolerance of the system.
- System adaptation for nuclear application.

2.4.3 Sulfide-Oxidase-Based Biosensor

Measurement Principle

Haile, et al. (2010, 2011) developed a sulfide-oxidase-based biosensor for simultaneously monitoring SRB and corrosion rate. This online probe has four sensing elements: (i) carbon steel working electrode, (ii) stainless steel counter electrode, (iii) saturated calomel reference electrode, and (iv) enzyme electrode. For monitoring SRB activity, the combination of an enzyme electrode, counter electrode, and reference electrode was used. For monitoring corrosion rate, the combination of a working electrode, counter electrode, and reference electrode was used. The enzyme electrode was based on a biosensor in which sulfide oxidase was the sulfide-sensing element. A sulfide-oxidase-producing micro-organism is cultured in a glucose–yeast extract medium. A glassy carbon electrode is used to prepare the enzyme electrode. The correlation between the biosensor response and corrosion rate was established. A schematic diagram and simultaneous monitoring results of corrosion rate and SRB activity are shown in Figures 2-15(a) and (b).

Maturity

The feasibility of an online probe for simultaneously monitoring corrosion rate and SRB activity has been demonstrated in the laboratory. In a laboratory test, the SRB reactor has a 500-mL [0.132-gal] container with four electrodes connected to a potentiostat and a PC. A 16-day experiment was conducted. The SRB activity was monitored every day, and the corrosion rate was recorded every hour. No commercially available sensors of this type were identified, and field testing of this type of system has not been conducted.

Measurement Range, Sensitivity, and Longevity

The probe responded linearly to an abiotic sulfide concentration in the range of 0–130 ppm. Because only short-term data are available, the longevity of the system is unknown.

Space and Power Requirements

A portable online four-probe sensor has been recently reported (Haile, et al., 2013). The portable system is 1.9 cm [0.75 in] in diameter and 8.0 cm [3.2 in] in height. The space required for the system is estimated to be 500–2,000 cm^3 [30.5–122 in^3]. The power requirement is 66 watts from 110 V AC.

Monitoring Area and Data Acquisition

The monitoring area is in the immediate vicinity of the sensor. Using the dimension of the portable four-probe sensor, the monitoring area has a diameter of 18 mm [0.71 in]. SRB activity is monitored by applying a small voltage versus the reference electrode or enzyme electrode and recording the current generated. Data acquisition mode is continuous.

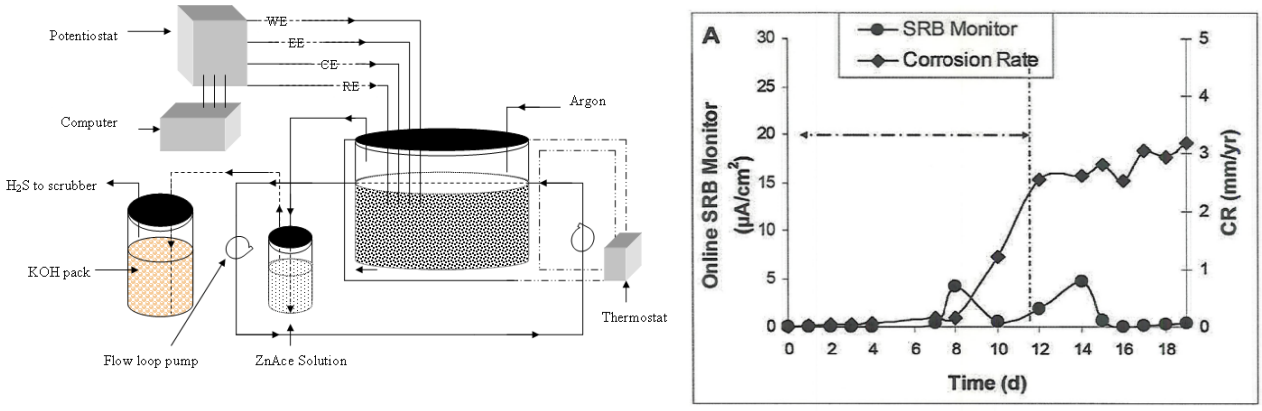

(a) **(b)**

Figure 2-15. An Online Probe for Monitoring Corrosion Rate and SRB Activity. (a) Schematic Diagram of the Online Probe and (b) Test Results of Monitoring Corrosion Rate and SRB Activity Simultaneously (Haile, et al., 2011). (Reproduced With Permission of NACE International)

Temperature and Radiation Tolerance

There is no information on the temperature and radiation tolerance of the system.

Strengths and Weaknesses

Strengths include the fact the technique utilizes an online probe for simultaneously monitoring corrosion rate and SRB activity.

Weaknesses are the technique has only been used in the laboratory and it has not been field tested. The maximum reported test time for the technique was 16 days.

Potential DCSS Use

A four-probe sensor for simultaneous monitoring of SRB activity and corrosion rate has been demonstrated in the laboratory. The method has not been field deployed. Additional development work will be needed and more information would need to be made available to evaluate the applicability of this sensor for MIC monitoring in a DCSS.

Unknowns

- Device specifications including size, power requirements, and measurement range.
- Longevity and maintenance requirements.
- Temperature and radiation tolerance.

2.4.4 Culturing Methods

Measurement Principle

Culturing methods to detect MIC involve taking a small sample of the in-service environment media (e.g., liquid or deposit) and placing it into a broth or agar that is specifically designed

to promote the growth of a specific type of micro-organism, if it is present in the system (Little, et al., 2006).

The American Petroleum Institute developed the broth bottle method for detecting SRB (Tatnall and Pope, 1993). In this method, lactate is added to the collected field sample. When SRB are present, they reduce the sulfate in the medium to sulfide to produce black iron sulfide. The blackening of the medium within 28 days indicates the presence of SRB.

Melt agar tubes are a modification of the broth bottle method (Tatnall and Pope, 1993). An agar culture medium tube is placed in boiling water to liquefy the agar and then cool the tube before adding the sample. The tube is then incubated from 1 to 3 weeks and checked for blackening. Relative numbers of bacteria are estimated by noting the rapidity with which blackening occurs.

Maturity

Both broth and agar culturing techniques are standardized methods (NACE International, 2004, 2012, 2006) for conducting assays of in-service environments for MIC.

Measurement Range, Sensitivity, and Longevity

The measurement range to identify certain micro-organisms is limited by the culture media that is used. Moreover, Kaeberlein, et al. (2002) suggest that 99 percent of the micro-organisms from the natural environment resist cultivation in the laboratory, so the sensitivity and measurement range are limited. Sensitivity greatly depends on the culture media. These methods are one-time use systems, so longevity is not applicable.

Space and Power Requirements

These requirements are not applicable because only the sample needs to be taken from the area of interest; the culturing is performed offsite.

Monitoring Area and Data Acquisition

Samples can be taken from any area of interest that is accessible. Each measurement identifies the presence of certain micro-organisms. The data acquisition mode is a single-use sample.

Temperature and Radiation Tolerance

Temperature and radiation tolerance is not an issue because the sample is taken from the in-service environment and cultured offsite in a controlled environment. For the culturing environment, there are a number of media with different characteristics designed for culturing organisms in a range of natural and production environments. Because these methods typically use aqueous-based media, the upper temperature limit would be the boiling point of the solution or the temperature where decomposition of the media would occur.

Strengths and Weaknesses

Strengths include the fact these methods have been routinely used to assess the possibility of MIC in field environments. Specific test systems have been developed to assess many types of

microbes that can be found in a range of environments, including freshwater, salt water, and concentrated brines.

Weaknesses are the necessity to collect a sample under radiation from the system environment and the long incubation time (5 to 28 days) in a controlled environment that is required to promote the growth of potentially relevant bacteria. Culturing is media specific and cannot approximate the complexity of a natural environment, so the detected bacteria may not represent all the micro-organisms present at the sampling location. The culturing method depends on single-use samples and cannot monitor *in situ* conditions continuously.

Potential DCSS Use

Additional information is necessary to evaluate whether this system may be applicable for microbial corrosion monitoring in DCSS applications. Media would need to be collected from inside the overpack or concrete to use these methods. In addition, suitable incubation conditions would need to be established to culture the micro-organisms that may be present in the DCSS. Micro-organisms can adapt to specific environments. Consequently, specific incubation environments may be necessary to use this method to detect organisms that may lead to MIC of the DCSS SSCs.

Unknowns

- Sample collection methods.
- Appropriate broth or agar chemistry, requirements for environmental conditions, and time for incubation.

2.5 Stress Corrosion Cracking Monitoring of Canister Body and Weld

Dry storage canisters typically are composed of stainless steel materials and are sealed by welding. Stainless steel degradation is strongly related to the environmental conditions, including temperature, RH, and chemical species (i.e., chloride). The monitoring techniques for these environmental conditions are included in previous sections. Atmospheric SCC of welded stainless steel storage casks may occur if aggressive species (e.g., chloride and sea salt particles) enter the concrete HSM and deposit on the stainless steel canister surface. Table 1-1 lists the technical information needs for external components of welded stainless steel. SCC is considered a degradation mechanism with high priority in the technical information needs report (NRC, 2014). Several mature and novel nondestructive examination (NDE) technologies exist for detecting SCC degradation of stainless steels. Typical NDE methods used for SCC detection include ultrasonic, nonlinear elastic wave spectroscopy; acoustic emission (AE); guided wave; and eddy current. Because the use of these NDE approaches to detect SCC are detailed in the NRC-sponsored project at Pacific Northwest National Laboratory (PNNL) as discussed in Section 1.1, no further evaluation was pursued in this project. Instead, the work presented here is devoted to reviewing and assessing technologies that are suitable for *in-situ* crack initiation and propagation monitoring but not based on NDE methods, such as ultrasonic test methods.

The reviewed and assessed non-NDE techniques for monitoring SCC listed in Table 2-6 include (i) fiber optic sensors, (ii) the Luna crack growth sensor, and (iii) the crack propagation sensor. Details of each sensor are provided in the following sections.

Table 2-6. Stress Corrosion Cracking Monitoring Techniques			
Features	**Fiber Optic Sensors (Section 2.5.1)**	**Luna Crack Growth Sensor (Section 2.5.2)**	**Crack Propagation Sensor (Section 2.5.3)**
Maturity	Field deployed	Field deployed	Unknown
Measurement Range	As large as 3 percent strain	Between 2 and 4 mm [0.08 and 0.2 in]] of crack measurement in depth	Not specified
Sensitivity	Crack opening resolution of 40 μm [1.6 mils]	Crack depth resolution of 1 μm [0.04 mil]	Crack depth resolution of 250 μm [9.75 mils]
Longevity	Unknown	~2 yr for a constant crack growth rate of 10^{-10} m/sec [4×10^{-6} mils/sec]	~1.6 yr for a constant crack growth rate of 10^{-10} m/sec [4×10^{-6} mils/sec]; unknown for irradiated environment
Space Requirements	Gauge lengths 10 cm [4 in] to more than 100 m [328 ft] with a 75–250 μm [2.9–9.8 mils] diameter	Cylindrical fracture specimen of 1.2 cm [0.5 in] diameter and 10 cm [4 in] long placed in the assembly of 11.5 cm [4.5 in] in diameter and 19 cm [7.5 in] in length	2.5 cm [1 in] × 0.5 cm [0.2 in] and 0.043 mm [1.7 mils] thick
Power Requirements	Power consumption ranging from 90–300 watts	0.05 watts per measurement	Low; less than 1 watt
Monitoring Area	Local and general cracking	Local cracking	Local cracking
Data Acquisition Mode	Continuous or intermittent	Continuous or intermittent	Continuous or intermittent
Temperature Tolerance	>1,100 °C [2,012 °F]	~120 °C [248 °F] or greater	−269 to +230 °C [−452 to 446 °F]
Radiation Tolerance	Total gamma radiation up to 53 Mrad	Unknown	Total gamma radiation of ~10^2 Mrad
Strengths	Electromagnetic immunity, small size, high-temperature tolerance, corrosion resistance, large area monitoring with single sensor, light weight, long record of field testing	Highly sensitive, sensor does not need bonding to canister, low power consumption	Simple to implement, wide operational temperature, sensor does not need to be bonded to canister, small size, low power consumption
Weaknesses	Gamma radiation interference, sensor deployment may be problematic, temperature calibration required	Relatively large size, surrogate sensor (does not measure cracking of actual canister, needs to assume a residual stress value of welds), temperature compensation required, local cracking monitoring, limited field testing	Surrogate sensor (does not measure cracking of actual canister; needs to assume a residual stress value of welds), modest crack propagation resolution, unknown field testing, local cracking monitoring

2.5.1 Fiber Optic Sensors

Measurement Principle

Fiber optic sensors measure the elongation or contraction of the fiber when it is bonded to a structure. The fiber structure consists of a core surrounded by a cladding with different indexes of refraction so the light is concentrated around the core of the fiber. Optical fibers are made of a dielectric material and, as such, are chemically inert and popular for use in detecting changes in temperature, pressure, and strain. There are several types of materials for construction of optical fibers. Several pure silica core fibers have been successfully tested in nuclear environments, including the step-index polymer clad, grated-index fluorine-clad multimode, and pure silica single-mode fibers. Recently, photosensitive fibers (e.g., silica-based fibers doped with germanium dioxide[1]) have shown promising results, including a long lifespan under harsh environments (Lacy, 1982; Gusarov, et al., 1999; Hill, et al., 1978; Udd, et al., 1998). More information on the effects of gamma dose appears in Appendix A.

There are several types of fiber optic sensors classified based on intensity, phase, wavelength, polarization modulations, and intrinsic and extrinsic sensors. However, most of the current sensor designs are based on wavelength or frequency modulations (i.e., FBG) and based on phase modulations (i.e., interferometric sensors). An FBG sensor consists of a periodic structure of multiple gratings along a single optical fiber, fabricated by exposing a photosensitive fiber to ultraviolet light. When a source light interacts with the grating, a single Bragg wavelength is reflected back while the rest of the signal is transmitted. An external mechanical strain in the fiber shifts the Bragg wavelength through expansion or contraction (strain) of the grating periodicity. The strain in the fiber (related to the strain in the host surface where the fiber is attached) is detected as a shift in the wavelength of the reflected light. Figure 2-16 shows a diagram of the FBG sensor operation.

It has been reported that FBG sensors were applied to detect cracks in carbon-fiber-reinforced polymer composites (Okabe, et al., 2002). A typical FBG sensor, however, has a limited gauge length and thus works as a “point” sensor (Schulz, et al., 2001). Although the sensing gauges can be multiplexed, the number of multiplexible gauges is limited. Because the crack locations in a material are not known *a priori*, conventional point sensors, even if they can be multiplexed, are not effective in crack detection. A truly distributed sensor system is desired for detection and continuous monitoring of cracks. Recently, a study on crack detection using a distributed Brillouin[2] fiber optic sensor was reported (Ravet, et al., 2008).

Due to its robustness and ruggedness, Brillouin fiber optic sensors are fabricated in various gauge lengths that can exceed 100 m [328 ft], making fiber optics ideal for monitoring large areas using a few sensors.

For field deployment, fiber optic sensors can be bonded to the exterior surface of the component to be monitored, providing information on the in-plane surface strain fields. Strain is

[1]Germanium is a common dopant material used to increase the index of refraction of the core relative to the cladding, thus providing the light-guiding properties.

[2]The Brillouin effect is an inelastic scattering process between optical photons and vibration waves (phonons), which produces a few scattered photons with a certain wavelength shift with respect to the original wavelength. This shift has been found to be proportional to the temperature and to the strain.

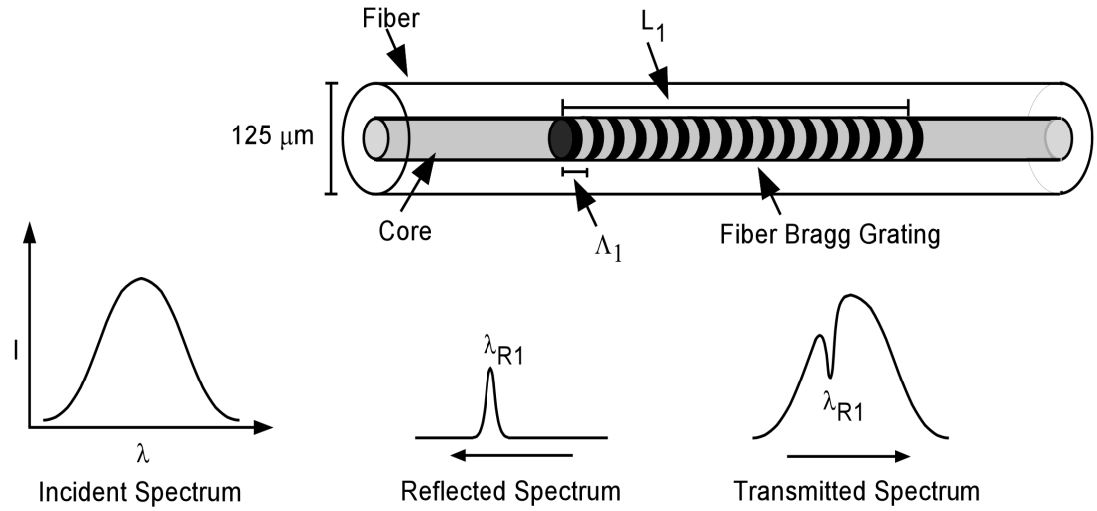

Figure 2-16. Diagram of the Fiber Bragg Gratings Sensor Operation

an alternative parameter that can be used to describe the initiation and propagation of SCC (Zou, et al., 2004). Crack formation is represented by degradation in the signal resulting from an increased distance traveled by the light in the fiber optics. When a crack forms, the fiber intersecting the crack bends and a sharp drop in the optical signal occurs as a result of elongation or contraction of the fiber. Sensor orientation with respect to the crack direction is critical for accurate crack detection. Consequently, it is recommended that *a priori* critical areas of the substrate that are prone to SCC (e.g., welds) be determined and the number of sensors in these critical areas be increased.

Maturity

In the past few decades, fiber optic sensors have been increasingly used in many infrastructures, such as transmission, monitoring of spacecraft, ships, refineries, pipelines, and civil engineering structures. The fiber optic sensors have been an integral part of structural health monitoring systems to monitor, in real time, global and local performances of a structure. For field applications, several types of fiber optic strain sensors have been developed, including those based on intensity, polarization, and interferometry (especially Fabry-Perot interferometric sensors), as well as Brillouin fiber sensors and FBG (Merzbacher, et al., 1996). As an example, real-time monitoring of the refinery process to detect SCC corrosion due to the presence of chlorides and sulfides has been carried out using fiber optic sensors. For almost two decades, real-time monitoring of steel and concrete civil engineering structures, including buildings, piles, large-span bridges, pipelines, tunnels, dams, and soil excavation, has been accomplished by fiber optic sensors (Lee, et al., 2003; Zhou and Ou, 2004; Kersey, et al., 1997; Morison and Tennyson, 2007).

Space and Power Requirements

Fiber optic sensors are typically fabricated in various diameters ranging from 75 to 250 μm [2.9 to 9.8 mils] and gauge lengths exceeding 100 m [328 ft]. Due to its low weight and size, a few fiber optic sensors can be deployed to monitor a large area of the structure under evaluation. The sensor is either bonded or embedded in the structure using adhesive or metal clamps. Then the sensor is hardwired to an external instrument for sensor interrogation and data collection.

Power consumption for the optical sensors is limited to the instrumentation for sensor interrogation. Newly developed instrumentation systems for fiber optic sensors are portable, compact, and use low power consumption {90 watts at 25 °C [77 °F]} with a single 9 V supply operation. Dimensions of portable instrumentation systems are 36 cm × 28 cm × 10 cm [14 in × 11 in × 3.9 in]. Some other fiber interrogators are 56 cm × 69 cm × 56 cm [22 in × 27 in × 22 in] in size and require AC power supply with a maximum power consumption of 100–300 watts.

Measurement Range, Sensitivity, and Longevity

The measurement range of this sensor is limited by the measurement range of the scanning instrument. Typically, it can be as large as 3 percent strain. Leung, et al. (2000) demonstrated that a single fiber optic sensor attached to a concrete beam in a zig-zag pattern can effectively detect and monitor cracks that are 0.1 mm [4 mils] wide. Another investigation by Feng, et al. (2010) demonstrated the detection of cracks 40 μm [1.6 mils] wide in ceramic materials by monitoring the change in strain profile, utilizing the distributed Brillouin sensor system. No information on longevity has been reported, but Udd (2011) indicated that fiber optic sensors deployed in steel bridges have been in service for over 25 years.

Monitoring Area and Data Acquisition

As mentioned previously, because the crack locations in a material are not usually known *a priori*, conventional point sensors, such as the FBG sensors, are not effective in crack detecting and monitoring. On the other hand, a single Brillouin fiber sensor can monitor a large area of a structure, depending on the length of the sensor. The small diameter flexible fiber allows the sensor to be packaged into configurations (e.g., the coil sensor shown in Figure 2-16) that are suitable for monitoring any type of local or large area. Both continuous and intermittent data acquisitions are possible.

Temperature and Radiation Tolerance

The temperature dependence of the Bragg wavelength is related to the temperature dependence of the index of refraction (or the Bragg wavelength) and the grating period. For instance, in fused silica and germanium-doped silica fibers exposed at room temperature, the change in the refractive index is 9×10^{-6}/°C (Takahashi and Shibata, 1979). For temperatures greater than 0 °C [32 °F], FBGs display linear temperature dependence. Previous work showed that optical fiber suffered significant attenuation at high temperatures due to dopant migration and devitrification. Despite the temperature dependency, fibers generally have high temperature tolerances. As an example, Fabry-Perot fiber-optic strain sensors can withstand temperatures up to 538 °C [1,000 °F].

Variations in temperature have a negative effect on the performance of the fiber optical sensing system. The temperature dependence of the Bragg wavelength is related to the temperature dependence of the index of refraction and the grating period. It has been demonstrated that the Bragg wavelength of fiber optic gratings depends nonlinearly on temperatures below 0 °C [32 °F] (Reid and Ozcan, 1998). Other studies, however, showed that on FBGs, temperature dependence of the Bragg wavelength response is usually linear for temperatures above 0 °C [32 °F] (Morey, et al., 1989; Takahashi and Shibata, 1979). As a result, temperature calibration is required. Although subzero temperatures are not expected for a DCSS, the statement is intended to demonstrate the dependency of temperature on the behavior of the fiber optics.

The radiation sensitivity of the fiber optics strongly depends on the chemical composition of the fiber and the photosensitization technique used for writing the fiber. Several investigations have been conducted to evaluate the FBG's radiation hardness under gamma-ray exposure in order to assess their possible use for temperature and stress corrosion monitoring in nuclear environments. The results of this research concluded that ionizing radiation produces attenuation of the wavelength in optical fibers (Griscom, 1995). In particular, there is a change in the wavelength saturation of the radiation-induced peak shift of FBG written in photosensitive germanium-doped fiber, depending on the total radiation dose and the dose rate, while the full-width, half-maximum of the peak remained unaltered (Gusarov, et al., 2000). Highly doped germanium optical fibers proved to be less sensitive to gamma radiation, while hydrogen-loaded optical fibers show higher radiation sensitivity (Gusarov, et al., 2002). It was reported the change of the Bragg wavelength can be as high as 100 pm [3.9×10^{-6} mils] at a dose level of 0.5 MGy. Gusarov, et al. (2002) showed that FBGs written in the germanium-doped photosensitive fiber exhibit a Bragg wavelength saturating shift of 20 pm [0.78×10^{-6} mils] after a total gamma dose of 80 kGy (at 3 kGy/h and a total gamma dose of 1.5 MGy). Due to the photosensitivity of the germanium dopant in the core, the index of refraction in the core increases under the influence of gamma radiation, resulting in an increase in the Bragg wavelength (Gusarov, et al., 1999). Neustruev (1994) reported that the formation of stable defect centers is induced by gamma radiation of germanium-doped silica glass. Further gamma radiation of FBGs would create additional color centers, resulting in a change of effective refractive index. Hence, a radiation-induced drift of the Bragg wavelength toward red, arising from the gamma radiation, is expected. On the other hand, Sporea and Sporea (2007) explored the possible use of sapphire optical fibers in high-radiation environments. The results of that investigation demonstrated that sapphire optic fibers are immune to gamma radiation for up to 530 kGy total dose.

While much research has been reported on the effects of radiation on optical fibers that have the potential to be used in fiber optic sensors to detect SCC, the combined effects of temperature and radiation may pose challenges to the operational lifetime of these devices. Additional testing and qualification in environments that are representative of those expected in a DCSS are necessary to evaluate the potential use and limitations of these sensors.

Strengths and Weaknesses

Strengths include the fiber optic sensors are fabricated from materials that are electric insulators, so these sensors can be used in high voltage environments. The sensors also are chemically passive and not susceptible to corrosion or galvanic interactions. The sensors are light and small in size with a wide temperature operation range and are immune to electromagnetic interference. A few sensors can be deployed to monitor large areas.

Weaknesses include the need for sensor calibration after exposure to elevated temperature and radiation exposure. Gamma radiation causes signal attenuation and displacement of the Bragg wavelength. Sensor bonding to the structure may be cumbersome, and sensor deployment in aggressive environments may be difficult.

Potential DCSS Use

For this DCSS application, fiber optic sensors need to be physically attached to the cask outer surface and remain in service for an extended period of time. For crack monitoring, the fiber optic sensors have to be located at strategic locations and be physically attached to the structure. The fiber/structure bonding usually is performed by adhesives or metallic clamps. As

a result, it is unclear whether successful application of this sensor to a DCSS is possible. Placement on a new or existing DCSS would require considerable planning and development so that it does not damage the sensor during DCSS installation and minimizes dose to personnel. In addition, the potential negative effects of attaching a fiber optic sensor system to a canister would need to be evaluated.

Unknowns

- Combined effects of temperature and radiation on the calibration and longevity of the system.
- Methods to identify locations where sensors could be installed.
- Availability of methods and specialized tools to install and maintain these sensors in high temperature and high radiation environments.
- System modifications and preparation required for deployment on a DCSS that was not designed for monitoring.

2.5.2 Luna Crack Growth Sensor

Measurement Principle

Luna, Inc. has developed a real-time *in-situ* crack growth sensor for atmospheric SCC monitoring of metallic components. The crack growth sensor design shown in Figure 2-17(a) consists of four major components: (i) tensile sample made of the same alloy as the structure under study, (ii) ported frame, (iii) compression load cell, and (iv) preload nut. The load frame contains apertures that allow the external environment to be in contact with the stressed specimen. To facilitate field deployment, Luna, Inc. developed a single ruggedized package that contains the crack sensor along with signal processing and communication electronics, as shown in Figure 2-17(b).

The Luna crack growth sensor is a type of surrogate sensor (i.e., the sensor does not measure actual cracking events on the component of interest). The working mechanism of the sensor relies on the application of a tensile load to a cylindrical fracture mechanics sample that changes gradually, resulting in displacement as the sample is cracked. A hydraulic bolt tensioner is used to place the sample under a desired static tensile stress. The present sensor unit contains the dedicated electronics unit for data collection and post-processing capability. If the atmospheric conditions are such that SCC can develop, the strain gauge in the load cell can capture the change in displacement, as cracks are initiating and propagating in the fracture specimen. In other words, the sensor estimates crack depth indirectly from a measured tensile force, comparing it to the initial force for an uncracked sample. Figure 2-18 shows the results of a finite element model in regard to the sample stiffness variation, as a function of the crack depth for Monel K-500 alloy, as well as the stiffness of the enclosure containing the sensor.

Note that for this surrogate sensor to properly reflect the cracking behavior of DCSS systems, the residual stresses commonly seen in DCSS applications need to be assessed. Such stress values will be used as input for the stressing element in the sensor to more accurately reproduce the cracking behavior of DCSS systems.

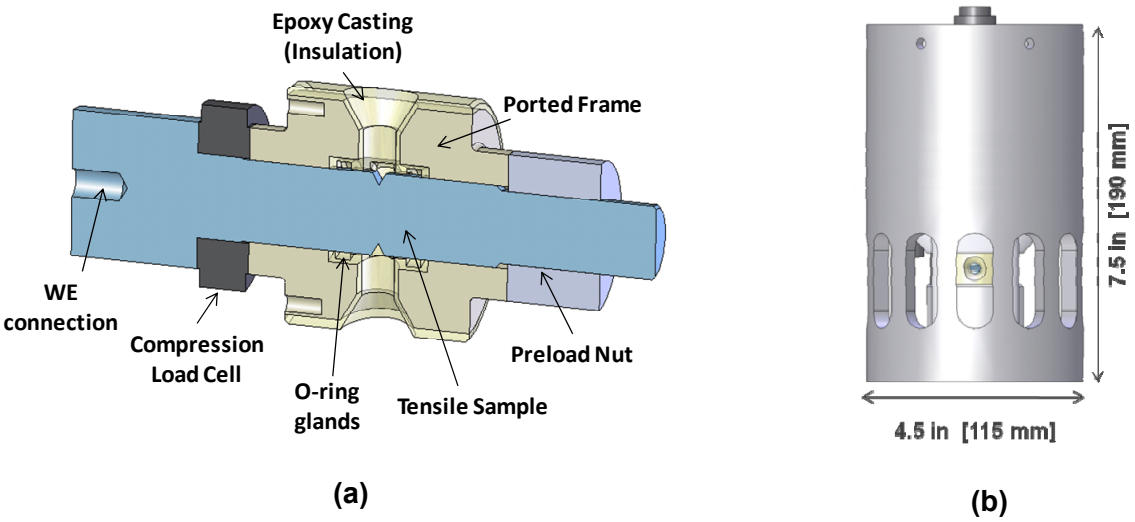

Figure 2-17. (a) Schematic Representation of the Load Frame and (b) Stress Corrosion Cracking Sensor Assembly (Reproduced With Permission of Luna, Inc.)

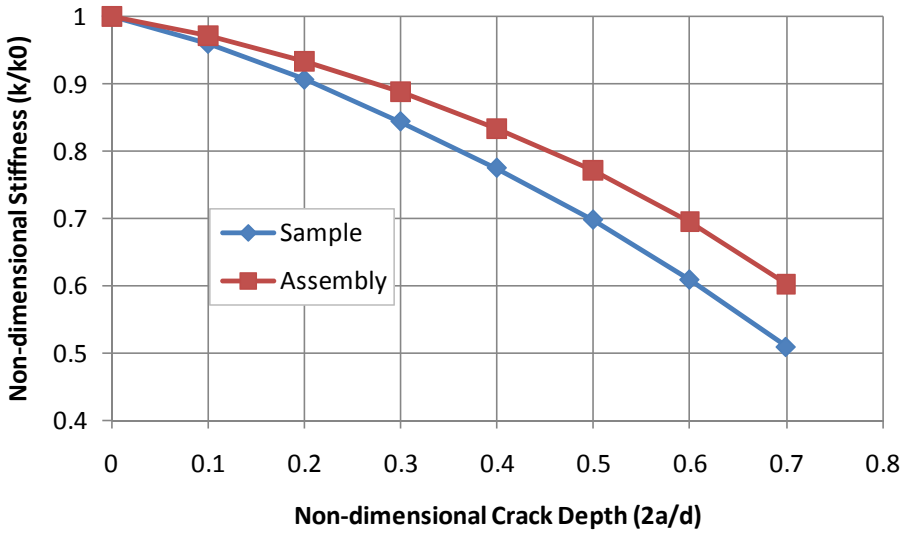

Figure 2-18. Normalized Stiffness Versus Crack Depth for the Sample Alone and for the Combined Assembly

Maturity

In early 2009, four crack growth sensors were field deployed at the U.S. Naval Research Laboratory at the Key West facility. Prior to field deployment, 30 sensors were tested in the laboratory under various accelerated conditions to study crack velocities. Although relatively newly developed, the Luna crack growth rate sensor is commercially available.

Space and Power Requirements

Figure 2-17 shows the diameter of the current assembly is 11.5 cm [4.5 in] and the length is 19 cm [7.5 in]. The sample geometry is 1.2 cm [0.5 in] in diameter, 10 cm [4 in] long, and is placed in a load frame 5 cm [2 in] in diameter connected to a strain gauge load cell.

The design life for the electronics is 3–5 years, with a target sampling interval of 30 minutes using three standard alkaline 1.5 V C-cell batteries and has a power consumption of 0.05 watts when a measurement is being recorded. This is achieved by the extremely low current draw when the unit is asleep (0.003 mA) and moderate draw when actively acquiring measurements (10 mA). The electronic compartment can be removed from the load cell so the load cell can be placed inside of a confined or remote location with the electronic enclosure hardwired to a more user accessible location. In doing this, the electronics compartment is separate from the fracture sample, allowing manual replacement of the batteries in the electronics enclosure and continuous sensor operation.

Measurement Range, Sensitivity, and Longevity

This sensor can measure a crack that is between 2 and 4 mm [0.08 and 0.2 in] deep. The more brittle alloys usually fracture at the shallower end of the depth range, while more ductile alloys will propagate further before fast fracture. This type of sensor can be custom tailored to specific applications, and the range and sensitivity can be customized accordingly. Experimental studies of crack propagation of Monel K-500 alloy in uncontrolled environments have shown crack depth resolution less than 1 μm [0.04 mils], with thermal compensation and crack propagation rates of 3×10^{-10} m/sec [1.2×10^{-5} mils/sec]. Note that sensor crack resolution is yet to be determined because no long-term studies have been conducted in nuclear environments, where radiation can pose challenges in the overall stability of the sensor.

The longevity of the sensor is dictated by the surrounding environment, the stress level applied to the sample, and the sample material. These combined factors will dictate the crack initiation and propagation rates. As an example, for a typical constant crack growth rate of 10^{-10} m/sec [4×10^{-6} mils/sec] in stainless steels, the sensor service life is estimated to be 2 years, assuming radial cracking in all directions.

Monitoring Area and Data Acquisition

As mentioned earlier, the Luna crack growth sensor is a surrogate sensor that does not directly monitor the surface of the component of interest. It is a stressed and instrumented sample that replicated the surface of interest.

For this sensor, an application software was developed for acquiring, converting, plotting, and storing data from multiple sensor nodes. The software code implements the crack depth/stiffness calibration and thermal compensation strategies outlined previously to reliably convert the raw measured force data into a useful crack depth metric. To validate proper

operation of the crack sensor mechanics, 17 4-PH stainless steel samples were tested. The logging interval is user configurable. Both continuous and intermittent data acquisitions are possible.

Temperature and Radiation Tolerance

The current sensor embodiment is rated for temperatures up to 120 °C [248 °F]. However, the implementation of custom strain gauges in place of the commercially available gauges currently used in the sensor may allow higher service temperatures.

The sensor is equipped with a calibration curve to convert the measured stiffness (related to the applied tensile load and the resulting deflection) to crack depth. Stiffness calibration curves are determined numerically and verified empirically for the tensile sample and loading frame. Significant analytical and experimental work was performed to develop the thermal compensation strategy that is now implemented in the data acquisition software, including the thermal calibration procedure required to obtain the necessary calibration constants.

To improve the accuracy of the crack depth measurement, a temperature correction of the sensor is required. As an example, the uncorrected output of the sensor has a crack depth error on the order of 30–40 μm [1.2–1.6 mils] per 1 °C [2 °F] temperature change, out of a total range of approximately 2,000 μm [78 mils]. Clearly, this effect must be compensated for to provide the most useful measurement for the intended environmental monitoring application, especially when crack growth rates are extremely low and easily obscured by uncorrected thermal transients. Temperature compensation is performed by explicitly measuring the sensor temperature with an embedded resistance temperature detector and applying the proper correction to the calculated crack depth. At the time of writing this report, the crack growth sensor has not been tested under radiation. Sensor components, such as the load cell, may be affected by the presence of radiation, but at this time, no research has been devoted to address this situation. As such, it is not known whether the sensor temperature compensation would be affected by radiation.

Radiation tolerance information is limited to the load cell element. According to the manufacturer, the load cell elements can absorb total gamma radiation levels on the order of 10^{11} rad. The effect of radiation on the sensor response currently is not known.

Strengths and Weaknesses

Strengths are that the Luna crack growth sensors are highly sensitive to crack initiation and propagation. The resolution for crack growth measurements is high. The sensor consumes low power without requiring AC power supply and does not need to be bonded to the canister surface.

Weaknesses are that this is a surrogate sensor, which does not measure crack initiation and propagation of the component of interest. The sensor requires temperature compensation and needs to know *a priori* the level of stress to be applied to the fracture sample in the sensor. The sensor only measures crack initiation and propagation locally. Multiple sensors may be needed for complete crack monitoring. Radiation tolerance has not been addressed in the current sensor technology, and field testing also is limited. The sensor also is quite large and somewhat complex.

Potential DCSS Use

For proper crack monitoring, the sensor has to be placed at strategic locations in the gap between the concrete overpack and the canister surface. Because this sensor acts as a surrogate inspection tool, the sensor does not need to be attached to the canister surface. Because of the large size of the sensor, placement inside existing DCSSs may be limited. In addition, successful sensor placement on an existing DCSS would require considerable planning and developing, as well as steps to minimize dose to personnel. For this surrogate sensor to properly reflect the cracking behavior of DCSS systems, the residual stresses commonly seen in DCSS applications need to be assessed. Such stress values would be used as input for the stressing element in the sensor to more accurately reproduce the cracking conditions of DCSS systems.

Unknowns

- Combined effects of temperature and radiation on the calibration and longevity of the system.
- Methods to identify locations where sensors could be installed.
- Availability of methods and specialized tools to install and maintain these sensors in high temperature and high radiation environments.
- System modifications and preparation required for deployment on a DCSS that was not designed for monitoring.
- The need for residual stress values before the sensor is deployed.

2.5.3 Crack Propagation Sensor

Measurement Principle

The commercially available crack propagation gauge provides a simple method to measure the propagation of a crack on a precracked surrogate specimen. The crack propagation sensor consists of a series of small strands (made of a high endurance alloy) connected in parallel and placed on a thin substrate in a ladder-like pattern. Typically, the sensor incorporates 10–20 resistor strands with a nominal thickness of 0.043 mm [1.7 mils] and a glass-fiber-reinforced epoxy matrix as sensor backing. The sensor can measure crack propagation in increments of 0.25 mm [9.8 mils]. When a crack forms beneath the gauge, it will induce a sequential local fracture of the sensing strands of the sensor, causing successive open circuiting of the strands and resulting in a stepped increase in the electrical resistance (ER) (Figure 2-19).

Note that for this surrogate sensor to properly reflect the cracking behavior of DCSS systems, the residual stresses commonly seen in DCSS applications need to be assessed. Such stress values would be used as input for the stressing element in the sensor to more accurately reproduce the cracking conditions of DCSS systems.

Data collection can be performed manually or continuously in real time via a wireless sensor network over Crossbow's Environmental Sensor Bus. The wireless sensor networks are composed of several nodes, typically known as "motes." Each mote is equipped with a radio, a

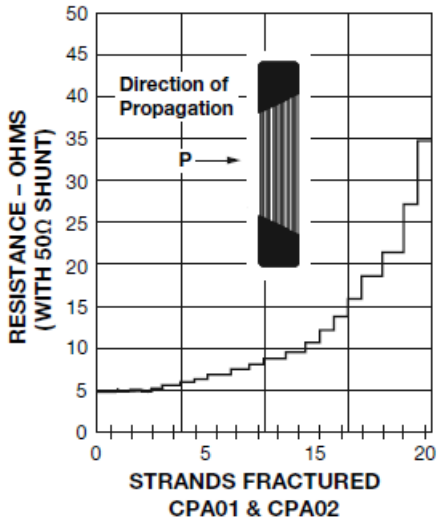

Figure 2-19. Resistance Correlation as a Function of the Number of Fractured Strands

power source (usually a battery), a microprocessor, specialized software, and usually one or more sensors. When deployed, a mote will record data from its sensors and transmit these data to a base station for processing or storage.

Maturity

Based on the literature review performed during this investigation, no field-deployed cases were reported.

Space and Power Requirements

The sensor geometry is 2.5 cm^2 × 0.5 cm^2 [1 in^2 × 0.2 in^2] with a thickness of 0.043 mm [1.7 mils]. Sensor interrogation can be accomplished manually using an ohmmeter with milliohm resolution. For this case, no power is needed. For automated sensor query, a low-powered, dedicated wireless network comprising numerous motes is required. Each mote is powered with 3 V using standard AA batteries. Typical power consumption for each mote is 0.001 watts. Because the crack propagation pattern is a purely resistive sensor, two precision resistors must be used to create a circuit that can convert the resistance output into a voltage that the mote can read.

Measurement Range, Sensitivity, and Longevity

The measurement range has not been specified. Based on the manufacturer specifications, the sensor crack resolution is modest and on the order of 250 μm [9.75 mils]. Sensor resolution is directly influenced by the separation between the strands. The longevity of the sensor is dictated by the surrounding environment, the stress level applied to the sample, and the sample material. These combined factors will dictate the crack propagation rates. Assuming a constant crack propagation rate of 10^{-10} m/sec [4 × 10^{-6} mils/sec], the sensor service life is estimated to be 1.6 years.

Monitoring Area and Data Acquisition

The crack propagation sensor is a surrogate sensor that can be positioned in close proximity to the actual component of interest. Ideally, the sensor is located in strategic locations where cracking is most likely to occur. The relatively small sensor size makes this technology a conventional point sensor for crack propagation measurements.

Sensor measurement can be obtained by measuring either the ER or voltage as a function of time. For manual measurements, a single data point is recorded at a given inspection time. For automated sensor interrogation, the recoded data include the measurement timestamp, sensor ID, and the value of the voltage across the sensor. Both continuous and intermittent data acquisitions are possible.

Temperature and Radiation Tolerance

The sensor does not require temperature compensation and can endure temperatures in the range of –269 to more than 230 °C [−452 to more than 446 °F]. In terms of radiation levels, the sensor can absorb total gamma radiation levels on the order of 10^8 rad, as reported by the manufacturer. The actual resolution of the sensor is yet to be determined because no long-term studies have been conducted in nuclear environments, where radiation can pose challenges in the overall stability of the sensor.

Strengths and Weaknesses

Strengths are the crack propagation sensors have a wide operational temperature range and are relatively simple systems. It needs low power without requiring an AC power supply. The sensor does not need to be bonded to the canister surface. The small size makes the sensor suitable to be placed in restricted areas.

Weaknesses are this is a type of surrogate sensor, which does not measure crack initiation and propagation of the actual component. It only has modest resolution of crack propagation. It does not measure crack initiation, but rather crack propagation locally. The radiation effect on sensor response and longevity has not been tested. Field testing has not been reported.

Potential DCSS Use

For proper crack monitoring, the sensor would need to be placed at strategic locations near the canister surface. A significant number of sensors would likely be necessary to cover the possible variations in conditions inside a storage overpack or concrete HSM. Successful sensor placement in an existing DCSS would require considerable planning and development, as well as steps to minimize dose to personnel. For this surrogate sensor to properly reflect the cracking behavior of DCSS systems, the residual stresses commonly seen in DCSS applications needs to be assessed. Such stress values would be used as input for the stressing element in the sensor to more accurately reproduce the cracking conditions of DCSS systems.

Unknowns

- Resolution of the sensor.
- Combined effects of temperature and radiation on the calibration and longevity of the system.

- Methods to identify locations where sensors could be installed.
- Availability of methods and specialized tools to install and maintain these sensors in high temperature and high radiation environments.
- System modifications and preparation required for deployment on a DCSS that was not designed for monitoring.
- The need for residual stress values before the sensor is deployed.

2.6 Concrete Degradation Monitoring

The degradation mechanisms considered for concrete structures listed in Table 1-1 include freeze-thaw degradation, chloride- and sulfate-induced chemical attack, aggregate reactions, leaching of $Ca(OH)_2$, settlement, creep, gamma and neutron irradiation, high temperature dehydration, reinforcing steel corrosion, and carbonation. For instance, corrosion of embedded reinforcing steel (rebar) can lead to cracking and spallation, which originates from debonding of the concrete from the reinforcing steel. The corrosion mechanism is often accompanied by several environmental indicators, including moisture level, pH, and concentrations of several chemical species (e.g., chloride, oxygen, and hydroxyl ions). The condition of the concrete may be assessed either indirectly by monitoring environmental factors (i.e., pH, chlorides, sulfates, and moisture level) relevant to concrete degradation or by direct measurement of physical deterioration in the structure.

The monitoring techniques that could be used to monitor some of the degradation mechanisms in Table 1.1 include embeddable corrosion sensors, external corrosion sensors, ultrasonic pulse velocity, acoustic emission, and fiber optic sensors. Details of these sensors are provided in Table 2-7 and the following sections.

2.6.1 Embeddable Corrosion Sensors

Measurement Principle

Several surrogate sensors have been developed and are commercially available to detect conditions that promote corrosion. These sensors, which can be embedded in close proximity to the rebar, may be used to identify the onset of rebar corrosion in concrete.[3] The ECI–1 corrosion sensor shown in Figure 2-20, developed by VTI (Reis and Gallaher, 2006), was designed to be embedded in the concrete to monitor several parameters related to corrosion of the steel reinforcement. These parameters include chloride ions, concrete resistivity, linear polarization resistance, corrosion potential, and concrete temperature.

The instrument contains an auxiliary reinforcement bar material used as a working electrode, a platinized niobium stainless steel mesh used as a counter electrode and an Mn/MnO_2 electrode used as a reference electrode for polarization resistance measurements. The unit also contains a resistivity sensor made of four gold wires and based on a modified Wenner four-pin method. A silver/silver chloride (Ag/AgCl) ion-specific electrode is used in combination with the MnO_2

[3]There are numerous sensing devices that have been developed for concrete evaluation. However, the ones presented in this investigation are those that hold promise for application in monitoring concrete used in nuclear applications.

Table 2-7. Monitoring Techniques for Concrete Overpack Degradation Mechanisms					
Features	**Embeddable Corrosion Sensors (Section 2.6.1)**	**External Corrosion Sensors (Section 2.6.2)**	**Ultrasonic Pulse Velocity (Section 2.6.3)**	**Acoustic Emission (Section 2.6.4)**	**Fiber Optic Sensors (Section 2.6.5)**
Maturity	Field deployed for non-nuclear applications	Field deployed for non-nuclear applications	Field deployed for non-nuclear applications	Field deployed for non-nuclear applications	Same as Table 2-6
Measurement Range	Not specified	Not specified	Not specified, measurements in the range of <2 to >4.5 km/s reported	Not specified	
Sensitivity	For ECI–1 sensor: 0.03 μA/cm^2 [0.19 μA/in^2]; for the multielectrode array sensor: 0.2 μA/cm^2 [1.3 μA/in^2]	0.1 μA/cm^2 linear polarization resistance (LPR), 5 kohm-cm (resistivity)	Detectable crack width >0.0254 mm [1 mil]	50 to 70 dB (depending on sensor type and model)	
Longevity	Decades possible	Not applicable, surface mounted and can be replaced	Not applicable, surface mounted and can be replaced	Not applicable, surface mounted and can be replaced	
Space requirements	ECI–1 sensor: 94 × 122 × 83 mm^3 [3.7 × 4.8 × 3.3 in^3]; multielectrode array sensor: 20 mm [0.78 in] diameter, and 20 mm [0.78 in] thickness	Linear polarization sensor: 180 mm [7.1 in] diameter × 20 mm [0.78 in]	180 × 110 × 160 mm^3 [7.09 × 4.33 × 6.30 in^3]	20 mm [0.79 in] (diameter) × 30 mm [1.2 in] (height)—transducer size	
Power requirements	Batteries, power consumption <0.6 watts	Batteries, power consumption <8.6 watts	Batteries or AC, power consumption not specified	Batteries or AC, power consumption as low as 4 watts	
Monitoring area or range	Local measurement in the immediate vicinity of the sensing element	Local measurement in the immediate vicinity of the sensing element	Linear depths or distances of 200 to 400 mm [7.87 to 15.7 in]	Not reported, area directly related to signal attenuation	
Data acquisition mode	Continuous or intermittent	Intermittent	Intermittent	Continuous or intermittent	
Temperature tolerance	−55 to 150 °C [−67 to 302 °F]	0 to 50 °C [32 to 122 °F]	0 to 45 °C [32 to 113 °F]	−20 to 80 °C [−4 to 176 °F]	
Radiation tolerance	Not specified	Not specified	Not specified	Not specified	
Strengths	Real time, monitors changes in conditions that promote corrosion of the reinforcing steel, wide temperature range	Easy to operate, highly sensitive to corrosion of the reinforcing steel, commercially available	Commercially available nondestructive, replaceable surface-mounted sensors, applicable ASTM standard	Mature technology, extensive field deployment, nondestructive	
Weaknesses	Requires concrete coring for sensor placement in structure, monitoring area limited to immediate vicinity of the sensor, surrogate sensors	Limited to outer surface layer assessment, requires electrical connection to reinforcing steel, monitoring area limited to immediate vicinity of the sensor, and time consuming	Difficulty in interpretation of results, inaccurate on rough concrete surfaces, data dependent on concrete moisture and temperature	Requires AC power source, cumbersome post-data analysis, background noise may interfere with test results	

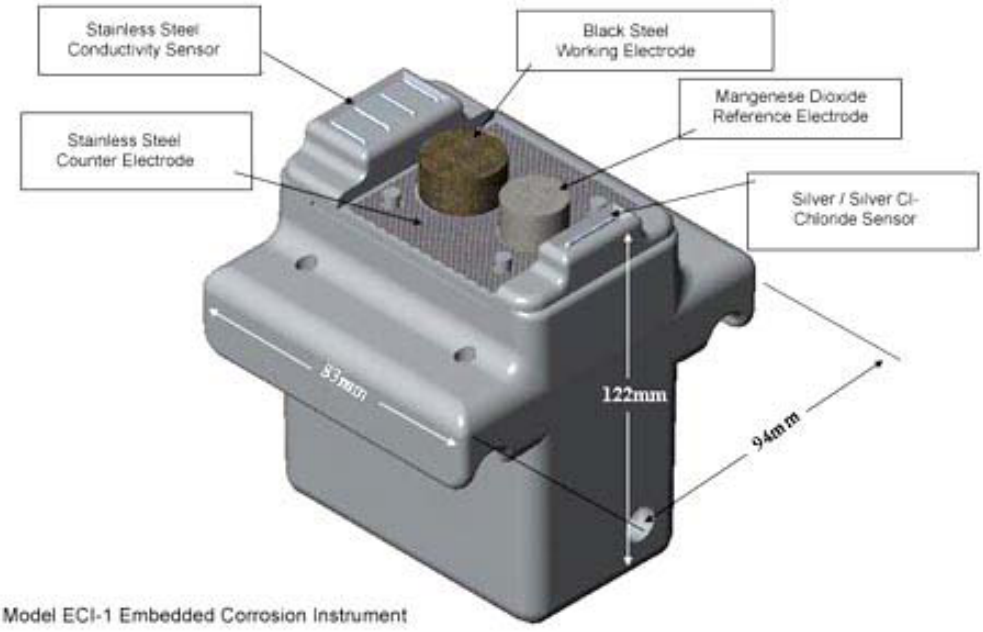

Figure 2-20. Schematic of VTI, ECI–1 Embedded Corrosion Instrument (Reproduced With Permission of VTI)

reference electrode as the chloride sensing unit. All sensing components are surface-mounted at or near the top of the device to provide a leveled measurement plane that can be directed to the area of interest.

The ECI-1 is currently considered the most successful corrosion monitoring instrument for reinforced structures. However, its design has deficiencies, which may limit its use in field applications. The most significant deficiency is its large size {94 mm × 122 mm × 83 mm [3.7 in × 4.8 in × 3.3 in]}, which restricts its application to new structures. For existing concrete structures, extensive concrete coring is needed to install the sensor within the concrete matrix, causing a significant disruption of the structure.[4] Also, there is uncertainty about the overall stability of the chloride-sensing electrode for long-term applications. Reports by Pawlick, et al. (1998), Schell and Manning (1985), and Bennett and Mitchell (1992) have suggested the reference electrode potentials tend to drift over time.

More recently, small coupled multielectrode array sensors (MAS) were developed for *in-situ* monitoring of various forms of corrosion of carbon steels, stainless steels, and nickel-based alloys (Yang, et al., 2001; Yang, 2008; Yang and Dunn, 2002). The surrogate sensors have been demonstrated to measure corrosion rates in concrete. Previous studies (Yang and

Sridhar, 2003) have shown the sensor can provide real-time measurements that are representative of the corrosion rate of reinforcing steel in concrete. Due to the nature of the sensor and the small area of the electrodes, the sensor can predict penetration rates typically encountered in localized corrosion processes (Yang, et al., 2001; Yang, 2008). While not

[4]When a hole is cored in an existing concrete structure for installing embeddable sensors, the prevention of preferential chloride penetration along the sensor/concrete interface is an important issue that needs to be further studied.

specifically designed for use in concrete, the small form factor of the sensor may allow it to be installed in existing concrete structures (and new structures) by coring a small diameter hole, resulting in minimal concrete disruption. Figure 2-21 shows a schematic of the sensor.

The sensor consisted of multiple miniature electrodes constructed of the metal of interest (e.g., rebar steel) in a nonconductive matrix, such as epoxy. The electrodes are coupled by connecting each of them to a common ground through independent resistors. Corrosion current measurements are made by reading the differential voltage across the resistors. The resistors are connected in series; each connection node is a port to an electrode of a corrosion probe array. In this manner, currents originating from the anodic or cathodic reactions at an individual electrode can be measured in sequence. The coupled multielectrode can be connected to a corrosion analyzer that has a high current resolution (10^{-12} A). One of the main advantages of this sensor is that it does not require calibration because the measurements are performed at the open circuit potentials. In addition, the sensor does not use a reference electrode, which is required in most electrochemical methods, such as linear polarization resistance, and must be maintained to ensure valid measurements. Also, this sensor can be set for wired and wireless operation.

Maturity

The ECI–1 developed by VTI (Reis and Gallaher, 2006) is commercially available and has been installed on a number of structures. The coupled multielectrode array was used for studying corrosion of pipelines in chemical plants as well as monitoring corrosion rates in concrete piles. To date there is no known use of this sensor in nuclear applications.

Space and Power Requirements

As stated previously, the ECI–1 device is 94 mm long × 122 mm wide × 83 mm thick [3.7 in × 4.8 in × 3.3 in], whereas the size of the MAS can be customized, depending on the application. Typically, the sensor diameter can be as small as 20 mm [0.78 in] and 20 mm [0.78 in] thick. For both sensing technologies, sensor measurement is restricted to the area where the sensor is positioned (highly localized), so that several units may be required for complete diagnostics of the structure.

The ECI–1 is wired to a microcontroller located within the polymer body of the device, which sequences all of the sensor measurements and stores and processes individual measurements. The microcontroller also is used to assign a unique data address to the device and to control the power sequencing of the device when used alone or in combination with other ECI–1 devices. Adding a data logging system with a cellular phone unit allows for remote access monitoring. The ECI–1 devices, data logger, and cellular phone unit can be powered by a solar power panel mounted near the sensor or by a 12 V DC battery or AC power supply. A gel-cell battery is used to store power from the solar panel. For DC- or AC-powered units, power consumption is rated at 0.054 watts during operation and 0.018 watts for the idle sensor. The MAS is powered with 3.6 V DC and has a power consumption rated at 0.01 watts during measurement and 0.6 watts for about a second during sensor communication.

Measurement Range, Sensitivity, and Longevity

The measurement range of the ECI–1 sensor is not specified. The manufacturer states the minimum detectable corrosion rate is 0.03 uA/cm^2 [0.19 uA/in^2]. This value is equivalent to a corrosion rate of 0.25 µm/yr [0.01 mils/yr] assuming carbon steel under the passive condition.

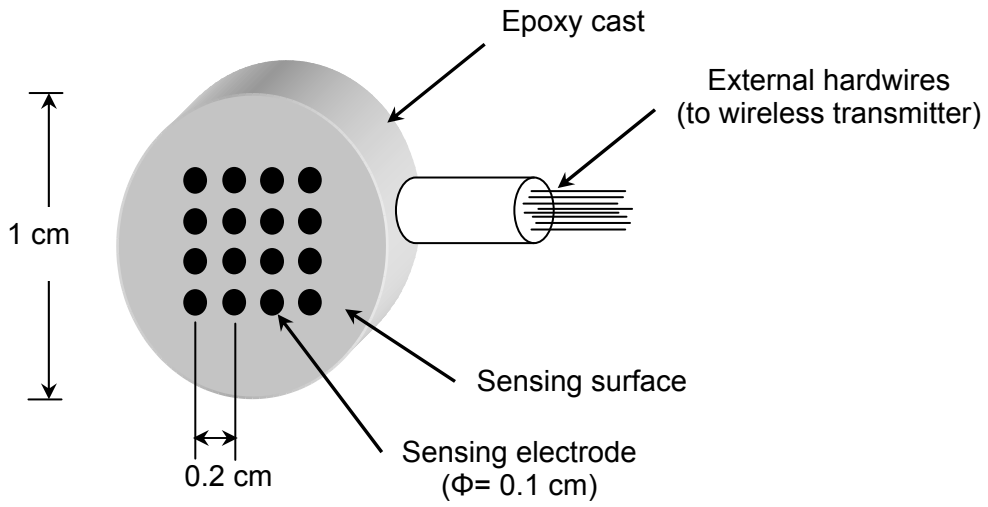

Figure 2-21. Schematic of the Multielectrode Array Sensor

For the MAS, minimum detectable corrosion currents are on the order of 0.2 μA/cm^2 [1.3 uA/in^2], equivalent to 2.5 μm/yr [0.1 mils/yr]. Based on these corrosion values, both sensing technologies have the capability to detect the passive/active corrosion transition of the reinforcing steel in concrete.

Based on these corrosion rates, both sensors are expected to last over decades, with decreasing longevity as the corrosion rate of the steel working electrode (ECI–1) or the sensing electrodes (multielement array sensor) increases. The actual sensor service life will strongly depend on the corrosive environment in concrete.

Monitoring Area and Amount of Data per Measurement

Because the sensor dimensions are relatively small compared to the area of inspection, the overall monitoring area is restricted to the location of the sensor. Typically, the sensors are positioned at the most susceptible locations for corrosion, adjacent to the rebar but on the side that will experience chloride or moisture ingress first. This will allow preventive measures to be taken before steel rebar corrosion begins. Sensor readings are taken at time intervals, and the current flow and/or corrosion rate is recorded. The amount of data per measurement is not specified but is estimated to be less than 0.1 kB/datum.

Temperature and Radiation Tolerance

The manufacturer states the ECI–1 sensor can withstand temperatures ranging from −55 to 150 °C [−67 to 302 °F]. The normal operation temperature range of the multielectrode probe is –30 to +50 °C [−22 to 122 °F] (Corr Instruments, LLC, 2013). Using diamond-like carbon-coated electrodes, the demonstrated upper temperature in the laboratory is increased to 150 °C [302 °F] (Chiang and Yang, 2010; Chiang, et al., 2008). The radiation tolerance for both sensing technologies is unknown.

Strengths and Weaknesses

Strengths of the EC–1 and the MAS include specific development for field applications, simple operation, small size, commercial availability, and adequate sensitivity for detecting the onset of conditions that are known to result in steel reinforcement corrosion. The units can provide real-time data and have a wide temperature operation range.

Weaknesses include the requirement for concrete coring for sensor placement in existing structures and the limited characterized area due to highly localized measurements. Additionally, these are surrogate sensors (i.e., the sensors do not measure the actual corrosion of the reinforcing steel but that of the working electrode). Sensor replacement can be difficult. Long-term performance and reliability is still under evaluation.

Potential DCSS Use

Either the ECI–1 or the MAS potentially could be used to monitor concrete in either new or existing DCSSs. For new structures, the sensors can be embedded in the concrete at the time of casting, preferably at locations near the reinforcing steel. For existing concrete structures, coring would be required for installation, followed by regrouting to avoid water ingress. The sensors are hardwired to the concrete exterior for data collection. For nuclear applications, the linear polarization resistance component of the sensor potentially is usable for extended periods of performance. The other sensing elements in the sensor (i.e., the chloride) are expected to be unstable over long periods of exposure.

Unknowns

- Measurement range and longevity of the embedded sensors.
- The effects of temperature and radiation on the sensor operation and longevity.

2.6.2 External Corrosion Sensors

2.6.2.1 Linear Polarization Resistance Sensor

Measurement Principle

In linear polarization resistance measurements, the reinforcing steel is perturbed by a small electrical signal (current or potential) applied by an auxiliary electrode on the concrete surface. Assuming the electrical signal is uniformly distributed throughout the reinforcement, the change of potential over the change of current ($\Delta E/\Delta I$) defines the polarization resistance. The corrosion current is inversely proportional to the polarization resistance and proportional to the extent of corrosion of the reinforcing steel (Table 2-8).

Direct measurement of the polarization resistance from $\Delta E/\Delta I$ measurements usually is not feasible in large concrete structures because the applied signal tends to diminish rapidly with distance from the signal application. This can lead to inaccurate estimates of the surface area of the steel polarized and lead to errors in calculating the corrosion current density. To overcome the problem of confining the current to a predetermined area, a second auxiliary guard ring electrode surrounding the inner auxiliary electrode is used. In principle, the outer guard ring electrode maintains a confinement current during the linear polarization resistance measurement (Gepraegs, et al., 2005; Liu and Weyers, 2003).

Table 2-8. Correlation Between Corrosion Current and Reinforcing Steel Extent of Corrosion*	
Corrosion Current Density	**Rebar Extent of Corrosion**
<0.1 μA/cm^2	Passive condition
0.1–0.5 μA/cm^2	Low to moderate corrosion
0.5–1.0 μA/cm^2	Moderate to high corrosion
> 1.0 μA/cm^2	High corrosion rate
*Broomfield, J.P. "Corrosion of Steel in Concrete." Uhlig's Corrosion Handbook. 2nd edition. R. Winston, ed. New York City, New York: John Wiley and Sons, Inc. pp. 581–599. 2000.	

The measurement is made by applying a galvanostatic pulse (using the galvanostatic pulse method), lasting up to 100 seconds, from the central counter electrode. Then, an additional current is applied from the external ring, and this external current is modulated by means of two reference electrodes, which equilibrate the internal and external currents. This allows for a correct current confinement and thus a more accurate account of the polarization resistance (Figure 2-22). The galvanostatic pulse method has been used since 1988 for evaluating reinforcement corrosion both in the laboratory and the field (James Instruments, Inc., 2010; Wojtas, 2004).

Maturity

The linear polarization resistance technique has become a well-established method of determining the instantaneous corrosion rate of reinforcing steel in concrete (Kessler, 2001). The technique is rapid and nonintrusive, requiring only localized damage to the concrete cover to enable an electrical connection to the reinforcing steel. One of the most reliable methods is linear polarization resistance by means of the modulated confinement of the current (James Instruments, Inc., 2010). This technique has been extensively used in the laboratory and in the field. Linear polarization resistance measurements on reinforcing steel in concrete have been used for corrosion rate estimation. Because of equipment constraints, the measuring technique was used in the laboratory rather than in the field. Studies using the linear polarization sensor were conducted throughout the 1990s (Feliu, et al., 1996, 1990). The sensor currently is used for field monitoring of bridges and concrete retention walls.

Space and Power Requirements

The sensor size placed in contact with the concrete is 180 mm in diameter × 20 mm thick [7.1 in × 0.78 in]. The sensor is electrically connected to the polarization recording unit, which has dimensions of 300 mm × 200 mm × 360 mm [11.8 in × 7.8 in × 14.1 in]. The unit contains rechargeable nickel hydride batteries capable of providing up to 8 hours of continuous operation at 13.7 V. Power consumption is rated at 8.6 watts. The instrument contains a verification box for sensor check. Inside this verification box is an electrical circuit that simulates the structure behavior.

Measurement Range, Sensitivity, and Longevity

The measurement range of this sensor is not specified, but available data indicate the sensor can measure corrosion rates over several orders of magnitude. Luping (2002) conducted a sensitivity study with a polarization recording instrument using the gravimetric method in concrete samples containing chloride concentrations ranging from 0 to 6 weight percent of

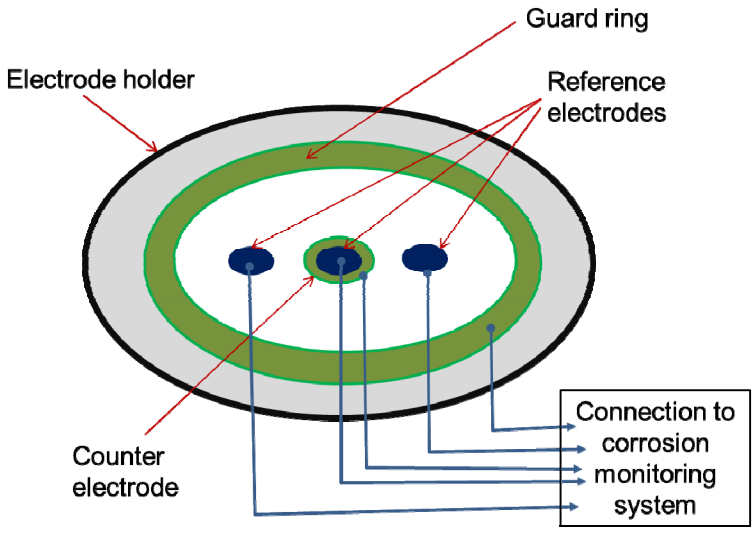

Figure 2-22. Schematic of the Linear Polarization With a Guard Ring for Current Confinement

cement (Figure 2-23). This study demonstrated the corrosion rate results matched closely (<2.6 factor) to the true values of the mean corrosion rate determined by the gravimetric

method. The polarization recording instrument values reported in Figure 2-23 were corrected by a pitting factor ranging from 4 to 8 to obtain the actual localized corrosion rate (Gonzalez, et al., 1995). Other uncertainties should be taken into account when evaluating onsite test results (e.g., the actual area of the reinforcement being polarized and the variation over time in corrosion rates due to fluctuations in temperature and moisture conditions). Exposure conditions, especially temperature and concrete humidity, can alter the corrosion rate by a factor of 10 or more.

Concerning the sensor longevity, there are no reported data that allow calculation of the sensor service life. According to the manufacturer, proper maintenance of the sensor is required to extend and improve sensor performance. Because the measurement of corrosion rate involving the polarization recording instrument requires placing the sensor on multiple areas of the concrete surface, the sensor can be easily maintained or replaced.

Monitoring Area and Amount of Data per Measurement

The duration for each corrosion rate measurement, including initialization and 100-second polarization, is 3 to 5 minutes. When the diameter of the reinforcement and the exposed length of the reinforcement (counter electrode diameter) are known, the instantaneous corrosion rate can be calculated. Note that the obtained corrosion rate is an instantaneous average rate for the confined area that strictly applies to the measuring conditions. This area corresponds to the steel reinforcement bars (with electrical contact between them) in the reinforcement layer close to the concrete surface and located within a 105-mm [4.13-in] diameter circle centered on the sensor schematically, which is shown as the measured area in Figure 2-22.

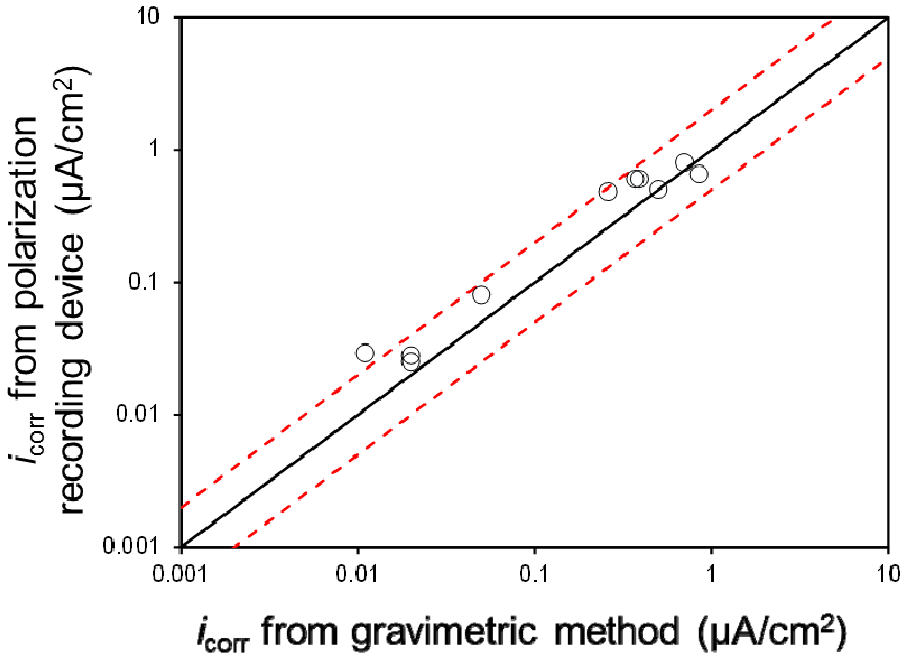

Figure 2-23. Comparison Between Corrosion Current Density Measured by the Polarization Recording Instrument and the Gravimetric Method (Luping, 2002). Dashed Lines Indicate the Upper and Lower Limits for a Tolerance Factor of 2, Which is Commonly Used in the Field of Corrosion Measurement Using Electrochemical Techniques.

For a single rebar of diameter D, with the sensor centered over it, the confined area under study is given Eq. (2-2)

$$A = 3.142 \times D \times 10.5 \text{ [cm}^2\text{]} \quad (2\text{-}2)$$

As a result of the confined area the sensor measures, structures have to be mapped at locations where corrosion is expected. Consequently, this monitoring technique can be time consuming.

Temperature and Radiation Tolerance

According to the manufacturer, the polarization recording device should not be operated in temperatures below 0 °C [32 °F] or exceeding 50 °C [122 °F]. The RH should not exceed 90 percent inside the unit. Radiation tolerance is unknown.

Strengths and Weaknesses

The linear polarization resistance sensors are lightweight, easy to operate, and commercially available and have adequate sensitivity to detect corrosion of steel in concrete. They can measure actual corrosion rates of reinforcing steel without major modification of the structure.

Weaknesses are that they require electrical connection to reinforcing steel, and the measurement is restricted to a confined area, and is time consuming. In addition, the maximum depth of the concrete structure that can be interrogated using this technique is unknown.

Potential DCSS Use

The linear polarization resistance sensor has demonstrated high accuracy for corrosion rate determination of the reinforcing steel in concrete. For proper analysis of the structure under study, the sensor must be manually positioned over different areas of the concrete surface for corrosion rate mapping. As a result, this technique is suited for the exterior surface only and cannot be used to access the inner surface of the concrete shielding structures (e.g., overpacks and HSMs).

Unknowns

- Applicability of this method to thick concrete sections and the effect of concrete coverage, or rebar depth, on the ability to perform measurements.

- Effect of concrete resistivity and concrete chemistry on the measurements.

2.6.2.2 Resistivity Sensor

Measurement Principle

The determination of concrete resistivity has become an established nondestructive test method, often used to assess moisture content in concrete and concrete durability (American Association of State Highway and Transportation Officials, 2011). One approach to measure concrete resistivity is by using the well-known Wenner probe. The Wenner probe consists of four equispaced shaft electrodes placed on cylindrical concrete samples in a fully saturated condition or on the surface of a concrete structure. Resistivity measurements are obtained by applying a potential between the outermost electrodes of the probe, which generates a current proportional to the concrete resistivity (ASTM International, 2012d). For instance, a few U.S. Department of Transportation agencies and universities (Florida Department of Transportation, 2005; Sagues, et al., 2001) are using the Wenner probe (Figure 2-24) in field applications for assessing concrete resistivity before the installation of a cathodic protection system. Two other resistivity test methods used in the field are related to using embeddable electrodes in the concrete and using the reinforcing steel and an external electrode placed on the concrete surface (Weydert and Gehlen, 1999). Resistivity measurements have been employed to characterize concrete quality, assess the likelihood of corrosion of the reinforcing steel, monitor the evolution of concrete hydration, and determine the transport of ionic species in concrete (Elkey and Sellevold, 1995; Hunkeler, 1996; Sagues and Lau, 2009).

The environmental factors that affect concrete resistivity are temperature and moisture. Surface layers of the concrete, aggregate size, structure geometry, resistivity probe electrode spacing, and the presence of steel embedded in concrete also affect concrete resistivity. Morris, et al. (1996) also provided correction factors for noninfinite geometry in resistivity measurements, to compensate for geometrical limitations. However, as the geometry becomes smaller than the ideal semi-infinite condition, resistivity measurements could be overestimated with respect to the actual concrete resistivity (Millard, 1991). Any variation on the surface of concrete, due to the ingress of external ions through a concrete cover, uneven moisture profile, or carbonation, could have an impact on resistivity measurements. Such situations can create concretes that are highly inhomogeneous.

Figure 2-24. Resistivity Measurements on Concrete Using the Wenner Probe

As a rule of thumb, a high degree of water saturation and an increased number and size of pores tend to decrease resistivity measurements. Resistivity increases as the concrete dries and when carbonation occurs. Additional factors that affect concrete resistivity (Millard, 1991; Pruckner and Gjorv, 2004) include

(1) Amount of cement per unit volume of concrete.

(2) Water-to-cement ratio. As the water-to-cement ratio increases, the pore structure in concrete becomes more connected, thus resistivity decreases.

(3) Concrete curing conditions (temperature, RH, and duration). An increase in curing temperature improves pore continuity, decreasing resistivity.

(4) Temperature (3 and 5 percent decrease in resistivity for saturated and nonsaturated concretes, respectively, per degree Celsius increase).

(5) Chlorides (a 2 percent increase in chloride concentration by weight of cement decreases the concrete resistivity by ~50–60 percent).

(6) Moisture content (~3 percent resistivity decrease per 1 percent increase in saturation). Typically, >70 percent degree of saturation is maintained for concrete covers beyond 2 cm [0.8 in].

(7) Cement type and the presence of pozzolanic additions (e.g., fly ash and silica fume) increase concrete resistivity (i.e., increase the long-term concrete strength and concrete density).

(8) Aggregate type.

(9) Admixtures (concrete inhibitors, water reducers).

Broomfield (2000) proposed a correlation between concrete resistivity and corrosion rates of the reinforcing steel as shown in Table 2-9.

Table 2-9. Correlation Between Concrete Resistivity and Reinforcing Steel Corrosion Probability	
Concrete Resistivity	**Likelihood of Corrosion Rate of the Steel**
>20 kohm-cm	Low corrosion rate (<0.1 μA/cm^2)
10–20 kohm-cm	Low/moderate corrosion rate (0.1–0.5 μA/cm^2)
5–10 kohm-cm	Moderate/high corrosion rate (0.5–1 μA/cm^2)
<5 kohm-cm	Very high corrosion rate (>1 μA/cm^2)

Maturity

The determination of concrete resistivity is an established nondestructive test method for studying the condition of concretes (e.g., permeability, curing efficiency, and water saturation in concrete) and for indicating corrosion of reinforcing steel in both laboratory and field applications (ASTM International, 2012d,e). The Wenner probe has been used for concrete resistivity measurement since the mid-1980s (Millard, et al., 1986; Ewins, 1990), and today few commercial products exist.

Space and Power Requirements

The concrete resistivity device is 197 mm × 53 mm × 69.7 mm [7.8 in × 2.1 in × 2.7 in], and the diameter of the probe shafts is 6 mm [0.24 in]. The device operates at a frequency of 40–1,000 Hz and AC voltage of 38 V. DC voltage is not recommended because it may involve errors due to electrode polarization. The maximum power consumption of the unit is estimated to be 0.0076 watts.

Measurement Range, Sensitivity, and Longevity

According to the manufacturer (GARDCO), concrete resistivity can be measured in the range of 0–1,000 kohm-cm (depending on the probe shaft spacing) with a resolution ranging from ± 0.2 kohm-cm (or 1 percent) for the nominal current of 200 μA and ± 2 kohm-cm (or 5 percent) for the nominal current of <50 μA. In practice, considerable scatter is expected in most sets of resistivity measurements. In any set of measurements on specimens, coefficients of variation of 10 percent are good and 20 percent must be considered normal. In the field, errors in the resistivity measurement of 25 percent are likely. Concerning instrument longevity, there are no reported data that allow calculation of its service life. According to the manufacturer, proper maintenance of the sensor is required to extend and improve performance.

Measurement of concrete resistivity is commonly limited to the outer 150-mm [5.9-in] layer of concrete, depending on the degree of concrete conductivity. As mentioned in Section 1.2, in some cases, the concrete thickness is greater than 59 cm [24 in]. Consequently, the resistivity of the inner concrete layers likely will not be measured if the sensor is placed on the outer concrete surface. The presence of reinforcing steels in concrete also can cause errors in the resistivity measurements.

Monitoring Area and Data Acquisition

Commonly used shaft spacing distances are 38 and 50 mm [1.5 and 2.0 in], according to the previous studies (ASSHTO, 2011, Millard, 1991) and the American Association of State

Highway and Transportation Officials surface resistivity test method. However, the presence of reinforcing steel may alter the resistivity measurement, especially if the concrete cover is less than 30 mm [1.2 in]. Thus, the location of the reinforcing steel must be assessed using a steel locator device. The concrete depth being monitored greatly depends on the separation of the sensor shafts. A wider shaft spacing is preferred for a more uniform current flow in the concrete due to the inhomogeneous nature of the concrete. For instance, concrete depths span between 114 and 150 mm [4.5 and 5.9 in] for 38-mm and 50-mm [1.5-in and 2.0-in] shaft separations, respectively. Each measurement results in a single value of resistivity so the amount of data per measurement is small. Data acquisition is typically manual and intermittent.

Temperature and Radiation Tolerance

According to the manufacturer, the concrete resistivity device can operate at temperatures between 0 and 50 °C [32 and 122°F]. Radiation tolerance is unknown.

Strengths and Weaknesses

Strengths include the resistivity sensors are lightweight, easy to operate, and commercially available and have adequate sensitivity to detect changes in concrete properties associated with the corrosion behavior of the steel. They do not require structure modification or physical access to the reinforcing steel.

Weaknesses are the measurement is qualitative and time consuming and the probe area is restricted by the shaft separation of the sensor. The measurement only is limited to the outer layer of the concrete.

Potential DCSS Use

The resistivity sensor could be placed on the concrete surface after wetting the shafts. The measurement is straightforward, but multiple measurements need to be performed to locate the areas of low resistivity that may be associated with higher anion penetration or likelihood of corrosion of the reinforcing steel. The technique cannot be used to interrogate thick concrete structures, and physical access to the internal surfaces of the concrete overpack or HSM would require considerable planning and effort to minimize worker dose. As a result, concrete resistivity is best suited for the exterior surface of the concrete overpack.

For sensor operation, no electrical connection to the steel is needed, so no modification of the DCSS systems is required. Concrete resistivity is manually collected and stored in the instrument. Several commercial handheld concrete resistivity sensors exist.

Unknowns

- Effects of concrete aging during DCSS operation on measured resistivity changes due to corrosion of the reinforcing steel.
- Initial concrete chemistry and atmospheric exposure effects on resistivity.
- Radiation tolerance.

2.6.2.3 Surface Potential Sensor

Measurement Principle

Corrosion processes on carbon steels, including those affecting reinforcing steel in concrete, have active (anodic) and passive (cathodic) regions. An electric current flows between the cathodic and anodic regions through the concrete, and the electrochemical potential difference can be detected by measuring the potential drop in the concrete at the surface (Broomfield, 2000). This qualitative and nondestructive technique allows for assessing the location of the active areas and indirectly detecting the probability of corrosion of the reinforcing steel in concrete before visual degradation is noted. Only two reference electrodes are required for surface potential measurements, and no electrical connection to the reinforcing steel is necessary. One of these electrodes is maintained at one location on the surface of the structure, while the other electrode is rastered along the surface. A high impedance voltmeter is commonly used to measure the potential difference between the two reference electrodes. A more positive potential reading represents an anodic area where corrosion is possible. The greater the potential difference between anodic and cathodic areas, the greater the probability of corrosion (Indian Lead Zinc Information Centre, 1995; Song and Saraswathy, 2007).

The surface potential measurements can be affected by the concentration of oxygen in concrete, concrete carbonation, chloride concentration, the type of reinforcing steel, and concrete resistivity, among other factors (Song and Saraswathy, 2007). Thus, surface potential measurements should be validated by complementary tests (e.g., visual inspection, concrete resistivity, and corrosion rate measurements) before an interpretation of corrosion probability is made.

The reference electrodes have to be checked against a standard reference electrode of known potential before starting the surface potential measurements. Typically, the potential difference between the known reference electrode and the reference electrodes under evaluation should be less than 10 mV. This calibration is commonly taken with a high input impedance voltmeter, so the current flowing through the reference electrodes does not disturb the stability of the reference electrode potential.

Maturity

The determination of surface potential is an established nondestructive test method for studying the condition of reinforcing steel in both laboratory and field applications (Song and Saraswathy, 2007). The technique is qualitative because it does not measure actual corrosion rates or assess the condition of the steel; rather, it indicates whether corrosion of the reinforcement may be occurring.

Space and Power Requirements

Reference electrodes for surface potential measurements come in different sizes, depending on the application {ranging from 4.5 to 40 mm [0.17 to 1.5 in] in diameter} and are 180 mm [7 in] long. The voltmeter used for recording the potentials is 150 mm × 80 mm × 45 mm [5.9 in × 3.1 in × 1.77 in]. The voltmeter usually operates with a 9 V battery with a power consumption rated at 0.0009 mW.

Measurement Range, Sensitivity, and Longevity

The measurement range is not specified but will be limited by the range of electrochemical potentials, which are dependent on the system pH and redox conditions. Typically, the accuracy of the surface potential measurements is dictated by the intrinsic accuracy of the voltmeter. Voltmeters are commonly specified with an accuracy of 1 percent of the potential reading. According to the manufacturer, proper maintenance of the sensor is required to extend and improve performance. Because the measurement of surface potential involving the use of reference electrodes requires placing the electrodes on multiple areas of the concrete surface, unit longevity is not an issue and replacement is simple.

Monitoring Area and Data Acquisition

Mapping is usually performed with a wheel arrangement and a grid. Areas may be scanned at rates exceeding 100 cm² [15.5 in^2] per hour with single or multiple electrode instruments and computer-assisted data acquisition. Potential drifts in a single measurement can be acceptable because 30–50 single potential measurements are taken per square meter of concrete surface. Vertical and horizontal surfaces from the underside can be measured with the same experimental arrangement, provided a suitable construction that presses the wheels onto the concrete surface is available. The potential data may be represented by color plots, equipotential contour plots, three-dimensional (3-D) plots, or other representations. The amount of data per measurement is small and could be in kilobytes.

Temperature and Radiation Tolerance

According to the manufacturers, voltmeters can operate at temperatures between −23 and 80 °C [−10 and 176 °F]. Radiation tolerance is unknown.

Strengths and Weaknesses

The surface potential sensors are lightweight, easy to operate, and commercially available. They do not require modifying the structure or physical access to the steel.

The technique has significant weaknesses causing measurements to become mostly qualitative indicators. The measurements are confined to the probe area defined by the location of the reference electrode. Characterization of large areas is time consuming. The measurements also are limited to the outer layer of concrete, and influenced by properties of concrete and reinforcing steel. The technique is not suitable for measurements of coated or galvanized steel reinforcement due to the high resistance provided by the coating or the mixed potential resulting from the zinc layer. Spatial variations of oxygen concentration at the concrete/steel interface significantly affect the surface potentials (Song and Saraswathy, 2007). For instance, a decrease in oxygen concentration at the steel surface can result in more negative corrosion potentials, which are not necessarily associated with a higher probability of corrosion. The concrete cover also plays a role in the surface potential measurements (i.e., a thicker concrete cover yields more positive surface potentials). In addition, a concrete cover in excess of 75 mm [3 in] thick can result in the averaging of adjacent reinforcement corrosion potentials. As a result, location of reinforcing steel and its depth are important parameters for analysis of surface potential values.

Potential DCSS Use

The sensing approach may be valuable for qualitative characterization of the condition of the steel reinforcement. The technique is inexpensive, easy to use, and nondestructive. However, due to its nature, this method can be time consuming, requiring several measurements to be manually performed to fully assess the condition of the structure. The technique cannot be used to interrogate thick structures, and physical access to the internal surfaces of the concrete overpack or HSM would require considerable planning and effort to minimize worker dose.

Unknowns

Combined effects of radiation, concrete chemistry, and concrete moisture content on surface potential measurements.

2.6.3 Ultrasonic Pulse Velocity Sensor

Measurement Principle

This nondestructive technique involves measuring the speed of sound through the concrete to predict its strength and detect internal voids, cracks, and other discontinuities indicative of degradation. The technique is used to determine uniformity in the concrete structure and monitor changes over time. It also can be used to measure the thickness of concrete layers of inferior quality, as well as the compressive strength of the concrete (ASTM International, 2009; British Standard Institute, 1986; Trtnik, et al., 2009). The concrete measured can also be correlated to accelerated corrosion of the reinforcing steel.

Two sensing elements, a transmitter, a receiver, an amplifier, and an electronic timing device for measuring the signal transit time are used. Pulses of longitudinal ultrasonic waves are generated by an electro-acoustical transducer in contact with the concrete surface being tested. After traversing the concrete, the pulses are received and converted into electrical energy by a second transducer. The pulse velocity is calculated from the distance between the two transducers and the electronically measured transit time of the pulse. Variable arrangements, as schematically shown in Figure 2-25, may be used for sensor placement, resulting in different transmission modes (Malhotra and Carino, 1991; Tomsett, 1980):

(1) **Direct transmission**: Transducers are placed directly opposite each other on both sides of the concrete structure. The direct method is most sensitive for transit time measurements, so this approach is used wherever possible for assessing concrete quality. The indirect (see item 3 below) and direct methods could be statistically similar, provided the concrete has uniform properties, including moisture gradient along the surface and the depth (Yaman, 2001).

(2) **Semi-direct transmission**: Transducers are placed across corners of the concrete. The sensitivity of this approach is reduced compared to the direct method.

(3) **Indirect or surface transmission**: Transducers are attached to the same concrete surface and separated by a known distance. The indirect method is the least sensitive approach because the received signal amplitude may be less than 3 percent of that for a comparable direct transmission. The pulse velocity will be predominantly influenced by the condition of the concrete surface, which may not be representative of the concrete

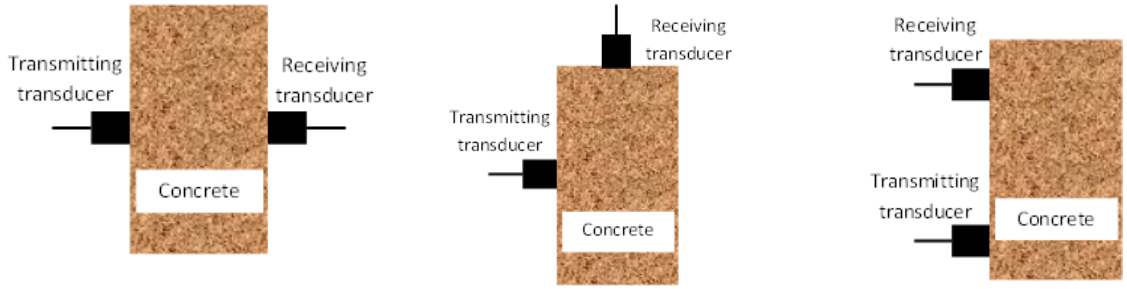

(a) (b) (c)

Figure 2-25. Schematics of the Different Configurations for Propagation and Reception of Ultrasonic Pulses: (a) Direct Transmission, (b) Semi-Direct Transmission, and (c) Indirect or Surface Transmission (British Standard Institute, 2004)

bulk. Also, the indirect method can cause attenuation of the transmitted pulse. The path length also is less clearly defined due to the finite transducer size.

The time for signal transmission is measured, and the signal velocity is computed based on the transducer separation. The relationship between ultrasonic pulse velocity and the quality of concrete is shown in Table 2-10. However, this relationship is not always practicable. For instance, the technique is ineffective for determining crack depths if the crack is water filled. The performance also is often poor in very rough surfaces and measurements are affected by temperature, concrete moisture, and the reinforcement presence of steel. Measurement interpretation can be very difficult because a large number of factors affect the pulse velocity. In general, crack widths >0.0254 mm [1 mil] are detectable by this method due to the negligible acoustic energy transmission across air-filled voids below this size.

Maturity

The first report of velocity measurements of mechanically generated pulses through concrete appeared in the United States in the mid-1940s (Leslie and Cheeseman, 1949; Elvery, 1973). At the same time, work was undertaken in Canada and the United Kingdom using electro-acoustic transducers, which were found to offer greater control on the type and frequency of pulses generated. The method has become widely accepted around the world, and commercially produced, robust, lightweight equipment suitable for field and laboratory use is readily available (Germann Instruments, Inc., 2014).

Space and Power Requirements

The transducers are connected to an external portable unit with dimensions of 114 mm × 223 mm × 267 mm [4.5 in × 8.5 in × 10.5 in], which provides a means of generating a pulse, transmitting the pulse to the concrete, receiving and amplifying the pulse, and measuring and displaying the time taken to transmit and receive the pulse. This transducer is typically 50 mm [2.0 in] in diameter. The equipment can be set up to run on both rechargeable batteries and standard AC power. The voltage required by the unit is 14 V. Transducers with natural frequencies between 50 and 80 kHz are the most suitable for use with concrete, and these may be of any type, although the piezo-electric crystal is most popular.

Table 2-10. Correlation Between Ultrasonic Pulse Velocity and Concrete Quality*†		
Pulse Velocity (km/sec) [mile/sec]	**Compressive Strength (MPa) [ksi]**	**Concrete Quality**
<2 [1.2]	—	Very poor
2–3 [1.2–1.9]	4 [0.58]	Poor
3–3.5 [1.9–2.2]	<10 [1.4]	Fairly good
3.5–4 [2.2–2.5]	<25 [3.6]	Good
4–4.5 [2.5–2.8]	<40 [5.8]	Very good
>4.5 [2.8]	<50 [7.2]	Excellent
*Song, H.W. and V. Saraswathy. "Corrosion Monitoring of Reinforced Concrete Structures: A Review." *International Journal of Electrochemical Science.* Vol. 2. pp. 1–28. 2007. †Neville, A.M. "Properties of Concrete." UK, London: Longman Group. 1995.		

Measurement Range, Sensitivity, and Longevity

The measurement range is not specified, but the relationship between pulse velocity and concrete quality is shown in Table 2-10. According to the manufacturer, the ultrasonic pulse velocity has an accuracy of 0.1 microseconds. The direct arrangement should be used whenever possible to ensure the highest signal amplitude between the transducers. The semidirect arrangement is less sensitive than the direct, although more sensitive than the indirect arrangement. The indirect method is particularly useful for determining crack depth or surface quality or for the case when access to only one surface is practical. According to the manufacturer, proper maintenance of the transducers is required to extend and improve performance. Because the measurement of pulse velocity involving the use of transducers requires placing the transducers on multiple areas of the concrete surface, the transducers and electronics can easily be removed and replaced.

Monitoring Area and Data Acquisition

The ultrasonic pulse technique can be used to map the structure by placing the transducers at different locations. Transducer separation can range from a few centimeters to 100 cm [39.3 in], depending on the type of defect and concrete properties to be examined. The only data collected during a single pulse velocity measurement is the transmission time, generally in microseconds. The pulse velocity then is computed with the known path length between the transducers. The amount of data per measurement is small and could be in kilobytes.

Temperature and Radiation Tolerance

According to the manufacturers, ultrasonic pulse devices can operate at temperatures between −10 and 60 °C [0 and 140 °F] (Germann Instruments, Inc., 2014). Radiation tolerance is unknown.

Strengths and Weaknesses

The ultrasonic pulse velocity sensors are lightweight, easy to operate, and commercially available. They do not require modification of the structures. The monitoring area can be significant depending on the path length between the transducers. The sensor provides the only readily available method of determining the extent of cracking within concrete.

Weaknesses are the operators must be well trained and aware of factors affecting the readings. For increased sensitivity, access to both sides of the concrete is needed. Detection of flaws within the concrete is not reliable when the concrete is wet. The method is time consuming. It is important to ensure adequate acoustic coupling of the transducers to the concrete surface. For that, a thin layer of couplant (e.g., petroleum jelly, liquid soap, or grease) should be applied to the transducer and the concrete. In some cases, it may be necessary to prepare the surface by smoothing it. For compound measurements and uniformity testing, a test grid should be drawn out on the concrete surface. As expected, the reinforcing steel affects the ultrasonic measurements because the signal will travel faster through the steel than through the concrete. Thus, the location of steel in the concrete matrix should be determined using a steel locator and ultrasonic transducers should be positioned to avoid the reinforcing steel. For practical purposes, for pulse velocities exceeding 4.0 km/s [2.5 miles/s], 20-mm [0.79-in] diameter steel bars running transversely to the pulse path will have no significant influence upon the measured values. However, steel bars exceeding 6 mm [0.24 in] in diameter and running parallel to the pulse path may have a significant effect.

Potential DCSS Use

This sensing approach is qualitative and focuses on the concrete properties. The properties can be directly correlated to accelerated corrosion or other degradation mechanisms in concrete. Due to the nonintrusive nature of the test, the ultrasonic pulse velocity technique could be applied to both new and existing DCSS configurations without cask modification. For the direct transmission approach, the placement of transducers could be problematic because of limited access to the interior concrete surfaces and the high temperatures and radiation doses inside the concrete overpack or HSM. As a result, assessment of the concrete bulk properties may not be possible, especially for thick concrete sections.

Unknowns

- Applicability of this method to conduct direct assessments given the requirement to have transducers on both sides of the concrete structure.

- Maximum thickness of a concrete structure that can be examined with this method.

2.6.4 Acoustic Emission Sensor

Measurement Principle

Acoustic emission (AE) testing has been increasingly used to ensure the integrity and performance of concrete bridges. AE is the transient elastic wave that is released by materials when they undergo deformation, dislocation movement, irreversible change, and initiation and propagation of microcracks (ASNT, 2005). More specifically, AE is a stress wave inside a material (e.g., concrete), leading to a displacement (e.g., crack) of concrete and inducing a pressure in a transducer positioned on the concrete surface (ASTM International, 2005a).

The AE technique consists of a transducer, commonly piezoelectric, in the frequency range of 60 to 300 kHz, which detects displacement and yields an electrical signal. For data collection and processing, typical AE equipment also involves a series of preamplifiers, filters, and amplifiers connected to a computer for data storage. AE sensors are broadly classified into two types: (i) resonant (narrow band), which are highly sensitive at a specific frequency and (ii) broadband, which possess a constant sensitivity across a wide band of frequencies. In most

practical field applications, resonant sensors are preferred over broadband sensors (Pollock, 1995). A typical AE sensor has a sensitivity of 50 to 70 dB.

Transducer mounting is an integral part of the success of AE monitoring (ASTM International, 2005b). First, the concrete surface where the sensors will be mounted must be cleaned and smoothed. Poor contact from rough surfaces decreases the amplitude of the acoustic signal. As a common practice, a thin layer of a viscous medium is placed in between the concrete surface and the transducer. In many cases, calibration is not required, because measurements are based on arbitrarily defined signal thresholds or the relative timing of wave arrivals. Alternatively, quantitative evaluation may be desirable to evaluate the absolute amplitude of recorded waves or discern the time history or shape of the waves emanating from the wave source. In addition, a calibration test can be used to identify sensors that have higher or lower sensitivities.

Background noise can have a large effect on AE testing and can prevent a test from providing usable data. This noise can be linked to mechanical sources, electrical sources, and environmental sources. The test may be ineffective if the noise sources cannot be removed. Additionally, the propagation of AEs through concrete is affected by nonuniformities in the structure (Uomoto, 1987).

During the formation of a concrete crack, a part of the energy is emitted as an elastic wave propagating spherically from the crack location and reaching the AE transducers at the concrete surface. By measuring specific signal parameters [i.e., counts, amplitude, duration, rise time, and counts energy (the area under the rectified signal envelope)], quantitative information can be obtained on the magnitude of the defect, its location, time of origination, and rate of propagation. Triangulation can be used to determine the location of certain discontinuities, where the location of discontinuities is computed as the product of signal travel times and sound speed (Pahlavan, et al., 2014).

Maturity

Obert (1941) first published initial studies on AE monitoring, followed by Kaiser (1950). Rüsch (1959) and L'Hermite (1959) carried out the first AE studies evaluating concrete under stress. Robinson (1965) showed that AE could be used to monitor microcracking between the cement and aggregates. Subsequent investigations were conducted to determine defect locations and failure mechanisms and to provide early warning about concrete failure (Green, 1970; Diederichs, 1983). More recently, Crystal River Power Plant employed AE to assess the repair of a concrete containment (Franke, 2011).

Space and Power Requirements

Prior to conducting an AE test, a preliminary visual survey of the existing DCSS should be conducted. Testing areas should be chosen based on accessibility and condition of the concrete. AE testing can be performed in the field with portable, lightweight instruments. The typical size of these portable units is 405 mm × 240 mm × 74 mm [16 in × 9.5 in × 2.9 in]. The units come with both a 12 V battery and AC options. No reported power consumption is available in the literature.

Measurement Range, Sensitivity, and Longevity

The measurement range is not specified but must be validated by calibration of the system. The National Institute of Standards and Technology developed the surface wave calibration method. This procedure subjects the sensor to a surface wave similar to that of an actual AE event (ASTM International, 2002). The preferred technique for conducting calibration tests is the pencil-lead break test, as specified in ASTM E2374 standard (ASTM International, 2004).

Sensitivity of an AE system often is limited by the background noise level. Examples of undesirable noise signals include frictional, impact, and mechanical vibrations. Some possible approaches to minimize noise involve fabricating special sensors with electronic gates for noise blocking, taking precautions to place sensors as far away as possible from noise sources and electronic filtering.

According to the manufacturer, proper maintenance of the transducers is required to extend and improve performance. Because measuring AE with transducers requires placing the transducers outside the concrete surface, sensor longevity is not an issue and unit replacement is simple.

Monitoring Area and Data Acquisition

There is no reported information about the magnitude of the concrete area that a single AE sensor can enclose. However, it is believed the monitored area will depend on several factors, such as the degree of external background noise and signal attenuation through the concrete matrix.

The AE testing produces large data sets. Extensive data analysis on the raw data is required before the damage onset can be detected and localized. Software-based AE systems can graphically display the recorded signals. These displays can be classified into four categories: (i) location, (ii) activity, (iii) intensity, and (iv) data quality. Location displays identify the origin of the detected AE events. Activity displays show AE activity as a function of time. Intensity displays are used to give statistical information concerning the magnitude of the detected signals and used to determine whether a few large signals or several small ones created the detected AE signal energy. Data displays are available to indicate the quality of the data collected.

Temperature and Radiation Tolerance

The types of transducers commonly used for AE testing vary depending on the application (Rhazi and Ballivy, 1993). For general purpose AE sensors, the operating temperature varies from −65 to 177 °C [−103 to 350 °F] (Vallen Systeme GmbH, 2012). Radiation tolerance is unknown.

Strengths and Weaknesses

AE sensors are commercially available. Their use does not require modification of the structures to be used, and measurements can be performed in real time. Because the elastic waves produced by the cracking events and the sudden redistributions of stresses in the concrete can travel considerable distances, the technique can be used to monitor for active defects over large areas.

Weaknesses are the operators must be well trained to execute this technique and interpret the data. This technique provides only qualitative information on damage in a structure. Continuous monitoring is necessary to detect the propagation of degradation processes, such as cracking.

Potential DCSS Use

This technique is a mature nondestructive method that can be used to monitor the formation of cracks or other defects in concrete in field applications. For the extended storage application, the AE technique could be applied to both new and existing DCSS system configurations, with limited system preparation. Multiple transducers, mounted on a cleaned and smoothed concrete surface, can be used to determine different sources of emission, and triangulation can be used to determine the location of certain discontinuities.

Unknowns

- Applicability of this method to the present design and construction of a DCSS.
- Size of monitored area for DCSS designs.
- Applicability for concrete overpacks encased in welded steel structures.
- Influence of operational background noise on monitoring resolution.

2.6.5 Fiber Optic Sensors

As discussed in Section 2.5.1, fiber optic sensors have been an integral part of health monitoring of steel and concrete civil engineering structures. In addition to the potential application for monitoring the SCC of the canister, fiber optic sensors can be used to monitor degradation of the concrete overpack. The features discussed in Section 2.5.1 for monitoring the SCC of the canister are the same as those for monitoring degradation of the concrete overpack. The difference is the radiation level and the temperature outside the concrete overpack are expected to be much lower than those on the canister surface. As a result, the effects of radiation and temperature on the fiber optic sensors are expected to be negligible. Sensor deployment, longevity, and radiation tolerance are not anticipated to be issues. The difference is reflected in Table 2-7.

2.7 Cask Bolt Degradation Monitoring

Figure 1-3, in Section 1.2, shows that for bolted casks, the confinement environment is sealed via vessel closure from primary and secondary lids, which are fastened to the metal vessel using bolts. Because the cask bolts are under tensile stress and exposed to atmospheric conditions (the protective cover shown in Figure 1-3 does not shield the bolts from atmospheric exposure), degradation of bolts by general and localized corrosion, SCC, by hydrogen embrittlement, and thermal–mechanical degradation (see Table 1-1) may be possible during long-term use. Corrosion of lid bolts and outer metallic lid seals has been observed in the Surry ISFSI site (Chopra, et al., 2012). Similar to the welded stainless steel canister system, environmental conditions (i.e., temperature, humidity, chloride ion, and microbes) are important factors affecting the system performance. The monitoring techniques for these conditions are discussed in Sections 2.1 through 2.4. In this section, a literature review was conducted to assess available techniques for monitoring SCC, hydrogen embrittlement, and general and localized corrosion of cask bolts. Several potential techniques were identified, including (i) conventional and phased array (PA) ultrasonic testing (UT), (ii) coupled MAS for monitoring localized corrosion, (iii) electrochemical noise probe for monitoring localized corrosion,

(iv) electrical resistance probe for monitoring general corrosion, (v) acoustic emission (AE) sensors, and (vi) impedance-based *in-situ* sensors for monitoring environment-assisted cracking. Visual inspection of the bolts using a camera could be a viable method to monitor corrosion. However, this approach is not addressed further in this report because this is a common technology and the information is readily available. The attributes of sensors and methods assessed in this section are summarized in Table 2-11. Details of each sensor and method are provided in the subsequent sections.

2.7.1 Conventional and Phased Array Ultrasonic Testing for Detecting Stress Corrosion Cracking of Cask Bolts

Measurement Principle

Conventional UT techniques have long been known to be able to detect cracks and flaws in bolts. UT transducers are coupled to the bolt head, allowing sound to be transmitted through the shank of the bolt. If a strong reflection is observed from the bottom of the shank with minimal additional reflections, the bolt integrity is confirmed. If, however, reflections are observed before the bottom-of-shank reflection is detected and/or the bottom-of-shank reflection is reduced, a compromised bolt is indicated. Ultrasonic inspection techniques are commonly divided into three primary classifications: (i) pulse-echo, (ii) beam, and (iii) contact or immersion. In pulse-echo testing, a transducer sends out a pulse of energy and the reflected energy is recorded.

The UT techniques can be divided into two subcategories: conventional UT and PA UT. Conventional UT also is known as the cylindrically guided wave technique (Light and Joshi, 1987). The technique is based on the principle that an ultrasonic wave traveling in a long cylinder (i.e., a bolt) becomes trapped and guided by the geometry of the cylinder. The ultrasonic beam is redirected within the bolt throughout its length, converting from longitudinal energy to shear energy and back to longitudinal. These “mode converted” waves are effective

Maturity

The conventional UT technique has been field deployed for inspection of bolts in nuclear power plants (IAEA, 2007; INETEC, 2003). The technique has been used for inspection of corrosion and corrosion-induced cracks. The conventional UT and PA UT techniques were used to detect notches (simulated cracks) in carbon steel bolts. All notches were detected by the conventional UT method, 2-D PA, and 3-D PA methods. It was demonstrated that visualization by the PA method improves crack identification. Figures 2-26 (a,b) show images of notches detected by the 2-D and 3-D PA methods, respectively. The 3-D PA method provides imaging of cracks for bolts in a wide region (Kitazawa, et al., 2010).

Measurement Range, Sensitivity, and Longevity

This technique measures reflected sound to identify cracks, and the measured range may vary based on the system settings. Conventional UT, 2-D PA, and 3-D PA have all been shown to be able to detect a 1.6-mm [0.06-in]-deep notch (TEPCO, 2010). Using conventional UT, a 2-mm [0.08-in]-sized crack can be detected (Jeskanen, et al., 2001). No information on longevity has been reported for nuclear applications.

Table 2-11. Monitoring Techniques to Address Technical Information Needs of Cask Bolt			
Features	**Ultrasonic Testing (Section 2.7.1)**	**Multielectrode Array Sensor (Section 2.7.2)**	**Electrochemical Noise Probe (Section 2.7.3)**
Maturity	Field deployed	Field deployed	Field deployed
Measurement Ranges	Varies depending on transducer size, frequency, and geometry of the component under inspection	0.001–50 mm/yr [0.04–2000 mil/yr]	Depends on electrode design
Sensitivity	2 mm [0.08 in] or larger crack size	0.001 mm/yr [0.04 mil/yr]	Corrosion rate near 25 µm/yr [1 mil/yr]
Longevity	Not specified	Decades depending on corrosion rate and probe size	Decades depending on corrosion rate and probe size
Space Requirements	10–25 mm [0.39–0.98 in] in diameter and 20–60 mm [0.78–2.3 in] in length	57mm × 135mm × 180mm (2.25 in × 5.3 in × 7.2 in), probes can be customized with diameters as small as 10 mm [0.4 in] and 1 cm [0.4 in] thick	Sensor can range from 1 to 10 cm [0.4 to 3.9 in] in diameter and 5 to 20 cm [2 to 7.9 in] in length; probe size can be customized
Power Requirements	66 or 132 watts power	66 or 132 watt power; battery	66 watt power
Monitoring Area	Bolt length 0.5–2.0 m [20–79 in], diameter 20–60 mm [0.8–2.4 in]	Immediate vicinity of cask components	Immediate vicinity of cask components
Data Acquisition Mode	Intermittent	Continuous	Continuous
Temperature Tolerance	450 °C [842 °F] or greater if special couplings are used	−30 to +50 °C [−22 to 122 °F] with typical probe, may be increased to 150 °C [302 °F] with special electrode coatings	Up to 200 °C [400 °F]
Radiation Tolerance	Given prior application on baffle-former bolts, should be sufficient for a DCSS	Given prior application on baffle-former bolts, should be sufficient for a DCSS	Given prior application on baffle-former bolts, should be sufficient for a DCSS
Strengths	Demonstrated inspection method in nuclear applications and in high radiation environments; sensitivity to small surface and subsurface discontinuities; when the UT pulse-echo technique is used, only one single-sided access is needed	Can be used for a variety of materials, sensor is able to determine localized or uniform corrosion rates, sensor size can be customized for DCSS applications, sensor calibration is not needed	Highly sensitive to detect and measure localized corrosion and corrosion tendency, sensor calibration is not needed
Weaknesses	Evaluation function not user friendly; equipment calibration needed; data intensive; for continuous monitoring, DCSS modification may be needed for sensor deployment; transducer bonding to the structure may be cumbersome	Low operating temperature range, surrogate sensor (does not measure corrosion of actual bolts), selection of sensor electrodes may not represent the actual metallurgical state and stress condition of the bolts, DCSS modification may be needed for sensor deployment	Surrogate sensor (does not measure corrosion of actual bolts), selection of sensor electrodes may not represent the actual metallurgical state and stress condition of the bolts, DCSS modification may be needed for sensor deployment.

Table 2-11. Monitoring Techniques to Address Technical Information Needs of Cask Bolt			
Features	**Electrical Resistance Probe (Section 2.7.4)**	**Acoustic Emission (Section 2.7.5)**	**Impedance-Based *In Situ* (Section 2.7.6)**
Maturity	Field deployed	Field deployed	Experimental
Measurement Ranges	0.0001 to 10 mm/yr [0.004 to 400 mpy], depends on probe design	1 kHz – 2 MHz	Not specified
Sensitivity	Minimum thickness loss on the order of 1 µm [0.04 mils]	50-100 dB	Not specified
Longevity	Years to decades, depending on the corrosion rate and size of probe	Not specified	Not specified
Space Requirements	Diameter of the probe could typically range from 1 to 5 cm [0.4 to 2 in] and the length of the probe could range from 5 to 20 cm [2 to 7.9 in]; probe size varied with applications and can be customized to be small	Up to 2.5 cm [1 in] diameter × 2.5 cm [1 in] height	Not specified
Power Requirements	66 watt power; battery	Unknown	Not specified
Monitoring Area	Immediate vicinity of cask components	Entire bolt volume	Immediate vicinity of cask components
Data Acquisition Mode	Intermittent or continuous	Continuous	Continuous
Temperature Tolerance	Up to 260 °C [500 °F]	−65 to 177 °C [−85 to 350 °F]	Not specified
Radiation Tolerance	Not specified	Not specified	Not specified
Strengths	Probe is functional in both aqueous and nonaqueous environments, sensor calibration is not needed, probes are equipped with a reference electrode for temperature compensation	Highly sensitive to detection of cracking or corrosion damage of bolts, real-time monitoring is possible	Real-time monitoring
Weaknesses	Not sensitive to localized corrosion, surrogate sensor (does not measure corrosion of actual bolts), selection of sensor electrodes may not represent the actual metallurgical state and stress condition of the bolts, DCSS modification may be needed for sensor deployment	Experienced operator needed to execute and interpret data, background noise needs to be assessed and identified, calibration needed, transducer bonding to the structure may be cumbersome and deployment may be difficult	Very early in development, never commercially deployed

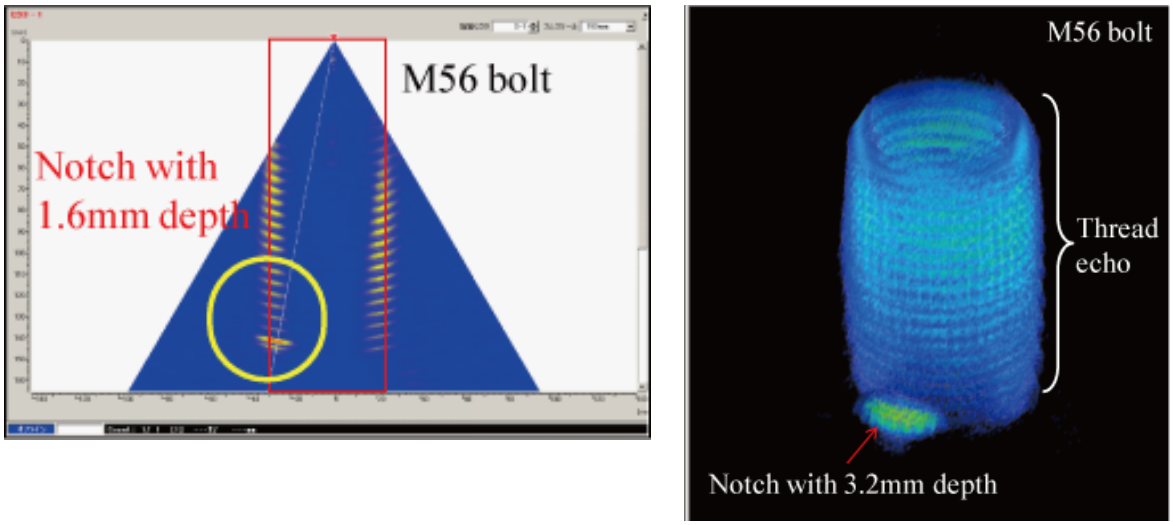

(a) (b)

Figure 2-26. Notches in Bolts Detected Using Phased Array Ultrasonic Testing Method. (a) Two-Dimensional Imaging and (b) Three-Dimensional Imaging (TEPCO, 2010). (Reproduced With Permission of E-Journal of Advanced Maintenance)

Space and Power Requirements

A conventional UT transducer is approximately 10–25 mm [0.39–0.98 in] in diameter and 20–60 mm [0.78–2.3 in] in length, with cables for signal transmissions. The transducer is set on top of the bolts and scanned mechanically on the end surface. Inspection data are displayed to show locations of cracks and ultrasonic intensity as a function of time. Power consumption for the UT transducers is limited to the instrumentation for sensor interrogation. Newly developed

instrumentation systems for UT are portable and compact and use low power consumption {2.5 watts at 25 °C [77 °F]} with a single 5 V supply operation. Dimensions of typical portable instrumentation systems are less than 35.0 cm × 25.0 cm × 15.0 cm [13.8 in × 9.8 in × 5.9 in]. Some UT instruments can function on AC or battery power.

Monitoring Area and Data Acquisition

As mentioned previously, the UT transducer must be bonded to the bolt head for defect detection. UT instruments are suitable for detecting flaws in bolts ranging from 1.3 to over 2 m [0.5 to 7 ft] in length and have a bolt diameter from 1.3 to 25.4 cm [0.5 to 10 in]. For instance, the UT technique was successfully employed to measure small flaws in foundation carbon steel bolts with diameters of 2–6 cm [0.8–2.4 in] and lengths of 0.5–2.0 m [20–79 in]. For reactor pressure vessels, stud bolts 15.0 cm in diameter and 40.0 cm long were successfully examined by PA UT. For conventional UT, the data generated are a line scan (A-scan, B-scan, and C-scan) that includes the initial pulse and all reflected pulses. Data acquisition mode is intermittent.

Temperature and Radiation Tolerance

McLay and Verkooijen (2012) showed that UT can be successfully applied to temperatures up to 450 °C [842 °F] using appropriate transducers. When the temperature exceeds 450 °C

[842 °F], a single transducer with a heat-resistant standoff can be used with a flaw detector. To eliminate sources of errors in high temperature environments, temperature correction can be obtained by Eq. (2-3)

$$T_a = T_m \times [1.007-(0.0001\times t)] \quad (2\text{-}3)$$

where Ta is the corrected thickness of the test piece, Tm is the measured thickness, and t is the surface temperature of the test article in °F. The radiation tolerance of the UT sensor is unknown. However, given its prior application on baffle-former bolts in reactor internals and the expected radiation dose for bolted cask systems, radiation tolerance of UT systems should be sufficient for DCSS applications.

Strengths and Weaknesses

UT is a very useful and versatile nondestructive method. Some of the advantages of UT monitoring of cracking or corrosion damage of bolts include its sensitivity to small surface and subsurface discontinuities with its superior depth of penetration for flaw detection. When the UT pulse-echo technique is used, only one single-sided access is needed.

Some of the weaknesses of the UT method include the need for calibration, potential difficulty in bonding the transducer to the structure and deploying it, and the need for a high degree of operator skill. Reference standards are required for both equipment calibration and the characterization of flaws. This technique is data intensive.

Potential DCSS Use

For crack monitoring in a DCSS application, UT transducers need to be physically attached to the bolt head surface and remain in service for an extended period of time. As a result, the protective cover in bolted casks needs to be removed temporarily for one-time monitoring. For continuous monitoring, the protective cover must be modified to electrically connect the UT transducers for data collection and transmission.

Unknowns

- System modifications and preparation required for deployment on a DCSS that was not designed for monitoring.
- Longevity of UT transducers for continuous monitoring of cracking and corrosion in DCSS applications.

2.7.2 Coupled Multielectrode Array Sensor for Localized Corrosion Monitoring of Cask Bolts

Measurement Principle

Coupled multielectrode array sensors (CMAS) were originally developed for *in-situ* monitoring of various forms of corrosion, with special emphasis on localized corrosion. The sensors have been tested extensively with carbon steels, stainless steels, and nickel-based alloys as probe elements in a wide range of aqueous solutions and in the process streams of industrial plants. Past studies have demonstrated the sensor can measure, in real time, the corrosivity of the environment. Due to the nature of the sensor and the small area of the electrodes that

comprises the sensor, the sensor also offers the ability to predict localized penetration rates typically encountered in localized corrosion. Additionally, the coupled multielectrode sensor does not require the presence of bulk electrolytes; it can be used to measure corrosion not only in an aqueous solution, but also under salt deposits. However, literature data on the sensor response in dry atmospheres and near deliquescence environments are scarce. Importantly, this sensor is not intended to measure cracking events, but rather corrosion events in the form of localized or uniform modes. These probes give simple parameters, such as maximum localized corrosion rate, maximum localized corrosion penetration depth, and average corrosion rate.

In a corroding environment, anodic currents flow in the more corroding electrodes (anodes) and the counteracting cathodic currents flow out of the less corroding electrodes (called cathodes). As mentioned earlier, the CMAS is suitable to measure corrosion rates in nonuniform corrosion processes where the electrochemical reactions may differ on the different electrodes. As a result, each electrode would develop its own electrochemical potential and current. The total anodic corrosion current may be expressed in Eq (2-4)

$$I_a = I_a^t + I_a^c \quad (2\text{-}4)$$

where I_a^t is the external anodic current that flows between electrodes and I_a^c is the internal anodic current that flows from the cathodic sites within each electrode. To measure I_a, the CMAS relies on the measurement of I_a^t, because I_a^c cannot be directly measured.

This type of sensor system consists of a multielectrode probe, a CMAS corrosion analyzer, and associated software. Data transmission is through an Ethernet port, with optional wireless data transmission. The typical number of electrodes in a CMAS probe is 9, 16, 25, or 50 for online corrosion monitoring. The sampling rate is less than 30 seconds for a 50-electrode probe, and data can be reviewed daily, weekly, or monthly. Data analysis software is supplied for downloading data and changing sampling parameters. Real-time graphical display and data analysis can be performed on a PC.

The CMAS sensor is a type of surrogate sensor (i.e., the sensor does not measure actual damage on the component of interest). As such, it is important to note that for this surrogate sensor to properly reflect the damage characteristics of bolted casks, the sensor needs to be placed in a representative environment and configuration (i.e., size of crevice region) and be constructed of the same material as that used in the bolts.

Maturity

Schiessl (1991) developed the first coupled multielectrode system. In 2003, the CMAS corrosion monitoring system was initially field deployed in process piping in a chemical plant at elevated temperatures to measure localized corrosion. The results of the CMAS were in agreement with model predictions for localized corrosion (Anderko, et al., 2003). In 2004 and 2005, the CMAS sensors were deployed to measure real-time localized corrosion rates of cooling water systems. The measured localized corrosion rate was consistent with the pitting rate measured from companion coupons (Dorsey, et al., 2004; Anderko, et al., 2005).

The corrosion monitoring system has been field deployed in chemical power plants and oil/gas pipeline systems. The systems are commercially available.

Measurement Range, Sensitivity, and Longevity

Measurement range for a field-designed instrument is reported to be 0.001–50 mm/yr [0.04–2,000 mils/yr] with a sensitivity of 0.001 mm/yr [0.04 mil/yr]. Sensor longevity is dependent on the present corrosion rates. Higher corrosion rates consume the electrodes in the sensor at a faster rate. Because the length of the sensor electrodes can be customized, the sensor can be built to last for decades.

Space and Power Requirements

As mentioned previously, the sensor size can be tailored, depending on the application and space requirements. The CMAS sensor can be as small as 1 cm [0.4 in] in diameter and 1 cm [0.4 in] thick. For bolted casks, the CMAS sensor needs to be placed in the region between the protective cover and the cask lid. The power requirement is 60 or 130 watts from 110 V or 220 V AC, with a 9–30 V battery as backup, limited to the instrument used to query the sensor.

Monitoring Area and Data Acquisition

The CMAS is a type of surrogate sensor; it does not measure the corrosion rate of the actual bolts. The monitoring area is restricted to the sensor region. Therefore, it is important to locate the sensor in the vicinity of the bolts so the sensor experiences a comparable environment. The measured corrosion rate is logged to an electronic data file. The user can specify the frequency of the corrosion rate measurements. Data acquisition mode is online, real-time continuous monitoring.

Temperature and Radiation Tolerance

The normal operation temperature range of the probe is −30 to +50 °C [−22 to 122 °F] (Corr Instruments, LLC, 2013). Using diamond-like carbon-coated electrodes, the demonstrated upper temperature in the laboratory can be increased to 150 °C [302 °F] (Chiang and Yang, 2010; Chiang, et al., 2008). When used above these temperatures, crevice formation between the electrodes in the sensor and the epoxy mounting material makes the corrosion rate measurement erroneous. The radiation tolerance of the CMAS system is unknown.

Strengths and Weaknesses

Among the strengths of the CMAS system is the ability of the sensor to detect and measure both localized and uniform corrosion. Also, the sensor can be used to measure corrosion rates for a variety of materials. In addition, the sensor size can be customized for each particular application. Another important advantage of the CMAS system is that sensor calibration is not required.

Weaknesses are that this system uses a probe that simulates the surface of the system or component that is exposed to the environment and does not actually measure corrosion processes on the component of interest. Commercially available CMAS systems used to monitor deliquescence-induced corrosion processes in a laboratory setting are limited to temperatures below 70 °C [158 °F]. Higher temperature operation up to 150 °C [302 °F] may be possible using a diamond-like, carbon-coated electrode system to eliminate the crevice formation between the electrode and epoxy mounting material (Chiang and Yang, 2010; Chiang, et al., 2008). As mentioned previously, the sensor uses a set of small electrodes

because the smaller the electrodes, the greater the chance of anodic reactions completely covering a given electrode surface. This, however, may not be practical for all situations. In addition, if the electrodes are too small, the anodic reaction may no longer represent the corrosion behavior of a large component (i.e., bolts). Because the electrode areas are small and low levels of current can be measured, precautions must be taken to minimize external noise interference. Care also must be taken in the electrode preparation to ensure that the metallurgical state and stress condition of the actual bolts is adequately represented by the electrodes. In addition, there are limited data on the sensor performance in dry atmospheres and on deliquescence conditions that may be present in bolted casks. The radiation tolerance of the system also is unknown.

Potential DCSS Use

Additional evaluation is necessary to determine whether this type of sensor can be used to monitor real-time cask bolt localized corrosion in a DCSS. While it may be possible to place the system in the immediate vicinity of the cask bolts, it is not clear that the data collected would be an accurate measure of the cask bolt localized corrosion rates.

For continuous corrosion monitoring in bolted casks, the CMAS sensor needs to be placed in the region between the protective cover and the cask lid and remain in service for an extended period of time. As a result, the protective cover needs to have provisions for electrical connection of the CMAS sensor for data collection and transmission.

Unknowns

- Applicability of this corrosion monitoring system as a surrogate for cask bolts.
- System modifications and preparation required for deployment on a DCSS that was not designed for monitoring.
- Performance of CMAS probes at temperatures above 150 °C [302 °F].

2.7.3 Electrochemical Noise Probe for Localized Corrosion Monitoring of Cask Bolts

Measurement Principle

Researchers at ANL developed the electrochemical noise (ECN) probe (Lin, et al., 2003, 2001) as an online, real-time method to monitor localized pitting corrosion so that treatment chemicals (e.g., biocides and chemical inhibitors) can be applied only when needed. ANL researchers used both laboratory and field experiments to ensure the probe can detect pitting corrosion as well as cracking events from ECN measurements. The onset of corrosion results in transient fluctuations in the corrosion current and corrosion potential during different corrosion processes (Bertocci and Huet, 1997). Corrosion phenomena can be studied by analyzing random current and/or potential fluctuations that can be detected by electrochemical measurements using zero resistance ammeters (ZRAs). There has been a tendency to relate all potential fluctuations to corrosion activity. However, potential noise can be misleading in cases where small fluctuations in mass transport control can produce sizable changes of the corrosion potential (e.g., passive stainless steels in neutral, aerated environments).

ECN measurements have been reported for experiments both under potentiostatic control and at the free corrosion potentials (Loto and Cottis, 1989; Stewart, et al., 1992). Cracking events can produce transient changes in the measured anodic currents similar to pit initiation. Thus, it is difficult to discern among pitting corrosion, crevice corrosion, and SCC using this technique.

One of the approaches for characterizing a random signal is to estimate its power spectral density (PSD) [i.e., the distribution of the power of the signal in the frequency domain using the Fourier transform (FFT) algorithm (Mansfeld and Xiao, 1994; Gusmano, et al., 1997)]. The ANL researchers have reexamined the ECN analysis of corrosion by using hardware, signal collection, and signal processing designs that are different from those used in conventional ECN analysis techniques. Specifically, a new data acquisition system was designed to identify and monitor the progress of localized corrosion by analyzing the power spectral density of the trend of the corrosion potential noise level. The low-frequency portion of the potential noise PSD is used to characterize pitting corrosion.

The ECN probe is a type of surrogate sensor (i.e., the sensor does not measure actual damage on the component of interest). As such, it is important to note that for this surrogate sensor to properly reflect the damage characteristics of bolted casks, the sensor needs to be placed in a representative environment, have a particular configuration (i.e., size of crevice region), and be constructed of the same material as that used in the bolts.

Maturity

ECN probes in corrosion and electrochemical laboratory studies were first reported in the 1960s (Hagyard and Williams, 1961; Iverson, 1968). The early application of the ECN approach involved the measurement of the transient open circuit potential, believed to be associated with the presence of localized corrosion. For these initial investigations, a pair of aluminum electrodes was immersed in solutions and the potential response was measured. Follow on investigations by Hashimoto, et al. (1992a,b) in 1992 presented the theoretical basis of the ECN analysis to study corrosion processes.

The online ECN analysis system was field tested in a natural gas storage facility. The ECN analysis system demonstrated it could detect sustained localized corrosion on the monitored facilities.

Measurement Range, Sensitivity, and Longevity

The ECN probes include a pair of working electrodes made from the same material as the monitored components and a reference electrode formed from a corrosion-resistant material. One pair of working electrodes has reduced roughness, which increases sensitivity to sustained localized pitting corrosion in the working electrode (Lin, et al., 2001). Corrosion rate measurement sensitivity for this technique is 25 μm/yr [1 mil/yr]. The probe may be placed in the immediate vicinity of the cask bolt to monitor localized corrosion. The longevity of the corrosion monitoring system is 10 years, and replacement of the sensor is possible.

Space and Power Requirements

The sensor size can be tailored to the application and space requirements, but typically, the sensor can range from 1 cm to 10 cm [0.4 in to 3.9 in] in diameter and 5 cm to 20 cm [2 in to 7.9 in] in length. For bolted casks, the sensor needs to be placed in the region between the

protective cover and the cask lid. The power requirement is 66 watts from 115 V AC, limited to the instrument used to record the data from the sensor.

Monitoring Area and Data Acquisition

As mentioned earlier, the ECN probe is a type of surrogate sensor; it does not measure the corrosion rate of the actual bolts. The monitoring area is restricted to the sensor region. Therefore, it is important to locate the sensor in the vicinity of the bolts so the sensor experiences a comparable environment. The amount of data per measurement can be quite large compared to other measurements (up to a few megabytes per measurement) and is dependent on the data sampling rate and the data collection time span. Typically, data are continuously collected for 10–20 minutes at selected time intervals.

Temperature and Radiation Tolerance

As stated earlier, the ECN probe can be custom made for the required application. Commercially available high temperature ECN probes can withstand temperatures on the order of 200 °C [400 °F]. The radiation tolerance of the ECN probes is unknown.

Strengths and Weaknesses

Among the strengths of the ECN system is the high sensibility of the ECN sensor to detect and measure localized corrosion and corrosion tendency. Data acquisition mode is online, real-time, continuous monitoring. Another important advantage of the ECN system is that sensor calibration is not required.

Weaknesses are that this system uses a probe which simulates the surface of the system or component that is exposed to the environment and does not actually measure corrosion processes on the component of interest. A moderate degree of operator skill may be needed to interpret and analyze the ECN data. In addition, the recorded signal has to be significantly higher than the noise level introduced by external interference. As such, disturbing external noise sources have to be identified and, if possible, minimized. Care also must be taken in the electrode preparation to ensure the metallurgical state and stress condition of the actual bolts is adequately represented by the ECN sensor. In addition, there are limited data on the sensor performance in dry atmospheres and for deliquescence conditions that may be present in bolted casks. The radiation tolerance of the system also is unknown.

Potential DCSS Use

Additional evaluation is necessary to determine whether this type of sensor can be used to monitor real-time cask bolt localized corrosion in a DCSS. While it may be possible to place the system in the immediate vicinity of the cask bolts, it is not clear the data collected would be an accurate measure of the cask bolt localized corrosion rates. The ability of this system to be used with a variety of cask bolt materials and the longevity of the system also need to be determined.

For continuous corrosion monitoring in bolted casks, the ECN sensor needs to be placed in the region between the protective cover and the cask lid and remain in service for an extended period of time. As a result, the protective cover needs to have provisions for electrical connection of the ECN sensor for data collection and transmission.

Unknowns

1. Applicability of this corrosion monitoring system as a surrogate for cask bolts.

2. System modifications and preparation required for deployment on a DCSS that was not designed for monitoring.

2.7.4 Electrical Resistance Probe for General Corrosion Monitoring of Cask Bolts

Measurement Principle

ER probes, widely used for monitoring general corrosion (Brossia, 2008; Yang and Chiang, 2010), consist of a metal sensing element whose resistance is measured while the element is exposed to the environment of interest. As corrosion occurs and metal loss takes place, the cross-sectional area of the sensing element will decrease and the ER (R) will increase, according to Eq. (2-5)

$$R = \rho \, l / A \tag{2-5}$$

where ρ is the resistivity of the sensing element, l is the length of the element, and A is the cross-sectional area. The ER can be measured by determining the potential drop across the sensing element when a small current is applied using Ohm's law. Practical measurement is achieved using (i) ER probes equipped with an element that is freely exposed to the environment and (ii) a reference element that is sealed within the probe body. The ER of the reference and the samples are expressed as ratios, and because both elements are at the same temperature, any change is solely due to the loss of metal from the sample. Any two metal loss measurements separated in time may be used to calculate the rate of loss.

Maturity

ER probes have been field deployed in petroleum, chemical processing, and other environments where online corrosion rates must be monitored. Various forms of sensing elements (i.e., flush, cylindrical, wire loop, strip loop, or band probes) are commercially available. Recent developments in ER probe technology have produced high sensitivity ER probes (Rohrback Cosasco Systems, 2013; Teledyne Corman, 2013). The high sensitivity ER probe has substantially increased the speed of response, thus providing rapid information when corrosion rates increase. An online monitoring system with an ER probe, transmitter, communication cable, and data logger is now commercially available.

Measurement Range, Sensitivity, and Longevity

The measurement range depends on the size and composition of the probe, but the range of corrosion rates can be many orders of magnitude, spanning from passive rates to rates associated with localized corrosion. Probes for most engineering materials are available to measure rates from 0.0001 to 10 mm/yr [0.004 to 400 mpy]. The sensitivity of thickness loss measurement is on the order of 1 μm [0.04 mils]. The ER life is limited. The probe life is reached when one-half of the thickness is consumed. Under low corrosion rates, the probes can have a usable lifetime of many years.

Space and Power Requirements

As mentioned previously, the sensor size can be tailored to the application and space requirements. For bolted casks, the ER probes need to be placed in the region between the protective cover and the cask lid. The space requirement for the monitoring system is approximately 600 cm^3 [36.6 in^3]. The diameter of the probe could typically range from 1 cm to 5 cm [0.4 in to 2 in], and the length of the probe could range from 5 cm to 20 cm [2 in to 7.9 in]. The power requirement is 66 watts from 115 V AC, or battery, limited to the instrument used to query the sensor.

Monitoring Area and Data Acquisition

The ER is a type of surrogate sensor; it does not measure the corrosion rate of the actual bolts. The monitoring area is restricted to the sensor region. Therefore, it is important to locate the sensor in the vicinity of the bolts so the sensor experiences a comparable environment. Corrosion rate is calculated by the change in the measured resistance of the element that is interpreted as loss of material from corrosion and is typically logged to a data file for real-time monitoring. Both continuous and intermittent data acquisitions are possible.

Temperature and Radiation Tolerance

The ER probe can be custom made for the required application. Commercially available high temperature ER probes can withstand temperatures on the order of 150 °C [302 °F] for epoxy resin probes, while glass variants are suitable to 260 °C [500 °F]. Typically, ER probes are equipped with a reference electrode for temperature compensation.

Strengths and Weaknesses

Strengths of the ER technique are corrosion monitoring in both aqueous and nonaqueous environments can be measured. The measured signal is directly related to metal loss, and data show the evolution of corrosion rates. The data acquisition mode is online, real-time, continuous monitoring. Another important advantage of the ER system is sensor calibration is not required. The ER probes are equipped with a reference electrode for temperature compensation.

Weaknesses are this system uses a probe, which simulates the surface of the system or component that is exposed to the environment and does not actually measure corrosion processes on the component of interest. Additional limitations include (i) the change of ER due to corrosion is relatively small, resulting in a slow response (usually weeks to hours; for improved sensitivity, the probe sensing element must be very thin) and (ii) the ER probe is not sensitive to nonuniform corrosion (i.e., pitting, crevice corrosion, or SCC), which can lead to measurement error. Care also must be taken in the electrode preparation to ensure the metallurgical state and stress condition of the actual bolts is adequately represented by the electrodes. The radiation tolerance of the system also is unknown.

Potential DCSS Use

Additional evaluation is necessary to determine whether this type of sensor can be used to monitor real-time cask bolt localized corrosion in a DCSS. While it may be possible to place the system in the immediate vicinity of the cask bolts, it is not clear that data collected would be an accurate measure of the cask bolt localized corrosion rates. The ability of this system to

be used with a variety of cask bolt materials and the longevity of the system also need to be determined.

For continuous corrosion monitoring in bolted casks, the ER sensor needs to be placed in the region between the protective cover and the cask lid and remain in service for an extended period of time. As a result, the protective cover needs to have provisions for electrical connection of the ER sensor for data collection and transmission.

Unknowns

- Applicability of this corrosion monitoring system as a surrogate for cask bolts.
- System modifications and preparation required for deployment on a DCSS that was not designed for monitoring.

2.7.5 Acoustic Emission Sensors

Measurement Principle

The AE technique is the transient elastic wave that is released by materials when they undergo deformation, dislocation movement, irreversible change, and initiation and propagation of microcracks (ANST, 2005). This technique involves the use of ultrasonic transducers (e.g., piezoelectric sensors mounted at a particular location on the structure) that typically operate at frequencies in the range of 20–1,000 kHz (for materials with high attenuation, lower frequencies may be used to better distinguish AE signals). During the formation of a crack, a part of the energy is emitted as an elastic wave propagating spherically from the crack location and reaching the AE transducers at the metal surface. By measuring the signal parameters, such as counts, amplitude, duration, rise time, and counts energy, quantitative information on the magnitude of a crack, location, time of its origination, and the rate of crack propagation can be assessed.

The AE transducers convert the surface movement in any direction caused by an elastic wave into an electrical signal (output voltage), which can be processed by the measurement equipment. AE sensors are broadly classified into two types: (i) resonant (narrow band), which is highly sensitive at a specific resonance frequency and (ii) broadband, which possesses a constant sensitivity across a wide band of frequencies. In most practical field applications, resonant sensors are preferred over broadband sensors (Pollock, 1995). Broadband AE sensors usually are desired if the frequency of interest is still unknown or if different frequencies in one signal should be analyzed. A common AE apparatus involves the AE sensors, preamplifiers, coaxial cables, and data acquisition device. The data acquisition device performs filtration, signal evaluation, and data analysis.

Typically, AE monitoring is carried out in the presence of background noise and electromagnetic interference, resulting from mechanical, electrical, and environmental sources. For instance, background noise from production machinery usually is more prominent at frequencies <100 kHz. To minimize interference, a preamplifier is placed close to the AE transducer. In fact, many AE transducers are equipped with integrated preamplifiers (named integral sensors). Depending on noise conditions, further filtering or amplifying may be necessary.

Transducer mounting is an integral part of the success of AE monitoring. First, the metal surface where the sensors will be mounted must be cleaned and smoothed. Rough surfaces

decrease the acoustic contact signals. As a common practice, a thin layer of a viscous medium is placed between the metal surface and the AE transducer.

Maturity

AE testing is a mature, nondestructive process that has been used to monitor structural integrity and characterize materials behavior for the past 50 years. AE testing has been demonstrated as a viable complement to the other nondestructive methods used in a variety of applications (e.g., aerospace, chemical, nuclear, and petroleum industries). In early 1965, at the National Reactor Testing Station, researchers detected the loss of coolant in a nuclear reactor using AE testing (Harris and Dunegan, 1974).

Measurement Range, Sensitivity, and Longevity

The measurement range is not specified but must be validated by calibration of the system. The National Institute of Standards and Technology developed the surface wave calibration method. This procedure subjects the sensor to a surface wave similar to that of an actual AE event (ASTM E1106–86, Standard Method for Primary Calibration of AE Sensors).

The output voltage amplitude/input motion amplitude ratio is a measure of the AE sensor sensitivity. Sensor sensitivity depends strongly on the frequency, magnitude of the background noise, and the direction of the motion. Available sensor calibration curves [normally in decibels (dB)] allow determination of the sensor sensitivity with frequency as well as the amplitude of the input motion in displacement units, velocity, or pressure. A typical AE sensor has a sensitivity of 30 to 100 dB.

According to the manufacturer, proper maintenance of the transducers is required to extend and improve performance. Because the measurement of AE involving the use of transducers requires the placement of the transducers between the cover lid and protective cover in a bolted cask, sensor longevity may be an issue and unit replacement can be compromised.

Space and Power Requirements

The diameter and height of the probe is generally on the order of 25.4 mm [1 in] or less (Mistras, 2013). AE testing can be performed in the field with portable, lightweight instruments. The typical size of these portable units is 405 mm × 240 mm × 74 mm [16 in × 9.5 in × 2.9 in]. The units come with both a 12 V battery and AC options. No power consumption is reported in the literature.

Monitoring Area and Data Acquisition

There is no information on the monitoring area using a single transducer. It is believed the monitoring area will be affected by several factors, such as degree of external background noise and signal attenuation.

AE testing produces large data sets. Several analysis procedures need to be applied to the raw data before onset detection and localization of damage can be assessed. Software-based AE systems are able to generate graphical displays for analysis of the signals recorded during an AE test. These displays can be classified into four categories: (i) location, (ii) activity, (iii) intensity, and (iv) data quality. Location displays identify origin of the detected AE events. Activity displays show AE activity as a function of time. Intensity displays are used to give

statistical information concerning the magnitude of the detected signals and used to determine whether a few large signals or many small ones created the detected AE signal energy. Data quality displays the quality of the data collected. Data acquisition mode is continuous.

Temperature and Radiation Tolerance

General purpose AE sensors can operate from −65 to 177 °C [−85 to 350 °F] (Mistras, 2013). High temperature AE sensors, reaching up to 500 °C [932 °F], have been developed. The radiation tolerance of the AE sensor is unknown.

Strengths and Weaknesses

Strengths of AE technique are the superior detection of cracking or corrosion damage of bolts, as well as its sensitivity to small surface and subsurface discontinuities. Crack detection can be performed in real time. Multiple transducers can be used to determine different sources of emission, and triangulation can be used to determine the location of active defects.

Weaknesses include operators must be well trained to execute this technique and interpret the data, background noise needs to be checked prior to testing, and this technique only qualitatively gauges how much damage is contained in a structure. Calibration tests should be conducted to ensure testing equipment is fully functional and to check sensitivity of the transducers. Transducer bonding to the structure may be cumbersome, and deployment may be difficult.

Potential DCSS Use

For crack monitoring in a DCSS application, AE transducers need to be physically attached to the bolt head surface and remain in service for an extended period of time. As a result, the protective cover in bolted casks needs to be removed temporarily. For continuous monitoring, modification of the protective cover is needed for electrical connection of AE transducers for data collection and transmission.

Unknowns

- System modifications and preparation required for deployment on a DCSS that was not designed for monitoring.
- Longevity of AE sensors and maintenance requirements.
- Influence of operational background noise on monitoring resolution.

2.7.6 Impedance-Based, *In-Situ* Sensors

Measurement Principle

The basic principle of the impedance method is to use high-frequency vibrations to monitor the local area of a structure for changes in electrical and mechanical impedance of the piezoelectric sensor resulting from localized corrosion. Of key importance is the electromechanical coupling of the piezoelectric actuator/sensor bonded to the structure. The electromechanical property of the piezoelectric material serves two purposes. First, the material generates an electric charge when subjected to mechanical stresses. Second, a mechanical strain is generated in response

to an applied electric field. The mechanical impedance is defined as the ratio of the applied force to the resulting velocity, while the electrical impedance is defined as the ratio of the applied voltage to the resulting current. This electromechanical coupling approach allows for the extraction of mechanical impedance information from a purely electrical impedance measurement, which can be easily made with commercially available impedance analyzers. The impedance analyzers provide a constant small voltage (less than 1 V) to the piezoelectric transducer over a preset frequency range (typically from 50 to 500 kHz). Under this high-frequency range, the wavelength of the excitation is small and sensitive enough to detect minor changes in the structural integrity (Stokes and Cloud, 1993). The magnitude and phase of the current of the piezoelectric is recorded in real and imaginary admittance for each frequency. A diagram of the components involved in the impedance method is shown in Figure 2-27.

This technique is envisioned to be most useful in identifying and tracking damage in those areas of structures where high structural integrity must be assured at all times. This technique would be ideal for areas that, over the service life of the structure, have been identified to be weak, and as yet, are difficult to inspect.

Maturity

The theoretical development of the application of impedance measurements to monitor structural degradation was first proposed by Liang, et al. (1994) and subsequently developed by Chaudhry, et al. (1996, 1995) for use in aerospace applications and Sun, et al. (1995a), among others. Lalande, et al. (1996) used the impedance method to investigate the corrosion behavior and structural integrity of complex precision parts, like those found in gear sets. Additionally, Park, et al. (2000) noted the ability of the impedance method to detect minor structural changes and described the mass loss condition associated with corrosion. Later work by Bhalla, et al. (2002a,b) and Naidu, et al. (2002), and more recently by Mascarenas (2006) and Brown and Friedersdorf (2011), expanded the knowledge of the application of this technique to monitor cracking of pipeline fasteners subjected to cathodic protection. The localized effect, the capability of detecting very small defects, and the insensitivity to the normal aircraft operation were demonstrated.

Measurement Range, Sensitivity, and Longevity

Measurement range for this sensing technique has not been specified. An investigation by Giurgiutiu (2003) demonstrated the impedance method can effectively detect 12.7 mm [0.5 in] cracks in aircraft panels. Another investigation (Simmers, 2005) proved the impedance method detected, within 95 percent confidence intervals, corrosion of an aluminum beam instrumented with a piezoelectric sensor and corroded to 1.4 percent surface coverage of light precrack corrosion.

Based on the information collected in this investigation, longevity of the piezoelectric sensor cannot be assessed. However, it is speculated the measurement of impedance involving the use of transducers requires bonding of the transducers over the bolted cask. Sensor longevity may be an issue, and unit replacement can be compromised. To that end, an investigation Simmers (2005) conducted showed piezoelectric sensors can be subjected to corrosion damage when exposed to harsh environments; however, the exact cause is not known.

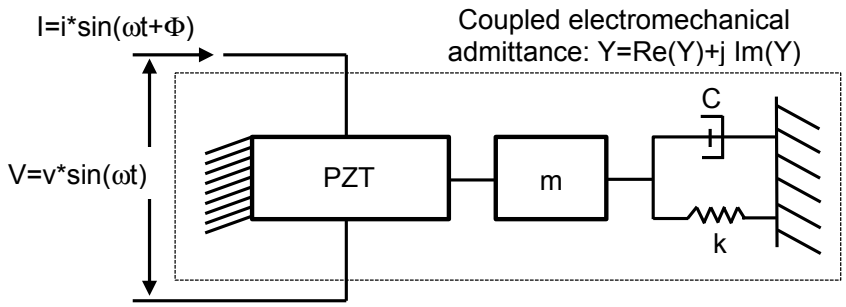

Figure 2-27. A Simplified Schematic of the Components of the Impedance-Based Method a One Degree of Freedom Fixed-Free Structure Is Represented by a Mass M, Spring, and Damper. PZT Represents the Piezoelectric Sensor.

Space and Power Requirements

The size of the piezoelectric actuator/sensor can be customized, depending on the required application. For most cases, the typical size of a circular piezoelectric actuator/sensor is 5.5 mm [0.2 in] in diameter and 0.2 mm [0.01 in] in thickness.

Peairs, et al. (2004) developed a miniaturized, low-cost impedance measuring device to increase the accessibility and portability of the impedance method. Previously, implementing the impedance method required costly, bulky {425 mm × 375 mm × 620 mm [16.7 in × 14.7 in × 24.4 in]}, and expensive impedance analyzers that required a 120 V source and consumed a total of 400 W. Because commercial hardware and software now allows for FFT on a single chip, the whole system can be implemented on small computer chips. Usually, these chips consume power in a fraction of 1 watt. With these low power units, it is conceivable this new technology could take, analyze, record, and send one measurement per day for well in excess of 5 years on two conventional AA batteries.

Monitoring Area and Data Acquisition

Under the high-frequency ranges used in the impedance-based method, the sensing region of the piezoelectric is limited to an area close to the piezoelectric actuator/sensor. Extensive numerical modeling, based on the wave propagation theory, has been performed to identify the sensing region of the impedance-based method (Esteban, 1996). It has been estimated the sensing area of a single piezoelectric sensor can vary from 0.4 m [15.7 in] (sensing radius) on composite structures to 2 m [78.7 in] on simple metal beams, depending on the frequency range, the material properties, and geometry of the structure. Experimentally, it was shown 1 percent and 0.25 percent surface coverage of corrosion damage could be identified at distances up to 125 cm [49.2 in] from a single piezoelectric sensor using the impedance method. Data acquisition mode is continuous.

Temperature and Radiation Tolerance

In an investigation by Park, et al. (1999), the impedance method was implemented to monitor damage of bolted joint structures exposed to a temperature range of 482–593 °C [900–1,100 °F]. The authors demonstrated the impedance measurements varied with temperature. However, these variations were small compared to the variations caused by corrosion damage. It is known that the piezoelectric strain coefficient and dielectric permittivity

are both temperature dependent and increase as the temperature increases. Also, the complex Young's modulus of the piezoelectric sensor at zero electric field changes slightly with respect to temperature.

The radiation tolerance of the piezoelectric actuator/sensor is unknown.

Strengths and Weaknesses

Strengths of this technique are the sensors are light and small in size and the new data acquisition units consume low power without requiring AC power supply. The sensors have the capability of detecting small corrosion damage. The sensor has high temperature tolerance.

Weaknesses of this technique include the piezoelectric sensors tend to be brittle and can withstand very little bending. This brittleness presents difficulties in handling, bonding, and adapting the sensor to curved surfaces of the structure to be monitored. To that end, new piezo-composite materials were developed. These materials are capable of being repeatedly manufactured at low cost, are tolerant to damage, and are capable of conforming to complex or curved surfaces. However, these materials need to be investigated for long-term field applications. Also, the sensor needs to be bonded to the canister surface. The piezoelectric material is sensitive to temperature changes. Corrosion of the piezoelectric sensor may be an issue if harsh corrosive environments are present.

Potential DCSS Use

For crack monitoring in a DCSS application, transducers need to be physically attached to the bolt head surface and remain in service for an extended period. As a result, the protective cover in bolted casks needs to be removed temporarily. For continuous monitoring, modification of the protective cover is needed for electrical connection of the transducers for data collection and transmission.

Unknowns

- Measurement range.
- Resolution of the sensor.
- Combined effects of temperature and radiation on the calibration and longevity of the system.
- System modifications and preparation required for deployment on a DCSS that was not designed for monitoring.
- Longevity of the sensor in elevated temperature environments and maintenance requirements.
- Methods to identify locations where sensors could be installed.

3 TECHNIQUES FOR FUNCTIONAL MONITORING OF INTERNAL ENVIRONMENTAL CONDITIONS AND DEGRADATION OF COMPONENTS INSIDE THE CONFINEMENT BOUNDARY

The process of placing fuel assemblies in the cask includes loading fuel assemblies in a spent fuel pool, followed by draining, drying, and filling the void space in the cask with helium. The helium gas prevents corrosion of internal components and aids in removal of decay heat from the spent fuel with its high thermal conductivity. The environment inside the confinement boundary (hereafter referred to as the internal environment) consists of helium gas and some residual water that is left in the canister during the process of placing the fuel assemblies in the cask. The conditions inside the sealed fuel rods are not considered part of the internal environment here.

The internal environment conditions affect the degradation of internal components, and they may be indicators of the cask confinement function and cladding integrity. If the cask is sealed, only the residual water would decompose by radiolysis to produce hydrogen and oxygen, which could change the internal pressure with time. The oxygen may oxidize cask internal components. However, a detailed analysis has indicated that the extent of oxidation due to the residual water is expected to be limited and not cause any significant changes in the integrity of the components (Jung, et al., 2013). Besides decomposition of the residual water, the internal environment is expected to change in a predictable fashion with time.

Any unexpected variations or changes in the internal environment conditions could be related to breach or failure of the internal components. For example, changes in the gas composition may be related to leakage, failure of fuel cladding, and/or incomplete drying. If the internal environment is affected by breaches in fuel rod cladding, it could be indicated by the presence of Kr-85 activity in the fill gas in the short term and xenon in the long term. Similarly, any unexpected change in temperature, humidity, and pressure of the internal environment could be an indication of the leakage from the confinement boundary. Therefore, monitoring the internal environment conditions may provide information on the functionality of the dry cask storage systems (DCSS) and integrity of the internal components. Hanson, et al. (2012) mentioned that monitoring of the temperature, humidity or moisture, pressure, Kr-85 activity, and elements such as helium, O_2, N_2, and H_2 in the gas of the internal environment could provide an indication of a breach in the canister or failure of the internal components. Saltzstein, et al. (2014) presented conceptual ideas using techniques to monitor the internal environment of high burnup dry storage demonstration casks. Passive instruments, such as the gas sampling apparatus and active instruments, such as ultrasonic sensors and millimeter wave detectors, are proposed to be used to monitor free water, humidity, temperature, and pressure inside the cask.

This chapter summarizes the reviewed techniques to monitor several internal environmental conditions, including temperature, humidity, pressure, and degradation of components inside the cask. The monitoring techniques to detect the concentration of hydrogen and oxygen that could exist inside the canister are not assessed in this report, because the concentration and amount of helium, O_2, N_2, and H_2 could be inferred through other parameters, such as pressure and relative humidity. For example, if hydrogen is produced by radiolysis of residual water inside the system, the pressure of the backfill gas will increase and the humidity will decrease inside the canister, and the extent of changes are predictable. Similarly, the presence of excess oxygen produced from radiolysis can be detected by monitoring the cask pressure and humidity of the internal environment.

These internal monitoring techniques are categorized by the parameters being monitored and are organized into four sections: (i) temperature, (ii) humidity, (iii) pressure, and (iv) degradation of cladding and other internal components. A discussion of potential common challenges in applying the various methods in Section 3.1 precedes the four sections. Section 3.1 on monitoring challenges also discusses various options to overcome the challenges.

Most of the techniques to monitor temperature and humidity inside the cask are the same as those described in Sections 2.1 and 2.2. Their features, where the same, are not repeated here, but they are evaluated individually for potential DCSS use to monitor internal temperature and humidity considering the monitoring challenges described in Section 3.1. The techniques for monitoring pressure and degradation of internal materials are evaluated in detail, but these assessments are mostly in nonradiation environments. A table summarizing the key features of these applicable techniques is provided in each subsection. Details of the sensor capabilities, operational requirements, advantages, and limitations are provided for each sensor. Based on assessment of the information available for each sensor or monitoring method, potential applicability for a DCSS is described along with a listing of the unknowns for such an application.

3.1 Monitoring Challenges

Three main challenges affect the practicality of monitoring the internal environment of a DCSS:

- Temperature range
- Radiation field
- Ease of access

The temperature during the drying process could exceed 200 °C [392 °F] when the canister is loaded with the fuel assemblies. The temperature inside the DCSS could reach 400 °C [1,058°F] during storage (NRC, 2003), which is higher than the expected maximum temperature outside the canister (EPRI, 2006; Suffield, et al., 2012). This requires additional evaluation of a sensor system for its temperature tolerance.

The radiation levels are strongest inside the DCSS and could be significantly higher than the radiation field outside the DCSS, depending on the system design. As such, radiation shielding or hardening of the sensors may be needed to protect a sensor from radiation effects. The amount of shielding or hardening that would be needed to protect the sensors is not evaluated in this report.

Regarding the ease of access, the internal environment is sealed to maintain its safety function, so it is not easily accessible. Observations of conditions in the interior may be performed by using a sight glass or by using sensing techniques to which the cask is transparent. If a sight glass is used, the effects of the sight glass or window installation on structural integrity and containment function would need to be considered. Current designs of storage canisters used in a DCSS do not include instrument penetrations, sight glasses, or power sources, such as batteries. Any penetrations, devices, or features for instrumentation inside the confinement boundary would have to be designed and evaluated for confinement and leakage under normal, off-normal, and accident conditions. For an existing DCSS, making penetrations and mounting instruments through them would require considerable planning, effort, expense, and safety assessments. For a new DCSS, penetrations would need to be part of the design structure, and sensors would likely be premounted inside the canister or cask before it is deployed. Some monitoring techniques are subjected to drift, and periodic recalibration is usually required. The

removal and replacement of sensors that require recalibration and/or replacement inside the canisters/casks would be a significant undertaking and much more difficult than replacing an external sensor.

Another possibility to alleviate the accessibility challenge is to deploy the sensors inside the cask and use various means of powering sensors and transferring data without penetrations. This would require use of precharged or chargeable power sources. This possibility and challenges associated with supplying power using batteries and data transmission through wireless technologies are discussed next.

3.1.1 Power Supply

Precharged batteries could be placed inside the canister and used to power the sensor assemblies. The number of precharged batteries needed to power a sensor assembly and the suitability and safety of placing batteries inside the DCSS are not evaluated in this report.

Another alternative is to use atomic batteries (NASA, 2014; Sheila, et al., 2011; Lal, et al., 2005), which use energy from the decay of a radioactive isotope to generate electricity. Atomic batteries have an extremely long life and high energy density and are used as power sources for equipment that must operate unattended for long periods of time, such as spacecraft, underwater systems, and automated scientific stations in remote parts of the world.

Atomic batteries already exist but may require technological evaluations and modifications for DCSS applications. The atomic batteries could be charged from the radiation field inside the canister. Specific details of the atomic batteries and the number of atomic batteries needed to power a sensor system are not assessed in this report.

3.1.2 Wireless Data Transmission

Sensor systems for temperature, humidity, and pressure monitoring generally consist of two parts: (i) probe and (ii) analyzer. The probe needs to be in direct contact with the environment, whereas the analyzer is typically connected to the probe via a cable, which will pose a challenge if the probes are placed inside the canister and the analyzer is outside. This arrangement would require penetration through the canister wall. One alternative is to have a wireless connection between the probe and the analyzer. Another possibility is to place both analyzer and probe inside the canister and output data via wireless transmission.

If wireless technology is used, it will need to be modified and evaluated to meet the requirements of data transmission of the sensor and constraints of the canister internal environment. For example, the existing and pervasive wireless data-transmission technology uses MHz-GHz range frequencies to transmit data. This frequency range is not suitable for the canister internal environment, because the signal emanating from the wireless transmitter will not overcome the canister thickness. In this case, the frequency of the wireless transmission should be a few tens of Hz.

A literature search on wireless transmission through sealed containers identified a patent by Tice (2005), where similar technology has been discussed. The work by Tice (2005) was for sealed shipping containers where the condition of the inside of the sealed container was monitored using impulse radio wireless techniques. Contemporary shipping containers are manufactured utilizing materials such as Corten™ Steel. The thickness of the shipping container wall is 1 in [25 mm]. To adopt a technology such as that of Tice (2005) for internal

environment monitoring, additional evaluations and modifications may be needed for the DCSS applications, especially to determine whether it is feasible for the components making up the wireless electronics to operate within the internal temperature, pressure, and radiation environment.

3.2 Temperature Monitoring

As indicated in Table 1-1, the temperature of the internal environment can be monitored to assess degradation of cladding and other internal components. Temperatures inside the DCSS are expected to range from near ambient up to 400 °C [1,058 °F] during storage (NRC, 2003). Section 2.1 reviewed and assessed eight temperature measurement methods for measuring temperature at the canister surface. The applicability of those methods for monitoring temperatures in the internal environment is discussed in Section 3.2.1. Sections 3.2.2 and 3.2.3 address the use of several other types of devices to monitor internal temperature, such as bimetallic sensors, pyrometric cones, and thermoscope bars. The main features of the various temperature monitoring techniques are summarized in Table 3-1.

3.2.1 Temperature Monitoring Methods Assessed in Section 2.1

Thermocouples, Resistance Temperature Detectors, and Fiber Optic Temperature Sensors

Thermocouples, resistance temperature detectors, and fiber optic temperature sensors have been described in detail in Section 2.1 and are considered collectively here due to their similarities in size, maximum measurement temperature, and other features.

Each of these sensors measures temperature by sensing an electric signal as a function of temperature. Current versions of these sensors consist of a probe and an analyzer that are electrically connected via a cable. The probe needs to be in direct contact with the internal environment. One advantage of these sensor systems is that the probes are small in size–typically less than 6 mm [0.250 in] in diameter—and the various lengths that are available. The cavity space in canisters of the existing DCSSs is sufficiently large to hold a probe placed inside the canister. In addition, the small size of the probes may allow the installation of multiple sensors to obtain information on the spatial variation in temperature. These sensors have an upper measurement temperature above the expected maximum internal temperature of 400 °C [1,058°F] and can have high radiation tolerance, which makes them potentially suitable for internal temperature monitoring of a DCSS.

The connection between the probe and sensor via a cable poses a challenge, if the probes are placed inside the canister and the analyzer is outside. Such an arrangement would require penetration at the canister wall. The size of the analyzer is much bigger than the probe, and if the analyzer is placed inside the canister, its location needs to be evaluated based on the temperature limit of the accompanying electronics, size and shape of the analyzer, and cavity space configuration.

As described in Section 2.1, thermocouples and resistance temperature detectors are subjected to drift, so periodic recalibration is usually required. Fiber optic temperature sensors are subject to gamma-induced fiber darkening and embrittlement that introduce temperature offsets, and calibration may be needed to mitigate or compensate for these effects. Removing the sensor for recalibration or replacing a sensor and achieving a reliable thermal bond with the measurement site would pose significant challenges for internal monitoring.

Table 3-1. Temperature Monitoring Sensors for Internal Environment			
Features	**Temperature Measurement Methods Described in Section 2.1**	**Bimetallic Sensors (Section 3.2.2)**	**Pyrometric Cones Thermoscope Bars (Section 3.2.3)**
Maturity	Same as Table 2-1	Field deployed in non-nuclear applications	Field deployed in non-nuclear applications
Measurement Ranges	Same as Table 2-1	−70 to 550 °C [−100 to 1,000 °F]	590 to 2,000 °C [932 to 3,632 °F]
Sensitivity	Same as Table 2-1	~0.5 to 5 °C [1 to 10 °F]	~20 °C [36 °F]
Longevity	Same as Table 2-1	Decades	Unknown
Space Requirements	Same as Table 2-1	Typically 50 mm × 50 mm × 12 mm [2 in × 2 in × ½ in] but various sizes available	5–10 cm^3 [0.3–0.61 in^3] per cone; cone height 3–10 cm [1.2–3.9 in]
Power Requirements	Same as Table 2-1	None for sensor, power needed for imaging system	None for cone or bar, power needed for Imaging system
Monitoring Area	Same as Table 2-1	Immediate vicinity of the strip	Immediate vicinity of the cone or bar
Data Acquisition Mode	Same as Table 2-1	Continuous or intermittent	Continuous or intermittent data collection, but one-time use
Radiation Tolerance	Same as Table 2-1	Unknown	Unknown
Strengths	Same as Table 2-1	Mechanically based, no power needed for sensor operation, wireless	Mechanically based, no power needed for sensor operation, wireless
Weaknesses	Most require penetration through the cask, or window installed	Imaging system required if used remotely, unknown radiation tolerance and possible embrittlement	One-time use, imaging system required if used remotely, limited temperature range, and unknown radiation tolerance

Radiation Thermometers

Radiation thermometers measure a portion of the thermal radiation emitted by the object being measured. It is a noncontact wireless technology, and some devices can measure up to 1,800 °C [3,252 °F], which is significantly above the expected maximum internal temperature of a DCSS. The line-of-sight measurement capability combined with large standoff distances and the availability of portable systems make them potentially useful for internal temperature monitoring of a DCSS. However, a window that is transparent at the frequencies of the radiation used to measure the temperature is not currently included in existing DCSS designs. Such a feature would need to be added to the canister and cask wall to allow the thermal

radiation from the internal components to be sensed, and it would have to be designed and evaluated for confinement and leakage under normal, off-normal, and accident conditions. The transparent window would not only need to allow the radiation from the internal components being measured to pass through, but the window would need to not produce sufficient radiation from its own temperature to interfere with the ability to determine the temperature of the internal components. At present, the radiation tolerance of the detectors themselves is unknown. The impact of radiation on the material making up the windows also would need to be considered, as well as the impact of changes in the window over time due to the environment or deposition of volatiles from breached elements on the window. In addition, it would appear that the physical arrangement of the structures, systems, and components (SSCs) in the canisters/casks would only allow a limited number of internal surfaces to be measured using a radiation thermometer.

Depending on what surface is being examined and whether oxidation occurs with time, emissivity values of internal components may not change with time as a result of internal environment changes. Any changes in emissivity would likely be a result of oxidation, which would make the surfaces better suited for radiation thermometer measurements. For example, cladding could be oxidized further by oxygen produced from radiolysis of residual water (Jung, et al., 2013), in which case it will be a black body, so no change in emissivity would be expected. Stainless steel surfaces may not be oxidized, so the measurement could be a problem because of its low emissivity. As such, changes of emissivity values of internal components with time, as a result of internal environment changes, and their effect on the measurement accuracy, may not be an issue for potential DCSS use.

Ultrasonic Measurement

As described in Section 2.1.4, some ultrasonic thermometers measure the average temperature between known locations or, using an echo, along a path followed by a reflected wave. Specialized versions of ultrasonic temperature detection using thin calibrated wires can provide direct measurements over specific routes. This is a mature technique that has been demonstrated in extremely harsh environments, including those with high-radiation fields. Some of these ultrasonic thermometers could be used to measure up to 2,500 °C [4,532 °F] with accuracy less than 1 °C [1.8 °F]. These strengths make ultrasonic temperature measurement a potentially useful technique for monitoring the internal temperature. Use of these ultrasonic methods would require insertion of wires into the medium to be measured along with sonic coupling to external sources and sensors for the sonic waves. This requirement would likely limit this technique to new casks. Maintenance and ensuring continued calibration of the inserted wire may be difficult.

Using other ultrasonic wave techniques to measure the temperature of materials inside a cask might require additional research to separate out the impact of the changes in factors other than temperature, including pressure and composition of the internal gases, as well as changes in the material properties of the encasing and enclosed materials. The use of multiple frequencies and receivers might provide information about a number of internal properties.

Semiconductor Temperature Sensors

As described in Section 2.1.6, the measurement range for semiconductor temperature sensors is generally limited to the nominal (IC) operating range of −55 to +150 °C [−67 to 302 °F], which is much lower than the expected maximum internal temperature (the nonoperating range is slightly larger). The sensors are easily damaged at elevated temperatures, and many semiconductors are known to be highly susceptible to radiation effects (Appendix A). Even if

radiation hardening or shielding of the semiconductors could be applied, the maximum temperatures would be a problem. The current maximum for standard high-temperature semiconductors is 220 °C [428 °F] derated to short lifetimes. Given these drawbacks, semiconductor temperature sensors are not likely to be suitable for internal temperature monitoring.

Thermistors

Because of their small size and low cost, thermistors could be a candidate to measure internal temperature. Some thermistors are available to measure temperatures up to 600 °C [1,112 °F]. However, most thermistors have upper temperature limits that are below the maximum internal temperatures expected for a DCSS.

Similar to thermocouples and resistance temperature detectors, electric wiring and good thermal contact are required for the measurement. The use of this type of sensor also would be affected by the data communications and power options discussed in Section 3.1.

Johnson Noise Thermometers

Johnson noise thermometry is based on the fundamental properties of thermal fluctuations in conductors. Johnson noise thermometers are capable of providing reliable temperature measurements at temperatures as high as 1,500 °C [2,732 °F] (White, et al., 1996) and high radiation environments. Because Johnson noise is a fundamental representation of temperature, the sensor is immune from chemical and mechanical changes. As a result, the temperature can be measured to high accuracy and the noise thermometers do not require calibration as frequently as some other sensors (Britton, et al., 2012; ANL, 2012). These strengths make Johnson noise thermometers a candidate to measure internal temperature. However, because the system is still under development, the frequency of calibration is not specified. Calibration frequency will depend on advances in digital signal processing as well as progressive improvements in the measurement electronics design required to extract the Johnson noise signal (Britton, et al., 2012).

In addition, this technique commonly needs to be combined with other devices, such as resistance temperature detectors, to function, and as such, these systems are subject to the power and data communications issues addressed in Section 3.1. There presently are no commercial systems or standard specifications for this technique. Potential DCSS use should depend greatly on further development of this system.

3.2.2 Bimetallic Sensors

Measurement Principle

A bimetallic sensor consists of two pieces of metal, with differing rates of thermal expansion, that are bonded together along their lengths forming a strip, as shown schematically in Figure 3-1. When the temperature of the strip changes, each metal expands or contracts in proportion to the change in temperature. Because the pieces are bonded together along the length of the strip, the strip will bend due to the thermal expansion. This is the basic principle of mechanical thermostats and bimetallic coil thermometers.

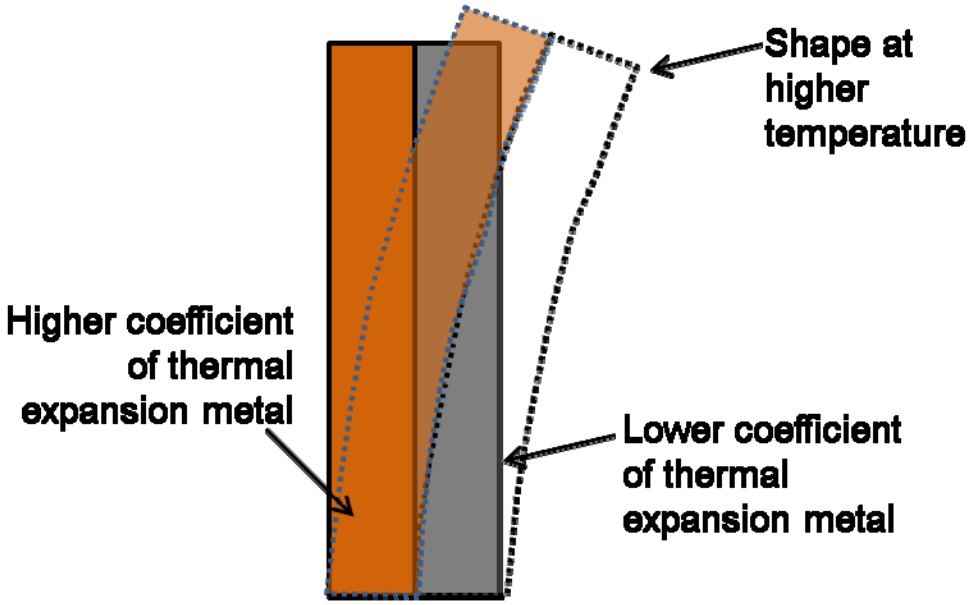

Figure 3-1. Schematics of Bimetallic Sensors

Maturity

This type of sensor has been deployed in the field for non-nuclear applications, but analysis, testing, and qualification are necessary to determine the applicability of bimetallic sensors to a DCSS. No published reports on the effect of gamma and neutron radiation on the performance of bimetallic temperature sensors were located. Expansion of the materials, as a result of radiation exposure, would need to be considered. Imaging (via, for example, acoustic, electromagnetic, or particle radiation) a bimetallic sensor inside a cask and in a gamma and neutron radiation environment would be a novel application and may require significant development.

Measurement Range, Sensitivity, and Longevity

Measurement range and sensitivity of bimetallic sensors depend on the combinations of materials selected, but these devices are usually designed for operational temperatures from −70 to 550 °C [−100 to 1,000 °F]. Measurement sensitivity depends on the device design and measurement range but can be ±1 percent of the measurement range or between 0.5 and 5 °C [1 and 10 °F]. Longevity of these devices can be years to decades in typical applications, such as thermostats. The longevity in high temperature and radiation environments has not been determined.

Space and Power Requirements

Bimetallic strips and coils can be manufactured in many different shapes, sizes, and configurations and are typically sized for a specific purpose. The size of the strip is dependent on the required use. Typical sensors for surface applications have a diameter of 50 mm [2 in] and a height of 12 mm [0.5 in]. Sensors designed for thermowell use also are available with measurement stems of 61 cm [24 in]. The bimetallic strip or coil does not require a power source; however, an external imaging system, if feasible, would require power and must be capable of withstanding the external radiation and temperature environment.

Monitoring Area and Data Acquisition

The monitoring area is the immediate vicinity of the strip or coil. Though a measurement ultimately consists of a single number, the data acquisition systems would likely need to be an imaging system that views and records the displacement angle and calculates the temperature. Both continuous and intermittent data acquisition modes are possible.

Temperature and Radiation Tolerance

Maximum temperatures for these devices are at least 550 °C [1,000 °F]. The radiation tolerance, including the effects of gamma and neutron radiation on measurement accuracy and sensor drift of these devices and the imaging system needed to calculate the temperature, is unknown.

Strengths and Weaknesses

Strengths are that these devices do not require a power source to operate and could potentially be used in applications where no power is available or in locations where gaining access to power is not feasible.

Weaknesses are that temperature monitoring with a bimetallic sensor requires either direct or remote observation of the sensor. In difficult-to-access locations, the use of this type of sensor would be limited by the ability to obtain readings in a high radiation environment. In addition, the strip or coil may be subject to radiation-induced embrittlement that could decrease sensitivity. At present, there are no known uses of bimetallic sensors in radiation levels similar to those expected in a DCSS. Further, there are no known reports of assessments of these devices in harsh radiation environments, such as those defined in IEEE (2003, IEEE-323).

Potential DCSS Use

This temperature sensor is a mechanically based device that requires no power to operate. Because no electrical or fiber optic connection is required for operation, this sensor technology was examined for potential remote applications where power and signal cable routing would be difficult. Internal temperature monitoring is one remote application where power and signal cables would require the need for a penetration of the canister or cask.

For temperature measurements inside a DCSS, the bimetallic sensor would likely need to be premounted inside the canister, such that the angle or distance of displacement of the device due to temperature changes could be determined from external measurements. Depending on the capability of imaging from outside the cask or canister, the sensor can be potentially small; however, the indicator connected to the bimetallic strip or coil would have to be large enough to be viewable via an external imaging system against the background of the SNF, canister or cask structures, and shielding. To meet radiation attenuation requirements for external radiographic imaging, significant changes to the materials, size, and proportions of the bimetallic strip may be necessary, but details of these aspects have not been investigated. If challenges can be overcome for imaging the sensor, the temperature in the immediate vicinity of the bimetallic strip could be inferred.

The feasibility of using bimetallic sensors as internal temperature sensors inside a DCSS without a penetration depends on several factors, including the capabilities of external imaging to provide a sufficiently high resolution image of the bimetallic strip or coil and the radiation

tolerance of the sensor. External measurement of the temperature sensor by either radiographic or tomographic imaging using an external gamma-ray source would be difficult (refer to Section 3.5.3 for additional information on gamma-ray radiographic and computed tomographic imaging). For radiographic imaging, the bimetallic strip or coil would have to be large and dense enough that its gamma-ray attenuation would be a significant and measurable fraction compared to at least twice the wall thickness of the canister or cask. For computed tomographic imaging, manufacturing a mechanical thermostat or bimetallic coil thermometer to include a strong point source of gamma rays is required, so that the physical deformation of the sensor in response to the ambient internal temperature could be imaged and effectively read outside of the canister. Use of SNF gamma rays as an internal source for imaging is not described further, due to additional complexities caused by source gamma rays not being collimated and by scattered gamma-ray contributions.

For internal use, removing the sensor for recalibration or replacing a sensor would require considerable planning, effort, and expense. The sensor therefore would be an unlikely choice for internal temperature monitoring of existing DCSSs because the canister or cask would need to be opened to mount the sensor.

Unknowns

- No information was found describing the gamma and neutron radiation tolerance of this type of sensor.
- The technology necessary to use this type of sensor in applications where remote imaging in a high radiation field is required to determine temperature has not been evaluated or reported.
- It is unclear whether it is possible to produce an operational sensor that meets the size constraints necessary for DCSS applications that can be imaged while within the cask.

3.2.3 Pyrometric Cones and Thermoscope Bars

Measurement Principle

Pyrometric cones (also called Seger cones) and, similarly, thermoscope bars are ceramic indicators that mechanically deform to indicate heat work (Stephenson, et al., 1999). These devices are used to gauge heat work, the combined effect of temperature and time, during the firing of ceramic materials (Dodd and Murfin, 1994; Hamer and Hamer, 1991). Typically three cones or a set of bars indicating different heat work limits are used to provide a visual indication of firing time and temperature. As shown in some examples in Figure 3-2, one cone begins to curl over before the proper thermal exposure has been reached, the second cone begins to drop at the correct thermal exposure, and the third indicates when the optimum exposure has been exceeded. Pyrometric cones and thermoscope bars are one-time devices; after they have curled or drooped, they do not return to the initial shape.

Maturity

Pyrometric cones and thermoscope bars have been deployed in the field as relatively inexpensive indicators. The most common use of these devices is thermal processing operations, such as firing of ceramics.

Figure 3-2. Examples of Pyrometric Cones

At present, there are no known uses of these devices, as temperature indicators in gamma and neutron radiation environments similar to those expected in a DCSS.

Measurement Range, Sensitivity, and Longevity

Pyrometric cones and thermoscope bars are available with discrete temperature ratings from 590 to 2,000 °C [932 to 3,632 °F] at increments of approximately 20 °C [36 °F]. The cones are limited to one-time use. Longevity of the pyrometric cones and thermoscope bars in humid atmospheric conditions or in high-radiation environments is unknown.

Space and Power Requirements

Pyrometric cones and thermoscope bars are manufactured for a specific temperature range and are approximately 3–10 cm [1.2–3.9 in] tall. The space requirement of pyrometric cones and thermoscope bars is on the order of 5–10 cm^3 [0.3–0.61 in^3]. Unless only a maximum upper limit is of interest, multiple cones or bars may be needed. Space might be an issue, but they can be made small and tied to some internal components with metallic wire. These devices do not require a power source; they indicate temperature by mechanical deformation.

Monitoring Area and Data Acquisition

The monitoring area would be in the immediate vicinity of the cone or bar. Although the device is an indicator of whether the heat work threshold has been exceeded, the data acquisition system would likely need to be an imaging system for viewing the deformation of the cones or bars. The data acquisition mode is intermittent.

Temperature and Radiation Tolerance

Pyrometric cones and thermoscope bars are available for a number of discrete temperatures between 590 and 2,000 °C [932 and 3,632 °F]. These are one-time use indicators for thermal processing, typically over a period of hours. Long-term temperature tolerance is not available. The radiation tolerance of these devices is unknown.

Strengths and Weaknesses

Strengths of pyrometric cones and thermoscope bars are similar to the bimetallic sensor described previously, in that they may be used remotely in applications where it is not feasible to run power or signal cables.

Weaknesses are that these temperature indicators are limited to one-time use and they provide information on the overall heat work done on the sensor rather than on the current temperature. Once an over-temperature condition has been reached for a specific cone, the cone is permanently altered and no longer provides useful feedback. These devices also are limited to temperatures above 590 °C [932 °F]. Even if lower temperature range sensors were developed, the elevated temperatures experienced in drying operations after SNF is loaded would limit the useful range of the sensors to temperatures above those reached in drying operations. The possibility of temperature monitoring in difficult-to-access locations would likely be limited by the ability to obtain remote readings in a high radiation environment. Pyrometric cones have not been used as temperature sensors in gamma and neutron radiation environments, and there are no known assessments of these devices in harsh radiation environments, such as those defined in IEEE (2003, IEEE-323).

Potential DCSS Use

Similar to bimetallic sensors in Section 3.1.2, this type of sensor also is mechanically based and it could be investigated as a means to measure internal temperatures without penetrating the canister or cask. Such an application, if determined to be feasible, would require sensor installation prior to fuel loading or in the process of fuel loading while the cask or canister is underwater. Because pyrometric cones and thermoscope bars are one-time use devices, they will be permanently changed if the temperature heat-work threshold has been exceeded during the dry storage installation operations, such as vacuum or forced helium drying operations. Given their one-time use and available temperature ranges, it appears that these devices would be limited to detecting maximum temperature during loading and drying operations.

Imaging pyrometric cones and thermoscope bars in a gamma and neutron radiation environment would be a novel application that may require significant development. This sensor could be mounted inside the canister, such that the shape of the device can be imaged via an external imaging system to indicate the internal temperature (assuming challenges, similar to those discussed in Section 3.2.2, could be overcome with external imaging measurements of the shape of the cone or bar). The imaging system would have to provide a sufficiently high resolution image, such that the curvature of the cone or bar could be measured to determine whether an over-temperature condition has been reached. If the sensor was feasible for internal use, it would likely be considered only for a new DCSS because the sensor would need to be mounted inside the canister before sealing the system.

Unknowns

- The radiation tolerance of this type of sensor is unknown. Although the technology is mature and pyrometric cones are used in commercial applications, no information was found describing the gamma and neutron radiation tolerance of this type of sensor.

- An operational sensor has not been developed or demonstrated that meets the size constraints necessary for internal DCSS applications, which can be measured using radiographic, tomographic, or other imaging methods.

- These sensors are designed for one-time use in relatively short-term thermal processes that are typically hours in duration. The stability of these sensors over the range of temperatures and environmental conditions expected in a DCSS is unknown.

- The useful temperature range of this indicator is higher than normal storage temperatures for a DCSS, and the useful measurement range may be limited to temperatures greater than the maximum temperature allowed during loading and drying operations.

3.3 Humidity Monitoring

The humidity inside a spent nuclear fuel (SNF) canister could indicate the presence of residual water left after drying following removal from the spent fuel pool. The residual water could form oxygen and hydrogen gas by radiolysis, thereby leading to a flammable condition, or it could corrode the internal metallic structures. Further, any intrusion of the water from the external environment during a dry storage period also can aggravate the corrosion of the internal metallic structure or can further increase the risk of flammability inside the canister due to radiolysis.

Humidity of the canister internal environment can be determined by placing a humidity sensor inside the canister or by sampling the internal environment through a probe. Section 2.2 reviewed and assessed six types of humidity sensors for monitoring humidity of the external environment.

This section focuses on the humidity sensors discussed in Section 3.1, in terms of their applicability for measuring humidity of the internal environment. Several enhancements are suggested to apply the technologies for internal monitoring. The main features of these techniques are summarized in Table 3-2.

Capacitance-Based Humidity Sensors

Capacitance-based humidity sensors measure humidity by sensing the capacitance of a ceramic or a polymer-deposited film that absorbs or releases water as a function of humidity. The film is mounted on the probe, which needs to be in direct contact with the internal environment. The probe also needs to be electrically connected to the analyzer. The current versions of the capacitance-based humidity sensors consist of a separate probe and analyzer. The two parts are connected via a cable, which will pose a challenge if the probes are placed inside the canister and the analyzer is outside. This arrangement would require penetration at the canister wall. The data transmission options detailed in Section 3.1.2 would eliminate the need for penetrating the canister.

These capacitance-based sensor systems are small in size and require approximately 0.1–0.5 L [0.03–0.13 gal] of cavity space for their placement inside the canister. A capacitance-based sensor unit consists of a probe 5–10 cm [2–4 in] long and 2–4 cm [0.8–1.6 in] in diameter. The analyzer unit of the sensor is approximately 5–10 cm [2–4 in] long, 4–6 cm [1.6–2.4 in] wide, and 2–5 cm [0.8–2 in] thick. The cavity space in current DCSS canisters is sufficient to place either the probe or both the probe and analyzer inside the canister. However, the placement location of the sensor depends on the temperature limit of the sensors, size and shape of the probe and analyzer, and cavity space configuration.

The polymer-capacitance-based humidity sensors have low radiation tolerance. This limitation can be overcome by using the appropriate shielding for the probes. The level and configuration

Table 3-2. Humidity Monitoring Sensors for Internal Environment						
Features	**Capacitance-Based (Section 3.3)**	**Electrical-Resistance-Based (Section 3.3)**	**Chilled-Mirror-Based (Section 3.3)**	**Leakage Monitoring Sensors (Section 3.3)**	**Fiber Optic Humidity Sensors (Section 3.3)**	**Psychrometer (Section 3.3)**
Maturity	Same as Table 2-3					
Measurement Ranges						
Sensitivity						
Longevity						
Space Requirements	Existing void space is sufficient for sensor placement		Modifications are needed to create cavity space for sensor placement		Cannot be determined	Same as Table 2-3
Power Requirements	Power supply using precharges or rechargeable batteries when the sensor system is placed inside the canister. Section 3.1.1 provides details on various power supply options.					Same as Table 2-3
Monitoring Area	Same as Table 2-3					
Data Transmission	Wireless data transmission when the probe or whole sensor system is placed inside without penetration. Section 3.1.2 provides discussion on wireless data transmission technology.					
Radiation Tolerance	Same as Table 2-3					
Strengths						
Weaknesses	Needs radiation shielding and canister penetration					Needs a liquid water source inside the canister to saturate the thermometer to function

of shielding can be determined by laboratory testing. The radiation hardening also can be used for the ceramic-capacitance-based humidity sensors.

The sensing probes of the capacitance-based sensors require periodic calibration. This would require placing the probe in the canister in such a way that it can be periodically removed from the environment for its calibration or replacement. This challenge has to be resolved before using the capacitance-based humidity sensor for internal monitoring.

Another limitation of the capacitance-based sensors is the operational temperature limit. Most capacitance-based sensors only can operate effectively up to 100 °C [212 °F], except $MgCr_2O_4$–TiO_2-based sensors, which have temperature tolerance up to 300 °C [572 °F] (see Table 2-3). The canister temperature is expected to be well above 100 °C [212 °F]. This poses a challenge in using the capacitance-based humidity sensor technology, and the temperature range of the polymer-capacitance-based sensor would have to be enhanced before it could be used for internal monitoring.

These sensors require external power to operate. The current version of the sensors is battery operated or needs an external power source. The power supply options detailed in Section 3.1.1 could provide a substitute for an external power supply.

Chilled-Mirror-Based Humidity Sensors

The principal operating mechanism of these sensors is based on cooling of a mirror to measure dew point or frost point temperature of the environment. The sensor system consists of a sampling probe and analyzer, both integrated in one unit. The probe simply acts as a conduit between the environment and mirror, which is part of the analyzer. These sensors can be used by placing them inside the canister and by including the following modifications: (i) radiation hardening, (ii) power supply, and (iii) wireless communication.

These sensor systems are relatively larger than capacitance-based sensors and need cavity space of approximately 5–15 L [1.32–3.96 gal]. The sensor system consists of a probe, which is approximately 13 cm [5 in] long and 5 cm [2 in] in diameter, and the analyzer is 25 cm × 20 cm × 12 cm [10 in × 8 in × 5 in]. The cavity space and configurations inside the canisters of the DCSS need to be evaluated for placing the sensor inside the canister. Certain design modifications in a DCSS may be needed to make room for the sensor system inside the canister. The sensors can be radiation hardened by placing them inside a radiation-shielded casing. This will allow sensors to operate without being degraded by the radiation field inside the canister.

The sensors require significantly more power compared to the capacitance-based humidity sensors. The power supply options involving batteries (detailed in Section 3.1.1) would provide a substitute for external supply. The battery system and the sensor can be programmed such that the sensor is used at discrete intervals. This will reduce power load on batteries and extend battery service life. Several precharged or chargeable atomic batteries could cover the power requirement for a sensor system for a certain monitoring period. The data from the sensor system can be transmitted using the wireless data transmission options detailed in Section 3.1.2.

Vendors' literature indicates that chilled-mirror-based humidity sensors only can operate up to 115 °C [239 °F] (Omega Engineering, 2013; GE, 2007, 2011; Michell Instruments, 2012; Kahn Instruments, Inc., 2012). This temperature limit is based on the cooling capacity of the

analyzers in the sensor systems. The sensor systems can be mounted in locations where the temperature is below 115 °C [239 °F] inside the canister. Another alternative is to increase the cooling capacity, and thus the operating temperature limit, of the sensor systems by technological enhancement.

The operating mechanism of this sensor system involves cooling the mirror. This could pose a serious challenge for the sensor cooling system, considering there is a large heat load inside the canister, and it will be difficult for the sensor cooling system to reject the heat generated from the cooling to the internal environment. In addition, the consequences of having the heat generated by the fuel assemblies inside the canister for the sensor cooling system would need to be evaluated.

Electrical-Resistance-Based Humidity Sensors

The electrical-resistance-based humidity sensors measure humidity by sensing change in either resistance or conductivity of a reference material with humidity of the environment. These sensor systems consist of a probe and analyzer. The size and power requirements of these sensor systems are comparable to the capacitance-based humidity sensors.

Similar to the capacitance-based humidity sensors, the probe and analyzer in these sensor systems are connected via a cable. The data transmission options, including wireless transmission detailed in Section 3.1.2, would eliminate the need for penetrating the canister. The resistance-based sensor systems need approximately 0.1–0.5 L [0.03–0.13 gal] of the cavity space for their placement inside the canister. The dimensions of the sensor probe and analyzer are expected to be comparable to the capacitance-based humidity sensors—5–10 cm [2–4 in] long and 2–4 cm [0.8–1.6 in] in diameter, and the analyzer unit approximately 5–10 cm [2–4 in] long and 4-6 cm [1.6–2.4 in] wide and 2-5 cm [0.8–2 in] thick. The current cavity space inside the DCSS is deemed sufficient to place either the probe or both the probe and analyzer inside the canister.

The radiation tolerance of the resistance-based humidity sensors is limited and not known for the level of radiation expected inside the canister. It is expected that various metallic and nonmetallic components could require radiation hardening. The radiation shielding options discussed in Section 3.1 also would be applicable for the internal use of this sensor technology.

Similar to capacitance-based humidity sensors, the sensing probes of the resistance-based sensors require periodic calibration. This would require the probe placed in the canister to be periodically removed from the canister for its calibration or replacement. This challenge has to be overcome before using the capacitance-based humidity sensor for internal monitoring.

The resistance-based sensors have an operational temperature limit of 200 °C [392 °F], which is higher than other humidity sensors. These sensor systems can be placed at several locations inside the canister where the temperature is below 200 °C [392 °F]. The temperature of the canister environment varies along its length and diameter with spent fuel loading. The sensor systems can be placed at appropriate locations, which can be identified by conducting thermal analysis of a DCSS and its temperature limit of 200 °C [392 °F].

The power requirement of these sensors is comparable to that of capacitance-based humidity sensors. Various power supply options discussed for the capacitance-based humidity sensors also are applicable for the resistance-based humidity sensors.

Fiber Optic Humidity Sensors

The fiber optic sensors are not commercially available; hence, evaluating their applicability in the internal environment is difficult. An analysis of the operation principle and sensing mechanism of the sensors indicates that these sensors are resistant to electromagnetic interference. Therefore, the sensors could be used for internal environment humidity monitoring with some modifications. These modifications would include radiation hardening, installing wireless communication, and sourcing independent power supply, which are discussed in Section 3.1.

The fiber optic cable and other sensor equipment would require radiation hardening before the sensor is placed in the canister. The wireless communication mechanism could be used to transmit and receive the collected data from the sensor. Further, the power for the sensors can be derived from the precharged battery and rechargeable batteries. The power supply and wireless data transmission options discussed in Sections 3.1.1 and 3.1.2 also are applicable for this sensor technology.

Leakage Monitoring Sensors

The leakage monitoring system captures the gas sample with a passive element and transfers it to a remote humidity analyzer, which is connected through a sealed tube to the passive element. Both Areva Flüs (Areva, 2009) and the Westinghouse Leakage Monitoring (Westinghouse Electric Company, 2011) systems have fairly large sized analyzers that are connected to the passive element through the long tubes. This technology is not deemed to be suitable for measuring the internal environment humidity in its current state because the removal of gas from the canister internal environment would reduce the gas amount in the canister, change heat transfer characteristics of the canister internal environment, and generate a waste stream to be processed. This will have an undesirable effect on storage capacity of the canister; therefore, the sensor system only can be used by placing it inside the canister. However, the analyzer and the passive elements cannot both be placed inside an existing DCSS, due to the large sizes of the analyzers of the two available sensor systems.

Psychrometer

A psychrometer functions with two thermometers, one dry and the other moist. The moist thermometer is saturated with water. A liquid water source must be present inside the canister to saturate the thermometer to make the psychrometer to work. This requirement may be counter to the original dry storage requirement, which is having a dry (i.e., moisture free) environment inside the canister. If a liquid water source is placed inside the canister, it could interfere with dry storage capability of the DCSS by increasing the risk of flammability, oxidation of cladding material, and corrosion of internal structural components. For these reasons, particularly the need for maintaining a liquid water source inside the canister, a psychrometer is not likely to be useful for humidity measurements inside the canister.

3.4 Pressure Monitoring

Helium backfill gas maximizes heat transfer from the SNF. One motivation to monitor internal pressure from outside the system is to provide a global indication of confinement boundary integrity. For casks with bolted lids, Figure 1-3 shows that a pressure monitoring system has been built into the system to directly confirm confinement (leak tightness) in the gas space between the inner and outer lids. The industry has put this system into actual application in

independent spent fuel storage installations (ISFSIs), so it will not be evaluated in this report. Currently there are no direct methods for testing the leak tightness of an SNF canister with welded primary and secondary lids.

As indicated in Table 1-1, helium pressure is one parameter that may be monitored to assess degradation of cladding. Estimates of volume and pressure in the SNF rods are 0.02 L [20 cm^3] and ~5 MPa [~50 atm] (NRC, 2007, pp. D–4 and D–15). These quantities are approximately 7,000 L [1,849 gal] and 1 to 5 atm [0.1 to 0.5 MPa] for storage casks (NRC, 2007, pp. D–4 and D–15). Applying the ideal gas law for combining gas releases from SNF rods with the gas in the cask (NRC, 2007, p. D–16), the estimated relative increase in cask pressure from gas releases ranges from 0.003 percent per rod [(0.02 L) (50 atm)/(7,000 L) (5 atm)] to 0.01 percent per rod {(0.02 L) [50 atm]/(7,000 L) [1 atm]}. This corresponds to pressure change of 0.00015 to 0.0001 atm. For a high-precision pressure gauge with a full scale of 2 to 10 atm and accuracy of 0.1 percent of full scale (Higham and Paros, 2010), the gauge can measure pressure change accurately up to 0.002 to 0.01 atm, which is well above the pressure change from one rod failure. To cause a pressure change that can be accurately measured by a high-precision gauge, more than 10 rods would have to fail. However, this is not likely to be the normal case. This scoping calculation suggests that pressure change because of failure of one or several rods is too low to be detected.

Another motivation for monitoring pressure is to detect the presence of hydrogen and oxygen. When the canister is sealed, it is filled with helium, with the overall pressure of helium (hereafter referred as backfill pressure) ranging between 1 and 5 atm [14.7 and 73.5 psi]. The backfill pressure inside the canister would gradually decrease with time as decay heat of the fuel assemblies decreases. The initial backfill pressure and its gradual decrease with time is referred to as the baseline backfill pressure. If there was any residual water during the drying process, the water would vaporize over time and increase the baseline backfill pressure. The amount of increase in the backfill pressure will be proportional to the amount of the residual water inside the canister. Scoping calculations are conducted to determine the increase in the baseline backfill pressure due to the presence of the residual water. Further, the water would gradually dissociate to form hydrogen and oxygen due to the radiation field inside the canister. This also could result in an increase in baseline backfill pressure inside the canister.

Simplified scoping calculations are conducted to quantify the magnitude of the backfill pressure with temperature and effects of the residual water on the baseline backfill pressure. While the backfill pressure in a canister would be a complex function of the temperature field and would vary with position inside the canister, it is assumed that the backfill pressure follows the ideal gas law. It also is assumed that the canister pressure is proportional to the bulk average temperature inside the canister. The bulk average temperature is defined as the overall average of the internal environment temperature field. Further, Dalton's Law for partial pressure is used to account for the effects of residual water on the backfill pressure. The calculated baseline backfill pressure and effects of various amounts of residual water on the pressure are shown in Figures 3-3(a,b) for a canister void volume of 2,100 and 7,000 L [554.8 and 1,849 gal], respectively.

The scoping calculations show that the baseline backfill pressure decreases with temperature. Because the canister temperature is expected to decrease with time, the backfill pressure also will decrease with time. The normal condition in Figure 3-3 corresponds to no water being present. The residual water amounts will increase the baseline backfill pressure, and the increase is expected to be proportional to the water amount, as shown in Figures 3-3(a,b). When the canister void volume is lower, the residual water effects will be more pronounced on

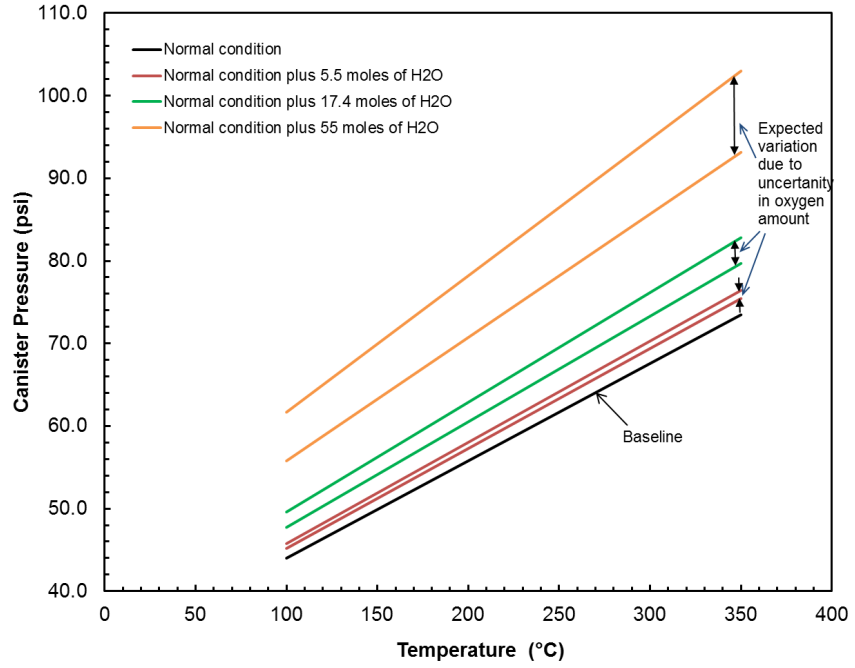

(a)

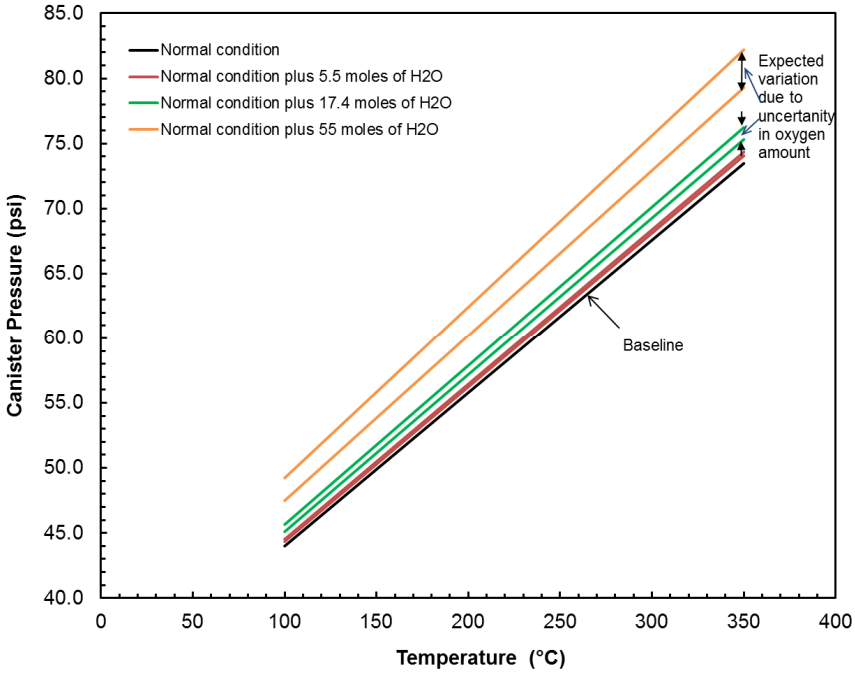

(b)

Figure 3-3. Canister Pressure Versus Temperature for Various Conditions. Canister Void Volume of (a) 2,100 L, (b) 7,000 L. The Normal Condition Corresponds to the Case Where There Is No Residual Water in the Canister. The Red, Green, and Orange Lines Correspond to the Conditions Where There Is Either 5.5, 17.4, or 55 Moles of the Residual Water in the Canister, Respectively.

the baseline backfill pressure. The scoping calculations also show that the residual water will result in a noticeable increase in the baseline backfill pressure. The increases in the baseline backfill pressures are likely to be high enough to be detected by the pressure sensor. For example, 5.5 moles of residual water increases the baseline backfill by several tenths of atm [several psi], which is above the detection limit of several pressure monitoring sensors (Higham and Paros, 2010).

The canister pressure also can be used to infer the oxygen amount in the canister. The residual water will dissociate into oxygen and hydrogen due to the radiation field inside the canister. Some of the oxygen produced from the radiolysis of the water will be consumed in the oxidation of the canister internal structural materials, such as cladding. The extent of oxygen consumption will depend on the cladding temperature and rate of water dissociation. However, there are several scenarios when the oxygen from radiolysis will be left in the canister. These scenarios are detailed in Jung, et al. (2013). The baseline backfill pressure will increase due to the presence of oxygen in the internal environment. This increase is quantified and shown in Figures 3-3(a,b) for the canister void volumes of 2,100 and 7,000 L [554.8 and 1849.2 gal], respectively.

As seen in Figures 3-3(a,b), the increase is more than 0.07 atm [1 psi] when residual water amounts are 17.4 and 55 moles. The scoping calculations account for uncertainty in the oxygen amount due to oxygen consumption by oxidation of cladding, any exposed spent nuclear fuel, and the recombination reaction between hydrogen and oxygen that produces water. Note that the upper values of the baseline pressure increases in Figures 3-3(a,b) are calculated assuming no consumption of oxygen inside the canister. If there is oxidation of the internals due to the radiolysis-produced oxygen, the oxygen amount in the canister will decrease and so will its effect on the backfill pressure. Thus, the baseline backfill pressure and any variation in it from the baseline case can be used to infer the presence of residual water, hydrogen, and oxygen inside the sealed canister.

This work reviews the following pressure monitoring methods that may be of interest for DCSS monitoring: (i) installation of magnetically coupled Bourdon tube pressure gauges in shield plugs; (ii) external measurement of internal pressure from the spectral analysis of airborne sound resonances created from ball bearing strikes on the container; (iii) installation of a pressure transducer inside the cask as part of a remote monitoring system with pressure signal routing through canister-wall transducers, a wireless transmitter, and a wireless receiver; (iv) Booth-Cromer type, null-balance pressure transducers to measure the internal pressure in mixed oxide fuel rods in the Plutonium Recycle Test Reactor; (v) container material hoop strain-based embedded sensor; and (vi) container material deflection-based measurement. Radiographic imaging of a small pressure-sensitive insert, which Ghosh, et al. (1983) described for measuring internal pressure of nuclear fuel rods, was not assessed, because its usefulness for DCSS applications is precluded by the high ambient radiation levels and placement of radiographic imaging equipment within the container.

The main features of these techniques are summarized in Table 3-3, with additional details described in subsequent sections.

Table 3-3. Internal Pressure Monitoring Sensors				
Features	**Bourdon Tube Pressure Gauges (Section 3.4.1)**	**Ball Bearing Strikes-Generated Sound Resonance Spectra (Section 3.4.2)**	**Remote Sensing of Pressure Transducer Inside Canister (Section 3.4.3)**	**Booth-Cromer Type, Null-Balance Pressure Transducer (Section 3.4.4)**
Maturity	Field deployed in non-nuclear applications	Tested in laboratory	Tested in laboratory	Old technology, tested in laboratory
Measurement Ranges	<0.1 to tens of MPa [<1 atm to hundreds of atm]	Not specified	0 to 1.72 MPa [0 to 17 atm] for Omega PX1009 pressure transducer	Up to 1.03 MPa [150 psi]
Sensitivity	Sensitivity of 0.0125 percent and accuracy up to 0.1 percent of its full scale	Not specified	Not specified	Not specified
Longevity	Decades in nonradiation field; radiation effects on longevity unknown	Not specified	Not specified	Not specified
Space Requirements	Minimal, less than 7.6-cm [3-in] diameter and 3.0-cm [1.2-in] height as designed to fit in canister port	The striking ball is 32 mm [1.2 in] in diameter	Not specified	Not specified
Power Requirements	None for visual or boroscope readout (sending unit power required for remote readout)	Not specified	Not specified	Not specified
Monitoring Area	Internal cask	Internal pressure	Internal pressure	Internal pressure
Data Acquisition Mode	Continuous or intermittent	Intermittent	Continuous	Continuous
Temperature Tolerance	Robust, in excess of 400 °C [752 °F]	Not specified	−54 to 343 °C [−65 to 650 °F]	Not specified
Radiation Tolerance	Robust, in excess of 1,000 Mrad (unconfirmed)	Not specified	Not specified	Not specified
Strengths	Long-term monitor, reliable detection of leakage out of the canister, no power required, decay heat harvesting system may be feasible for generating sufficient electrical power to enable remote instrument readout for long time periods	External measurement of internal pressure without penetration	Wireless, *in situ*	*In situ*
Weaknesses	A retrofit is required to the shield plug port	Mechanical impact on canister, lower sensitivity at higher internal pressure, geometry may not allow space for striking ball	A retrofit is required to make a cavity in the shield plug. Numerous unknowns.	Need electrical wires and cables. Numerous unknowns.

Table 3-3. Internal Pressure Monitoring Sensors		
Features	**Container Material Hoop Strain-Based Embedded Sensor (Section 3.4.5)**	**Container Material Deflection-Based Measurement (Section 3.4.6)**
Maturity	Field deployed for health monitoring	Tested in laboratory
Measurement Ranges	Not specified	Not specified
Sensitivity	Unknown	Not specified
Longevity	Unknown	Not specified
Space Requirements	Sensor embedded in host material	Close proximity to canister surface to measure deflection
Power Requirements	Power consumption ranging from 90–300 watts (Section 2.5.1)	Not specified
Monitoring Area	Internal pressure	Internal pressure
Data Acquisition Mode	Continuous or intermittent	Intermittent
Temperature Tolerance	>1,100 °C [2,012 °F]	Not specified
Radiation Tolerance	Unknown	Not specified
Strengths	In-service, nondestructive external monitoring	External measurement of internal pressure without penetration
Weaknesses	Possible low sensitivity because of thick-walled canister, gamma radiation interference, sensor deployment may be problematic, temperature calibration required	Possible low sensitivity because of thick-walled canister, installation and measurement difficulty. Numerous unknowns.

3.4.1 Bourdon Tube Pressure Gauges

Measurement Principle

Sexton (2000) described a plan for monitoring the internal pressure of a U.S. Department of Energy (DOE) multicanister overpack (MCO). The plan called for the installation of a magnetically coupled Bourdon tube pressure gauge in the shield plug port that was intended to eliminate "any impact to the MCO pressure boundary." Figures included in the plan (Sexton, 2000, Figures 1 and 2) apply to a proposed DOE MCO and depict the potential installation of a pressure gauge and magnet in the drain port below the solid plug material that establishes the pressure boundary. A simplified rendering is shown in Figure 3-4 of this report. Although there are container design differences among dry storage systems for commercial spent nuclear fuel and the DOE MCO, the technique was assessed because it was proposed for the storage and monitoring of spent nuclear fuel (Sexton, 2000). Discussion of the measurement principle is brief because a Bourdon tube pressure gauge is a well-developed technology. Features of this monitoring technique are summarized in Table 3-3.

Maturity

The technology is mature. Although its use in the proposed configuration has not been demonstrated for dry storage applications, the gauge technology is well developed and has been field deployed.

Measurement Range, Sensitivity, and Longevity

Instrument measurement range and sensitivity are not directly stated in the monitoring plan (Sexton, 2000). The range is approximated in Table 3-3. Higham and Paros (2010) indicate that the Bourdon tube pressure gauge can have sensitivity of 0.0125 percent and accuracy up to 0.1 percent of its full scale. The pressure change of the internal environment could be reliably detected by this method; however, reliable detection of these pressure differences needs to be demonstrated for storage conditions. Concurrent temperature monitoring may improve sensitivity of the technique for assessing pressure variations over short and long time periods.

A high confidence of instrument availability is expected for periods longer than 40 years. This long-term monitoring technique does not require hardware placement within the canister and would readily detect the pressure drop from helium leakage out of the canister.

Gauge installation is required during canister closure. Gauge replacement would be difficult following its installation into the shield plug port and closure of the canister. Sexton (2000, p. 10) proposed installation of a magnetically coupled Bourdon tube pressure gauge in a DOE MCO and indicated that maintenance of the pressure gauge would be possible "while still in the shield plug only configuration." The degree to which maintenance also would be possible for other dry cask storage designs was not evaluated in this project, because long-term gauge operation does not rely on periodic maintenance.

Space and Power Requirements

By design, the pressure gauge does not require maintenance or calibration during its lifetime (Sexton, 2000, p. 10). No calibration is required following installation. Gauge size is tailored to the dimension of the shield plug port. Gauge dimensions of less than 7.6-cm [3-in] diameter

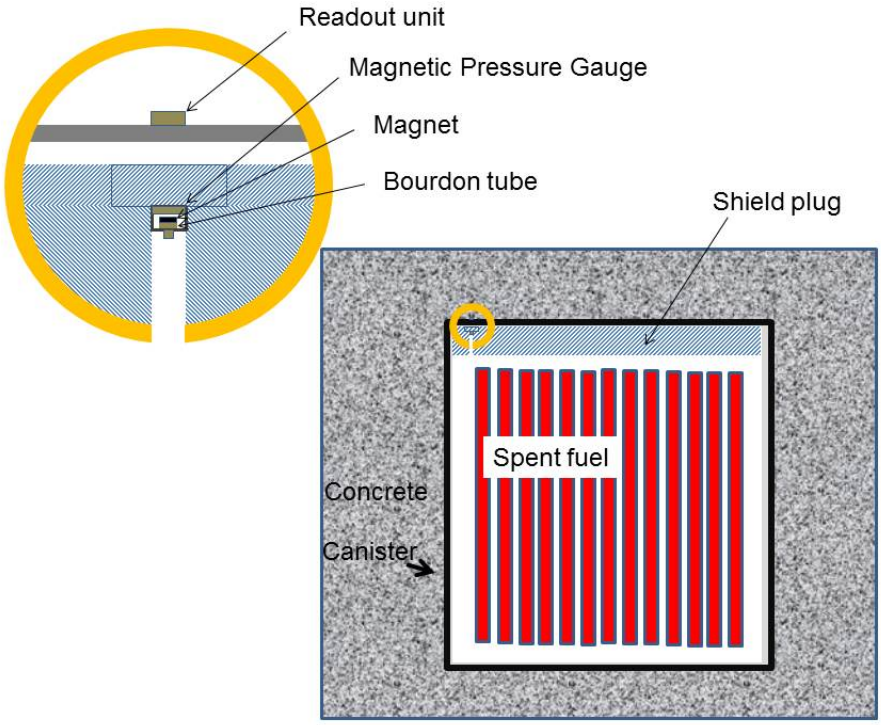

Figure 3-4. Schematics Showing the Bourdon Tube Pressure Gauges for Internal Pressure Monitoring

and 3.0-cm [1.2-in] height were approximated in Table 3-2. Space requirements are minimal and limited to boroscope access to the sender readout unit for remote readings. There are no power requirements for this pressure gauge.

Monitoring Area and Data Acquisition

The gauge provides a direct measure of internal cask pressure; no data analysis is required. The pressure data can be digitized and transmitted to a data acquisition system. Data acquisition can be continuous or intermittent.

Temperature and Radiation Tolerance

Temperature and radiation tolerance for the pressure gauge is high. The temperature tolerance in excess of 400 °C [752 °F] is presented in Table 3-3 to merely indicate the pressure gauge can withstand temperatures exceeding those expected in a DCSS for SNF. Pressure gauges have been designed for operation at higher temperatures.

The Bourdon tube pressure gauge was selected for the long-term monitoring of a DOE MCO (Sexton, 2000), but radiation tolerance data were not presented. Gauge lifetimes of more than 40 years are expected but remain uncertain. As described in the MCO monitoring plan (Sexton, 2000, p. 1), “MCOs are likely to be stored for 40 years or longer.” Inside an SNF container and at its ends without shielding, an exposure time of 40 years relates to a total integrated dose on the order of 1,000 Mrad, which is the minimum value presented in Table 3-3 for the radiation tolerance of this pressure gauge. The pressure gauge may withstand higher total integrated doses, but data to substantiate the claim are lacking.

Strengths and Weaknesses

A remote system was described in Sexton (2000) with magnetic coupling that eliminates effects on the cask pressure boundary by the propagation of a magnetic signal from the pressure gauge on one side of the metal plug to a readout unit on the other side. This long-term monitoring technique does not require hardware placement within the canister and would readily detect the pressure drop from helium leakage out of the canister. Decay heat harvesting may be feasible for generating sufficient electrical power to enable remote instrument readout over long time periods (Carstens, et al., 2013). Thermal-electric generation is a mature technology due to its utility in space missions as a source of long-term electrical power. A detailed assessment of current technological options was not conducted as part of this project. Shield plug modification and retrofitting are required to allow for instrument installation. Dry cask designs with carbon steel lids may inhibit magnetic coupling. A scoping assessment suggested that pressure monitoring alone would be unable to detect a small number of rod failures but could detect a substantial number of rod failures in a cask. Overall, the technique seems to have a limited value for detecting fission gas releases from SNF rods into a sealed canister.

Potential DCSS Use

Hanson, et al. (2012, Section 4.6.3.2) indicated that internal pressure can be monitored in the headspace using a commercially available pressure transducer. Sensor access can be provided by vent or drain ports, as schematically shown in Figure 3-4. A pressure gauge provides instantaneous indication of internal pressure; remote access and visual gauge reading may be continuous or intermittent. Sexton (2000) proposed remote pressure gauge readings using a boroscope by either (i) removing the cover cap to access the pressure gauge at the shield plug port or (ii) adopting an alternative design with a sender readout unit at the top of the cover cap that did not require cover cap removal. Although structural integrity during an accident has not been assessed for gauge installation in the drain port with a magnetic interface at the sealed pressure boundary as Sexton (2000) proposed, such an assessment should be performed during DCSS-use considerations.

Using a boroscope with a welded cover in place, a sender readout unit allows for remote visual gauge reading and pressure monitoring. As Sexton (2000) indicated for installation in an MCO, the standard indicating needle of the Bourdon pressure tube will be replaced by a magnetic couple, and the gauge will be installed in one of the MCO shield plug ports. Mounted outside the MCO, a compass with a modified face to reflect pressure will be used to provide an external readout and a direct reading of MCO internal pressure. Mounting in this manner and installing the existing designed port cover eliminates any impact to the MCO pressure boundary.

Unknowns

- Maintaining confinement following accident sequences.
- Measurement range and sensitivity for an instrument robust enough to maintain confinement following accident sequences.
- Decay heat harvesting system for generating electrical power to enable remote instrument readout for long time periods.
- Magnetic signal transmission through metal components of the confinement boundary for dry storage system designs.

3.4.2 Ball Bearing Strikes-Generated Sound Resonance Spectra

Measurement Principle

The airborne sound resonance spectrum created from ball bearing strikes is a function of the internal pressure. Ball bearing striking on a structure generates vibrations whose frequencies increase with internal pressure. A higher pressure increases the stiffness of the structure and thus changes the resonance frequencies of the individual vibration modes. These resonance frequencies are determined by spectrum analysis of airborne sound signals, which can be used to determine the internal pressure of the structure. A detailed assessment of acoustic properties and sensitivities associated with DCSS designs was not conducted as part of this project.

Maturity

Eisenblätter (1995) tested an external measurement technique for internal pressure by performing a spectral analysis of airborne sound resonances created from ball bearing strikes on nuclear waste drums. Following impact, the complex sound response, registered during the initial 15 μs, developed into periodic sound resonances, which were recorded for time periods of 15 and 65 μs post-impact. Spectral analyses of the first and second sound resonances showed a clear dependence on internal pressure. Greater frequencies were observed for internal pressure increases. Supralinear curves were plotted for internal pressure versus resonance frequency for both the first and second sound resonances. The internal pressure, wall thickness, and dimensions of SNF canisters are different from waste drums. Feasibility for measuring internal pressure of SNF canisters using this approach was not demonstrated and warrants further evaluation.

Measurement Range, Sensitivity, and Longevity

The measurement range was not specified, but Eisenblätter (1995) reported an accuracy of pressure measurement between 0.005 and 0.01 MPa [0.05 and 0.1 atm]. Because higher internal pressures corresponded to smaller changes in sound resonance frequencies, sensitivity of the approach decreased for increasing internal pressures. Internal pressures were less than 2 atm for the nuclear waste drums tested. Compared to nuclear waste drums, SNF canisters have significantly greater wall thicknesses, and resonant frequencies will differ for SNF canisters. Assessment of the measurement sensitivity at higher internal pressures (~5 atm) requires additional information on anticipated resonant frequencies for SNF canisters or metal casks.

The lifetime of the striking ball could be limited depending on the striking force, but it can be replaced externally. Longevity is not likely to be a limitation.

Space and Power Requirements

The striking ball is 32 mm [1.2 in] in diameter. Other facilities are needed to operate the ball. The power requirement was not specified in Eisenblätter (1995).

Monitoring Area and Data Acquisition

This technique only measures the internal pressure. The data measured each time are the sound resonance spectra. The data acquisition mode is intermittent.

Temperature and Radiation Tolerance

Temperature and radiation tolerance were not specified.

Strengths and Weaknesses

The strength of this technique is that it is an external technique to measure internal pressure. Weaknesses are that the ball needs to mechanically strike the canister and thicker canister wall, and higher internal pressure could affect the measurement sensitivity. Limited space available between a canister and either an overpack or a horizontal storage module (HSM) would require modification to accommodate such a system.

Potential DCSS Use

This approach has been tested for the waste drum and may have potential for long-term canister internal pressure monitoring. Further investigations are needed to establish a sufficient basis on its appropriateness for dry storage monitoring.

Unknowns

- Measurement sensitivity at higher internal pressures (~5 atm) and thicker walls for canisters compared to nuclear waste drums.
- Effect of canister internals, including the potential degradation of those components, on the resulting resonance frequencies.
- Depending on its striking force, the ball bearing impact may have negative effects on that localized area of the canister for repeated measurements over long time periods.

3.4.3 Remote Sensing of Pressure Transducer Inside Canister

Measurement Principle

Pressure transducers are installed inside the cask as part of a remote monitoring system with pressure signal routing through canister wall transducers, a wireless transmitter, and a wireless receiver. The system was designed without a canister wall penetration.

Maturity

Massie (2008) proposed this system to remotely monitor the temperature and pressure inside an SNF canister in dry storage. Several items were identified for further consideration, improvement, or verification (Massie, 2008, Section 11). The system includes components inside and outside the canister. Inside components are a temperature sensor (thermocouples), pressure sensor (diaphragm and strain gauges), power supply (thermopiles), multiplexer, integrated circuit (amplifier, voltage regulator, and voltage oscillator), and internal canister wall transducer. Outside components are an external canister wall transducer, thermopiles, wireless transmitter, and wireless receiver.

Measurement Range, Sensitivity, and Longevity

Massie (2008) introduced various methods of measuring pressure and recommended diaphragm and strain gauges for the SNF monitoring application. Massie (2008) suggested using the Omega PX1009 pressure transducer. For this device, the stated absolute pressure range of 0 to 1.72 MPa [0 to 17 atm] is adequate for normal dry storage conditions. Sensitivity and longevity are unknown.

Space and Power Requirements

Not specified.

Monitoring Area and Data Acquisition

This technique monitors internal pressure. The system uses a signal conditioner that outputs to a data acquisition system. The data acquisition mode is continuous, and the data are stored as an electronic file.

Temperature and Radiation Tolerance

For the Omega PX1009 pressure transducer Massie (2008) suggested, the stated operating temperature range of −54 to 343 °C [−65 to 650 °F] is adequate for normal dry storage conditions.

Radiation tolerance of the device was not documented.

Strengths and Weaknesses

The strength is that this is an *in-situ* internal pressure monitoring technique and it is wireless. The weakness is that this monitoring approach requires a retrofit to existing dry cask designs for implementation, as well as the installation of sensors and electronics inside the canister.

Potential DCSS Use

The proposed design involves a retrofit to create a cavity in the shield plug for internal electronics with a diagonal shaft for wires to the thermocouples and thermopiles, located within the canister away from the shield plug. Outside of the canister near the modified shielding, the gamma dose rate was calculated to be approximately 10 times higher than the unmodified design. This increase applies to a localized region near that end of the canister; dose rates at other locations were unaffected. The neutron dose rate was much less sensitive to the retrofit. As Massie (2008, Section 8) suggested, additional shielding could be added to reduce or remove the estimated dose rate increase, but it was not included in the retrofit design used for the shielding calculation. Electronics survivability also was considered.

Unknowns

- Sensitivity of measurement.
- Power requirements, radiation tolerance, and longevity of components inside the canister.

- Space accommodations for monitoring equipment inside the canister.

3.4.4 Booth-Cromer-Type, Null-Balance Pressure Transducer

Measurement Principle

The pressure sensor operates by deflection of a thin diaphragm that opens an electrical circuit.

Maturity

Burley (1969) used the Booth-Cromer-type, null-balance pressure transducers to measure the internal pressure in mixed oxide fuel rods in the Plutonium Recycle Test Reactor. Pressure measurements were acquired over 15 months of reactor operation. If the transducer diaphragm failed during the experiments, fission gases could have passed through the failed diaphragm and exposed personnel. A safety system was devised to prevent operator exposure in the event of diaphragm failure. The diaphragms did not fail during the tests.

Measurement Range, Sensitivity, and Longevity

Maximum internal pressures of approximately 1.03 MPa [150 psi] were measured. Sensitivity and longevity were not specified.

Space and Power Requirements

The space requirement was not specified. Power requirements for the pressure sensor were not described, presumably because electrical wires and cables were used instead of configuring sensor operation with a remote power source.

Monitoring Area and Data Acquisition

The technique monitors the internal pressure. The system uses a signal conditioner that outputs to a data acquisition system. The data acquisition mode is continuous, and the data are stored as an electronic file.

Temperature and Radiation Tolerance

Temperature and radiation tolerance were not specified. This sensor technology was able to withstand the greater neutron and gamma-ray fluxes during reactor operation. Due to the relatively short timeframe associated with the experiments, the in-reactor tests do not rule out the possibility of greater accumulated dose and aging effects for long-term monitoring of a dry storage system.

Strengths and Weaknesses

It is an in-service pressure monitoring technique, but electrical wires and cables are needed.

Potential DCSS Use

It is an old technology and was not deployed with remote power.

Unknowns

1. Measurement range, sensitivity, longevity, space and power requirements, amount of data per measurement, temperature, and radiation tolerance.

2. Applicability in DCSS use.

3.4.5 Container Material Hoop Strain-Based Embedded Sensors

Measurement Principle

Fiber Bragg grating (FBG) optical sensors and polyvinylidene-fluoride (PVDF) polymetric piezoelectrodes are embedded in composite overwrapped pressure vessels. The measurement principle of FBG sensors was described in Section 2.5.1 and shown in Figure 2-15. Hoop strain in the host material surface where the fiber or the PVDF polymer is attached generates optical or piezoelectric signals. Strain changes are correlated to internal pressure changes. As a result, the internal pressure is monitored externally.

Maturity

Several researchers (Podskarbi, 2010; Frias, et al., 2010; Faria, et al., 2010) have examined internal pressure determinations from hoop strain measurements. Testing and demonstration were geared toward oil and gas pipeline and steel pressure vessel applications.

Measurement Range, Sensitivity, and Longevity

The measurement range of the sensor was not specified. Faria, et al. (2010) tested the sensors embedded in the steel liner-composite interface of a composite overwrapped pressure vessel over a pressure range of 0.5 to 4 MPa [5 to 40 bar]. Sensitivity and longevity are not specified. Hoop strain for thick-walled dry storage systems could be very small during normal dry storage conditions. Sensor sensitivity to pressure change inside the canister is unknown. Radiation degradation of fiber optic materials could limit sensor lifetime.

Space and Power Requirements

Space and power requirements for FBG optical sensors were evaluated in Section 2.5.1. They are typically fabricated in various diameters ranging from 75 to 250 μm [2.9 to 9.8 mils] and gauge lengths exceeding 100 m [328 ft]. Because of low weight and size, a few fiber optic sensors can be deployed to monitor a large area of the structure under evaluation. The sensor is hardwired to an external instrument for sensor interrogation and data collection. The PVDF piezoelectric sensors are expected to be similar.

Monitoring Area and Data Acquisition

The sensors monitor internal pressure. Both continuous and intermittent data acquisition modes are possible.

Temperature and Radiation Tolerance

Temperature and radiation tolerance were evaluated in Section 2.5.1.

Strengths and Weaknesses

Strengths include that the sensors provide in-service nondestructive monitoring of internal pressure without penetrating the confinement boundary. Sensor calibration to a specific DCSS design is expected to include demonstrations of the pressure and strain relationship. Other strengths and weaknesses are similar to those evaluated in Section 2.5.1.

Potential DCSS Use

For this DCSS application, sensors need to be physically embedded in composite and the composite needs to be overwrapped around the canister and remain in service for an extended period of time. As described in Section 2.5.1, sensor placement on an existing DCSS would require considerable planning and development.

Unknowns

- Feasibility for thick-walled casks and sensitivity for various canister designs.
- Combined effects of temperature and radiation on the calibration and longevity of the system.
- Availability of methods and specialized tools to install and maintain these sensors in high temperature and high radiation environments.

3.4.6 Container Material Deflection-Based Measurement

Measurement Principle

Eisenblätter (1995) demonstrated a pressure compensation method to measure internal gas pressure of sealed nuclear waste drums. The method involves measuring the deflection in container material due to an internal overpressure. External counter pressure exerted on the cover reverses this deformation; the internal pressure is derived from the counter pressure that is needed.

Maturity

This method has been tested in the laboratory. The measured compensation pressure exhibits a relatively good linear increase with the internal pressure.

Measurement Range, Sensitivity, and Longevity

The measurement range and longevity were not specified. Eisenblätter (1995) showed that an internal pressure of 0.12 or 0.16 MPa [1.2 or 1.6 bar] causes the measured compensation pressure to be increased by up to [0.25 bar]. For the small internal overpressures anticipated, measurable deflection in the canister wall is uncertain.

Space and Power Requirements

Displacement gauges were used in the measurement, and measurement needs to be done in close proximity to the canister surface. The power requirement was not specified in Eisenblätter (1995).

Monitoring Area and Data Acquisition

This technique only measures the internal pressure. The data measured each time are the internal pressure. Details of the data acquisition system were not available. Data acquisition mode is intermittent.

Temperature and Radiation Tolerance

Temperature and radiation tolerance was not specified.

Strengths and Weaknesses

The strength for this technique is that it is an external technique to measure internal pressure. Weaknesses are that the measurement is based on canister deflection, which may not be sensitive because of the thick wall of the canister. The measurement needs to be performed in close proximity to the canister surface.

Potential DCSS Use

This approach has been tested for waste drums and may have potential for long-term canister internal pressure monitoring. Further investigations are needed to establish a sufficient basis on its appropriateness for dry storage monitoring.

Unknowns

- Measurement sensitivity of thicker wall for canisters compared to nuclear waste drums.
- Availability of methods and specialized tools to install and maintain these sensors in the narrow canister and overpack gap under high temperature and high radiation environments.
- Size of mechanical monitoring system.

3.5 Cladding Confinement and Other Internal Components Degradation Monitoring

External monitoring methods for assessing the performance of internal components are evaluated in this section. The reviewed and assessed monitoring techniques are (i) external gamma-ray spectrometry measurement for Kr-85 concentrations in canister voids, (ii) external piezoelectric probes for speed of sound measurements across void space above the SNF basket, and (iii) gamma-ray radiography and computed tomography imaging. The main features of these techniques are summarized in Table 3-4, with additional details described in Sections 3.5.1, 3.5.2, and 3.5.3.

3.5.1 Gamma-Ray Spectrometry for Kr-85

Measurement Principle

Cladding is susceptible to progressive degradation and potential failure over long time periods during dry storage (NRC, 2014). Initial cladding breaches due to slow degradation processes are expected to be small and result in the release of pressurized gases from the fuel rod into the

Table 3-4. Cladding Confinement and Internal Components Degradation Monitoring Sensors			
Features	**Gamma-Ray Spectrometry for Kr-85 (Section 3.5.1)**	**Piezoelectric Probes for Speed of Sound Measurement (Section 3.5.2)**	**Radiography and computed Tomography Imaging (Section 3.5.3)**
Maturity	Feasibility assessed	Proposed idea only	Field deployed in industry and medical field using gamma rays Cosmic-ray muon imaging demonstrated for high atomic number material, nuclear fuel
Measurement Ranges	From ~1 TBq* to >1,000 TBq of Kr-85	Not specified	Not specified
Sensitivity	About 1 TBq* of Kr-85	Not specified	Not specified
Longevity	Not applicable for portable equipment	Not specified	Not an issue for intermittent measurements
Space Requirements	Line of sight needed to ~40-cm^2 [6.2-in^2] area on canister surface for alignment with briefcase-sized detector and collimation shielding	Less than13 cm $\times$ 8 cm $\times$ 5 cm [5 in $\times$ 3 in $\times$ 2 in]	Large
Power Requirements	Internal instrument battery or external power, less than 400 watts for electrically powered mechanical cooling	Not specified	Large
Monitoring Area	~10–40 cm^2 [1.6–6.2 in^2] view of internal canister void volumes	Free space between canister SNF basket and inner lid	Potential to image majority of the canister interior
Data Acquisition Mode	Intermittent	Not specified	Intermittent, requiring long measurement times
Temperature Tolerance	Temperature-induced detector drift for external measurements is manageable during the anticipated intermittent data acquisition mode	Not specified, likely high	Temperature-induced detector drift for external measurements is manageable during the anticipated intermittent data acquisition mode
Radiation Tolerance	Detector collimation required to shield gamma rays from SNF	Not specified, likely high	High radiation emission rates from SNF complicate transmission measurements of radiation from external sources
Strengths	Applicable to aged systems currently in service, good sensitivity	Small size and nondestructive examination of internal components from outside of the SNF confinement boundary	Nondestructive examination of internal components from outside of the SNF confinement boundary. Cosmic-ray muons are well suited for imaging spent nuclear fuel and can penetrate DCSS gamma-ray shielding.
Weaknesses	Line of sight needed to canister surface, not amendable to continuous monitoring. Over time, radioactive decay increases the effective number of rod inventories of Kr-85 corresponding to the minimum detectable activity of Kr-85. Reduction in the scattered background over time due to reductions in gamma-ray emission rates from SNF was not assessed. Requires retrofit to DCSS.	Limited to canisters with free space. A significant fractional release of the total noble gas inventory may be needed for detection.	Significant modification to gamma-ray energies and emission intensities would be required to yield suitable transmission signals. Detector interference from SNF radiation emissions.
* An activity of about 1 TBq corresponds to the total Kr-85 inventory in 5 rods of typical PWR SNF with a cooling time of 25 years.			

void spaces of the canister. For pinholes and hairline cracks in fuel rod cladding, fine particulates that may be entrained by flowing gas within the rod could be prevented from escaping through such small openings. Under these conditions, gaseous species released from degraded rods are distributed within the canister void volume. Particulate releases may accompany the gaseous releases. While this section focuses on a method for the detection of Kr-85, a radioactive noble gas, detection of SNF particulates also would be possible by the same method, but this has not been assessed in detail.

Detection of radioactive gases (e.g., noble gases) in the void volume would signify that cladding degradation and releases into the canister have occurred. For example, Kr-85 can provide an early indication of new releases from cladding breaches (NWTRB, 2010, p. 86). Kr-85 is a noble gas and a radioactive fission product in SNF with a radioactive half-life of approximately 11 years. Radioactive decay of Kr-85 results in a 514-keV gamma-ray emission with a yield of 0.4 percent. In general, the concentration of radioactive material in canister voids relates to the current confinement provided by cladding within the canister. Incremental releases and concentration increases of radioactive gases over time would indicate an increase in the number of fuel rods with degraded cladding.

In addition to Kr-85 detection, a gamma-ray spectrometer also would allow external measurement of SNF particulates. Detection of SNF particulates is more straightforward than Kr-85 detection due to the larger activity associated with SNF particulates and the wide variety of emitted gamma rays. Gamma-ray spectrometry can differentiate among activated corrosion products, fission product gases, SNF particulates, and residual water in canister void volumes.

In other words, gamma-ray spectrometry can more easily detect large cladding breaches through which SNF particulates have been released to the canister volume compared to Kr-85 detection within the canister.

Matsumura, et al. (2008) used precise collimation to ensure that only the Kr-85 concentration in the canister gas is measured, not the fission gas contained within the fuel cladding (which also implies that fission gases released from the fuel pellet into the rod plenum are not measured). Figure 3-5 shows the layout of gamma-ray spectrometry measurements for Kr-85 in canister voids (Matsumura, et al., 2008). As Figure 3-5 shows, an alternative measurement alignment may not require a DCSS retrofit but could still provide access to the canister surface. Perpendicular to the original measurement alignment, the alternative measurement alignment is further discussed in the section on strengths and weaknesses.

Maturity

Matsumura, et al. (2008) performed computations and a small-scale mock-up experiment in a feasibility study. A refinement to the Matsumura, et al. (2008) approach was investigated, as described in the section on measurement range, sensitivity, and longevity. For the alternative measurement alignment described as the refinement, scoping simulations were performed for Kr-85 gamma-ray emissions in canister voids and scattered gamma rays from SNF. No experiments have been conducted for the alternative measurement alignment. Field testing of the technique has not been performed.

Measurement Range, Sensitivity, and Longevity

For the measurement configuration proposed, Matsumura, et al. (2008) determined that the approach is sensitive enough to detect a cumulative Kr-85 release to the canister of 10^{11} Bq,

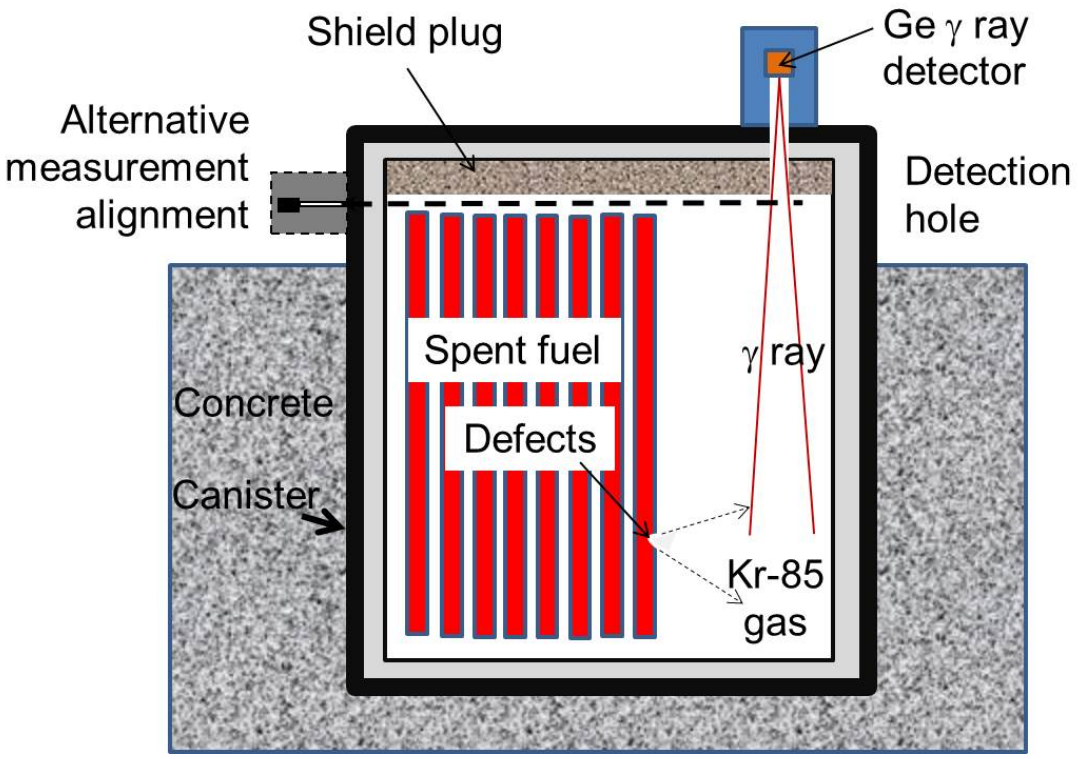

Figure 3-5. Gamma-Ray Spectrometry Measurements for Kr-85 in Canister Voids. Dimensions Are Not to Scale. The Original Measurement Alignment (Matsumura, et al., 2008) Creates a Vertical Detector Field of View. Dashed Lines Indicate an Alternative Measurement Alignment for the Void Space Above Spent Nuclear Fuel and Below the Canister Shield Plug. The Dashed Arrow Depicts an Example Gamma-Ray Path to the Detector, Shown With Access to the Canister Surface.

which is approximately 10 percent of the total Kr-85 inventory in a single fuel rod. In general, it is expected that a breached rod will release 2–7 percent of its Kr-85 inventory. The Matsumura, et al. (2008) measurement configuration was based on a measurement along the axis of the canister and included drilling a detection hole in the shield plug as a retrofit to the shield design. The sensitivity presented in Table 3-3 relates to a refinement for an alternative measurement alignment that does not require a retrofit to the shield plug. The measurement range is expected to be 1 TBq of Kr-85 (equivalent to approximately 5 total rod inventories of Kr-85 for PWR SNF with a cooling time of 25 years) to more than 1,000 TBq of Kr-85. Considering both approaches, the sensitivity is estimated to range from as low as a few breached rods up to about a hundred breached rods at early times following emplacement.

In the refinement to the Matsumura, et al. (2008) approach, radiation transport computations were performed to assess the signal-to-noise ratio for measurements of Kr-85 in the distributed background of scattered gamma rays from SNF using an alternative collimation and detector alignment. Canister dimensions were modeled after the NUHOMS 24P configuration. SNF was modeled as 24 homogenized cylindrical volumes within the canister. The fraction of gamma rays that was transported outside of the canister along a single collimated path with a radius of 1.5 cm [0.59 in] to a detector surface was calculated. The collimated path was aligned with the center of the 3.4-cm [1.3-in] void between the end fittings at the top of the assemblies and the lead shield plug. The alternative collimation and detector alignment differs from the

Matsumura, et al. (2008) measurement configuration; both are shown in Figure 3-5. The number of "signal" gamma rays at 514 keV from Kr-85 emissions was compared to the number of "noise" gamma rays anticipated at this energy from scattered SNF emissions. Based on these initial computations, the suggested alternative measurement alignment appears to be a suitable candidate for external measurements on aged systems currently in service.

In a scoping calculation, gamma-ray emissions from Kr-85 were simulated in the upper void region (near the radial collimation opening), representing a volumetric disc that is 1.2 percent of the free volume in the canister, to determine whether the 514-keV gamma-ray signal from Kr-85 could be detected amongst the "background" of scattered gamma rays from SNF. A canister configuration with 24 assembly positions of SNF from a pressurized water reactor was modeled with a circumferential (or "radial") collimation opening. For 5×10^{12} Bq Kr-85 released into the canister volume, a peak at 514 keV associated with Kr-85 was clearly visible in the scoping calculation, and the Kr-85 contribution exceeds the 2-standard-deviation statistical uncertainty in background counts. The detectable activity of Kr-85 gas in the canister is expected to be lower than 5 TBq, due to a better signal-to-noise ratio that may be achievable with more restrictive collimation (such as pinhole collimation instead of radial collimation) at the penalty of longer measurement times. In summary, the lower end of the detectable range was assigned to 1 TBq of Kr-85 gas in the canister [equivalent to a total Kr-85 inventory in 5 rods of pressurized water reactor (PWR) SNF with a cooling time of 25 years]. Although less verify if this is correct, than one total rod inventory of Kr-85 released into the canister may be detectable, as reported by Matsumura, et al. (2008) on related measurements, further simulations and calculations with the refined geometries would be required to yield a higher fidelity determination of the detection sensitivity.

For its described use as an inspection technique, longevity is not an issue because measurements can be repeated as long as access to the surface of the canister is provided for equipment setup. Longevity is considered to be very long for this external measurement approach because detection equipment can be maintained over long time periods, replaced as needed, and deployed for dry storage measurements at recommended intervals. Battery power is sufficient for single shift operation before swap out and recharging.

Space and Power Requirements

Collimated gamma-ray spectrometry measurements outside the SNF container have been proposed to assess the Kr-85 concentration in the canister (Matsumura, et al., 2008). Assuming reasonable access is provided to the outer surfaces of the canister, shielding or collimation for the gamma-ray spectrometer improves detection by focusing the detector field of view on the narrow void space between SNF assemblies, canister walls, and shield plugs, where no SNF is present, and reducing direct and scattered gamma-ray contributions from radionuclides contained within SNF cladding.

High purity germanium detectors typically have sufficient energy resolution to detect and differentiate 514-keV gamma rays from 511-keV annihilation photons arising from electron-positron pairs produced by the interactions of higher energy gamma rays (Knoll, 1989, Figure 12-9, p. 401). Portable systems with sufficient energy resolution and typical detection efficiency are shoebox to briefcase size. Smaller systems have lower detection efficiency and require longer counting times. Battery or external power operations are possible. For high-resolution gamma-ray spectrometry systems, cryogenic cooling is accomplished either with liquid nitrogen or electrically powered mechanical cooling, which requires less than 400 watts of power.

A collimated detector is aligned with a canister void (purposely avoiding SNF pellets, rods, and assemblies in the field of view). A free line of sight is needed to an area of 40 cm^2 [6.2 in^2] on the canister top or bottom aligned with internal void space. New geometric calibration is required for each dry storage design. Collimators are heavy and require rigging or support for proper alignment.

Monitoring Area and Data Acquisition

The monitoring area is a 10–40 cm^2 [1.6–6.2 in^2] cross-sectional view of a gas-filled space inside the canister between SNF assemblies, canister walls, and shield plugs. The volume of gas present in the detector field of view depends on the orientation of gamma-ray collimation and physical dimensions of void regions in the canister. The measurement yields energy-dependent gamma-ray counts over time. Data analysis is straightforward with geometric calibration. Measurement and assessment time were estimated to be 1 day per dry storage canister (Matsumura, et al., 2008). The data acquisition mode is intermittent.

Temperature and Radiation Tolerance

Temperatures encountered for this external measurement technique are expected to be manageable. Detector drift is more likely during longer measurement durations (several hours) in higher ambient temperatures, but excessive spectral resolution degradation is not expected for the measurement duration envisioned. With access to the canister surface by way of a port within the concrete overpack or bunker, operators are expected to be exposed to elevated dose rates for short durations during measurement setup and tear down. Because collimation is required to shield the detector from gamma rays originating from SNF, radiation shielding is integral to the assessment of this radiation detection measurement technique.

Strengths and Weaknesses

A key strength is that the original and refined techniques do not require physical penetration of sealed canisters and provide potentially acceptable sensitivity for detecting the loss of cladding confinement.

Aligning the collimated measurement with the region of the canister between the top of the SNF assemblies and the shielding plug at the end of the canister is advantageous because the alternative measurement alignment does not require shielding plug drilling or retrofitting. Additionally, the alternative measurement alignment allows measurements to be performed with multiple detectors, which could increase the detection efficiency and reduce the measurement time needed for each canister. A scoping assessment determined 1 TBq of Kr-85 gas in the canister (or approximately 5 total rod inventories of PWR SNF with a cooling time of 25 years) could be detected using an alternative measurement alignment across the void between the top of the fuel assemblies and below the shield plug, which does not require canister design changes or retrofitting. Unlike the original approach that uses a single detector aligned with a retrofitted hole bored in the lead shield plug, the alternative measurement alignment enables simultaneous measurements by multiple gamma-ray detectors (i.e., in a radial fan beam orientation at the top of canister) to increase the detection field of view and reduce measurement times.

One weakness is that measurements require a direct line of sight to the canister surface, because the concrete overpack diminishes detection signals from Kr-85 gamma rays to unusable levels. To provide this access for the rather large detection equipment and heavy

collimation, the canister could be pulled out of the concrete overpack during the measurement (~1 to 4 hours). Access only is needed to the top of canister; full removal of the canister is not required. Alternatively, the line of sight to the canister surface could be accomplished by drilling a hole in the concrete overpack, which requires repair of the overpack following the measurement. These measurement configurations are not amenable to continuous monitoring.

Another weakness is that a reduced sensitivity over time is expected due to Kr-85 decay with a half-life of 11 years. Further assessments may consider how reductions in SNF gamma-ray emissions over time will lower scattered radiation contributions at the gamma-ray detector and change the minimum detectable activity of Kr-85 gas in the canister.

The assessment considered a uniform distribution of krypton within the canister volume. Because krypton is heavier than helium, a nonuniform distribution of krypton concentration may result within the canister if gas circulation in the canister is insufficient to provide well-mixed conditions. Depending on the canister orientation, nonuniform distributions of krypton in the canister may influence the selection of external measurement locations and determination of detection sensitivity. These secondary effects were not investigated in this project but are highlighted for future consideration.

Potential DCSS Use

External measurement of Kr-85 gamma rays in canister gas appears to be a viable technique for indicating the degree to which cladding is providing its confinement function. Features of this technique are summarized in Table 3-4 for as-needed inspection measurements. The assessment in this section considered both prior and new measurement alignments. During storage, an inspection frequency of no more than one measurement per canister per year seems sufficient. To verify cladding confinement within intact canisters, measurements could be performed following packaging, repacking, transporting, or off-normal events during storage.

Unknowns

- Line-of-sight access to the canister surface to enable measurements.
- Extent of gas circulation and mixing within the sealed canister.

3.5.2 Piezoelectric Probes for Speed of Sound Measurement

Measurement Principle

Argonne National Laboratory (ANL, 2012) proposed the potential use of external piezoelectric probes for speed of sound measurements across void space above an SNF basket. The ultrasound piezoelectric probes are positioned on opposite sides of a canister at a location where there is void space. The sound travels from one side to the other side. The speed of sound is different for different gases. Released fission gas from fuel rods changes the composition of the gas in the void space. As a result, the speed of sound changes.

Maturity

Although proposed by ANL (2012), use of external piezoelectric probes has not been put into practice for this application. The method may warrant further evaluation.

Measurement Range, Sensitivity, and Longevity

Measurement range was not specified. Instrument sensitivity was not documented. Ten rods releasing 20 percent of their xenon and krypton inventories into the canister would represent molar fractions in helium fill gas of <0.0002 for xenon and <0.00002 for krypton. A significant fractional release of the total noble gas inventory seems to be required for detection.

Space and Power Requirements

The early hand-held prototype speed of sound detectors are 13-cm [5-in] long, 8-cm [3-in] wide, and 5-cm [2-in] thick. Smaller versions can be developed. Power requirements are not issues, because this is an external technique.

Monitoring Area and Data Acquisition

The monitoring area is limited to the location where there is free space between the SNF basket and the inner lid. The data acquisition mode was not specified.

Temperature and Radiation Tolerance

Piezoelectric devices are likely to be tolerant to temperature and high levels of radiation.

Strengths and Weaknesses

Strengths include small size and nondestructive examination of internal components from outside of the SNF confinement boundary. Weaknesses include that piezoelectric probes only can be used in canister free space, which may exist in only certain DCSSs. A significant fractional release of the total noble gas inventory may be required for detection.

Potential DCSS Use

Much more additional information is necessary to evaluate whether this technique may be applicable for cladding confinement and SNF degradation monitoring, including measurement range and sensitivity.

Unknowns

- Device specifications, including measurement range; sensitivity, including the noble gas quantities released from SNF needed for detection given dependencies of the speed of sound on temperature and its variation due to gas circulation inside the canister; longevity; and data acquisition measurements

- Long-term stability in elevated temperature and high radiation environments

3.5.3 Radiography and Computed Tomography Imaging of Internal Components

Measurement Principle

Radiography and computed tomography are imaging techniques that use penetrating radiation to view the internal structure of a material. Discussion of the measurement principle for gamma

rays is brief because these imaging techniques is a well-developed technology for application in industry and the medical field. Features of this category of monitoring techniques are summarized in Table 3-3. Cosmic-ray muon imaging also is identified.

Maturity

Gamma-ray radiography has been applied to piping degradation (Kajiwara, 2005; Edalati, et al., 2006), weld flaw detection (Cho, et al., 2011; Kasban, et al., 2011), and pressure vessel inspections (HEDRad—High Energy Digital Radiography System, Computerized Information Technology Limited, 2013). Current system designs are not suitable for SNF dry storage applications due to the large physical dimensions, very large density thicknesses, and strong gamma-ray emission rates from the object to be imaged. Typical radiography detectors do not provide energy discrimination of gamma rays, an essential requirement when imaging strong gamma-ray emitters. Medical computed tomography is well developed but is inappropriate for imaging SNF containers due to the low gamma-ray energies and source intensities used. Because radiation detectors, source energies, and intensities of industrial gamma-ray tomography (IAEA, 2008) make tailoring to SNF applications more feasible, industrial gamma-ray tomography technologies were assessed further.

Due to the very large density thickness of SNF assemblies and large physical dimensions of stainless steel canisters, high gamma-ray energies and emission intensities would be required to yield suitable transmission signals for computed tomography. A simple assessment was performed assuming a gamma-ray source energy of 10 MeV to account for Bremsstrahlung x-ray sources (common monoenergetic sources tend to have lower maximum energies of 1–2 MeV) and a very high dose rate of 1 Mrad h^{-1} to determine whether adequate transmission could be achieved for a loaded SNF canister.

Despite the strong source intensity and hypothetical 10-MeV energy for deriving attenuation properties, denser regions of the canister and SNF assemblies cannot be sufficiently penetrated to yield usable transmission signals. For each equivalent of 15 rod diameters traversed, the transmission signal is attenuated by a factor of more than 1,200. Although sufficient transmission signals (thousands to millions of gamma-ray arrivals at the detector) could be expected along transmission paths within a canister through the equivalent of 15 up to 30 rod density thicknesses, the transmission signal becomes too weak beyond 30 rod diameters (dense path across two fuel assemblies). Usable transmission signals may be reduced to only those paths through much fewer than 30 rod diameters because the elevated background of SNF emissions reduces the signal-to-noise ratio of transmission measurements. For a 24 pressurized water reactor configuration with 6 assemblies side by side along the canister diameter, the thickest transmission path is ~90 rod diameters, which equates to a density thickness that far exceeds the penetrating power of the intense source strength and hypothetical high gamma-ray energy assumed for this assessment. Because classical computed tomography requires usable transmission signals through all paths of an object, opaque transmission paths without usable transmission signals are expected to severely degrade the resulting image and may prevent the reconstruction algorithm from converging on a solution (especially for the large number of opaque paths anticipated in the SNF canister case). Therefore, computed tomography using gamma rays also was concluded to not be a viable method for monitoring of the cask internals.

Cosmic-ray muon imaging appears to be more promising, however, due to much longer mean free path lengths through materials compared to gamma rays. Although a detailed assessment of this technique was not conducted in this project, several researchers have reported on the

cosmic-ray muon technique (Gilboy, et al., 2007; Schlutz, et al., 2004; Borozdin, et al., 2003) and assessed its feasibility for imaging nuclear fuel (Morris, et al., 2014; Miyadera, et al., 2013). Commercial systems for cosmic-ray muon imaging are currently unavailable.

Measurement Range, Sensitivity, and Longevity

Because a commercially available system is not available and critical issues were identified in the assessment described in the preceding section, measurement range and sensitivity have not been specified and were not assessed further. For its described use as an inspection technique, longevity is not an issue because measurements can be repeated as long as access to the surface of the canister is provided for equipment setup. Longevity is considered to be very long for this external measurement approach because detection equipment can be maintained over long time periods, replaced as needed, and deployed for dry storage measurements at recommended intervals.

Space and Power Requirements

The technology needs strong radiation to image internal components. Space and power requirements are expected to be large.

Monitoring Area and Data Acquisition

The technology images an internal structure along its radiation path. Data acquisition mode is intermittent. Images are generated from multiple detector measurement positions surrounding the object.

Temperature and Radiation Tolerance

The technique is an external imaging technique. The temperature-induced detector drift for external measurements is manageable during the anticipated intermittent data acquisition mode. Radiation tolerance is less of an issue for intermittent measurements. However, high radiation emission rates from SNF complicate transmission measurements of radiation from external sources.

Strengths and Weaknesses

The technique is an external technique to image internal components through the thick-walled canister without penetrating the wall. Critical issues on the source emission rate and individual gamma-ray transmission probabilities through SNF (for yielding acceptable signal-to-noise ratios amid the high ambient levels of gamma-ray radiation from SNF) need to be overcome for this technique to be considered a viable approach. For cosmic-ray muon imaging, detector interference would be expected from gamma rays emitted from SNF and should be factored into any further viability assessments.

Potential DCSS Use

Due to the very large density thickness of SNF assemblies and large physical dimensions of stainless steel canisters, high gamma-ray energies and emission intensities would be required to yield suitable transmission signals for computed tomography. Significant modifications for stronger external sources and increased gamma-ray transmission energies will be needed for

DCSS use. Cosmic-ray muon imaging is still in the research phase, but nuclear fuel imaging demonstrations have been performed.

Unknowns

- Future technology advancements to overcome critical issues anticipated in the SNF canister case, such as the large number of opaque paths (through the very high density thickness of SNF in multiple assemblies), usable transmission signals through those paths, resulting image degradation, and reconstruction algorithm convergence.
- Space and power requirements.
- Measurement range and sensitivity.
- Timeframe for commercialization of a cosmic-ray muon imaging system or experimental DCSS demonstrations using cosmic-ray muon imaging.

4 SUMMARY

U.S. Nuclear Regulatory Commission (NRC)-licensed dry cask storage systems (DCSSs), in addition to pools, are presently used for storage of spent nuclear fuel (SNF). NRC initially licensed DCSSs in the mid-1980s. These systems were intended to provide additional SNF storage capacity and allow operating plants to maintain full core offload capacity in the spent fuel pools. Initially, these independent spent fuel storage installations (ISFSI) with DCSSs were licensed for periods up to 20 years. When initially licensed, ISFSIs were an effective short-term solution until a nuclear waste repository was operational. The absence of a repository for the disposal of the SNF has led to additional licensed ISFSI locations, and operating ISFSIs have applied for and received license renewals for up to an additional 40 years. With the lack of a permanent disposal option for SNF, the already licensed ISFSI sites may be required beyond 60 years.

Aging and environmentally induced degradation must be considered for the extended storage of SNF in DCSSs. These phenomena are commonly encountered in many industrial applications, including operating nuclear power plants. Preventing unexpected failure in these systems has been accomplished by the use of engineering codes and standards for design, construction and operation, mandated inspections, and monitoring of key parameters. When originally licensed, the DCSSs were designed to be passive systems. Inspection and monitoring were limited to visual examination of accessible structures, systems, and components (SSCs) to validate licensing conditions and were not intended to determine whether conditions existed where degradation processes may be initiated or detect the onset of environmentally induced degradation.

The objective of this review was to identify and evaluate currently available technologies that may be adapted and utilized to monitor environmental conditions and degradation mechanisms relevant to a DCSS. Monitoring methods were reviewed for external environmental conditions, including temperature, relative humidity, chloride deposition, and microbial activity, because these parameters are known to control the onset and rate of degradation processes. Direct methods for monitoring degradation processes were examined, including atmospheric stress corrosion cracking (SCC) of welded stainless steel canisters, concrete degradation, corrosion, and mechanical degradation of cask bolts. Reviews also included monitoring methods for internal temperature, relative humidity, pressure, and degradation of cask internals. Key findings of this review follow:

- Temperature and relative humidity measurements are routinely performed in nuclear applications. Technology to measure these parameters is well developed and has been adapted to both nuclear and other specialized applications. The most promising methods to measure temperature include thermocouples and resistance temperature detectors. Relative humidity measurements used in leak detection systems in operating nuclear power plants have been specifically designed for continuous monitoring in aggressive environments that exist near the reactor pressure vessel head of an operating pressurized water reactor.

- No method was identified for monitoring atmospheric deposition of solid chloride salts. Presently available methods used in non-nuclear applications rely on manual collection and analysis of the dissolved samples to determine the presence and amount of chloride contamination. Significant additional development is necessary to adapt an existing method of chloride analysis for DCSS monitoring.

- Detection of microbial activity using online monitoring has been developed for liquid handling systems. It is unclear whether these sensors could be adapted for use in DCSSs. Sampling techniques for microbial activity also are available but rely on manual collection of a sample and require long incubation times to obtain a result.

- SCC sensors are available but have limited field experience. Surrogate sensors deployed as an instrumented SCC coupon have been developed for condition monitoring in field applications. It is unclear whether such sensors could be used for DCSS monitoring.

- Concrete degradation monitoring methods are well developed and have sufficient sensitivity to detect degradation before physical deterioration begins. The main limitation for some of the available methods is the relatively shallow interrogation depths. Embeddable sensors would require significant effort to install in existing DCSSs. Embedding sensors in concrete overpack could have detrimental effects on the system and will require evaluation.

- Methods are available to monitor cask bolts degradation including general and localized corrosion, stress corrosion cracking, and mechanical degradation. Ultrasonic testing has been field deployed for nuclear applications. Most other sensors have been deployed for non-nuclear applications. The main limitation for some methods is the deployment difficulty. Modification of DCSS is needed and its effect on the system will require evaluation.

- Monitoring of canister or cask internal environmental conditions and degradation of internal components would likely be limited to new DCSSs, given the difficulty and operational challenges of retrofitting an existing canister or cask. Methods to conduct monitoring also are limited and pose significant challenges. Internal pressure monitoring may be used to monitor the presence of residual water, hydrogen, and oxygen inside the canister. External gamma-ray spectrometry for Kr-85 monitoring in canister voids for cladding confinement integrity monitoring do not require physical penetration of sealed canisters and provide a direct measure of internal cask pressure without the need for a pressure boundary penetration. Significant analyses and tests would be necessary to qualify these methods. In addition, adverse effects, such as material incompatibility, would need to be rigorously evaluated.

Finally, it is recognized that specialized sensors and monitoring systems may need to be developed and modifications of existing DCSS designs may be required to retrofit monitoring systems. While not addressed in this review, a number of technical issues must be evaluated prior to considering any sensor or monitoring system for DCSS application, including sensor size and the dimensions of the DCSS, the effects of placement and confinement boundary penetration on the required functions of the DCSS SSCs, material compatibility, and monitoring system maintenance.

5 REFERENCES

American Association of State Highway and Transportation Officials (AASHTO). "Standard Method of Test for Surface Resistivity Indication of Concrete's Ability to Resist Chloride Ion Penetration." AASHTO TP095-11-UL. Washington, DC: American Association of State Highway and Transportation Officials. 2011.

ASNT. *Nondestructive Testing Handbook*. 3rd Edition. Columbus, Ohio: American Society for Nondestructive Testing. 2005.

Anderko, A., N. Sridhar, L. Yang, S.L. Grise, B.J. Saldanha, and M.H. Dorsey. "Validation of a Localized Corrosion Model Using Real-Time Corrosion Monitoring in a Chemical Plant." *Corrosion Engineering, Science and Technology*. Vol. 40. pp. 33–42. 2005.

Anderko,, A., N. Sridhar, C.S. Brossia, D.S. Dunn, L.T. Yang, B.J. Saldanha, S.L. Grise, and M.H. Dorsey. "An Electrochemical Approach to Predicting and Monitoring Localized Corrosion in Chemical Process Streams." CORROSION/2003, Paper No. 03375. Houston, Texas: NACE International. 2003.

ANL. "Extended *In-Situ* and Real Time Monitoring for Long-Term Dry Cask Storage of Spent Nuclear Fuel." ANL/NE–12/18. Argonne, Illinois: Argonne National Laboratory. 2012.

Archer, D. "Comparing Preparation and Calibration Techniques for Ultrasonic Bolt Tension Measurement–Part 1." *Fastener Technology International*. pp. 56–57. 2007.

AREVA NP GmbH. "FLÜS For Rapid Detection and Localization of Steam and Water Leaks System." FLÜS Brochure, Erlangen, Germany: AREVA NP GmbH. 2009.

ASTM International. "Standard Specification for Type K and Type N Mineral-Insulated, Metal-Sheathed Thermocouples for Nuclear or for Other High-Reliability Applications." Designation E235. West Conshohocken, Pennsylvania: ASTM International. 2012a.

_____. "Standard Specification and Temperature-Electromotive Force (emf) Tables for Standardized Thermocouples." Designation E230. West Conshohocken, Pennsylvania: ASTM International. 2012b.

_____. "Standard Specification for Industrial Platinum Resistance Thermometers." Designation E1137. West Conshohocken, Pennsylvania: ASTM International. 2012c.

_____. "Standard Test Method for Bulk Electrical Conductivity of Hardened Concrete." ASTM C1760–12. West Conshohocken, Pennsylvania: ASTM International. 2012d.

_____. "Standard Test Method for Electrical Indication of Concrete's Ability to Resist Chloride Ion Penetration." ASTM C1202-12. West Conshohocken, Pennsylvania: ASTM International. 2012e.

_____. "Standard Test Method for Pulse Velocity Through Concrete West Conshohocken." ASTM C597-09. West Conshohocken, Pennsylvania: ASTM International. 2009.

_____. "Standard Test Method for Determining Atmospheric Chloride Deposition Rate by Wet Candle Method." ASTM G140–02. West Conshohocken, Pennsylvania: ASTM International. 2008.

_____. "Standard Terminology for Nondestructive Testing." ASTM E1316–05. West Conshohocken, Pennsylvania: ASTM International. 2005a.

_____. "Standard Guide for Mounting Piezoelectric Acoustic Emission Sensors." ASTM E650/E650M–12. West Conshohocken, Pennsylvania: ASTM International. 2005b.

_____. "Guide for Acoustic Emission System Performance Verification." ASTM E 2374–14. West Conshohocken, Pennsylvania: ASTM International. 2004.

_____. "Standard Method for Primary Calibration of Acoustic Emission Sensors." ASTM E1106-86. West Conshohocken, Pennsylvania: ASTM International. 2002.

Bakhtiari, S., K. Wang, T.W. Elmer, E. Koehl, and A.C. Raptis. "Development of a Novel Ultrasonic Temperature Probe for Long-Term Monitoring of Dry Cask Storage Systems." 39th Annual Review of Progress in Quantitative Nondestructive Evaluation, AIP Conference Proceeding. Vol. 1,511. pp. 1,526–1533. 2013.

Bennett, J.E. and T.A. Mitchell. "Reference Electrodes for Use With Reinforced Concrete Structures." *CORROSION/92.* Paper No. 191. Houston, Texas: NACE International. 1992.

Berruti, G., M. Consales, M. Giordano, L. Sansone, P. Petagna, S. Buontempo, G. Greglio, and A. Cusano. "Radiation Hard Humidity Sensors for High Energy Physics Applications Using Polyimide-Coates Fiber Bragg Gratings Sensors." *Sensors and Actuators B: Chemical*. Vol. 177. pp. 94–102. 2013.

Berruti, G., M. Consales, A. Cutolo, A. Cusano, G. Breglio, S. Buontempo, P. Petagna, and M Giordano. "Radiation Hard Humidity Sensors for High Energy Physics Applications Using Polymide-Coated Fiber Bragg Gratings Sensors." Proceedings of IEEE Sensors 2011 Conference in Limerick, Ireland. pp. 1,484–1,487. Institute of Electrical and Electronics Engineers. October 28–31, 2011.

Bertocci. U. and F. Huet. "Noise Resistance Applied to Corrosion Measurements III. Influence of the Instrumental Noise on the Measurements." *Journal of the Electrochemical Society*. Vol. 144. pp. 2,786–2,793. 1997.

Bhalla, S., A.S.K. Naidu, and C.K. Soh. "Influence of Structure–Actuator Interactions and Temperature on Piezoelectric Mechatronic Signatures for NDE." Proceedings of ISSS-SPIE 2002 International Conference on Smart Materials Structures and Systems. Bangalore, India: ISSS-SPIE. 2002a.

Bhalla, S., A.S.K Naidu, C.W. Ong, and C.K. Soh. "Practical Issues in the Implementation of Electromechanical Impedance Technique for NDE." Proceedings of the SPIE International Symposium on Smart Materials. Nano-, and Micro-Smart Systems. Melbourne, Australia: SPIE. 2002b.

Borozdin, K.N., G.E. Hogan, C. Morris, W.C. Priedhorsky, A. Saunders, L.J. Schultz, M.E. Teasdale. "Radiographic Imaging with Cosmic-ray Muons." *Nature*. Vol. 422. p. 277. 2003.

Brenner, R., N. Bingefors, and B. Mohn. "Evaluation of a Humidity Sensor for Use in an Environment Exposed to Radiation." *Journal of Testing and Evaluation.* Vol. 35, No. 5. pp. 469–476. 2007.

British Standard Institute. "Testing Concrete. Determination of Ultrasonic Pulse Velocity." BS EN12504-4. British Standard Institute. London. 2004.

_____. "Testing Concrete, Recommendations for Measurement of Velocity of Ultrasonic Pulses in Concrete." BS1881-203. British Standard Institute. London. 1986.

Britton Jr., C.L., M. Roberts, N.D. Bull, D.E. Holcomb and R.T. Wood. "Johnson Noise Thermometry for Advanced Small Modular Reactors." ORNL/TM-2012/346, SMR/ICHMI/ORNL/TR-2012/01. Oak Ridge, Tennessee: Oak Ridge National Laboratory. 2012.

Broomfield, J.P. *Corrosion of Steel in Concrete*. Uhlig's Corrosion Handbook, 2nd Edition, R. Winston editor. New York City, New York: John Wiley and Sons, Inc. pp. 581−599. 2000.

Brossia, C.S. "Electrical Resistance Techniques." *Techniques in Corrosion Monitoring*. Cambridge, United Kingdom: Woodhead Publishing. pp. 277–292. 2008.

Brown, N.K. and F.J. Friedersdorf. "*In-Situ* Sensors and Methods for Monitoring Environment Assisted Cracking of Structural Components." U.S. Patent Application Number 20110100131. Washington, DC: U.S. Patent Office. 2011.

Burley, T.B. "The Measurement of Internal Pressure Buildup in Full Sized Fuel Rods During Irradiation." Lewis Research Center National Symposium on Development in Irradiation Testing Technology. Houston, Texas: National Aeronautics and Space Administration (NASA). pp. 296–306. 1969.

Burns, G.W. and M.G Scroger. "The Calibration of Thermocouples and Thermocouple Materials." NIST Special Publication 250-35. Gaithersburg, Maryland: National Institute of Standards and Technology. 1989.

Caproco. "Microbially-Influenced Corrosion (MIC) Analyzer." Edmonton, Alberta, Canada: Caproco. <www.caproco.com> (19 March 2013).

Carnevale, E.H., S. Wolnik, G. Larson, and C. Carey. "Simultaneous Ultrasonic and Line Reversal Temperature Determination in a Shock Tube." *Physics of Fluids*. Vol. 2, No. 7. pp. 1,459–1,467. 1967.

Carstens, T., M. Corradani, J. Blanchard, and Z. Ma. "Gamma Radiation Influence on Thermoelectric Powered Wireless Sensors for Dry-Cask Storage." *Electrical and Power Engineering Frontier*. Vol. 2, No. 2. pp. 30–36. 2013.

Chaudhry, Z., F. Lalande, A. Ganino, and C. Rogers. "Monitoring the Integrity of Composite Patch Structural Repair via Piezoelectric Actuators/Sensors." AIAA-1996-1074-CP. Reston, Virginia: American Institute of Aeronautics and Astronautics. 1996.

Chaudhry, Z., T. Joseph, F.P. Sun, and C.A. Rogers. "Local-Area Health Monitoring of Aircraft Via Piezoelectric Actuator/Sensor Patches." SPIE 1995. San Diego, California: North American Conference on Smart Structures and Materials. 1995.

Chen, Z. and C. Lu. "Humidity Sensors: A Review of Materials and Mechanisms." *Sensor Letters.* Vol. 3. pp. 274–295. 2005.

Cheng, J., J.-C. Chou, T.-P. Sun, S.-K. Hsiung, and H.-L. Kao. "Study on All-Solid-State Chloride Sensor Based on Tin Oxide/Indium Tin Oxide Glass." *Japan Journal of Applied Physics*. Vol. 50. pp. 037001-1–037001-8. 2011.

Cheymol, G., H. Long, J.F. Villard, and B. Brichard. "High Level Gamma and Neutron Irradiation of Silica Optical Fibers in CEA OSIRIS Nuclear Reactor." *IEEE Transactions on Nuclear Science*. Vol. 55, No. 4. pp. 2,252–2,258. 2008.

Chiang, K.T. and L. Yang. "High-Temperature Electrochemical Sensor for Online Corrosion Monitoring." *Corrosion.* Vol. 66, No. 9. pp. 095002-1–095002-8. 2010.

Chiang, K.T., L. Yang, R. Wei, and K. Coulter. "Development of Diamond-Like Carbon Coated Electrodes for Corrosion Sensor Applications at High Temperatures." *Thin Solid Films.* Vol. 517, Issue 3. pp. 1,120–1,224. 2008.

Cho, H.S., J.E. Oh, S.I. Choi, H.M. Cho, Y.O. Park, D.K. Hong, M.S. Lee, Y.J. Yang, U.K. Je, D.S. Kim, T.H. Woo, B.S. Lee, and H.K. Lee. "Performance Evaluation of a Gamma-Ray Imaging System for Nondestructive Testing of Welded Pipes." *Nuclear Instruments and Methods in Physics Research.* Vol. A652. pp. 650–653. 2011.

Chopra, O.K., D. Diercks, D. Ma, V.N. Shah, S-W Tam, R.R. Fabian, Z. Han, and Y.Y. Liu. "Managing Aging Effects on Dry Cask Storage Systems for Extended Long-Term Storage and Transportation of Used Fuel." FCRD–UFD–2013–000294. ANL/NE–13/15. Argonne, Illinois: Argonne National Laboratory. 2012.

Chu, B.-H., H.-W. Lin, S. Gwo, Y.L. Wang, S.J. Pearton, J.W. Johnson, P. Rajagopal, J.C. Roberts, E.L. Piner, K.J. Linthicuni, and F. Ren. "Chloride Ion Detection by Inn Gated Algan/Gan High Electron Mobility Transistors." *Journal of Vacuum Science and Technology B*. Vol. 28. pp. L5–L8. 2010.

Computerised Information Technology Limited. "High Energy Digital Radiography System." Buckinghamshire, United Kingdom: Computerised Information Technology Limited. 2013. <www.cituk-online.com/acatalog/HEDRad.pdf> (21 March 2013).

Consales, M., A. Buosciolo, A. Cuolo, G. Breglio, A. Irace, S. Buontempo, P. Petagna, M. Giordano, A. Cusano. "Fiber Optic Humidity Sensors for High-Energy Physics Applications at CERN." *Sensors and Actuators B: Chemical*. Vol. 159. pp. 66–74. 2011.

Corr Instruments, LLC. "NanoCor Monitoring Systems." San Antonio, Texas: Corr Instruments, LLC. <http://www.corrinstruments.com> (21 March 2013).

Daw, J., J. Rempe, P. Ramuhalli, R. Montgomery, H.T. Chien, B. Tittman, B. Reinhardt. "NEET In-Pile Ultrasonic Sensor Enablement-FY 2012 Status Report." INL/EXT-12-27233 Idaho Falls, Idaho: Idaho National Laboratory. 2012.

Daw, J., J. Rempe, S. Taylor, J. Crepeau and S.C. Wilkins. "Ultrasonic Thermometry for In-Pile Temperature Detection." NPIC&HMIT 2010, INL/CON-10-18293. Idaho Falls, Idaho: Idaho National Laboratory. 2010.

Dickey, E.C., O.K. Varghese, K.G. Ong, D. Gong, M. Paulose and C.A. Grimes. "Room Temperature Ammonia and Humidity Sensing Using Highly Ordered Nanoporous Alumina Films." *Sensors*. Vol. 2. pp. 91–110. 2002.

Diederichs, U., U. Schneider, and M. Terrien. "Formation and Propagation of Cracks and Acoustic Emission." *Fracture Mechanics of Concrete.* Vol. 3. 5 p. 1983.

Dodd, A. and D. Murfin, eds. *Dictionary of Ceramics: Pottery, Glass, Vitreous Enamels, Refractories, Clay Building Materials, Cement and Concrete, Electroceramics, Special Ceramics*. 3rd Edition. Cambridge, United Kingdom: Woodhead Publishing Limited. ISBN 0–901716–56–1. 1994.

Dorsey, M.H., L. Yang and N. Sridhar. "Cooling Water Monitoring Using Coupled Multielectrode Array Sensors and Other On-line Tools." CORROSION/2004, Paper No. 04077. Houston, Texas: NACE International. 2004.

Edalati, K., N. Rastkhah, A. Kermani, M. Seiedi, and A. Movafeghi. "The Use of Radiography for Thickness Measurement and Corrosion Monitoring in Pipes." *International Journal of Pressure Vessels and Piping*. Vol. 83. pp. 736–741. 2006.

Eisenblätter, J. "Non-nuclear Non-destructive Testing Methods To Determine Free Water, Gas Pressure and Matrix Level in Waste Drums." EUR 16190. ISSN 1018-5593. Luxembourg: European Commission. 1995..

Elkey, W. and E. Sellevold. "Electrical Resistivity of Concrete." Publication No. 80. Oslo, Norway: Norwegian Road Research Laboratory. 36 p. 1995.

Elvery, R. H. "Estimating Strength of Concrete in Structures. Current Practice Sheet 10." *Concrete*. Vol. 11. pp. 49–51. 1973.

Engineers Handbook.com. "Mechanical Components: Thermocouples, Temperature Sensors." *Engineers Handbook.* 2013. <http://www.engineershandbook.com/Components/temperaturesensors.htm> (11 March 2013).

EPRI. "Extended Storage Collaboration Program Progress Report and Review of Gap Analyses." EPRI 1022914. Palo Alto, California: Electric Power Research Institute. 2011.

_____. "Climatic Corrosion Considerations for Independent Spent Fuel Storage Installations in Marine Environments." EPRI 1013524. Palo Alto, California: Electric Power Research Institute. 2006.

Esteban, J. "Modeling of the sensing region of a piezoelectric actuator/sensor." Ph.D. dissertation. Virginia Polytechnic Institute and State University. Blacksburg, Virginia. 1996.

Ewins, A.J. "Resistivity Measurements on Concrete." *British Journal of Nondestructive Testing.* Vol. 32. pp. 120–126. 1990.

Faria, H., C. Frias, O. Frazão, P. Vieira, and A.T. Marques. "Development and Validation of Online Monitoring Techniques for Composite Overwrapped Pressure Vessels." Report No. PVP2010–25812. Proceedings of the ASME 2010 Pressure Vessels & Piping Division/K-PVP Conference, Bellevue, Washington, July 18–22, 2010. New York City, New York: American Society of Mechanical Engineers. 2010.

Feliu, S., C. Andrade, J.A. Gonzales, and C. Alonso. "A New Method for *In-situ* Measurement of Electrical Resistivity of Reinforced Concrete." *Materials and Structures/Matériaux et Constructions*. Vol. 29. pp. 362–365. July 1996.

Feliu, S. J.A. Gonzalez, S. Feliu, Jr., and C. Andrade. "Confinement of Electrical Signal for *In-situ* Measurements of Polarization Resistance in Reinforcement Concrete." *Materials Journal of the American Concrete Institute.* Vol. Sep–Oct. pp. 457–460. 1990.

Feng, M., L. Zou, and M. Imai. "Detection of Ceramic Cracks Using a Distributed High-Resolution Brillouin Fiber Optic Sensor." *SICE Journal of Control, Measurement, and System Integration.* Vol. 3, No. 4. pp. 279–284. 2010.

Fieldpiece Instruments, Inc. "HVAC Guide System Analyzer, Field Manual, Model HG3." Anaheim, CA, Fieldpiece Instruments, Inc., 2010. http://fieldpiece.com/PDF/Manuals/HVAC-Guide3-manual-v17.pdf.

Florida Department of Transportation (FDOT). "Florida Method of Test for Concrete Resistivity as an Electrical Indicator of Its Permeability." FM5-578. Tallahassee, Florida: Florida Department of Transportation, State Materials Office. 2005.

Fox, B.P., Z.V. Schneider, K. Simmons-Potter, W.J. Thomes, Jr., D.C. Meister, R.P. Bambha, D.A.V. Kliner, and M.J. Söderlund. "Gamma Radiation Effects in Yb-Doped Optical Fiber." *Fiber Lasers IV: Technology, Systems, and Applications.* Vol. 6,453. p. 645–328. 2007.

Franke, J. "Crystal River Unit #3 Repair Update Briefing to the Florida Public Service Commission." St. Petersburg, Florida: Progress Energy. 2011. <http://psc-fl.granicus.com/MetaViewer.php?view_id=2&clip_id=350&meta_id=14119.> (14 October 2014)

Frias C., H. Faria, O. Frazão, P. Vieira, and A.T. Marques. "Manufacturing and Testing Composite Overwrapped Pressure Vessels With Embedded Sensors." *Materials and Design.* Vol. 31. pp. 4,016–4,022. 2010.

Fuhr, P. and D.R. Huston. "Fiber Optic Chloride Threshold Detectors for Concrete Structures." *Journal of Structural Control.* Vol. 7. pp. 77–102. 2000.

Gao, X., J. Zhang, Y. Yang, and H. Deng. "Fabrication and Performance of All-Solid-State Chloride Sensors in Synthetic Concrete Pore Solutions." *Sensors*. Vol. 10. pp. 10,226–10,239. 2010.

Gaston, A., I. Lozano, F. Perez, F. Auza, J. Sevilla. "Evanescent Wave Optical-Fiber Sensing (Temperature, Relative Humidity, and pH Sensors)." *IEEE Sensors Journal*. Vol. 3. pp. 806–811. 2003.

Geddes, C.D. "Optical Halide Sensing Using Fluorescence Quenching: Theory, Simulations and Applications—A Review." *Measurement Science and Technology*. Vol. 12. pp. R53–R88. 2001.

General Electric (GE). "OptiSonde™ General Eastern Chilled Mirror Hygrometer." *GE Measurement & Control Solutions*. Issue 920–423B. Schenectady, New York: General Electric. 2011. <http://www.gemcs.com/download/moisture-humidity/920-423B-LR.pdf> (12 March 2013).

_____. "OptiSonde™ General Eastern Chilled Mirror Hygrometer User's Manual." *GE Measurement & Control Solutions*. October 2007. <http://www.ge-mcs.com/download/sensing-manuals/910-282A.pdf> (5 May 2013).

_____. "NTC Type B Series Thermometrics Glass Coated Bead Thermistors." 2006. <http://www.ge-mcs.com/download/temperature/920_177a.pdf> (5 May 2013).

_____. "M Series Panametrics Aluminum Oxide Moisture Probe." 920-046C. Billerica, Massachusetts: General Electric. 2005.

Gepraegs O.K. and C.M. Hansson. "A Comparative Evaluation of Three Commercial Instruments for Field Measurements of Reinforcing Steel Corrosion Rates." *Journal of ASTM International.* Vol. 2, No. 8. pp. 1–16. 2005.

Germann Instruments Inc. "Manual of Portable Ultrasonic Nondestructive Digital Indicating Tester." Evanston, Illinois. 2014. <http://www Germann.org/TestSystems/PUNDIT/pundit.pdf> (3 August 2014).

Ghosh, J.K., J.P. Panakkal, K.N. Mahule, and P.R. Roy. "Monitoring Internal Pressure of Sealed Nuclear Fuel Pins: A Simple Technique." *NDT International*. pp. 17–18. February 1983.

Gilboy, W.B., P.M. Jenneson, S.J.R. Simons, S.J. Stanley, D. Rhodes. "Industrial Radiography With Cosmic-ray Muons: A Progress Report." *Nuclear Instruments and Methods in Physics Research.* Section A: Accelerators, Spectrometers, Detectors and Associated Equipment. Vol. 580. pp. 785–787. 2007.

Giurgiutiu, V. "Multifunctional Vehicle Structural Health Monitoring Opportunities With Piezoelectric Wafer Active Sensors." AIAA-1568. Reston, Virginia: American Institute of Aeronautics and Astronautics. 2003.

Gonzalez, J.A., C. Andrade, C. Alonso, and S. Feliu. "Comparison of Rates of General Corrosion and Maximum Pitting Penetration on Concrete Embedded Steel Reinforcement." *Cement and Concrete Research.* Vol. 25, No. 2. pp. 257–264. 1995.

Green, A.T. "Stress Wave Emission and Fracture of Prestressed Concrete Reactor Vessel Materials." Proceedings of the 2nd Interamerican Conference on Materials Technology, Mexico City, Mexico, August 24–27, 1970. Vol. I. p. 635. New York City, New York: American Society of Mechanical Engineers. 1970.

Griscom, D.L. "γ-Ray-Induced Optical Attenuation in Ge-Doped-Silica Optical-Fiber Waveguides." *Journal of Applied Physics.* Vol. 78. pp. 6,698–6,704. December 1995.

Gusarov, A., A. Fernandez, S. Vasiliev, O. Medvedkov, M. Blondel, and F. Berghmans. "Effect of Gamma-Neutron Nuclear Reactor Radiation on the Properties of Bragg Gratings Written in Photosensitive Ge-Doped Optic Fiber." *Nuclear Instruments and Methods in Physics Research.* Vol. B187. pp. 79–86. 2002.

Gusarov, A.I., F. Berghmans, O. Deparis, A. Fernandez, Y. Defosse, P. Me'gret, M. De'creton, and M. Blondel. "Behaviour of Fibre Bragg Gratings Under High Total Dose Gamma Radiation." *IEEE Transactions on Nuclear Science*. Vol. 47, No. 3. pp. 688–692. June 2000.

Gusarov, A.I., F. Berghmans, O. Deparis, A. Fernandez Fernandez, Y. Defosse, P. Megret, M. De'creton, and M. Blondel. "High Total Dose Radiation Effects on Temperature Sensing Fiber Bragg Gratings." *IEEE Photonics Technology Letters.* Vol. 11, No. 9. September 1999.

Gusmano G., G. Montesperelli, S. Pacetti, A. Petitti, and A. D'Amico. "Electrochemical Noise Resistance as a Tool for Corrosion Rate Prediction." *Corrosion*. Vol. 53, No. 11. pp. 860–868. 1997.

Hagyard, T. and J.R. Williams. "Potential of Aluminum in Aqueous Chloride Solutions. Part I, Part II." *Transactions of the Faraday Society*. Vol. 57. pp. 2,288–2,294 and 2,295–2,298. 1961.

Haile, T., S. Papavinasam, and W.D. Gould. "Evaluation of a Portable Online Sensor for Simultaneously Monitoring of Corrosion Rate and Sulfate Reducing Bacteria Activity." Proceedings of the CORROSION 2013 Conference, Orlando, Florida, March 17–21, 2013. Paper No. 2148. Houston, Texas: NACE International. 2013.

_____. "Further Evaluation of an Online Probe for Simultaneous Monitoring Corrosion Rate of SRB Activity: Influence of FeS Surface Layer." Paper No. 11221. *Corrosion 2011.* Houston, Texas: NACE International. 2011.

Haile, T., R. Sooknah, S. Papavisnasam, W.D. Gould, and O. Dinardo. "Simultaneous Online Monitoring of SRB Activity and Corrosion Rate." Paper No. 10255. *Corrosion 2010.* Houston, Texas: NACE International. 2010.

Hamer, F. and J. Hamer. *The Potter's Dictionary of Materials and Techniques*. 3rd Edition. London, England: A & C Black Publishers, Limited. 1991.

Hanson, B., H. Alsaed, C. Stockman, D. Enos, R. Meyer, and K. Sorenson. "Gap Analysis to Support Extended Storage of Used Nuclear Fuel." FCRD–USED–2011–000136. PNNL–20509. Rev. 0. Richland, Washington: Pacific Northwest National Laboratory. 2012.

Harris, D.O. and H.L. Dunegan. "Continuous Monitoring of Fatigue Crack Growth by Acoustic Emission Techniques." *Experimental Mechanics*. Vol. 14, No. 2. pp. 71–81. 1974.

Hasegawa, S. "Performance Characteristics of a Thin-Film Aluminum Oxide Humidity Sensor." 1980. Washington, DC: National Bureau of Standards. <http://manalytical.com/documents/Hasegawa_Report.pdf> (13 March 2013).

Hashimoto, M., S. Miyajima, and T. Murata. "A Stochastic Analysis of Potential." *Corrosion Science*. Vol. 33. p. 885. 1992a.

Hashimoto, M., S. Miyajima, and T. Murata. "A Stochastic Analysis of Potential." *Corrosion Science*. Vol. 33. p. 905. 1992b.

Higham, E.H. and J.M Paros. *Chapter 14: Measurement of Pressure*. Instrumentation Reference Book. W. Boyes, ed. 4th Edition. Butterworth-Heinemann. 2010.

Hill, K.O., Y. Fujii, D.C. Johnson, and B.S. Kawasaki. "Photosensitivity in Optical Fiber Waveguides: Application to Reflection Filter Fabrication." *Applied Physics Letters.* Vol. 32. p. 647. 1978.

Holtec International. "Final Safety Analysis Report for the Holtec International Storage, Transport, and Repository Cask System (HI-STAR 100 Cask System)." Report HI–2012610. Rev 3. ML093070147. Marlton, New Jersey: Holtec International. 2009.

Honeywell International. "HCH-1000 Series Capacitive Humidity Sensors." 000699-2-EN. Golden Valley, Minnesota: Honeywell International. November 2011.

Hung, S.C., Y.L. Wang, B. Hicks, S.J. Pearton, D.M. Dennis, F. Ren, J.W. Johnson, P. Rajagopal, J.C. Roberts, E.L. Piner, K.J. Linthicum, and G.C. Chi. "Detection of Chloride Ions Using an Integrated Ag/AgCl Electrode with AlGaN/GaN High Electron Mobility Transistors." *Applied Physics Letters*. Vol. 92, No 19. p. 193,903. 2008.

Hunkeler, F. The Resistivity of Pore Water Solution—A Decisive Parameter of Rebar Corrosion and Repair Methods." *Construction and Building Materials*. Vol. 10. p. 381. 1996.

Hygrometrix. "Xeritron Datasheet V2.0." Alpine, California: Hygrometrix. May 2005.

IAEA. "Industrial Process Gamma Tomography." Report No. IAEA–TECDOC–1589. Vienna, Austria: International Atomic Energy Agency. 2008.

_____. "Assessment and Management of Aging of Major Nuclear Power Plant Components Important to Safety: PWR Vessel Internals." Vienna, Austria: International Atomic Energy Agency. 2007.

Indian Lead Zinc Information Centre (ILZIC). "Protection of Reinforcement in Concrete—An Update, Galvanizing and Other Methods." New Delhi, India: Indian Lead Zinc Information Centre. 1995.

Institute for Nuclear Technology (INETEC). "Ultrasonic Inspection of Baffle to Former Bolts." 2003. Croatia: Institute for Nuclear Technology. <www.inetec.com> (21 March 2013).

IEEE. "Standard for Qualifying Class 1E Equipment for Nuclear Power Generating Stations." IEEE-323. New York, New York: Institute of Electrical and Electronics Engineers, Inc. 2003.

ISO. "Preparation of Steel Substrates Before Application of Paints and Related Products—Tests for the Assessment of Surface Cleanliness—Part 6: Extraction of Soluble Contaminants for Analysis—The Bresle Method." Report No. ISO 8502-6. Geneva, Switzerland: International Organization for Standardization. 2006.

_____. "Preparation of Steel Substrates Before Application of Paints and Related Products—Tests for the Assessment of Surface Cleanliness—Part 9: Field Method for the Conductometric Determination of Water-Soluble Salts." Report No. ISO 8502-9. Geneva, Switzerland: International Organization for Standardization. 1998.

Iverson, W.P. "Transient Voltage Changes Produced in Corroding Metals and Alloys." *Journal of Electrochemical Society*. Vol. 115. pp. 617–618. 1968.

James Instruments Inc. "Rebar Corrosion and Its Effects." Chicago, Illinois: James Instruments Inc. 2010. <http://www.ndtjames.com> (20 March 2013).

Jeskanen, H., P. Kauppinen, and J. Pitkanen. "Applicability of Ultrasonic Techniques to the Inspection of Copper Canisters Used for High Active Waste Disposal." Working Report 2001-08. Espoo, Finland: VTT Manufacturing Technology, Materials and Structural Integrity. March 2001.

Ju, S., P.R. Watekar, and W.-T, Han. "Highly Sensitive Temperature Sensor using Fiber Bragg Grating on Pb/Ge-codoped Fiber." Proceeding of Conference on Optical Fiber Communication, Technical Digest Series. 2009.

Jung, H., P. Shukla, T. Ahn, L. Tipton, K. Das, X. He, and D. Basu. "Extended Storage and Transportation: Evaluation of Drying Adequacy." ML13169A039. Washington DC: U.S. Nuclear Regulatory Commission. 2013.

Kaeberlein, T., K. Lewis, S.S. Epstein. "Isolating 'Uncultivabte' Microorganisms in Pure Culture in a Simulated Natural Environment." *Science*. Vol. 296. pp. 1,127–1,129. 2002.

Kahn Instruments, Inc. "Chilled Mirror Optical Hygrometers." Wethersfield, Connecticut: Kahn Instruments, Inc. August 2012.

Kaiser, J. "Untersuchungen über dem Auftreten Geräuschen beim Zugversuch." Ph.D. Thesis. Technische Hochschule. Munich, Germany. 1950.

Kajiwara, G. "Improvement to X-Ray Piping Diagnostic System Through Simulation (Measuring Thickness of Piping Containing Rust)." *Journal of Testing and Evaluation*. Vol. 33, No. 5. pp. 295–304. 2005.

Kasban, H., O. Zahran, H. Arafa, M. El-Kordy, S.M.S. Elaraby, F.E. Abd El-Samie. "Welding Defect Detection from Radiography Images with a Cepstral Approach." NDT & E International 2011 Vol. 44. pp.226–231. 2011.

Kersey, A.D., M.A. Davis, and H.J. Patrick. "Fiber Grating Sensor." *Journal of Lightwave Technology*. Vol. 15. pp. 1,442–1,461. 1997.

Kessler, R. "Corrosion Rate Based on Polarization Resistance." Washington, DC: American Association of State Highway and Transportation Officials. 2001.

Kisner, R., C.L. Britton, U. Jagadishl, J.B. Wilgen, M. Roberts, T.V. Blalock, D. Holcomb, M. Bobrek, and M.N. Ericson. "Johnson Noise Thermometry for Harsh Environments." IEEE Aerospace Conference Proceedings 01/2004. DOI: 10.1109/AERO 2004. DOI: 10.1109/AERO 2004. pp. 2,586–2,596. 2004.

Kitazawa, S., N. Kono, A. Baba, Y. Adachi, M. Odakura, and O. Kikuchi. "Three-Dimensional Visualization and Evaluation Techniques for Volumetrically Scanned Data of Ultrasonic Phased Arrays." *Insight.* Vol. 52, No. 4. pp. 201–205. 2010.

Knoll, G.F. *Radiation Detection and Measurement*. 2nd Edition. New York City, New York: John Wiley & Sons. p. 115. 1989.

Korsah, K., R. Wetherington, R. Wood, L.F. Miller, K. Zhao, and A. Paul. NUREG/CR-6888, "Emerging Technologies in Instrumentation and Controls: An Update." Washington, DC: U.S. Nuclear Regulatory Commission. 2006.

Lacy, E. *Fiber Optics.* Englewood Cliffs, New Jersey: Prentice-Hall. 1982.

Lal, A., R. Duggirala, L. Hui. "Pervasive Power: A Radioisotope-Powered Piezoelectric Generator." IEEE Pervasive Computing. 2005.

Lalande, F., B. Childs, Z. Chaudhry, and C.A. Rogers. "High Frequency Impedance Analysis for NDE of Complex Precision Parts." Conference on Smart Structures and Materials. Proceedings of SPIE. San Diego, California: SPIE Publishing, Bellingham, AA. Vol. 2,717. pp. 237–245. 1996.

Lam, C., R. Mandamparambil, T. Sun, K.T.V. Grattan, S. Nanukuttan, S.E. Taylor, and P.M.A. Basheer. "Optical Fiber Refractive Index Sensor for Chloride Ion Monitoring." *IEEE Sensors Journal*. Vol. 9. pp. 525–532. 2009.

Lambert, J.D., S. Bakhtiari, I. Bodnar, C. Kot, and J. Pence. "NRC Job Code V6060: Extended *In-Situ* and Real Time Monitoring Task 3: Long-Term Dry Cask Storage of Spent Nuclear Fuel." ANL/NE-12/18. Argonne, Illinois: Argonne National Laboratory. March 2012.

Lee, L.R., C.Y. Ryu, B.Y. Koo, S.G. Kang, C.S. Hong, and C.G. Kim. "In-Flight Health Monitoring of a Subscale Wing Using a Fiber Bragg Gating Sensor System." *Smart Materials and Structures.* Vol. 12. pp. 147–155. 2003.

Lee, N., I. Hwang, and H. Yoo. "New Leak Detection Technique Using Ceramic Humidity Sensor for Water Reactors." *Nuclear Engineering and Design*. Vol. 205. pp. 23–33. 2001.

Leslie J. R. and W.J. Cheeseman. "An Ultrasonic Method for Studying Deterioration and Cracking in Concrete Structures." American Concrete Institute Proceedings. Vol. 46. pp. 17–36. 1949.

Leung, N., N. Elvin, N. Olson, T.F. Morse, and Y.-Fei He. "A Novel Distributed Optical Crack Sensor for Concrete Structures." *Engineering Fracture Mechanics*. Vol. 65. pp. 1,333–1,348. 2000.

L'Hermite, R.G. "What We Know About the Plastic Deformation and Creep of Concrete?" *RILEM Bulletin*. Vol. 1. p. 21. 1959.

Liang, C., F.P. Sun, and C.A. Rogers. "Coupled Electromechanical Analysis of Adaptive Material Systems—Determination of the Actuator Power Consumption and System Energy Transfer." *Journal of Intelligent Material Systems and Structures*. Vol. 5. pp. 12–20. 1994.

Licina, G.J. "Monitoring Biofilms on Metallic Surfaces in Real Time." Paper No. 01442. *Corrosion 2001.* Houston, Texas: NACE International. 2001.

Licina, G.J. and C.S. Carney. "Monitoring Biofilm Formation and Incipient MIC in Real Time." Proceedings of the CORROSION 1999 Conference, San Antonio, Texas, April 25–30, 1999. Paper No. 175. Houston, Texas: NACE International. 1999.

Light, G.M. and N.R. Joshi. "Ultrasonic Waveguide Technique for Detection of Simulated Corrosion Wastages." *Nondestructive Testing Communications.* Vol. 3. pp. 13–27. 1987.

Lin, Y.J.P., E.J. St. Martin, and J.R. Frank. "Monitoring and Mitigation of Sustained Localized Pitting Corrosion." Argonne, Illinois: Argonne National Laboratory. 2003.

Lin, Y.J.P., E.J. St. Martin, J.R. Frank, and D.H. Pope. "Electrode Design for Corrosion Monitoring Using Electrochemical Noise Measurement." U.S. Patent No. 6,294,074. Washington, DC: U.S. Patent Office. 2001.

Little, B.J., J.S. Lee, and R.I. Ray. "Diagnosing Microbiologically Influenced Corrosion: A State-of-the-Art Review." *Corrosion*. Vol. 62, No. 11. pp.1,006–1,017. 2006.

Liu Y. and R.E., Weyers. "Comparison of Guarded and Unguarded Linear Polarization CCD Devices with Weight Loss Measurements." *Cement and Concrete Research*. Vol. 33. pp. 1,093–1101. 2003.

Liu, H., D.W. Miller, and J.W. Talnagi. "Performance Evaluation of Fabry-Perot Temperature Sensors in Nuclear Power Plant Measurements." *Nuclear Technology*. Vol. 143. pp. 208–216. 2003.

Loto, C.A. and R.A. Cottis. "Electrochemical Noise Generation During Stress Corrosion Cracking of the High-Strength Aluminum AA 7075-T6 Alloy." *Corrosion*. Vol. 45. pp. 136–141. 1989.

Louisville Solutions Incorporated. "SaltSmart® Accurate Soluble Salt Contamination Measurements in a Portable Low Cost Device." Louisville, Kentucky: Louisville Solutions Incorporated. 2013.

Luping, T. "Calibration of the Electrochemical Methods for the Corrosion Rate Measurement of Steel Concrete." Nordtest Project No. 1531-01, SP Report No. 2002:25. Sweden: SP Swedish National Testing and Research Institute. 2002.

Lynnworth, L.C. "Chapter 5: Temperature Applications." Ultrasonic Measurements for Process Control. San Diego, California: Academic Press Inc. pp. 369–422. 1989.

McLay, A. and J. Verkooijen. "Ultrasonic Inspections at Elevated Temperature." *Insight: Non-Destructive Testing and Condition Monitoring.* Vol. 54. pp. 307–309. 2012.

Malhotra, V.M. and N.J. Carino. "Handbook on Nondestructive Testing of Concrete." Boca Raton, Florida: CRC Press. p. 343. 1991.

Mansfeld, F. and H. Xiao. "Electrochemical Techniques for the Detection of Localized Corrosion Phenomena in MIC." In Microbiologically Influenced Corrosion (MIC) Testing. STP 1232. West Conshohocken, Pennsylvania: American Society for Testing and Materials. p. 12. 1994.

Marchal, R., N. Monfort-Moros, D. Festy, B. Tribollet, and I. Frateur. "Method and Device for Detecting Microbiologically Induced Corrosion." U.S. Patent No. 6,960,288. Washington, DC: U.S. Patent Office. 2005.

Mascarenas, D.D.L. "Development of an impedance method based wireless sensor node for monitoring of bolt joint preload." M.S. Thesis. University of California. San Diego, California. 2006.

Massie, M.E. "Device To Transmit Critical Information from the Interior of a Spent Fuel Cask." Honors Thesis. University of Tennessee. Knoxville, Tennessee. April 2008.

Mathew, J., Y. Semenova, G. Rajan, and G. Farrell. "Humidity Sensor Based on a Photonic Crystal Fibre Interferometer." *Electronics Letters*. Vol. 46. pp. 1,341–1,343. 2010.

Matsumura, T., A. Sasahara, Y. Nauchi, and T. Saegusa. "Development of Monitoring Technique for the Confirmation of Spent Nuclear Fuel Integrity During Storage." *Nuclear Engineering and Design*. Vol. 238. pp. 1,260–1,263. 2008.

Merzbacher, C.I., A.D. Kersey, and E.J. Friebele. "Fiber Optic Sensors in Concrete Structures: A Review." *Smart Materials and Structures.* Vol. 5, No. 2. pp.196–208. 1996.

Meyer, R.M., A.F. Pardini, J.M. Cuta, H.E. Adkins, A.M. Casella, A. Qiao, A.A. Diaz, and S.R. Doctor. "Assessment of HI-STORM 100 and NUHOMS® Dry Storage Modules or Implementation of NDE to Manage Atmospheric SCC in Canisters." PNNL–22495. Richland, Washington: Pacific Northwest National Laboratory. 2013.

Michalski, L., K. Eckersdorf, J. Kucharski, and J. McGhee. *Temperature Measurement.* 2nd Edition. New York City, New York: John Wiley & Sons, Ltd. 2001.

Michell Instruments. "S8000 Remote High Precision Chilled Mirror Hygrometer." Rowley, Massachusetts: Michell Instruments. 2012.

Miki, C and H. Shirahata. "Nondestructive testing for steel bridges in Japan." Nondestructive Testing in Civil Engineering. T. Uomoto, ed. 1st edition. Elsevier Science. pp. 13–22. 2000.

Millard, S.G. "Reinforced Concrete Resistivity Measurement Techniques." *Proceedings Institute of Civil Engineers*. Vol. 91. pp. 71–78. 1991.

Millard, S.G., J.A. Harrison, and A.J. Edwards. "Measurement of the Electrical Resistivity of Reinforced Concrete Structures for the Assessment of Corrosion Risk. *British Journal of Nondestructive Testing.* Vol. 31. pp. 617–621. 1986.

Miller, D.W., B. Hajek, J.W. Talnagi, A. Mutlak, H. Liu, and M. Holton. "Fiber Optic Sensors in Nuclear Power Plant Radiation Environments" Phase 1 TR-107326-V1. Palo Alto, California: Electric Power Research Institute. 1999.

Mistras. "General Purpose Sensor." web page. September 20, 2013. http://www.mistrasgroup.com/products/solutions/acousticemission/sensors/R15S.aspx. (20 September 2013).

Miyadera, H., K.N. Borozdin, S.J. Greene, Z. Lukić, K. Masuda, E.C. Milner, C.L. Morris, J.O. Perry. "Imaging Fukushima Daiichi Reactors with Muons." *AIP Advances*. Vol. 3. Article Number 052133. 2013.

Morey, W.W., G. Meltz, and W.H. Glenn. "Fiber Optic Bragg Grating Sensors." *Proceedings of SPIE.* Vol. 1169. Doi: 10.1117/12.963022. http://dx.doi.org/10.1117/12.963022. pp. 98–107. 1989.

Morison, D. and R. Tennyson. "Direct Assessment of Corrosion Using Fiber Optic Sensors." *Corrosion*. Paper No. 07385. Houston, Texas: NACE International. 2007.

Morris, C.L., J. Bacon, Y. Ban, K. Borozdin, J.M. Fabritius, M. Izumi, H. Miyadera, S. Mizokami, Y. Otsuka, J. Perry, J. Ramsey, Y. Sano, T. Sugita, D. Yamada, N. Yoshida, K. Yoshioka. "Analysis of Muon Radiography of the Toshiba Nuclear Critical Assembly Reactor." *Applied Physics Letters*. Vol. 104. Article Number 024110. 2014.

Naidu, A., S. Bhalla, and C.K. Soh. "Incipient Damage Localization with Smart Piezoelectric Transducers using High-Frequency Actuation." Proceedings of SPIE International Symposium on Smart Materials, Nano-, and Micro-Smart Systems, December 16–18, 2002. Melbourne, Australia. 2002.

NASA Glenn Research Center, Alpha- and Beta-voltaics. <https://rt.grc.nasa.gov/power-in-space-propulsion/photovoltaics-power-technologies/technology-thrusts/alpha-and-beta-voltaics/> (16 May 2014).

Neustruev, V. "Color Centers in Germanosilicate Glass and Optical Fibers." *Journal of Physics: Condensed Matter*. Vol. 6. pp. 6,901–6,936. 1994.

Ng, D. and G. Fralick. "Use of a Multiwavelength Pyrometer in Several Elevated Temperature Aerospace Applications." *Review of Scientific Instruments*. Vol. 72. p. 1,522. 2001.

Nguyen, T.H., Y.C. Lin, C.T. Chen, F. Surre, T. Venugopalan, T. Sun, and K.T.V. Grattan. "Fibre Optic Chloride Sensor Based Fluorescence Quenching of an Acridinium Dye." 20th International Conference on Optical Fiber Sensors. *Proceedings of SPIE*. Vol. 7503. pp. 750,311-750,315. 2009.

NRC. "Identification and Prioritization of the Technical Information Needs Affecting Potential Regulation of Extended Storage and Transportation of Spent Nuclear Fuel." ML14043A423. Washington, DC: U.S. Nuclear Regulatory Commission. 2014.

_____. "Regulatory Issue Resolution Protocol (RIRP) Pilot: Marine Atmosphere Stress Corrosion Cracking (SCC)." ML12128A200. Washington DC: U.S. Nuclear Regulatory Commission. 2012a.

_____. "Response to Request for Supplemental Information, RE: Calvert Cliffs Independent Spent Fuel Storage Installation License Renewal Application (TAC No. L24475)." Calvert Cliffs Nuclear Power Plant Independent Spent Fuel Storage Installation Material License No. SNM–2505. Docket No. 72-8. ML12212A216. Washington, DC: U.S. Nuclear Regulatory Commission. July 2012b.

_____. "Minutes of the ACRS Radiation Protection and Nuclear Materials Subcommittee Meeting on June 5, 2012." ML122140318. Washington DC: U.S. Nuclear Regulatory Commission. 2012c.

_____. "Staff Requirements: COMSECY–10–0007—Project Plan for Regulatory Program Review to Support Extended Storage and Transportation of Spent Nuclear Fuel." Memorandum (December 6) to R.W. Borchardt, NRC, from A.L. Vietti-Cook. ML103400287. Washington, DC: U.S. Nuclear Regulatory Commission. 2010a.

_____. "Davis-Besse Nuclear Power Station Special Inspection to Review Flaws in the Control Rod Drive Mechanism Reactor Vessel Closure Head Nozzle Penetrations 05000346/2010-008(DRS) and Exercise of Enforcement Discretion. " EA-10-087. ML102930380. Washington, DC: U.S. Nuclear Regulatory Commission. October 22, 2010b.

_____. NUREG–1864, "A Pilot Probabilistic Risk Assessment of a Dry Cask Storage System at a Nuclear Power Plant." Washington, DC: U.S. Nuclear Regulatory Commission. March 2007.

_____. "Cladding Considerations for the Transportation and Storage of Spent Fuel, Revision 3." Interim Staff Guidance–11. Washington DC: U.S Nuclear Regulatory Commission. 2003.

Nuclear Waste Technical Review Board (NWTRB). "Evaluation of the Technical Basis for Extended Dry Storage and Transportation of Used Nuclear Fuel." Washington, DC: Nuclear Waste Technical Review Board. 2010.

Obert, L. "Use of Subaudible Noises for Prediction of Rock Bursts. Report No. 3555. Washington, DC: U.S. Bureau of Mines. 1941.

Ohmic Instruments Company. "Absolute Humidity Sensor Model ABS-300." ABS-300. Rev. 2 Brochure. Easton, Maryland: Ohmic Instruments Company. 2013.

Okabe, Y., N. Tanaka, and N. Takeda. "Effect of Fiber Coating on Crack Detection in Carbon Fiber Reinforced Plastic Composites Using Fiber Bragg Grating Sensors." *Smart Material Structure.* Vol. 11. pp. 892–989. 2002.

Olinger, D., J. Gray, and R. Felice. "Successful Pyrometry in Investment Casting." Proceedings of the 55th Annual Technical Conference on Investment Casting, Cleveland, Ohio. Dallas, Texas: Investment Casting Institute. 2007.

Omega Engineering, Inc. "RHCM-40 SERIES Dew Point Transmitter With a Humidity Option Configuration." Stamford Connecticut: Omega Engineering, Inc. March 2013.

_____. "Omega Users Guide, RH511 Temperature/Relative Humidity Non-Contact Infrared/Thermocouple Handheld Meter & Logger with Wireless Temp/RH Probe Option." Stamford, Connecticut: Omega Engineering, Inc. 2012. <http://www.omega.com/Manuals/manualpdf/M4954.pdf> (6 August 2014).

Pahlavan, P.L., J. Paulissen, R. Pijpers, H. Hakkesteegt, R. Jansen. "Acoustic Emission Health Monitoring of Steel Bridges." 7th European Workshop on Structural Health Monitoring. July 8-11, La Cité, Nantes, France. 2014.

Park, G., H. Cudney, and D.J. Inman. "An Integrated Health Monitoring Technique Using Structural Impedance Sensors." *Journal of Intelligent Material Systems and Structures*. Vol. 11. pp. 448–455. 2000.

_____. "Impedance-Based Health Monitoring for Civil Structures." 2nd International Workshop on Structural Health Monitoring. Stanford, California: American Society of Civil Engineers. pp. 523–532. 1999.

Paul N. Gardner Co., Inc. "DSP Bresle Chloride Test Kit." 2013. <www.gardco.com.> (6 August 2014).

Pawlick, L.A., G.E. Stoner, and G.G. Clemenia. "Development of an Embeddable Reference Electrode for Reinforced Concrete Structures." VTRC 99-CR1. Charlottesville, Virginia: Virginia Transportation Research Council, Virginia Department of Transportation. 1998.

Pearis, D.M., G. Park, and D.J. Inman. "Improving the Accessibility of the Impedance-Based Structural Health Monitoring Method." *Journal of Intelligent Material Systems and Structures*. Vol. 15. pp.129–139. 2004.

Pieter, R.W. *Water Vapor Measurement: Methods and Instrumentation.* New York City, New York: Marcel Dekker. 1997.

Podskarbi, M. "Retrofitable External Hoop Strain Sensors to Monitor Changes in Internal Pressure during Hydrate Blockage Remediation in a Deep-Water Flowline." Proceedings of the International Conference on Offshore Mechanics and Arctic Engineering. Vol. 5. pp. 771–776. 2010.

Pollock, A.A. "Inspecting Bridges with Acoustic Emission." Guidelines prepared for the U.S. Department of Transportation and Federal Highway Administration (FHWA). Technical Report No. TR-103-12-6/95. Princeton Junction. New Jersey: Physical Acoustic Corporation. 1995.

Pruckner, F. and O.E. Gjorv. "Effect of $CaCl_2$ and NaCl Additions on Concrete Corrosivity." *Cement and Concrete Research.* Vol. 34. pp. 1,209–1,217. 2004.

Ravet, F., F. Briffod, B. Glisic, M. Nikles, and D. Inaudi. "Detection of Sub-Millimeter Faults With a Time Domain Distributed Brillouin Sensor." *Proceedings of SPIE*. Vol. 7004. p. 700,412. 2008.

Reid, M.B. and M. Ozcan. "Temperature Dependence of Fiber Optic Bragg Gratings at Low Temperatures." *Optical Engineering*. Vol. 37, No. 1. pp. 237–240. 1998.

Reis, R.A. and M. Gallaher. "Evaluation of the VTI ECI-1 Embedded Corrosion Instrument." Final Report FHWA/CA/TL–2003/07/ECI–1. Sacramento, California: California Department of Transportation. 2006.

Rhazi, J. and G. Ballivy. "Damage Study by Acoustic Emission: The Role of Transducer." *Canadian Acoustics.* Vol. 21. pp. 9−14. 1993.

Rittersma, Z.M. "Recent Achievements in Miniaturised Humidity Sensors—A Review of Transduction Techniques." *Sensors and Actuators A*. Vol. 96. pp. 196–210. 2002.

Robinson, G.S. "Methods of Detecting the Formation and Propagation of Microcracks in Concrete." Proceedings of the International Conference on the Structure of Concrete and It's Behaviour Under Load, Cement and Concrete Association. A.E. Brooks and K. Newman, eds. London, United Kingdom. pp. 131–145. 1965.

Rohrback Cosasco Systems. "Corrosion Management Solutions." Santa Fe Springs, California: Rohrback Cosasco Systems. 2013. <www.cosasco.com> (21 March 2013).

Ruedas-Rama, M.J., A. Orte, E.A.H. Hall, J.M. Alvarez-Pez, and E.M. Talavera. "A Chloride Ion Sensor for Time-Resolved Fluorimetry and Fluorescence Lifetime Imaging." *Analyst*. Vol. 137. pp. 1,500–1,508. 2012.

Rüsch, H. "Physical Problems in the Testing of Concrete." *Zement-Kalk-Gips*. Vol. 12. p. 1. 1959.

Saafi, M. and P. Romine. "Embedded MEMS for Health Monitoring and Management of Civil Infrastructure." Smart Structures and Materials 2004: Sensors and Smart Structures Technologies for Civil, Mechanical, and Aerospace Systems. *Proceedings of SPIE*. Vol. 5391. pp. 331–343. 2004.

Saegusa, T., K. Shirai, T. Arai, J. Tani, H. Takeda, M. Wataru, A. Sasahara, and P. Winston. "Review and Future Issues on Spent Nuclear Fuel Storage." *Nuclear Engineering and Technology*. Vol. 42. pp. 237–248. 2010.

Sagues, A.A and K. Lau. "Corrosion of Steel in Locally Deficient Concrete, Final Report." Tallahassee, Florida: Florida Department of Transportation. 2009.

Sagues, A.A., S.C. Kranc, L. Yao, F. Presuel-Moreno, and D. Rey. "Corrosion Forecasting for 75-Year Durability Design of Reinforced Concrete, Final Report." Tallahassee, Florida: Florida Department of Transportation. 2001.

Saltzstein, S., S. Marschman, and B. Hanson. "DOE Cask Monitoring Development: Public Meeting at the Nuclear Regulatory Commission." ML14059A209. Washington DC: U.S. Nuclear Regulatory Commission. 2014.

Schell, H.C. and D.G. Manning. "Evaluating the Performance of Cathodic Protection Systems on Reinforced Concrete Bridge Substructures." *CORROSION/85*. Paper No. 263. Houston, Texas: NACE International. 1985.

Schiessl, P. "Corrosion Measuring Cell." United States Patent 5,015,355. May 14, 1991.

Schultz, L.J., K.N. Borozdin, J.J. Gomez, G.E. Hogan, J.A. McGill, C.L. Morris, W.C. Priedhorsky, A. Saunders, M.E. Teasdale. "Image Reconstruction and Material Z Discrimination via Cosmic Ray Muon Radiography." *Nuclear Instruments and Methods in Physics Research, Section A: Accelerators, Spectrometers, Detectors and Associated Equipment.* Vol. 519. pp 687–694. 2004.

Schulz, W., J. Conte, and E. Udd. "Long-Gage Fiber Optic Bragg Grating Strain Sensors to Monitor Civil Structures. *Proceedings of SPIE.* Vol. 4330. pp. 56–65. 2001.

Schweitzer, P.A. *Corrosion Engineering Handbook: Corrosion of Polymers and Elastomers.* 2nd Edition. Boca Raton, Florida: CRC Press. 2007.

Scigiene Corporation. "Infrared Thermometer Emissivity Tables." Scarborough Ontario Canada: http://www.scigiene.com/pdfs/428_InfraredThermometerEmissivitytablesrev.pdf. 2013.

Sensirion. "Datasheet SHT7x (SHT71, SHT75) Humidity and Temperature Sensor IC." Stafa, Switzerland: Sensirion. December 2011.

Sexton, R.A. "MCO Monitoring Plan." SNF–5536. EDT 628541. Rev. 0. Richland, Washington: Fluor Hanford. September 2000.

Sheila, G.B., D.M. Wilt, R.P. Raffaelle, and S.L. Castro. "Alpha-Voltaic Power Source Designs Investigated, Research and Technology 2005." NASA TM–2006–214016. 2011.

Shu, X., B. Gwandu, Y. Liu, L. Zhang, and I. Bennion. "Sampled Fiber Bragg Grating for Simultaneous Refractive-Index and Temperature Measurement." *Optics Letters*. Vol. 26. pp. 774–776. 2001.

Sickafus, K.E., L. Minervini, R.W. Grimes, J.A. Valdez, M. Ishimaru, F. Li, K.J. McClellan, and T. Hartmann. "Radiation Tolerance of Complex Oxides." *Science*. Vol. 289, No. 5480. pp. 748–751. 2000.

Simmers Jr., G.E. "Impedance-based structural health monitoring to detect corrosion." M.S. Thesis. Virginia Polytechnic Institute and State University. Blacksburg, Virginia. 2005.

Sindelar, R.L., A.J. Duncan, M.E. Dupont, P.-S. Lam, M.R. Louthan, Jr., and T.E. Skidmore. "Materials Aging Issues and Aging Management for Extended Storage and Transportation of Spent Nuclear Fuel." NUREG/CR-7116. SRNL–STI–2011–00005. Washington, DC: U.S. Nuclear Regulatory Commission. 2011.

Solanki, R., W.H. Ritchie, and G.J. Collins. "Photodeposition of Aluminum Oxide and Aluminum Thin Films." *Applied Physics Letters*. Vol. 43, Issue 5. pp. 454–456. 1983.

Song, H.W. and V. Saraswathy. "Corrosion Monitoring of Reinforced Concrete Structures: A Review." *International Journal of Electrochemical Science.* Vol. 2. pp. 1–28. 2007.

Sporea, D. and A. Sporea. "Radiation Effects in Sapphire Optical Fibers." *Physica Status Solidi (c).* Vol. 4, No. 3. pp. 1,356–1,359. 2007.

Stephenson, R.J., A.M. Moulin, M.E. Welland, J. Burns, M. Sapoff, R.P. Reed, R. Frank, J. Fraden, J.V. Nicholas, F. Pavese, J. Stasiek, T. Madaj, J. Mikielewicz, and B. Culshaw. "Temperature Measurement." J.G. Webster, ed. Measurement Instrumentation and Sensors Handbook. CRC Press. 1999.

Stewart, J., D.B. Wells, P.M. Scott, and D.E. Williams. "Electrochemical Noise Measurements of Stress Corrosion Cracking of Sensitised Austenitic Stainless Steel in High-Purity Oxygenated Water at 288 °C." *Corrosion Science*. Vol. 33. pp. 73–88. 1992.

Stokes, J.P., and G.L. Cloud. "The Application of Interferometric Techniques to the Nondestructive Inspection of Fiber-Reinforced Materials." *Experimental Mechanics*. Vol. 33. pp. 314–319. 1993.

Suffield, S., J. Fort, J. Cuta, and H. Adkins. "Thermal Modeling of NUHOMS HSM15 Storage Module at Calvert Cliffs Nuclear Power Station ISFSI." FCRD–UFD–2012–000114. U.S. Department of Energy. 2012.

Sun, F.P., Z. Chaudhry, C. Liang, and C.A. Rogers. "Truss Structure Integrity Identification Using PZT Sensor–Actuator." *Journal of Intelligent Material Systems and Structures*. Vol. 6. pp. 134–139. 1995a.

Takahashi, S. and S. Shibata. "Thermal Variation of Attenuation for Optical Fibers." *Journal of Non-Crystalline Solids.* Vol. 30. pp. 359–370. 1979.

Tang, J.-T. and J.-N. Wang. "Measurement of Chloride-Ion Concentration With Long-Period Grating Technology." *Smart Materials and Structures*. Vol. 16. pp. 665–272. 2007.

Tang, J.-L., T.Y. Chiang, H.-P. Chang, and J.-N. Wang. "Studies on Measurement of Chloride Ion Concentration in Concrete Structures with Long-Period Grating Sensors." *Proceedings of SPIE*. Vol. 6174. pp. 61743R-61741 through 61743R-61711. SPIE. 2006.

Tasman, H.A., M. Campana, D. Pel, and J. Richter. "Ultrasonic Thin Wire Thermometry for Nuclear Applications, Temperature—Its Measurement and Control in Science and Industry." *American Institute of Physics*. pp. 1,191–1,196. 1982.

Tatnall, R.E. and D.H. Pope. "Identification of MIC." *A Practical Manual of Microbiologically Influenced Corrosion*. G. Korbin, ed. Houston, Texas: NACE International. 1993.

TDK Corporation. "Resistance Change Type Humidity Sensor Units with High-Accuracy Detection and Output Control CHS Series." TFL–SA06EA 2011.02.18. Tokyo, Japan: TDK Corporation. February 2011.

_____. "Humidity Sensor Units Element Type CHS-ESS Series." Tokyo, Japan: TDK Corporation. May 2010.

Teledyne Cormon. "Monitoring Systems." Middlesex, United Kingdom: Teledyne Cormon. 2013. <http://www.ortonceramic.com/shop/category.aspx?catid=3> (21 March 2013).

TEPCO. "Ultrasonic Integrity Assessment for Foundation Bolts of Nuclear Power Plants." *EJAM*. Vol. 2, No.2. NT23. Tokyo, Japan: The Tokyo Electric Power Co., Inc. 2010.

Texas Instruments Incorporated. “Thermocouples.” 2013. Dallas, Texas: Texas Instruments Incorporated. <http://www.ti.com/lit/an/snia015/snia015.pdf> (7 January 2013).

Tice, R.N. “Method for Enabling Communication and Condition Monitoring from Inside of a Sealed Shipping Container Using Impulse Radio Wireless Techniques.” Patent No. US 6,927,688B2. Washington, DC: 2005.

Tomsett, H. N.. “The Practical Use of Ultrasonic Pulse Velocity Measurements in the Assessment of Concrete Quality.” *Magazine of Concrete Research.* Vol. 32. pp. 7–16. 1980.

Trtnik G., F. Kavcic, and G. Turk. “Prediction of Concrete Strength using Ultrasonic Pulse Velocity and Artificial Neural Networks.” *Ultrasonics*. Vol. 49. pp. 53–60. 2009.

Udd, E. “25 Years of Structural Monitoring Using Fiber Optic Sensors.” *Proceedings of SPIE 7982, Smart Sensor Phenomena, Technology, Networks, and Systems.* Vol. 7982. p. 7982F. April 15, 2011.

Udd, E., J. Corones, and H.M. Laylor. “Fiber Optic Sensors for Infrastructure Applications, Final Report.” SPR 374, February 1998. Salem, Oregon: Oregon Department of Transportation, and Federal Highway Administration. 1998.

Uomoto, T. “Application of Acoustic Emission to the Field of Concrete Engineering.” *Journal of Acoustic Emission*. Vol. 6, No. 3. pp. 137–144. 1987.

Urbano, E., H. Offenbacher, and O.S. Wolfbeis. “Optical Sensor for Continuous Determination of Halides.” *Analytical Chemistry*. Vol. 56. pp. 427–429. 1984.

VAISALA. “Industrial Measurements.” Helsinki, Finland: VAISALA. 2012. <http:// www.vaisala.com/en/industrialmeasurements/products/humidity/Pages/default.aspx> (7 March 2013).

Vallen Systeme GmbH. “Acoustic Emission Sensors Specification.” Germany. <http://www.vallen.de/sites/default/files/sov1212.pdf> (3 August 2014).

Wang, Y., H. Mao, and L.B. Wong. “Dynamic [Cl-]i Measurement with Chloride Sensing Quantum Dots Nanosensor in Epithelial Cells.” *Nanotechnology*. Vol. 21. pp. 055101–055101 through 0055101–0055107. 2010.

Wataru, M., H. Kato, S. Kudo, N. Oshima, and K. Wada. “Measurement of Atmospheric Sea Salt Concentration in the Dry Storage Facility of the Spent Nuclear Fuel.” Proceedings of ICONE14 International Conference on Nuclear Engineering, Miami, Florida, July 17–20, 2006. New York City, New York: ASME International. 2006.

Watlow. “Thermocouples.” 2013. St. Louis, Missouri: Watlow <http://www.watlow.com/ downloads/en/catalogs/thermocouples.pdf> (7 January 2013).

Watters, D.G., A.J. Bahr, P. Jayaweera, and D.L. Huestis. “SMART PEBBLES™: Passive Embeddable Wireless Sensors for Chloride Ingress Monitoring in Bridge Decks.” Sacramento, California: SRI International. 2003.

Weed Instrument Company. "Nuclear Qualified Thermocouple Assemblies." Pub: 0015-002-1021 rev. 10/99. Round Rock, Texas: Weed Instrument Company. 1999.

_____. "Model 601 and 611 Nuclear Qualified RTD with Welded Fitting." Pub: 0015-002-1014 rev. 3/97. Round Rock, Texas: Weed Instrument Company. 1997.

Westinghouse Electric Company. "Nuclear Automation Leakage Monitoring System." Brochure NA-0081. Cranberry Township, Pennsylvania: Westinghouse Electric Company. 2011.

Weydert, R. and C. Gehlen. "Electrolytic Resistivity of Cover Concrete: Relevance, Measurement, and Interpretation." *Durability of Building Materials and Components*. Vol. 8, No. 1. Washington, DC: U.S. Nuclear Regulatory Commission Research Press. pp. 409–419. 1999.

White, D.R., R. Galleano, A. Actis, H. Brixy, M. De Groot, J. Dubbeldam, A.L. Reesink, F. Edler, H. Sakurai, R.L. Shepard, and J.C. Gallop. "The Status of Johnson Noise Thermometry." *Metrologia*. Vol. 33. pp. 325–335. 1996.

Wilkins, S.C. and R.P. Evans. "Assessment of High-Temperature Measurements for Use in the Gas Test Loop." INL/EXT–05–00298. Idaho Falls, Idaho: Idaho National Laboratory. 2005.

Wojtas H. "Determination of Corrosion Rate of Reinforcement with a Modulated Guard Ring Electrode; Analysis of Errors due to Lateral Current Distribution." *Corrosion Science.* Vol. 46. pp. 1621–1632. 2004.

Yaman, I.O., G. Inci, N. Yesiller, and H. Aktan. "Ultrasonic Pulse Velocity in Concrete using Direct and Indirect Transmission." *ACI Materials Journal*. Vol. 98. pp. 450–457. 2001.

Yang, L. "Multielectrode Systems." *Techniques in Corrosion Monitoring.* Cambridge, United Kingdom: Woodhead Publishing. pp. 187–243. 2008.

Yang, L. and K.T. Chiang. "On-Line and Real-Time Corrosion Monitoring Techniques of Metals and Alloys in Nuclear Power Plants and Laboratories." *Understanding and Mitigating Ageing in Nuclear Power Plants: Materials and Operational Aspects of Plant Management.* P.G. Tipping, ed. Woodhead Energy Series No. 4, Chapter 14. Cambridge, England: Woodhead Publishing Limited. pp. 417–455. 2010.

Yang, L. and N. Sridhar. "Coupled Multielectrode Online Corrosion Sensor." *Material Performance.* Vol. 42, No. 9. pp. 48–52. 2003.

Yang, L. and D.S. Dunn. "Evaluation of Corrosion Inhibitors in Cooling Water Systems Using a Coupled Multielectrode Array Sensor." Proceedings of the NACE International. Paper No. 02004. Houston, Texas: NACE International. 2002.

Yang, L., N. Sridhar, and O. Pensado. "Development of a Multielectrode Array Sensor for Monitoring Localized Corrosion." Proceedings of the Extended Abstract. Vol. I. Abstract No. 182. Washington, DC: The Electrochemical Society. p. 182. 2001.

Yeo, T.L., T. Sun, and K.T.V. Grattan. "Fibre-Optic Sensor Technologies for Humidity and Moisture Measurement." *Sensors and Actuators A*. Vol. 144. pp. 280–295. 2008.

Yeo, T.L., T. Sun, K.T.V. Grattan, D. Parry, R. Lade, and B.D. Powell. "Polymer-Coated Fiber Bragg Grating for Relative Humidity Sensing." *IEEE Sensors Journal*. Vol. 5. pp. 1,082–1,089. 2005.

Zaininger, K.H. "Radiation Resistance of Al_2O_3 MOS Devices." *IEEE Transactions on Electron Devices.* Vol. 16, Issue 4. pp. 333–338. 1969.

Zhou, Z. and J. Ou. "Development of FBG Sensors for Structural Health Monitoring in Civil Infrastructures." Proceeding of North American Euro-Pacific Workshop, Sensing Issues in Civil Structural Health Monitoring, Oahu, Hawaii, November 10–13, 2004. Winnipeg, Manitoba, Canada: International Society for Structural Health Monitoring of Intelligent Infrastructure. 2004.

Zielińska, R., E. Mulik, A. Michalska, S. Achmatowicz, and M. Maj-Żurawska. "All-Solid-State Planar Miniature Ion-Selective Chloride Electrode." *Analytica Chimica Acta*. Vol. 451. pp. 243–249. 2002.

Zou, L., X. Bao, S. Afshar, and L. Chen. "Dependence of the Brillouin Frequency Shift on Strain and Temperature in a Photonic Crystal Fiber." *Optics Letters.* Vol. 29. pp. 1,485–1,487. 2004.

APPENDIX A

RADIATION LEVEL AND RADIATION TOLERANCE OF MATERIALS

APPENDIX A

RADIATION LEVEL AND RADIATION TOLERANCE OF MATERIALS

Spent nuclear fuel (SNF) is highly radioactive. Ionizing radiation can present a challenge for sensor operation and longevity by resulting in spurious detection signals, increases in instrument background noise, radiation damage to electronics or sensor components, material degradation, and combinations thereof. SNF radiation characteristics are briefly described in the context of other harsh radiation environments. The discussion is geared toward sensor and component irradiation pertaining to the long-term monitoring of SNF dry storage systems. Occupational radiological dose considerations are beyond the scope of the assessment.

Gamma rays dominate SNF radiation emissions, and emission rates for gamma rays are orders of magnitude greater than those for neutrons (Office of Civilian Radioactive Waste Management, 2001; U.S. Department of Energy, 2008, Section 1.10). Gamma-ray contributions, therefore, are of primary importance to the irradiation assessment. Irradiation by gamma rays and neutrons has been performed by several investigators (e.g., Takada, et al., 1998; Fernandez, et al., 2001; Lee, et al., 2007; Dickerson, et al., 2009; Gusarov, 2009). Specifically, Lee, et al. (2007) states: "A comparison of the radiation effects with different technology for the semiconductors with a Cobalt-60 source and with spent fuel elements has been carried out by AEA Technology in Great Britain. This study shows a divergence lower than the measurement error after a Cobalt-60 irradiation and a spent fuel irradiation. There is therefore no detectable difference in the degradation induced by a Cobalt-60 source and by a spent fuel element." Because electronics and robotics are more sensitive to gamma radiation compared to neutron radiation (Lee, et al., 2007), this appendix focuses on available information for radiation tolerance and hardness to gamma ray irradiation.

Radiation dose rate is strongly dependent on the amount of radiation shielding between the SNF source (i.e., total shield density thickness) and the location on, within, or away from the various container surfaces relative to the SNF source. Estimates of dose rate at various locations relative to SNF and surrounding containers are provided in Table A–1. Dose rate data between shielding layers are more important to this assessment, yet relevant data available to the public are sparse. Representative information is presented in Table A–1. Because irradiation effects are much less severe outside the outer shield of dry storage systems and of lesser importance to this assessment, calculated dose rates at outer locations were not gathered and tabulated for the various storage designs. Radioactive decay over time is important in determining the radiation emission rates, dose rates, and accumulated doses. The dose rate of 10,000 rad/hr listed in Table A–1 compares well to the value of 10,800 rem/hr for peak radial dose rate at the inner surface of a waste package containing 21 average pressurized water reactor SNF assemblies without a canister for transportation, aging, and disposal (Bechtel SAIC Company, 2006, Table 1). The alternative, more conservative, or bounding source terms Bechtel SAIC Company (2006) presented were considered to be unrepresentative or unnecessarily conservative for estimating total integrated dose (TID) from multiple SNF assemblies in conventional dry cask storage systems over long time periods.

At this initial stage of the assessment, TID was approximated by multiplying the exposure time (40 years in Table A–1) by the reported dose rates, corresponding to SNF of various origins with ages of about 20 years. Starting with a 5-year cooled pressurized water reactor SNF, Massie (2008, Figure 8.12) showed a reduction in the shielded dose rate in an electronics region of a redesigned canister shield plug over time. Compared to the dose rate for SNF with a cooling time of 20 years, dose rates were factors of 5 and 2 times higher at cooling times of 5 and

Table A–1. Radiation Dose Rates and Total Integrated Dose Estimates			
Surface Location	**Rough Estimate Dose Rate (rad/hr)**	**40-Year TID Estimate (Mrad)**	**Remarks**
Inside Vessel (no shield)	600–5,000 (corner) 10,000 (middle)	200–1,800 (ends) 3,500 (middle)	Waste package with 21 PWR average SNF assemblies with 4 percent enrichment, 48 GWd/MTU, 21-year cooling time*
Outside 5-cm [2-in] steel§	60–400 (corner) 700 (middle)	20–140 (ends) 250 (middle)	
Outside 5-cm [2-in] steel and 2-cm [0.8-in] Alloy 22§	20–120 (corner) 180 (middle)	7–40 (ends) 60 (middle)	
Outside 5-cm [2-in] copper§	10 (average) 20 (maximum)	3.5 (average) 7 (maximum)	11 BWR SNF assemblies with 20-year cooling†
Outside steel canister in air vent annulus	20–270 (corner) 2,000 (middle)	7–95 (corner) 700 (middle)	Measurements of VSC–17 for 17 PWR SNF assemblies stored for 15 years‡
Outside VSC–17 8.9-cm [3.5-in] steel and 51-cm [20-in] concrete§	0.002 (corner) 0.009 (middle)	0.0007 (corner) 0.003 (middle)	

*Office of Civilian Radioactive Waste Management. "Dose Rate Calculation for the 21–PWR UCF Waste Package." CAL–UDC–NU–000002. Rev. 01. ML040550509. Las Vegas, Nevada: Office of Civilian Radioactive Waste Management. May 2001.
†Posiva Oy. "Gamma and Neutron Dose Rates on the Outer Surface of the Nuclear Waste Disposal Canisters." POSIVA–96–10. Helsinki, Finland: Posiva Oy. December 1996.
‡Winston, P. "Inspection and Gamma-Ray Dose Rate Measurements of the Annulus of the VSC–17 Concrete Spent Nuclear Fuel Storage Cask." INL/EXT–07–13129. Idaho Falls, Idaho: Idaho National Laboratory. September 2007.
§1 in = 2.54 cm
TID = total integrated dose
PWR = pressurized water reactor
SNF = spent nuclear fuel
BWR = boiling water reactor

10 years, respectively. After 20 years, dose rates dropped by a factor of about 1.6 for each additional 10 years of cooling time. At a cooling time of 40 years, the dose rate was roughly 13 times smaller than the dose rate at a cooling time of 5 years. For the gamma-ray emission rates, Massie (2008, Figure 8.7 and Table 8.3) presented a slightly slower reduction over time. Compared to the emission rate at 20 years, emission rates were factors of 2.6 and 1.4 times higher at cooling times of 5 and 10 years, respectively. After 20 years, emission rates dropped by a factor of about 1.3 for each additional 10 years of cooling time. Assuming that SNF is not loaded into a container within the first 5 years of being removed from the reactor core, this information suggests that dose rate data for 20-year-cooled SNF multiplied by 40 years of exposure without explicit treatment of radioactive decay can provide a good estimate of TID for the first 40 years of exposure in a container (within tens of percent). For monitoring over time periods longer than 40 years, TID should be increased with recognition for reduced dose rates at those longer cooling times.

Space, nuclear reactor, and particle accelerators represent other harsh radiation environments, within which instruments and sensors have been designed to function. Each environment is briefly discussed. Space radiation consists of primary radiation (typically electrons, protons, and heavier ions) and secondary radiation (Bremsstrahlung X-rays and neutrons), generated from

primary radiation interactions with the space craft, hardware, or planetary surface materials. Although space radiation can extend to higher individual particle energies compared to those for SNF emissions, dose rates encountered in space missions are lower than dose rates for interior locations of dry storage systems considered for potential instrument placement and long-term monitoring. For example, the environment surrounding Jupiter and its moons represents one of the most intense regions of radiation in our solar system (Benke, et al., 2013). For the entire Jupiter Icy Moons Explorer mission, the European Space Agency (2012, Table 26) specifies the total ionizing dose in silicon as 12.8, 1.9, and 0.8 Mrad for spherical aluminum shielding thicknesses of 1, 3, and 5 mm [0.04, 0.12, and 0.20 in]. For these combinations of shielding material and thickness, accumulated doses are dominated by electrons. Although these accumulated doses represent an upper bound for space missions, they are less than the rough 40-year TID estimates outside the canister or waste package (Table A–1).

Irradiation testing of sensors in nuclear reactors has been performed to total integrated doses exceeding 10 Mrad (Takada, et al., 1998; Fernandez, et al., 2001; Lee, et al., 2007; Dickerson, et al., 2009; Gusarov, 2009). In-core radiation consists of gamma rays and neutrons. With much higher neutron fluxes, the associated irradiation effects from neutrons are much more significant in the core compared to the minimal neutron effects expected from SNF in dry storage configurations. Nevertheless, data on nuclear reactor irradiation represent the best alternative to SNF irradiation data or controlled gamma-ray irradiation testing.

Particle accelerator irradiation also can result in instrument irradiation exceeding 10 Mrad. Because custom instrument designs are expected to be more widespread for particle accelerator and fusion device applications compared to in-core instruments for nuclear reactors, radiation tolerance and hardness data from particle accelerator or fusion device irradiation were not sought.

Radiation damage can be classified for two consequences: (i) atomic displacement (i.e., moving atoms due to the collisions) and (ii) ionization (i.e., creating electron-hole pairs) (Holmes-Siedle, 2002). Depending on the radiation particles and radiation levels, the radiation effect on materials varies. Metals are commonly used in nuclear reactor cores, where the neutron fluxes are high enough to significantly reduce the mechanical strength of metals or render them brittle. For semiconductors that are widely used in electric circuits, the effect of radiation on displacement damage is mostly on electrical changes caused by the change in minority carrier lifetime and concentration, which can have an important effect on p-n junctions in rectifiers and bipolar transistors, as well as solar cells. Ionization of insulators has a major impact on microelectronic devices, in particular for large-scale integration and VLSI MOS ICs. In polymers the ionization can break bonds and even create new ones. The mechanical properties of polymers can be strongly modified by ionizing and nonionizing radiation. Table A–2 shows the materials radiation tolerance ranking. More quantitative information on radiation tolerance of materials is available in Meyer, et al. (2013, Table 5.2)

In the industry, there are three main groups of radiation mitigation techniques: (i) implement methods during the design and fabrication process, (ii) shield the most critical subsystems or components, and (iii) design radiation-tolerant circuits or systems. For the various monitoring technologies assessed in this task, the radiation tolerance will be evaluated case by case depending on the design of the sensor and the location of the sensor placed in the dry cask storage system.

Because several sections in the main body of the report discuss sensors constructed with optical fibers, additional information is provided on irradiation effects for fiber optic materials.

Table A–2. Radiation Tolerance of Materials	
Radiation Tolerance	**Groups of Materials**
High	Metals, ceramics, and insulators
Fair	Bipolar integrated circuits, rectifying diodes, hardened metal oxide semiconductor circuits
Poor	Commercial metal oxide semiconductor circuits, analogue devices, solar cells, power transistors, and charge-coupled devices

Takada, et al. (1998) identify two main uses of optical fibers as transmitting signals or measuring physical changes to the fiber. For transmission-based operation, a signal originates from a detector or device at one end of the fiber and is collected by a photonic sensor at the other end of the fiber. Alternatively, when the fiber itself is used as the sensing medium, the intrinsic relationship of light emission and signal propagation in the fiber to the physical state of the fiber enables measurements of physical changes to fiber materials. In addition to remarks on optical fiber developments for high tolerances to radiation, Takada, et al. (1998) showed more severe radiation-induced losses for light transmission at shorter wavelengths {e.g., shorter than 700 nm [0.0273 mils]} and indicated that radiation losses induced by gamma rays, along with induced measurement errors, usually saturate, such that additional radiation exposure does not lead to further losses or increases in error.

Dickerson, et al. (2009) described that radiation induces fiber darkening, which reduces the transmission of visible light, but near-infrared light signals used for telecommunications, with wavelengths between 1,300 and 1,500 nm [0.0507 and 0.0585 mils], is much less sensitive to radiation effects in specially designed fibers. Addressing long-term pressure sensor use in nuclear reactors, Dickerson, et al. (2009) commented on plans to “include fiber optic radiation sensors within future designs to actively compensate for radiation flux and fluence effects.”

Fernandez, et al. (2001) discussed the strong dependence that the chemical composition of fiber Bragg grating sensor has on gamma-ray irradiation effects. In particular, hydrogen-loaded and non-hydrogen-loaded germanium-doped fibers responded with peak shifts that saturated at a gamma-ray dose of about 10 Mrad, whereas the N_2-doped fiber showed no saturation up to 150 Mrad. The standard highly germanium-doped photosensitive fiber exhibited the lowest radiation sensitivity without pre- or post-fabrication techniques. After photosensitization by hydrogen loading, the fiber Bragg gratings in a telecommunications fiber were found to be the most sensitive to radiation, as indicated by a larger peak shift and significant change in other parameters. From previous tests Fernandez, et al. (2001) performed, the temperature sensitivity of fiber Bragg gratings was not affected by gamma-ray irradiation up to 150 Mrad. In the more recent work by Fernandez, et al. (2001) on nuclear reactor testing of fiber Bragg grating sensors for in-core temperature measurements, radiation-resistant “pigtail” connections were necessary to maintain an acceptable signal-to-noise ratio.

Due to the wide variety of fiber optic materials and fabrication enhancements (including dopants and treatments, measurement techniques, measured parameters, and a clear dependency of the extent of radiation effects on each of the previously described factors), general conclusions on the radiation tolerance for sensors that incorporate fiber optic components are difficult to support. To reduce the uncertainty of sensor performance from the long-term irradiation of fiber optic components, the current approach others in related engineering fields have pursued to experimentally test, evaluate, and demonstrate the performance of specific sensors or

prototypes in harsh environments is endorsed. These concepts are embodied in the nuclear qualification process.

References

Benke, R.R., D.M. White, J.A. Trevino, and K.S. Pickens. "Comparison of Radiation Induced Noise Levels in Two Ion Detectors for Shielded Space Instruments in High Radiation Fields." *IEEE Transactions on Nuclear Science.* Vol. 60, No. 1. pp. 365–375. 2013.

Bechtel SAIC Company. "TAD Source Term and Dose Rate Evaluation." 000–30R–GGDE–00100–000–00A. ML090770282. Las Vegas, Nevada: Bechtel SAIC Company, LLC. August 2006.

Dickerson, B.D., M.A. Davis, M.E. Palmer, and R.S. Fielder. "Temperature Compensated Fiber Optic Pressure Sensor Tested Under Combined High Temperature and High Fluence." Presented at the 6th American Nuclear Society International Meeting on Nuclear Plant Instrumentation, Control, and Human-Machine Interface Technologies 2009, Knoxville, Tennessee, April 5–9, 2009. La Grange Park, Illinois: American Nuclear Society. 2009.

European Space Agency. "JUICE Environmental Specification." JS–14–09, Issue 4. Rev. 9. Noordwijk, Netherlands: European Space Research and Technology Centre. 2012.

Fernandez, A.F., F. Berghmans, B. Brichard, M. Decréton, A.I. Gusarov, O. Deparis, P. Mégret, M. Blondel, and A. Delchambre. "Multiplexed Fibre Bragg Grating Sensors for In-Core Thermometry in Nuclear Reactors." *Proceedings of SPIE*. Vol. 4204. Bellingham, Washington: SPIE. pp. 40–49. 2001.

Gusarov, A. "Long-Term Exposure of fiber Bragg Gratings in the BR1 Low-Flux Nuclear Reactor." Proceedings of the European Conference on Radiation and its Effects on Components and Systems. Article No. 5994686. *RADECS.* pp. 408–411. 2009.

Holmes-Siedle, A. and L. Adams. *Handbook of Radiation Effects.* 2nd Edition. Oxford, England: Oxford University Press. 2002.

Lee, H.J., K.H. Yoon, K.M. Lim, and B.S. Park. "Irradiation Test for ACP Equipment Components." Proceedings of the International Conference on Control, Automation and Systems 2007, Seoul, Korea, October 17–20, 2007. Korea: ICROS. pp. 412–415. 2007.

Massie, M.E. "Device To Transmit Critical Information from the Interior of a Spent Fuel Cask." Honors Thesis. University of Tennessee. Knoxville, Tennessee. April 2008.

Meyer, R.M., A.F. Pardini, J.M. Cuta, H.E. Adkins, A.M. Casella, A. Qiao, A.A. Diaz, and S.R. Doctor. "Assessment of HI-STORM 100 and NUHOMS® Dry Storage Modules or Implementation of NDE to Manage Atmospheric SCC in Canisters." PNNL–22495. Richland, Washington: Pacific Northwest National Laboratory. 2013.

Office of Civilian Radioactive Waste Management. "Dose Rate Calculation for the 21-PWR UCF Waste Package." CAL–UDC–NU–000002. Rev. 01. ML040550509. Las Vegas, Nevada: Office of Civilian Radioactive Waste Management. May 2001.

Takada, E., A. Kimura, F.B.H. Jensen, and M. Nakazawa. "Correction Techniques of Radiation Induced Errors for Raman Distributed Temperature Sensor and Experiment at the Experimental Fast Reactor: JOYO." *Journal of Nuclear Science and Technology.* Vol. 35, No. 8. pp. 547–553. 1998.

U.S. Department of Energy. "Yucca Mountain Repository License Application. Safety Analysis Report. Chapter 1: Repository Safety Before Permanent Closure." DOE/RW–0573. Rev. 1. Las Vegas, Nevada: U.S. Department of Energy, Office of Civilian Radioactive Waste Management. November 2008.